Aus dem Lehrstuhl für Stoffwechselbiochemie
des Adolf-Butenandt-Instituts
der Ludwig-Maximilians-Universität München
Vorstand: Prof. Dr. Dr. h.c. Christian Haass

Identification of ADAM10 5`UTR binding proteins – The RNA-binding protein Unr is involved in ADAM10 mRNA stability

Dissertation
zum Erwerb des Doktorgrades der Naturwissenschaften
an der Medizinischen Fakultät
der Ludwig-Maximilians-Universität München

vorgelegt von
Sonja Christina Renner
geb. Zilow
aus Heidelberg

2014

Gedruckt mit Genehmigung der Medizinischen Fakultät
der Ludwig-Maximilians-Universität München

Dissertation eingereicht am 06. Februar 2014

Betreuer:	Prof. Dr. Dr. h.c. Christian Haass
Zweitgutachter:	Priv. Doz. Dr. Christof Haffner
Mitbetreuung durch den promovierten Mitarbeiter:	Dr. Sven Lammich
Dekan:	Prof. Dr. med. Dr.h.c. Maximilian Reiser, FACR, FRCR

Tag der mündliche Prüfung: 12. Juni 2014

Eidesstattliche Versicherung

Renner, Sonja

Ich erkläre hiermit an Eides statt,
dass ich die vorliegende Dissertation mit dem Thema

Identification of ADAM10 5`UTR binding proteins-
The RNA-binding protein is involved in ADAM10 mRNA stability

selbständig verfasst, mich außer der angegebenen keiner weiteren Hilfsmittel bedient und alle Erkenntnisse, die aus dem Schrifttum ganz oder annähernd übernommen sind, als solche kenntlich gemacht und nach ihrer Herkunft unter Bezeichnung der Fundstelle einzeln nachgewiesen habe.

Ich erkläre des Weiteren, dass die hier vorgelegte Dissertation nicht in gleicher oder in ähnlicher Form bei einer anderen Stelle zur Erlangung eines akademischen Grades eingereicht wurde.

Mannheim, den 06.02.2014

(Sonja Renner)

Table of content

Acknowledgement

I want to thank everyone who contributed to my Ph.D. at the Adolf-Butenandt Institute of the Ludwig-Maximilians University.

In particular, I want to thank my scientific supervisor, Sven Lammich, for his constant support and advice throughout my thesis, and for always having his door open for me.

I am truly grateful to Christian Haass for giving me the opportunity to work in his laboratory, for all his support and mentoring, as well as for the nice atmosphere in the laboratory.

Especially, I have to thank the Hans & Ilse Breuer Foundation for supporting this work with a Ph.D. scholarship.

Some parts of this work were only possible due to the help I received. Therefore, I thank Ignasi Forne for the mass spectrometry measurements, Brigitte Nuscher for all the ELISA measurements and Sabine Odoy for her perfect lab organization and for all the pleasant conversations. I thank Elisabeth Kremmer for providing the monoclonal antibodies 2D8 against Aβ and 7C2 against Unr. Furthermore, I thank Barbara Bettegazzi for her help with the preparation of cytosolic mouse brain extract.

I would like to thank Ann-Katrin Ludwig for all her help in the lab and the nice atmosphere she created there, but especially for her friendship.

I thank the alpha-/beta and friends group members as well as former members: Sven Lammich, Michael Willem, Anja Capell, Frauke van Bebber, Daniel Fleck, Barbara Bettegazzi, Anja Krauss, Ann-Katrin Ludwig, Stephanie Kunath, Katrin Fellerer, Dominik Büll and Bozidar Novak for being good colleagues and giving active support to my work.

My thanks go to the table soccer and/or "Girls day" team: Ann-Katrin Ludwig, Katrin Fellerer, Claudia Abou-Ajram, Anja Krauss, Karin Görner, Susanne Schöbel, Ayako Yamamoto, Claudia Böhland, Stephanie Kunath for all the fun we had. Thanks to all the members of the lab for providing a great working atmosphere and for their help and chats.

I would like to thank my parents for their constant support. Thanks go to Isabel Vogler for her friendship and moral support during my Ph.D. time. Thanks to all my friends for sharing fun and relaxing lab-free time with me. In particular, I have to thank my husband Timo Renner for all his love and patience.

List of Abbreviations

Aβ	Amyloid-β peptide
AD	Alzheimer's disease
ADAM	A disintegrin and metalloprotease
AICD	APP intracellular domain
APH1	Anterior pharynx-defective
APLP	APP like protein
APP	Amyloid precursor protein
APS	Ammonium persulfate
ARE	AU-rich element
Asp	Aspartate
ATP	Adenosine triphosphate
BACE1	Beta-site APP cleaving enzyme
BACE1-AS	BACE1 antisense transcript
BSA	Bovine serum albumin
CD44	Cluster of differentiation 44
CID	Collision-induced dissociation
CSD	Cold shock domain
CSDE1	Cold-shock domain-containing protein E1
CTF	C-terminal fragment
CTP	Cytidine triphosphate
Da	Dalton
DEPC	Diethylpyrocarbonat
DMEM	Dulbecco`s modified Eagle`s medium
DNA	Deoxyribonucleic acid
DTT	Dithiothreitol
dNTP	Deoxyribonucleotide triphosphate
E.coli	Escherichia coli
ECL	Enhanced Chemiluminescence
EDTA	Ethylene diamine tetraacetic acid
ELISA	Enzyme-linked immunosorbent assay
EMSA	Electrophoretic mobility assay
end.	endogenous
ER	Endoplasmic reticulum

ESC	Embryonic stem cell
FAD	Familial Alzheimer's disease
FCS	Foetal calf serum
FXR	Fragile X-related
GAPDH	Glycerinaldehyd-3-phosphat-Dehydrogenase
GC	Guanine-cytosine
GFP	Green fluorescent protein
G-rich	Guanine-rich
GSH	Glutathione
GST	Glutathione-S-transferase
GTP	Guanosine triphosphate
h	Hour
HB-EGF	Heparin-binding EGF-like growth factor
HEK	Human embryonic kidney
HRP	Horse radish peroxidase
IL-1	interleukin-1
imm.	immature
IPTG	Isopropyl-beta-D-thiogalactopyranoside
IRE	Iron-response element
IRES	Internal ribosome entry site
IRP	Iron-regulatory protein
KD	Knockdown
Kuz	Kuzbanian
LB	Luria Bertani
LC	Liquid chomatrography
LRP	Low-density lipoprotein receptor-related protein
LTQ	Linear trap quadrupole
MBP	Myelin basic protein
min	Minute
miRNA	microRNA
MS	Mass spectrometry
msl-2	Male-specific lethal 2
Nct	Nicastrin
NPC	Neural progenitor cells

NRG	Neuregulin
nt	Nucleotide
NTF	N-terminal fragment
OD	Optical density
OPMD	Oculopharyngeal muscular dystrophy
ORF	Open reading frame
P30	Postnatal-day 30
PABP	Poly(A)-binding protein
PAGE	Polyacrylamide gel electrophoresis
PAIP	PABP- interacting protein
PAM	PABP-interaction motif
PB	Processing body
PBS	Phosphate buffered saline
PCBP	Polycytidylic acid binding protein
PCR	Polymerase chain reaction
PD	Parkinson disease
PEN2	Presenilin enhancer protein
PHF	Paired helical filament
PMA	Phorbol 12-myristate 13-acetate
PMSF	Phenylmethylsulphonylfluoride
PNS	Peripheral nervous system
PS	Presenilin
PSGL	P-selectin glycoprotein ligand
PTH	Parathyroid hormone
PVDF	Polyvinylidene fluoride
RBD	RNA-binding domain
rec.	recombinant
RGG	Arginine-glycine-glycine repeats
RNA	Ribonucleic acid
RNP	Ribonucleoprotein
rpm	Revolutions per minute
RT	Room temperature
RT-PCR	real-time PCR
SDS	Sodium dodecyl sulphate

sec	Second
SP	Signal peptide
SPECS	Secretome protein enrichment with click sugars
STRAP	Serine/threonine kinase receptor associated protein
SXL	Sex lethal
TACE	Tumour necrosis factor-α converting enzyme
TAE	Tris-Acetate-EDTA
TBE	Tris-Borat-EDTA
TBS	Tris buffered saline
TBST	Tris buffered saline with Tween
TEMED	N,N,N`,N`-Tetramethylethylendiamine
TMD	Transmembrane domain
Unr	Upstream of N-ras
Unrip	Unr interacting protein
uORF	Upstream open reading frame
UTP	Uridine triphosphate
UTR	Untranslated region
UV	Ultra violet

Summary

Alzheimer`s disease is the most common form of dementia. It is characterised by the accumulation of amyloid plaques and neurofibrillary tangles in the brain. Plaques mainly consist of the 40- or 42-amino-acid amyloid-β peptide (Aβ), which is derived through proteolysis of the amyloid precursor protein (APP) by β- and γ-secretase. In contrast, α-secretase prevents the formation of Aβ by cleaving APP within the Aβ domain. There is strong evidence that ADAM10 (a disintegrin and metalloproteinase) acts as α-secretase *in vivo* whereas BACE1 (beta-site APP cleaving enzyme) acts as β-secretase.

ADAM10 has a 444 nucleotide conserved 5`untranslated region (UTR) with potential upstream open reading frames (uORFs) and a guanine-cytosine (GC) content of 70%. Recently, our group could demonstrate that the 5'UTR of ADAM10 inhibits ADAM10 translation.

Since the protein expression of ADAM10 is repressed by its 5`UTR, the possible involvement of 5`UTR RNA-binding proteins in this process was examined in this work. Using Electrophoretic mobility shift assays (EMSAs) and UV crosslink experiments, I could show that proteins bind to the 5'UTR of ADAM10 and thus are potential candidates which might modify ADAM10 translation. To identify these interacting proteins, a streptavidin-based affinity chromatography purification method coupled to mass spectrometry was established and a UTR-database search was performed. Mass spectrometry analysis revealed several RNA-binding proteins as ADAM10 5`UTR interactors, including Unr, a protein involved in translational regulation and mRNA stability of certain transcripts. A UTR-database search revealed Unr, as candidate RNA-binding protein of the ADAM10 5`UTR.

The interaction of Unr with the ADAM10 5`UTR was confirmed by EMSAs with recombinant Unr. The formation of the ADAM10 5`UTR-Unr complex was visible in the gel through a delay in the running behaviour in comparison with the free RNA. Deletion of an 83 purine-rich nucleotide stretch within the 5'UTR abolished the binding of recombinant Unr to the 5'UTR of ADAM10 and resulted in an increase of ADAM10 expression. Moreover, upon Unr knockdown reduced levels of ADAM10 as well as reduced ADAM10 mRNA were observed. Due to the reduced ADAM10 protein levels, the ADAM10 dependent shedding of APP was reduced. Overexpression of Unr resulted in a minor change of ADAM10 expression with no change in ADAM10 mRNA.

In summary, this study demonstrated that the cytoplasmic protein Unr is able to bind to the 5'UTR of ADAM10. Unr may contribute to the translational repression of ADAM10 protein expression and in addition to the stabilisation of the ADAM10 mRNA.

Zusammenfassung

Die Alzheimer Krankheit ist die weltweit am häufigsten vorkommende Altersdemenz. Die Akkumulation von extrazellulären Amyloid-Plaques und von intrazellulären neurofibrillären Bündeln ist das charakteristische Merkmal der Alzheimer Krankheit. Amyloid-Plaques bestehen überwiegend aus dem 40-42 Aminosäuren langem Amyloid β-Peptid (Aβ), das durch sequenzielle proteolytische Spaltung durch die β- und γ-Sekretase aus dem β-Amyloid-Vorläuferprotein (APP) entsteht. Im Gegensatz dazu verhindert die α-Sekretase die Bildung von Aβ durch Spaltung von APP in der Mitte der Aβ-Domäne. Verschiedene Studien deuten darauf hin, dass ADAM10 *in vivo* als α-Sekretase fungiert und BACE1 als β-Sekretase.

ADAM10 hat eine 444 Nukleotide lange konservierte 5`untranslatierte Region (5`UTR) mit potenziellen uORFs und einem GC-Gehalt von 70%. Kürzlich konnte unsere Gruppe zeigen, dass die 5`UTR von ADAM10 die Translationsrate von ADAM10 inhibiert.

Da die Proteinexpression von ADAM10 durch ihre 5`UTR inhibiert wird, sollte in dieser Arbeit die mögliche Beteiligung von RNA-bindenden Proteinen an diesem Prozess untersucht werden. Mit Hilfe von Electrophoretic Mobility Shift Assays (EMSAs) und UV Crosslink Experimenten konnte ich zeigen, dass mehrere Proteine selektiv an die 5`UTR von ADAM10 binden. Um die möglichen Bindekandidaten zu identifizieren, wurde eine auf Biotin-Streptavidin-basierende Affinitätschromatographie als Reinigungsmethode entwickelt und eine UTR-Datenbanksuche durchgeführt. Mit Hilfe von Massenspektrometrieanalyse wurden mehrere potenzielle RNA-bindende Proteine, darunter Unr, als Bindekandidaten der ADAM10 5`UTR identifiziert. Unr ist ein zytosolisches Protein, das an der translationellen Kontrolle verschiedener Proteine beteiligt ist. Die UTR-Datenbanksuche bestätigte Unr als ADAM10 5`UTR bindendes Protein.

Anhand von EMSAs mit rekombinantem Unr konnte die Bindung von Unr an die 5`UTR von ADAM10 bestätigt werden. Die Deletion einer 83 Nukleotide langen, Purin-reichen Nukleotidsequenz in der 5`UTR verhindert die Bindung von rekombinantem Unr an die 5`UTR von ADAM10 und resultiert in einer erhöhten ADAM10 Expression. Des Weiteren wurden Zellen hergestellt, in denen Unr herrunterreguliert ist. In diesen Zellen werden sowohl reduzierte ADAM10 Proteinmengen als auch ADAM10 mRNA beobachtet. Auf Grund des reduzierten ADAM10 Proteinspiegels ist die Spaltung von APP durch die α-Sekretase ADAM10 reduziert. Die Überexpression von Unr resultiert in

einer minimalen Veränderung der ADAM10 Expression ohne Veränderung der ADAM10 mRNA Mengen.

Zusammenfassend konnte in dieser Arbeit gezeigt werden, dass das zytosolische Protein Unr an die 5`UTR von ADAM10 binden kann. Unr ist möglicherweise ein Translationshemmer für die ADAM10 Expression und ist wichtig für die Stabilität der ADAM10 mRNA.

1 Introduction

1.1 Histopathology of Alzheimer's disease

Alzheimer's disease (AD) is the most common form of dementia among older people and affects the parts of the brain that control thought, memory and language (Figure 1.1) (Selkoe, 2001a).

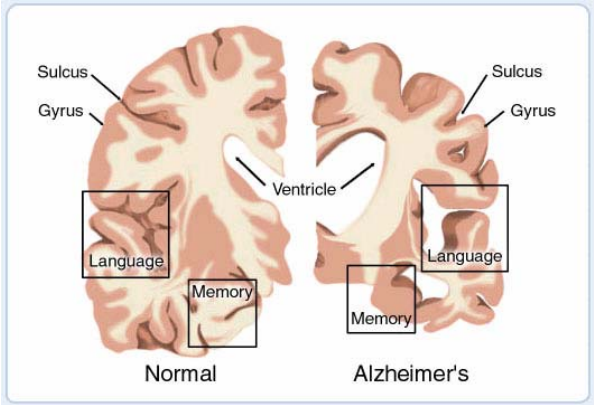

Figure 1.1 Representation of a cross-section of a brain as seen from the front.
The cross-section on the left represents a normal brain and the one on the right represents a brain with AD. (Resource: American Health Assistance Foundation (http://www.ahaf.org/))

About 18 million people worldwide are currently affected by AD. Since ageing is the major risk factor for AD, the number of people affected increases markedly with advanced age. The disease usually begins after age of 60. Of people over 65-year-olds only 5-10% develop AD symptoms, while for those over 85 years the probability increases to 30-50%. Thus, after the age of 65 the risk of AD doubles every five years (Evans *et al.*, 1989; Kawas *et al.*, 2000).

Symptoms of AD include memory loss, language deterioration, impaired ability to mentally manipulate visual information, poor judgement, confusion, restlessness and mood swings (Parihar and Hemnani, 2004). The early symptoms, which include forgetfulness and loss of concentration, are often missed because they resemble natural signs of ageing (Selkoe, 2001a).

The disease is named after Dr. Alois Alzheimer, a German physician. In 1906, Dr. Alois Alzheimer reported the first AD patient, Auguste D. (Figure 1.2). Dr. Alzheimer for the first time described changes in the brain tissue of Auguste D. who had died of an unusual mental illness (Alzheimer, 1907).

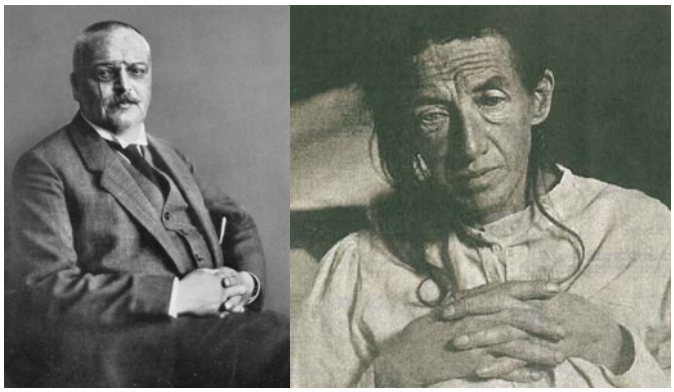

Figure 1.2 Alois Alzheimer and Auguste D. (Maurer and Maurer, 1998).
Photographs of Alois Alzheimer on the left and his patient Auguste D. on the right.

The symptoms described were progressive memory impairment, disordered cognitive function, altered behaviour including paranoia, delusions, loss of social appropriateness and a progressive decline in language function (Alzheimer, 1907). Post-mortem, the brain of the patient showed atrophy and *"many fibrils"* in the cell and *"miliary foci"* all over the cortex, especially in the upper layers, which were observed by silver staining. These lesions, that Alzheimer reported more than 100 years ago, are the pathological hallmarks of AD, which today are described as neuronal cell loss, the intracellular accumulation of neurofibrillary tangles and the extracellular deposition of senile plaques.

One of the hallmarks of AD is the presence of characteristic extracellular deposited senile plaques in the brains of patients (Figure 1.3). They are usually found in brain regions such as hippocampus, amygdala, cortical and subcortical areas (LaFerla and Oddo, 2005; Selkoe, 2001a; Selkoe, 2001b) and are primarily composed of the amyloid β-peptide (Aβ) (Glenner and Wong, 1984). The Aβ peptide is liberated from a larger membrane protein, the amyloid precursor protein (APP). The peptide is highly hydrophobic and aggregates to form oligomers and fibers. It is secreted by all cells throughout the body, but is produced in particularly large amounts by neurons in the brain. Analysis of the amyloid plaques found in the brains of AD patients revealed that they are mainly composed of peptides of either 40 or 42 amino acids. The ratio of Aβ40 to Aβ42 is usually 9:1 (Haass and Selkoe, 2007). The peptide ending at amino acid 42 (Aβ42) is more hydrophobic and thus particularly more prone to aggregation (Jarrett *et al.*, 1993a; Jarrett *et al.*, 1993b). Most plaques in the AD brain are diffuse plaques (Joachim *et al.*, 1989; Selkoe, 1997). There are also less frequent neuritic plaques, in which dystrophic neurites are a prominent and commonplace feature. Since diffuse plaques are also found frequently in healthy aged

brains, it is hypothesised that they are the precursor of neuritic plaques (LaFerla and Oddo, 2005; Selkoe, 2001a; Selkoe, 2001b).

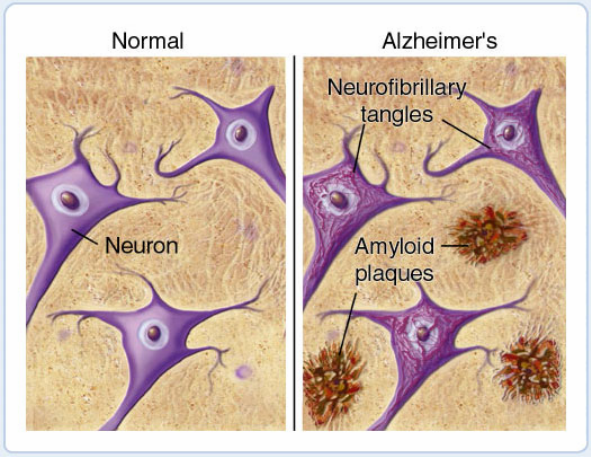

Figure 1.3 Amyloid plaques and neurofibrillary tangles.
The formation of amyloid plaques and neurofibrillary tangles contribute to the degradation of neurons in the brain and the subsequent symptoms of AD. (Resource: American Health Assistance Foundation (http://www.ahaf.org/))

A second hallmark of AD brains is the presence of intraneuronal lesions called neurofibrillary tangles (Figure 1.3). Neurofibrillary tangles are filamentous inclusions composed of hyperphosphorylated forms of the microtubule associated protein tau (Grundke-Iqbal *et al.*, 1986), which assembles into arrays of paired helical filaments (PHF). Normally, the tau protein is a soluble protein that is involved in the assembly and stabilisation of microtubules (Xie *et al.*, 1998). On the other hand, the pathological tau protein shows altered solubility properties, is abnormally phosphorylated, has less affinity for microtubules and forms filamentous structures (Goedert *et al.*, 1992; Grundke-Iqbal *et al.*, 1986). Due to the alterations of the cellular tau protein, PHFs are formed that appear as intraneuronal tangles at autopsy (Johnson and Hartigan, 1999). In other neurodegenerative disorders, such as frontal temporal dementia or Pick's disease, neurofibrillary tangles are also observed (Koo *et al.*, 1999; Lee *et al.*, 2001; Morris *et al.*, 2001). As tangles are a defined characteristic of a large number of neurodegenerative diseases, they are thought to be a secondary consequence of a primary neuronal injury and thus, an indication of disease progression (David *et al.*, 2002).

Additional pathogenic alterations found in the brains of AD patients are microgliosis, astrocytosis, selective neuronal degeneration, neuronal loss and multiple neurotransmitter deficits (Ding *et al.*, 1992; Norris *et al.*, 2005).

1.2 Molecular biology of Alzheimer`s disease

1.2.1 Amyloid precursor protein processing

In 1987, APP was cloned by using the information obtained through isolation and sequencing of Aβ (Kang *et al.*, 1987). The APP gene is located on chromosome 21 and encodes a type I transmembrane glycoprotein of 770 amino acids (Esch *et al.*, 1990; Kang *et al.*, 1987). The gene is alternatively spliced to encode for the APP protein variants of 695 and 751 amino acids. The APP splice variants of 770 and 751 amino acids are ubiquitously expressed (Selkoe, 2004). The 695 amino acid isoform is expressed at higher levels in neurons in comparison to the two longer splice variants (Rohan de Silva *et al.*, 1997).

Three different enzymes termed α-, β-, and γ-secretase process APP (Haass and Steiner, 2002; Kaether and Haass, 2004; Walter *et al.*, 2001). Cleavage of APP within the ectodomain by either α- or β-secretase generates the soluble APPα or APPβ and the membrane-bound APP C-terminal fragments, APP-CTFα (83 amino acids) or CTFβ (99 amino acids), respectively. The membrane bound cleavage products of α- and β-secretase (APP-CTFα and -CTFβ) are direct substrates for γ-secretase. γ-secretase generates the APP intracellular domain (AICD) (Sastre *et al.*, 2001) and p3 (Haass *et al.*, 1992a) by intramembrane cleavage of APP-CTFα. The cleavage of APP-CTFβ by γ-secretase yields AICD and Aβ that accumulates as amyloid deposits in senile plaques of aged individuals and patients with AD (Haass and Selkoe, 1993). In Figure 1.4, a schematic representation of APP processing is shown.

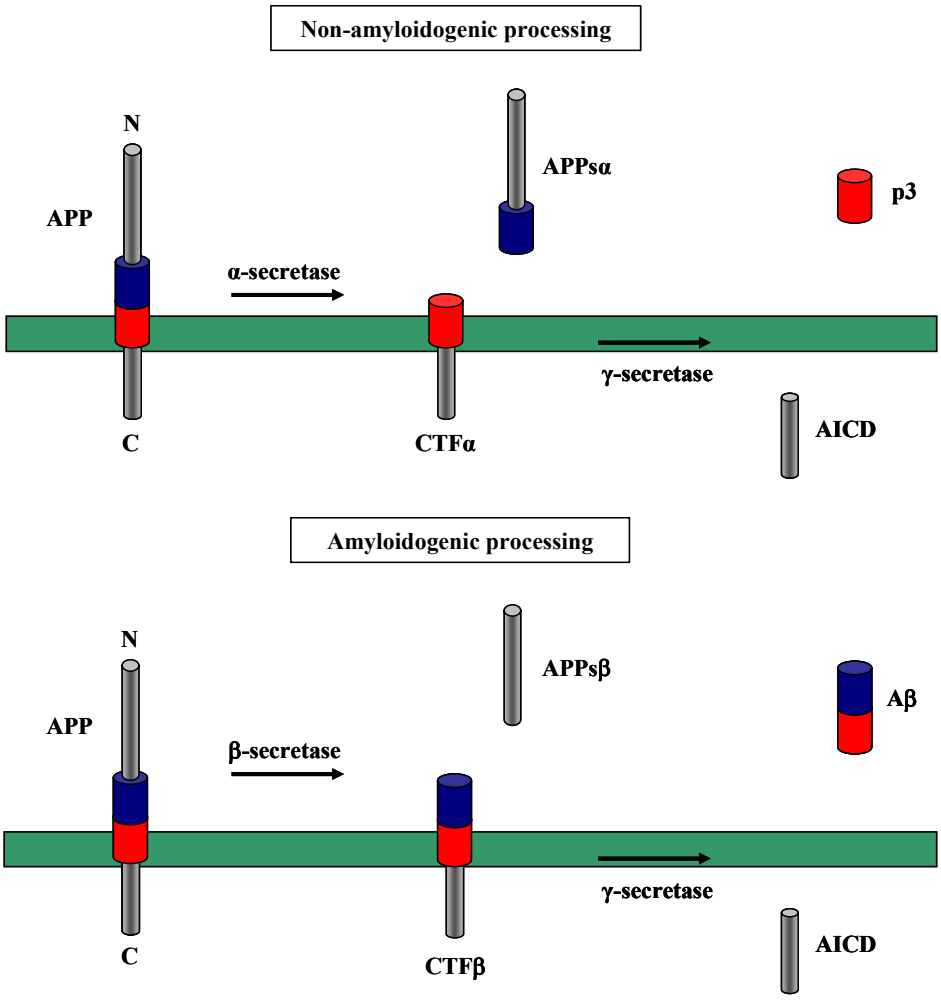

Figure 1.4 Schematic representation of APP processing (according to Walter *et al.* 2001). In the non-amyloidogenic pathway, α-secretase cleaves APP in the middle of the Aβ domain to generate extracellular APPsα, thereby preventing the formation of Aβ generation. The resulting APP-CTFα is subsequently cleaved by γ-secretase to yield p3 and AICD. In the amyloidogenic pathway, APP is first cleaved by β-secretase to generate APPsβ. The membrane-bound APP-CTFβ is then cleaved by γ-secretase. The released Aβ forms extracellular aggregates, which lead to amyloid plaque formation.

As the α-secretase cleaves APP between residues 16 and 17 of the Aβ domain and thus precludes Aβ generation, this process is referred to as the non-amyloidogenic pathway. On the other hand, β-secretase cleaves APP at the beginning of the Aβ domain resulting in Aβ peptide generation. Therefore, this process is referred to as the amyloidogenic pathway.

1.3 Genetics of Alzheimer's disease

The majority of AD cases are sporadic, while 5-10% of the cases are genetically inherited as familial AD (FAD) (Selkoe, 2001a). The onset of age of the disease is earlier in FAD than in sporadic AD. Three FAD causing genes, APP and presenilin (PS) 1 and PS2, have been revealed by genetic analysis of pedigrees with FAD (Goate *et al.*, 1991;

Levy-Lahad *et al.*, 1995b; Levy-Lahad *et al.*, 1995c; Rogaev *et al.*, 1995; Sherrington *et al.*, 1995; St George-Hyslop *et al.*, 1992). Mutations in the PS1 gene cause most of the FAD cases, whereas APP and PS2 mutations are rather rare. To date, 185 missense mutations are found in PS1 and 13 in PS2 (Alzheimer Disease and Frontotemporal Dementia Mutation Database: http://www.molgen.ua.ac.be/ADMutations) (Cruts *et al.*, 1998). For all tested missense mutations, the ratio of Aβ42 to Aβ40 is increased. For APP, so far, 33 missense mutations are found (Alzheimer Disease and Frontotemporal Dementia Mutation Database: http://www.molgen.ua.ac.be/ADMutations) (Cruts *et al.*, 1998). Interestingly, all the FAD missense mutations found in APP are located near to the three secretase-cleavage sites suggesting that they cause AD by an alteration of the APP cleavage. Predominantly the mutations localize close to the γ-secretase cleavage site and cause an increase in the production of Aβ42 peptides (Haass *et al.*, 1994; Suzuki *et al.*, 1994). There is also a rare mutation in a Swedish family that localizes to the β-secretase cleavage site. This mutation causes an increase in the production of all Aβ peptides (Cai *et al.*, 1993; Citron *et al.*, 1992). Recently, the APP mutation A673T was identified that protects against AD (Jonsson *et al.*, 2012). This mutation is close by the β-secretase cleavage site and reduces the formation of Aβ (Jonsson *et al.*, 2012). Mutations in the vicinity of the α-secretase cleavage site do not influence the processing of APP but rather alter the aggregation properties of Aβ (Selkoe, 2001a). Furthermore, individuals with Down`s syndrome, harbouring an extra copy of chromosome 21 containing the APP gene, invariably develop dementia and AD-like pathology (Head and Lott, 2004).

In contrary to the FAD cases, the reasons for the development of sporadic AD, which forms the majority of all AD cases, are unclear. However, a major genetic risk factor for late-onset AD, the ε4 allele of apolipoprotein E, has been identified (Levy-Lahad *et al.*, 1995a). Genetic analysis revealed that the likelihood of developing AD will increase with the inheritance of one or two ε4 alleles in comparison to subjects harbouring ε2 and/or ε3 alleles (Corder *et al.*, 1993). Recently, other risk loci within CLU, PICALM, CR1 and SORL1 were identified (Harold *et al.*, 2009; Lambert *et al.*, 2009; Lee *et al.*, 2007). On the other hand, the greatest risk factor of AD is ageing. However, the mechanism how ageing contributes to Aβ deposition in the brain is not well established. The cause of sporadic AD might be a deficiency in Aβ degradation (Yasojima *et al.*, 2001a; Yasojima *et al.*, 2001b) or an increase in β-secretase cleavage of APP (Holsinger *et al.*, 2002; Yang *et al.*, 2003). These observations suggest that the balance between generation and clearance of Aβ is altered by ageing. Moreover, the difference in the levels of alteration of Aβ

generation and clearance may account for the difference in the onset age of the disease. The imbalance between Aβ generation and clearance may result from an alteration of gene expression or from unknown factors involved in these processes. Such alteration could also cause an acceleration of the Aβ aggregation rate in the brain.

In Figure 1.5, the sequence of pathogenic events leading to AD is represented by the amyloid cascade hypothesis (Hardy and Selkoe, 2002).

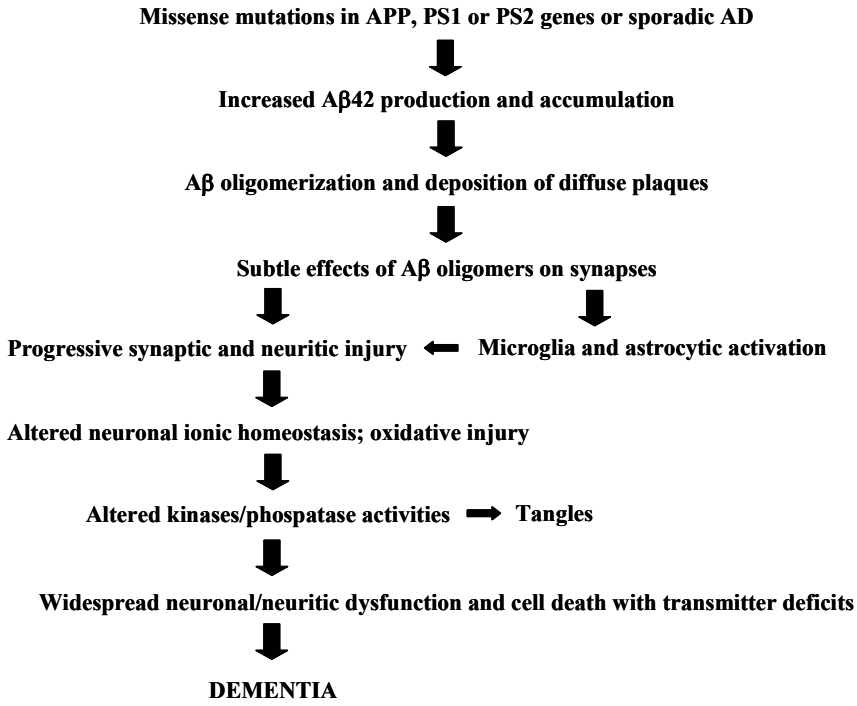

Figure 1.5 Amyloid cascade hypothesis (adopted from Hardy and Selkoe, 2002).
The sequence of pathogenic events leading to AD proposed by the amyloid cascade hypothesis. Aβ may directly injure the synapses and neurites of brain neurons, in addition to activating microglia and astrocytes (Haass and Selkoe, 2007; Hardy and Selkoe, 2002).

1.4 β-secretase

The β-secretase BACE1 (beta-site APP cleaving enzyme), also known as Asp2 or memapsin2, was discovered in 1999 independently by a number of different groups (Hussain *et al.*, 1999; Lin *et al.*, 2000; Sinha *et al.*, 1999; Vassar *et al.*, 1999; Yan *et al.*, 1999). BACE1 is a 501-amino-acid type I transmembrane protease belonging to the pepsin and retroviral aspartic protease family. It has a large ectodomain containing the dual active site motif (D-T/S-G-T/S), a transmembrane domain and a short cytoplasmic tail (Figure 1.6) (Vassar *et al.*, 2009; Walter *et al.*, 2001; Willem *et al.*, 2009).

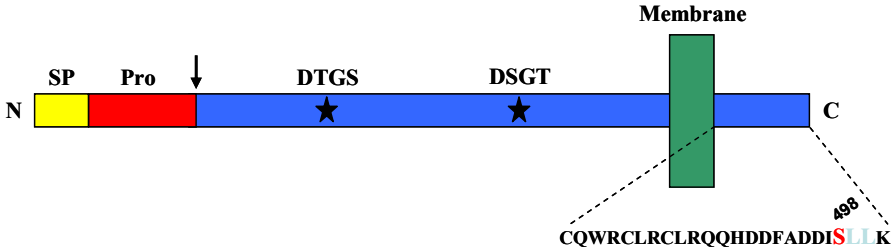

Figure 1.6 Schematic view of BACE1 (Walter *et al.*, 2001).
The signal peptide (SP) is shown in yellow, the prodomain (pro) in red, the aspartyl protease site motifs (DTGS and DSGT) in the luminal/ extracellular domain by stars and the furin cleavage site by an arrow. In the amino acid sequence of the cytoplasmic tail, given in single-letter code, the phosphorylation site is shown in red and the dileucine motive in light blue.

BACE1 is synthesized in the endoplasmic reticulum (ER) as an immature proenzyme with a molecular weight of 50 kDa. Mature BACE1 has a molecular weight of 70 kDa. Maturation involves disulphide bridge formation, N-glycosylation, carbohydrate sulphation, propeptide removal and palmitoylation (Benjannet *et al.*, 2001; Bennett *et al.*, 2000b; Capell *et al.*, 2000; Creemers *et al.*, 2001; Haniu *et al.*, 2000; Huse *et al.*, 2000).

Even though it is not well understood whether BACE1 in principal exists as a monomeric enzyme or a dimer, there is evidence that a high molecular complex variant of BACE1 has a higher β-secretase activity than the monomer (Schmechel *et al.*, 2004; Westmeyer *et al.*, 2004). BACE1 has an acidic pH optimum, and the enzyme is located in the Golgi apparatus, the endosomes, and at the cell membrane (Esler and Wolfe, 2001; Haass *et al.*, 1992b; Koo and Squazzo, 1994; Vassar *et al.*, 1999). It was shown that BACE1 is internalized from the plasma membrane to endosomes. This internalization process is mainly driven by the dileucine motive in the C-terminus (Figure 1.6) (Huse *et al.*, 2000; Pastorino *et al.*, 2002). From the endosomes, BACE1 is recycled to the Golgi apparatus. For this process the phosphorylation of a single serine residue (S498) in the C-terminus is required (Figure 1.6) (Walter *et al.*, 2000). In human cortical neurons, BACE1 co-localizes with its cleavage product APPsβ and the putative α-secretase ADAM10 (Marcinkiewicz and Seidah, 2000; Sennvik *et al.*, 2004).

There is a close homologue to BACE1, BACE2, which does not contribute to the amyloidogenic processing of APP. BACE2 seems to have α-secretase-like properties (Farzan *et al.*, 2000; Fluhrer *et al.*, 2002; Hussain *et al.*, 2000; Yan *et al.*, 2001) and is preferentially expressed in non-neuronal cells (Bennett *et al.*, 2000a).

Strong support for the pivotal (and exclusive) role of BACE1 as β-secretase comes from BACE1 knockout mice which show a complete absence of Aβ generation in their

brains, suggesting that BACE1 is the only protease mediating β-secretase activity (Cai *et al.*, 2001; Luo *et al.*, 2001; Roberds *et al.*, 2001). Initial reports indicated that BACE1 knockout mice develop normally, are healthy, fertile and appear to have no obvious morphological phenotype (Cai *et al.*, 2001; Luo *et al.*, 2003; Luo *et al.*, 2001; Roberds *et al.*, 2001). However, recent studies have shown that they are not completely normal. Behavioural assays revealed memory impairment and changes in spontaneous activity (Dominguez *et al.*, 2005; Harrison *et al.*, 2003; Laird *et al.*, 2005; Ohno *et al.*, 2004). Moreover, close analysis of BACE1 knockout mice revealed an important morphological phenotype. They show severe hypomyelination of the peripheral nervous system (PNS) similar to neuregulin-1 (NRG-1) heterozygous mice (Hu *et al.*, 2006; Willem *et al.*, 2006). It could be shown that NRG-1 is a physiological substrate of BACE1. BACE1 participates in the proteolytic processing of NRG-1 (Hu *et al.*, 2006; Willem *et al.*, 2006), a ligand for members of the ErbB family of receptor-tyrosine kinases. Since in BACE1 knockout mice NRG-1 cannot be cleaved by BACE1, full-length NRG-1 accumulates and failure of NRG-1 signalling causes reduced myelin sheath thickness of axons of both peripheral sciatic nerves (Hu *et al.*, 2006; Willem *et al.*, 2006) and central optic nerves (Hu *et al.*, 2006). Moreover, this abrogated cleavage of NRG-1 also impairs remyelination of injured sciatic nerves (Hu *et al.*, 2008).

Besides APP and NRG-1, BACE1 was found to process the Golgi-localized membrane-bound α2,6-sialyltransferase (Kitazume *et al.*, 2001), the P-selectin glycoprotein ligand-1 (PSLG-1) (Lichtenthaler *et al.*, 2003), the APP like proteins APLP1 and APLP2 (Eggert *et al.*, 2004; Li and Sudhof, 2004; Pastorino *et al.*, 2004), the low-density lipoprotein receptor-related protein (LRP) (von Arnim *et al.*, 2005), the voltage-gated sodium channel (Na_v1) β2 subunit ($Na_v\beta_2$) (Kim *et al.*, 2005; Wong *et al.*, 2005), and neuregulin-3 (NRG-3) (Hu *et al.*, 2008). Recently, Kuhn *et al.* identified 34 mostly novel substrates in primary neurons by secretome protein enrichment with click sugars (SPECS) (Kuhn *et al.*, 2012). Seizure protein 6, NCAM-L1, CHL1 and contactin-2, four of the identified substrates, were validated in BACE1 inhibitor-treated and BACE1 knockout mice (Kuhn *et al.*, 2012). In an independent study, Zhou *et al.* identified several putative BACE1 substrates in primary neuronal cultures by a quantitative proteomic approach (Zhou *et al.*, 2012). The adhesion molecules NCAM-L1 and CHL1 were confirmed in cell culture, in BACE1 inhibitor-treated and BACE1 knockout mice (Zhou *et al.*, 2012).

BACE1 is located on chromosome 11. So far no AD-causing mutation has been identified, but polymorphisms in the BACE1 gene seem to influence the risk for AD

(Kirschling *et al.*, 2003). It has been shown that β-secretase mRNA is ubiquitously expressed with its highest levels in the brain and pancreas (Vassar *et al.*, 1999; Yan *et al.*, 1999). However, the BACE1 activity in the pancreas is low due to BACE1 variants with reduced proteolytic activity which are generated from alternative spliced transcripts (Mowrer and Wolfe, 2008). Interestingly, several studies showed that levels of BACE1 protein and activity are elevated approximately 2-fold in AD brain without a parallel increase in mRNA expression (Fukumoto *et al.*, 2002; Holsinger *et al.*, 2002; Li and Sudhof, 2004; Preece *et al.*, 2003; Yang *et al.*, 2003).

1.5 γ-secretase

γ-secretase is an unusual aspartyl protease occurring as high molecular weight complex that catalyses intramembrane proteolysis of a variety of substrates apart from APP (Haass, 2004; Steiner, 2004). The Notch (1-4) receptors, which are essential for cell differentiation, are very important and well-studied substrates of γ-secretase (Berezovska *et al.*, 1999; Davis *et al.*, 1998; De Strooper *et al.*, 1999; Donoviel *et al.*, 1999; Herreman *et al.*, 1999; Herreman *et al.*, 2000; Levitan and Greenwald, 1998; Nakajima *et al.*, 2000; Qian *et al.*, 1998; Struhl and Greenwald, 2001; Wong *et al.*, 1997). Notch functions as a receptor at the cell surface and mediates cell-cell signalling interactions to specify cell fates during development (Bray, 2006). Apart from APP and Notch, there is a growing number of type I transmembrane proteins that have been identified as substrates of γ-secretase such as APLP1 and APLP2 (Scheinfeld *et al.*, 2002), CD44 (Cluster of differentiation 44) (Lammich *et al.*, 2002; Murakami *et al.*, 2003), N- and E-cadherin (Baki *et al.*, 2001; Georgakopoulos *et al.*, 1999; Marambaud *et al.*, 2002), Delta and Jagged (Ikeuchi and Sisodia, 2003; LaVoie and Selkoe, 2003) and ErbB4 (Ni *et al.*, 2001). Altogether, around 90 substrates have been described for γ-secretase until today (Lleo and Saura, 2011).

γ-secretase is composed of the four core components presenilin (PS1 or PS2), nicastrin (Nct), anterior pharynx-defective phenotype 1 (Aph1) and presenilin enhancer 2 (Pen2) (Haass, 2004). Edbauer and colleagues showed that when all four components were expressed together in yeast, which has no homologues of γ-secretase components and thus lacks γ-secretase activity, active γ-secretase was reconstituted (Edbauer *et al.*, 2003). This suggests that these four components are necessary and sufficient for the activity of the enzyme.

1.5.1 Presenilin

The genes encoding PS1 and PS2 are located on chromosome 14 and 1, respectively (Levy-Lahad *et al.*, 1995b; Levy-Lahad *et al.*, 1995c; Sherrington *et al.*, 1995). They are related multipass transmembrane proteins that share about 63% of sequence identity. PS1 and PS2 possess nine membrane-spanning segments (Henricson *et al.*, 2005; Kaether *et al.*, 2004; Laudon *et al.*, 2005; Oh and Turner, 2005a; Oh and Turner, 2005b) and a large cytoplasmic loop located between transmembrane domain 6 and 7 (Laudon *et al.*, 2005; Li and Greenwald, 1998; Periz and Fortini, 2004).

PS1 or PS2 are the catalytic subunit of the γ-secretase complex and provide the two critical aspartyl residues (Kimberly *et al.*, 2000; Wolfe *et al.*, 1999). PS1 and PS2 are synthesized as a holoprotein of 50 kDa. To generate the functional γ-secretase, PS1 or PS2 undergo endoproteolysis within the large cytoplasmic loop to generate a 30 kDa N- and a 20 kDa C-terminal fragment (NTF and CTF) in the cell (Fukumori *et al.*, 2010; Thinakaran *et al.*, 1996). The NTF and CTF of PS1 or PS2 form a heterodimer (Capell *et al.*, 1998; Saura *et al.*, 1999; Yu *et al.*, 1998) which are more stable than the holoprotein (Ratovitski *et al.*, 1997; Steiner *et al.*, 1998).

The following lines of evidence demonstrate that PS is the catalytic subunit of the γ-secretase complex: (1) The two crucial aspartate residues (Asp) are required for γ-secretase activity. Substitution of either of the two aspartate residues buried within the 6^{th} and 7^{th} transmembrane domains of PS abolished γ-secretase activity (Wolfe *et al.*, 1999; Yu *et al.*, 2000a). (2) γ-secretase activity was severely diminished in cells derived from PS1 knockout mice (De Strooper *et al.*, 1998) and completely abolished in PS1 and PS2 deficient embryonic stem cells (Herreman *et al.*, 2000; Zhang *et al.*, 2000). (3) γ-secretase inhibitors can be directly crosslinked to PS (Esler *et al.*, 2000; Li *et al.*, 2000).

1.5.2 Nicastrin

Nct, as well as Aph1 and Pen2 proteins, associate with presenilin heterodimers and are required for protease activity. Nct is a type I integral membrane glycoprotein comprising 709 amino acid residues in humans with a predicted size of 80 kDa for the native protein. It undergoes complex glycosylation and sialylation within the secretory pathway to yield the mature form of around 120 kDa, which exists in the active γ-secretase complex (Edbauer *et al.*, 2002; Leem *et al.*, 2002; Tomita *et al.*, 2002; Yang *et al.*, 2002; Yu *et al.*, 2000b). Shah and colleagues showed that Nct functions as a γ-secretase substrate receptor

(Shah *et al.*, 2005). It was shown that the ectodomain of Nct can bind to ectodomain-shedded APP and Notch before γ-secretase cleavage occurs.

1.5.3 Aph1

By genetic screening for mutants that enhance the Notch signalling defect phenotype in C.elegans, Aph1 was identified (Francis *et al.*, 2002; Goutte *et al.*, 2002). Aph1 is a multitransmembrane protein that spans the membrane seven times (Fortna *et al.*, 2004). It was shown that Aph1 interacts with PS NTF/CTF heterodimers and Nct in mammalian cells and *in vivo* (Lee *et al.*, 2002). In humans, two homologs of Aph1 genes, Aph1a and Aph1b, were identified. Furthermore, for Aph1a two splice variants are reported, Aph1aL and Aph1aS. It was shown that the two splice variants of Aph1a as well as Aph1b are not found in the same γ-secretase complex (Shirotani *et al.*, 2004). PS1 and PS2 are also in separate complexes, resulting in the formation of 6 different proteolytically active γ-secretase complexes with every possible combination of PS and Aph1 variants in human cells (Hebert *et al.*, 2004; Shirotani *et al.*, 2004). In mice, there are eight complex possibilities, as mice contain a third Aph1 homolog, Aph1c (Hebert *et al.*, 2004). So far, it is not well understood whether there exist any differences on the γ- secretase activity or any substrate preference of an individual γ-secretase complex. It has been demonstrated that the absence of Aph1 causes a decrease in the levels of the other γ-secretase complex components (Ma *et al.*, 2005; Serneels *et al.*, 2005; Shirotani *et al.*, 2004; Takasugi *et al.*, 2003), suggesting that Aph1 stabilises the γ-secretase complex. However, the Aph1 function for cleavage within an assembled complex is still unclear and further studies are required to elucidate the function of Aph1.

1.5.4 Pen2

As Aph1, Pen2 was identified by genetic screening for mutants that enhance the Notch signalling defect phenotype in C.elegans (Francis *et al.*, 2002; Goutte *et al.*, 2002). Pen2 is the smallest subunit of the γ-secretase complex with 101 amino acids (Francis *et al.*, 2002; Steiner *et al.*, 2002). It encodes a membrane protein of about 10 kDa that spans the membrane twice. Pen2 adopts a hairpin orientation in the membrane with its N- and C-terminal domains facing the luminal/extracellular space (Crystal *et al.*, 2003). It was shown that Pen2 is involved in the initiation of PS endoproteolysis (Takasugi *et al.*, 2003) and that it is necessary to stabilise the NTF and CTF of PS within the γ-secretase complex

(Hasegawa *et al.*, 2004; Prokop *et al.*, 2005; Prokop *et al.*, 2004). Whether and how Pen2 contributes to the catalytic function of γ-secretase is still unclear.

1.5.5 Assembly of the γ-secretase complex

How the γ-secretase complex is assembled and transported is not understood in full detail. It was shown that the four components of the γ-secretase undergo stepwise assembly in the ER and co-operatively exit the ER (Capell *et al.*, 2005; Kim *et al.*, 2004). Complex formation in the ER begins with binding of Aph1 to the transmembrane domain (TMD) of immature Nct. This immature Nct-Aph1 heterodimer then binds to PS holoprotein in the ER to form a ternary complex. In the final step of γ-secretase assembly in the ER, Pen2 binds to PS resulting in endoproteolytic cleavage of PS and structural changes in the Nct ectodomain (Dries and Yu, 2008). γ-secretase is then transported through the Golgi, where Nct is complex glycosylated and transported to the plasma membrane and the endosomal/lysosomal system. The fully assembled complex is known to exert its biological function in the late secretory pathway (De Strooper, 2003).

The non-assembled complex components appear to be unstable and/or to be retained within the ER. The following lines of evidence suggest this: (1) Decreased Nct expression by RNAi is accompanied by reduced PS1, Aph1a-L and Pen2 expression (Steiner *et al.*, 2002). (2) Decreased Pen2 expression by RNAi leads to loss of PS1 NTF and CTF and accumulation of immature Nct (Crystal *et al.*, 2003; Prokop *et al.*, 2004; Takasugi *et al.*, 2003). (3) Presenilin knockout cells have only immature Nct and Pen2 is lost (Steiner *et al.*, 2002). In addition it was shown that in the absence of PS Nct is retained in the ER (Edbauer *et al.*, 2002; Periz and Fortini, 2004). Retention of PS1 was shown to be due to a retention signal in the C-terminus (Kaether *et al.*, 2004). Also non-assembled Pen2 was shown to accumulate in the ER where it is degraded by proteosomal degradation (Bergman *et al.*, 2004; Crystal *et al.*, 2004).

Kaether and colleagues proposed a model for γ-secretase complex assembly and trafficking (Kaether *et al.*, 2004). According to this model the assembly of γ-secretase is governed by similar mechanisms that govern the assembly of complexes like ion channels and cell surface receptors. Here control mechanisms ensure that only fully assembled complexes leave the ER and travel to the cell surface. Quality control in the ER is crucial to prevent export of non-functioning or, worse, malfunctioning proteins. Retention of monomeric subunits is achieved by exposing ER-retention signals that can be cytosolic (Zerangue *et al.*, 1999) or within transmembrane domains (TMDs) (Bonifacino *et al.*, 1990; Bonifacino

et al., 1991; Hennecke and Cosson, 1993; Sato *et al.*, 2004). Upon complex assembly these retention signals are masked and ER-export is permitted.

1.6 α-secretase

ADAMs are membrane proteins containing a disintegrin and metalloprotease domain, which are widely distributed and play important roles in many cellular events (Wolfsberg *et al.*, 1995). The domain structure of the ADAMs consists of a pro-domain, a metalloprotease domain, a disintegrin and cysteine-rich domain, an EGF-like domain, a transmembrane domain and a cytoplasmic tail (Figure 1.7).

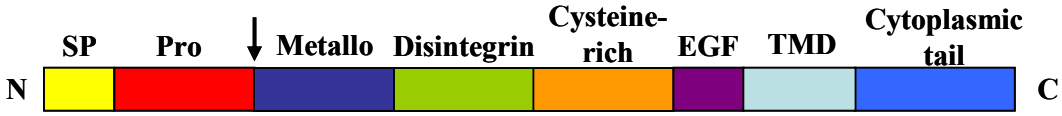

Figure 1.7 Representation of domain structure of a typical ADAM (Allinson *et al.*, 2003). The signal peptide (SP) is shown in yellow, the prodomain (pro) in red, the furin cleavage site by an arrow, the metalloprotease domain in dark blue, the disintegrin domain in green, the cysteine-rich domain in orange, the EGF-like domain in purple, the hydrophobic transmembrane domain in light blue and the cytoplasmic tail in blue.

At least 17 individual members of the ADAM family are expressed in the brain (Karkkainen *et al.*, 2000). They cleave a variety of different substrates including adhesion molecules, cytokines, growth factors and growth factor receptors (Pruessmeyer and Ludwig, 2009). By the work of several groups, ADAMs 9, 10 and 17 have been shown to be putative α-secretases for the cleavage of APP (Buxbaum *et al.*, 1998; Koike *et al.*, 1999; Lammich *et al.*, 1999).

1.6.1 ADAM9

ADAM9, also known as meltrin γ or MDC9, is a ubiquitously expressed 84 kDa glycoprotein. It was shown that ADAM9 mRNA is highly expressed in developing mesenchyme, heart and brain (Weskamp *et al.*, 2002). In adult tissue, it is ubiquitously expressed including the heart, brain, placenta, lung, skeletal muscle, digestive system and reproductive system (Weskamp *et al.*, 1996). ADAM9 is involved in various cellular processes. The heparin-binding EGF-like growth factor (HB-EGF), for example, is processed by ADAM9 upon TPA stimulation (Izumi *et al.*, 1998). In addition, it was shown that in COS cells co-expression of APP and ADAM9 leads to APP processing by ADAM9 (Hotoda *et al.*, 2002; Koike *et al.*, 1999). ADAM9 knockout mice developed normally, were viable and fertile, and did not show any abnormality. Isolated fibroblasts

or hippocampal neurons derived from these mice still show shedding of HB-EGF and APP, suggesting a redundant role of ADAM9 (Weskamp *et al.*, 2002).

1.6.2 ADAM17

ADAM17, also known as TACE (Tumor necrosis factor-α converting enzyme), was identified as being responsible for the shedding of the cytokine proTNF-α (Black *et al.*, 1997; Moss *et al.*, 1997). ADAM17 is widely expressed with high levels of expression in the heart, placenta, testis, ovary, lung and spleen (Black *et al.*, 1997; Sahin *et al.*, 2004). In the brain the expression of ADAM17 is more or less limited to the endothelia and glia (Goddard *et al.*, 2001). The expression pattern in the brain is more consistent with a role for ADAM10 and ADAM9 than ADAM17 as the APP α-secretase, although expression analysis is not a completely reliable indicator of where an enzyme might function (even low levels of an ADAM may be completely sufficient for its physiological activity) (Karkkainen *et al.*, 2000). Mice lacking ADAM17 are perinatal lethal with multiple defects in various organs which closely resemble those seen in mice lacking EGFR, TGF or HB-EGF (Mann *et al.*, 1993; Miettinen *et al.*, 1995; Peschon *et al.*, 1998). Concerning Notch, mice lacking ADAM17 do not show any apparent phenotype related to Notch or Notch ligand loss (Peschon *et al.*, 1998). It was shown that the absence of ADAM17 abolished regulated (PMA-stimulated), but not constitutive α-secretase activity in mouse embryonic fibroblasts (Buxbaum *et al.*, 1998). Apart from APP and TNFα, a substantial number of other substrates for ADAM17 have been identified, including EGFR ligands (Sahin *et al.*, 2004; Sunnarborg *et al.*, 2002), p75 TNFR (Peschon *et al.*, 1998), IL6R (Matthews *et al.*, 2003), prion protein (Vincent *et al.*, 2001), VCAM-1 (Garton *et al.*, 2001) and ErbB4 (Rio *et al.*, 2000).

1.6.3 ADAM10

ADAM10 was originally purified as a myelin-associated metalloprotease from brain myelin membranes. A preliminary characterization showed that it efficiently degrades myelin basic protein (MBP) in brain extracts (Chantry *et al.*, 1989). Peptide sequences obtained from the purified protein later allowed cloning of ADAM10 cDNA from a bovine cDNA library (Howard *et al.*, 1996). Subsequently, it became clear that ADAM10 is the mammalian homologue of Drosophila Kuzbanian (Kuz), which in turn has an essential role in Notch signalling (Pan and Rubin, 1997).

ADAM10 was found to be expressed ubiquitously in embryos, including the dermatome, myotome of the somites, epidermis, gut endoderm, epithelial tissues of the kidney, liver, heart and neural crest cells of chicks (Hall and Erickson, 2003). ADAM10 is also highly expressed in a variety of adult tissues as shown by Western blotting (Sahin *et al.*, 2004). In adult brains, ADAM10 was found to be widely expressed throughout the brain, including neurons. This is consistent with a putative role of this gene as an α-secretase for APP (Bernstein *et al.*, 2003; Karkkainen *et al.*, 2000). Interestingly, it was reported that ADAM10 protein levels are decreased in platelets of AD patients (Colciaghi *et al.*, 2002). Additionally, a decrease in APPsα release was found by these platelets as well as in the cerebrospinal fluid of sporadic AD patients and AD patients carrying the Swedish mutation (Colciaghi *et al.*, 2002; Fellgiebel *et al.*, 2009; Sennvik *et al.*, 2000). Overexpression of ADAM10 in HEK cells leads to an increased α-secretase activity, and endogenous α-secretase activity in these cells is inhibited by introducing a dominant negative form of ADAM10 (Lammich *et al.*, 1999). ADAM10 knockout mice are lethal around embryonic day 9.5 (Hartmann *et al.*, 2002) with multiple malformations strikingly similar to that of a complex Notch deficiency as seen in PS1/PS2 or notch1/notch4 double mutant mice (Herreman *et al.*, 1999; Krebs *et al.*, 2000). Due to the early embryonic lethality of ADAM10 knockout mice at a stage preceding neuronal development, APP processing can only be analysed in immortalized cell lines derived from ADAM10 knockout embryos. The results might therefore not directly reflect the actual contribution of ADAM10 in APP cleavage in the brain. Nevertheless, the data clearly showed that α-secretase activity was preserved in some ADAM10 knockout cell lines (Hartmann *et al.*, 2002). It remains to be determined whether there is compensation by, or redundancy between, different ADAMs or other enzymes in the processing of APP (Asai *et al.*, 2003) or whether different ADAMs have major roles in APP processing in distinct cells and tissues.

A study by Postina and colleagues showed that overexpression of ADAM10 in neurons alleviates amyloid plaque formation and hippocampal defects in an AD mouse model (Postina *et al.*, 2004). Overexpression of inactive ADAM10 however could increase the Aβ plaque load in an AD mouse model (Postina *et al.*, 2004). This study suggests that an increase of ADAM10 activity may be therapeutically desirable. To learn more about the function of ADAM10 during development and in adults as well as in APP processing in the brain, it will be critical to generate mice carrying a conditional mutation in this gene. Therefore, Jorissen and colleagues recently generated conditional ADAM10

knockout mice, limiting ADAM10 inactivation to neural progenitor cells (NPC) and NPC-derived neurons and glial cells (Jorissen *et al.*, 2010). In these mice, Notch1 processing is affected, leading to downregulation of several Notch-regulated genes in the brain of these mice. In addition, the α-secretase-mediated processing of APP was largely reduced in the neurons of these mice, demonstrating that ADAM10 represents the most important α-secretase in brain. These results were confirmed in primary neurons by another recently published study (Kuhn *et al.*, 2010). Using RNAi-mediated knockdown of ADAM10 in different cell lines and primary murine neurons, α-secretase cleavage of APP was completely suppressed. RNAi-mediated knockdown of ADAM9 and ADAM17, however, has no effect on α-secretase cleavage (Kuhn *et al.*, 2010).

Apart from processing APP and the Notch receptor, ADAM10 has also been implicated in regulating neuronal repulsion through cleaving ephrinA2 (Hattori *et al.*, 2000), and in the processing of various other cell surface molecules, including CD44 (Murai *et al.*, 2004), type IV collagen (Millichip *et al.*, 1998), L1 adhesion molecule (Mechtersheimer *et al.*, 2001), interleukin-6 receptor (Matthews *et al.*, 2003), CXC chemokine fractalkine (Hundhausen *et al.*, 2003), neurotensin receptor-3 (Navarro *et al.*, 2002), prion protein (Vincent *et al.*, 2001), betacellulin, EGF (Sahin *et al.*, 2004) and BACE1 (Hussain *et al.*, 2003). For most of these putative candidate ADAM10 substrates, the physiological relevance of the processing during development remains to be determined *in vivo*.

1.7 Translational control

1.7.1 Translational control of APP

Interestingly, several studies have already shown that the APP mRNA is subjected to extensive regulation at the post-transcriptional level. Studies in mammalian cell lines and primary neuronal cultures have indicated that RNA-binding proteins interact with regulatory regions of APP mRNA and modulate the expression of APP (Ruberti *et al.*, 2010). The 5`UTR of APP contains several elements that control the translation of APP mRNA. These include an internal ribosome entry site (IRES) (Beaudoin *et al.*, 2008), an interleukin-1 (IL-1) translation enhancer element (Rogers *et al.*, 1999) and an iron-response element (IRE) (Cho *et al.*, 2010; Rogers *et al.*, 2002), similar to the originally identified IRE that regulates the translation of the L- and H-ferritin mRNAs in response to intracellular iron levels (Hentze *et al.*, 1987; Klausner *et al.*, 1993). Furthermore, the APP coding sequence contains a guanine-rich (G-rich), G-quartet-like sequence that interacts

with either hnRNP C or FMRP (Lee *et al.*, 2010; Westmark and Malter, 2007). The RNA-binding proteins hnRNP C and FMRP associate with the same APP mRNA coding region element and influence APP translation competitively and in opposite directions (Lee *et al.*, 2010). Silencing hnRNP C increased FMRP binding to APP mRNA and repressed APP translation, while silencing FMRP enhanced hnRNP C binding and promoted translation of APP (Lee *et al.*, 2010). The repression of APP translation is linked to the recruitment of the FMRP-APP mRNA complex to processing bodies (PBs) and hnRNP C blocks the recruitment of APP mRNA to PBs (Lee *et al.*, 2010). Interestingly, it appears that hnRNP C not only regulates the translation of APP mRNA, but also increases its stability by binding to a highly conserved 29 nucleotides (nt) element within the 3`UTR, approximately 200 nt downstream of the stop codon (Rajagopalan *et al.*, 1998; Zaidi *et al.*, 1994; Zaidi and Malter, 1994; Zaidi and Malter, 1995). The same 29 nt sequence is also target of the RNA-binding protein nucleolin (Ceman *et al.*, 1999; Zaidi *et al.*, 1994; Zaidi and Malter, 1994; Zaidi and Malter, 1995). While the 29 nt sequence appears to destabilize the APP mRNA, another sequence located in the first 52 bases downstream of the stop codon seems to have the opposite effect and increases stability (Broytman *et al.*, 2009). The 52 nt stabilizing element is recognized by six cytosolic proteins YB1, La/SS-B, EF1α, nucleolin, Rck/p54 and PAI/RBP1 (Broytman *et al.*, 2009). Whether these proteins are present in a single complex or bind APP mRNA independently is unknown. The identified proteins may interact with each other or within a complex through both RNA dependent or independent interactions.

The described examples show that there is extensive evidence that APP expression is potently regulated by post-transcriptional mechanisms as APP mRNA stabilization and APP translation, indicating that the regulation of APP mRNA metabolism is an important event in AD pathophysiology (Beaudoin *et al.*, 2008; Hebert *et al.*, 2009; Patel *et al.*, 2008; Rajagopalan *et al.*, 1998; Rogers *et al.*, 2002; Westmark and Malter, 2001a; Westmark and Malter, 2001b; Westmark and Malter, 2007).

1.7.2 Translational control of BACE1

So far, several independent studies have reported that expression of BACE1 is regulated by different translational control mechanisms such as microRNA (miRNA), noncoding antisense transcript and translational repression via the 5`UTR (depicted in Figure 1.8).

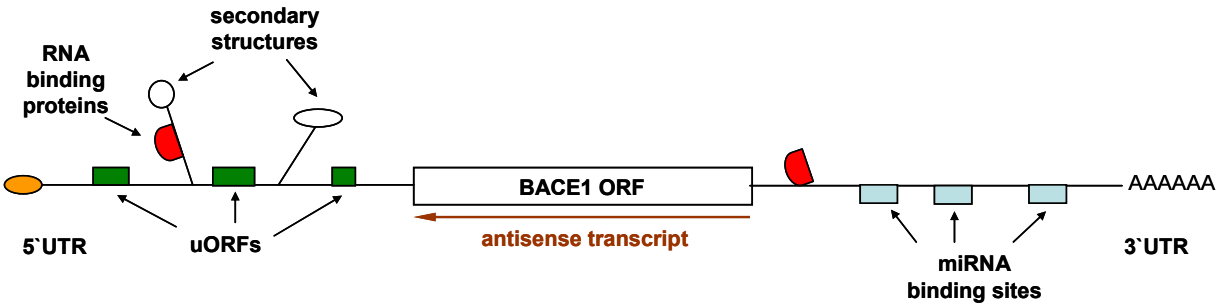

Figure 1.8 Translational control of BACE1 mRNA (adapted from Willem et al, 2009)

BACE1 expression is regulated by different post-transcriptional mechanisms which are depicted in this image. The 5`cap is shown in orange. uORFs (green), RNA binding proteins (red) and secondary structures are depicted in the 5`UTR. miRNA binding sites and RNA binding proteins in the 3`UTR are shown in light blue and red, respectively. The antisense transcript (brown) is shown below the BACE1 ORF.

miRNAs are small non-coding RNA molecules and function via base-pairing with complementary sequences within mRNAs, usually resulting in translational repression or target degradation (Bartel, 2009; Kusenda *et al.*, 2006). Hebert *et al.* showed that lowered levels of miR-9 and loss of miR-29a/b correlates with increased BACE1 expression (Hebert *et al.*, 2008). Consistent with these findings, it was shown that overexpression of miR29c downregulates BACE1 protein levels (Zong *et al.*, 2011). Another study by Wang *et al.* suggests that decreased miR-107 level tend to upregulate BACE1 expression (Wang *et al.*, 2008). Boissonneault and collegues demonstrated that miR-298 and miR-328 recognize specific elements in the BACE1 3`UTR and thereby downregulate BACE1 expression in cultured neuronal cells (Boissonneault *et al.*, 2009). Moreover, Zhu *et al.* showed that inhibition of miR-195 results in increased BACE1 protein level (Zhu *et al.*, 2012). Recently, it was suggested that miR-124 plays an essential role in the control of BACE1 expression (Fang *et al.*, 2012).

Besides the regulation via miRNAs, BACE1 mRNA and protein expression is regulated via a conserved noncoding antisense transcript for BACE1 (BACE1-AS) (Faghihi *et al.*, 2008). Faghihi *et al.* showed that BACE1-AS forms a RNA duplex with BACE1 which may alter secondary and tertiary structures thereby stabilizing BACE1 mRNA (Faghihi *et al.*, 2008). Through downregulation of BACE1-AS the formed RNA duplex between BACE1 and BACE1-AS is disrupted and thereby the stability of BACE1 mRNA is decreased and protein levels are downregulated (Faghihi *et al.*, 2008). Consistent with these findings, it was shown that the concentration of BACE1-AS transcripts is elevated in AD patients as well as APP transgenic mice (Faghihi *et al.*, 2008).

Finally, several studies independently showed that the 5`UTR of BACE1 represses the translation of BACE1 mRNA, but not the transcription (De Pietri Tonelli *et al.*, 2004; Lammich *et al.*, 2004; Mihailovich *et al.*, 2007; O'Connor *et al.*, 2008; Rogers *et al.*, 2004; Zhou and Song, 2006). Previously, we and other groups could show that the expression of BACE1 is controlled via its 5'UTR (De Pietri Tonelli *et al.*, 2004; Lammich *et al.*, 2004; Rogers *et al.*, 2004). BACE1 mRNA has a 446 nucleotides long GC-rich (70%) 5`UTR with three uORFs. It could be shown that the complex secondary structure and the second uORFs are involved in the translational repression of BACE1 expression (Lammich *et al.*, 2004; Mihailovich *et al.*, 2007; O'Connor *et al.*, 2008; Zhou and Song, 2006). In general, complex secondary structures, the presence of uORF and the binding of trans-activating factors to the 5'UTR are responsible for modulating the translational efficiency (Gebauer and Hentze, 2004). However, until now little is known about the factors that influence the BACE1 expression via its 5`UTR. So far, only O'Connor and colleagues determined that energy deprivation results in increased efficiency of BACE1 mRNA translation (O'Connor *et al.*, 2008). They showed that this increase in BACE1 expression was due to the phosphorylation of the translation initiation factor eIF2α (O'Connor *et al.*, 2008). Upon phosphorylation of eIF2α, the concentration of the ternary complex consisting of eIF2, GTP and Met-tRNA$_i^{Met}$, which is required for translation initiation, is reduced (Sonenberg and Hinnebusch, 2009). Thus, in the wake of eIF2α phosphorylation, the scanning 40S ribosomal subunit more likely bypasses secondary structures (Lu *et al.*, 2004; Vattem and Wek, 2004). Upon binding of the 60S ribosomal subunit, the production of the protein is then increased (Clemens, 2001; Holcik and Sonenberg, 2005). Under normal conditions, reinitiating ribosomes rebind the ternary complex and reinitiate at uORFs (Sonenberg and Hinnebusch, 2009). The observed increase in BACE1 translation is similar to the translation of GCN4 and ATF4 (Hinnebusch, 1997; Vattem and Wek, 2004).

1.7.3 Translational control of ADAM10

For ADAM10, it was reported that its expression could be repressed under hypoxia in the human neuroblastoma SH-SY5Y cells by post-transcriptional mechanisms (Marshall *et al.*, 2006; Webster *et al.*, 2004). Under hypoxic conditions ADAM10 protein levels were decreased by approximately 60%, resulting in a decrease of APPsα production. In contrast, no change in the expression of the ADAM10 mRNA could be detected (Marshall *et al.*, 2006). The protein levels of BACE1 were unchanged. In addition, ADAM10 expression is regulated by miRNAs. Bai *et al.* showed that the liver-specific miR-122

represses ADAM10 expression (Bai *et al.*, 2009). Recently, a computational approach predicted several miRNA binding sites for the ADAM10 3`UTR (Augustin *et al.*, 2012). Expression of miR103, miR107 and miR1306 reduced the activity of a luciferase reporter containing the ADAM10 3`UTR (Augustin *et al.*, 2012). Besides the miRNAs, nELAV was shown to bind to the 3`UTR of ADAM10 (Amadio *et al.*, 2009). Reduction of nELAV results in decreased ADAM10 protein levels (Amadio *et al.*, 2009).

Finally, Lammich and colleagues could show that the 5`UTR of ADAM10 represses the translation of ADAM10 mRNA, but not the transcription (Figure 1.9) (Lammich *et al.*, 2010). This was shown by transfection of HEK293 cells with ADAM10 with and without 5`UTR. Expression levels of ADAM10 in these cells were analysed by immunoblotting (Figure 1.9A). Deletion of the 5`UTR resulted in a 3-fold increase of ADAM10 expression (Figure 1.9B). In addition, analysis of mRNA levels demonstrated that the observed effect on protein expression is independent from an increase in transcription (Figure 1.9C). Moreover, the two potential uORFs within 444-nucleotide-long, GC-rich 5`UTR of ADAM10 had no influence on the translation of ADAM10 mRNA (Lammich *et al.*, 2010).

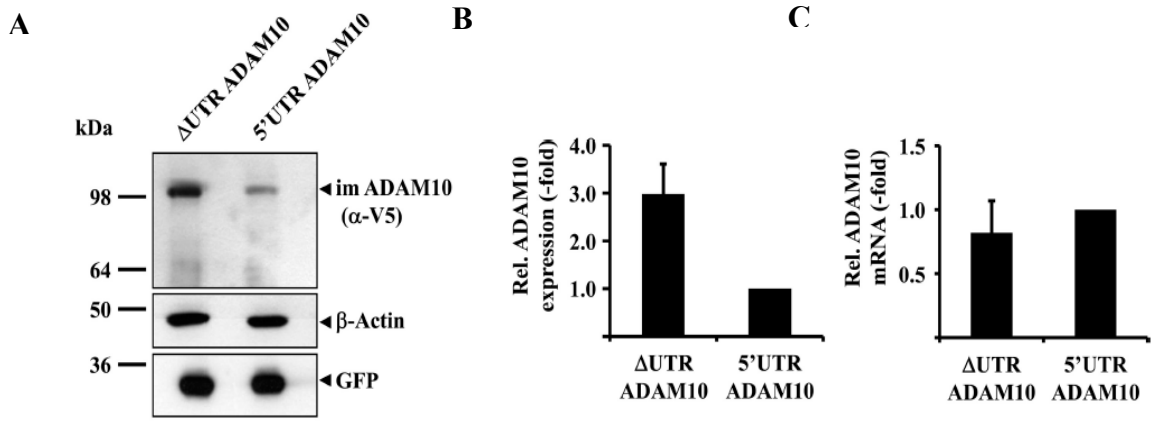

Figure 1.9 Translational regulation of ADAM10 expression (Lammich *et al.*, 2010).
(A) HEK293 cells were transiently transfected with ADAM10 or ADAM10 containing the 5`UTR together with GFP as transfection control. The upper Western blot shows immature (im) ADAM10 expression, the middle β-Actin expression and the lower GFP expression. (B) Western blots were quantified and ADAM10 protein was normalised to GFP and β-actin levels. The signal for ADAM10 containing the 5′UTR was set to 1. (C) The ADAM10 mRNA of the transfected cells was quantified by RT-PCR. ADAM10 mRNA levels were normalised to GAPDH mRNA levels using the $2^{-\Delta\Delta Ct}$ method. The result obtained for ADAM10 with 5`UTR mRNA was set to 1. Values are expressed as the mean ± standard deviation of 6 independent experiments made in triplicates.

Complex secondary structures in the 5`UTR of ADAM10 and/or RNA-binding proteins might be responsible for the translational repression of ADAM10 expression. Recently, it could be shown that the ADAM10 expression is inhibited by a G-quadruplex

secondary structure near the 5`end of the ADAM10 5`UTR (Lammich *et al.*, 2011). G-quadruplex structures can block the formation or scanning of the preinitiation complex (Huppert *et al.*, 2008). So far no further factors that influence the ADAM10 expression via its 5`UTR have been identified. However, the inhibition by the G-quadruplex could be modulated by RNA-binding proteins (Khateb *et al.*, 2004; Menon *et al.*, 2008).

1.8 Aim of the study

Several studies showed that in AD patients BACE1 levels were elevated by a factor of 2.7 in comparison to brains of patients having no AD (Fukumoto *et al.*, 2002; Holsinger *et al.*, 2002; Yang *et al.*, 2003), although mRNA levels were not increased (Holsinger *et al.*, 2002; Preece *et al.*, 2003; Yasojima *et al.*, 2001b). In addition, it was demonstrated that ADAM10 expression is also regulated by translational control mechanisms (Lammich *et al.*, 2010; Lammich *et al.*, 2011).

For BACE1, it could be shown that a complex secondary structure and the second uORF are involved in the translational repression of BACE1 expression (Lammich *et al.*, 2004; Mihailovich *et al.*, 2007; O'Connor *et al.*, 2008; Zhou and Song, 2006). Furthermore, deletion of the first half of the BACE1 5`UTR revealed a striking increase in BACE1 protein expression (Lammich *et al.*, 2004).

Furthermore, Lammich and colleagues could show that the 5`UTR of ADAM10 inhibits the translation of the ADAM10 mRNA (Lammich *et al.*, 2010). Again, in the absence of the 5`UTR, ADAM10 protein levels were significantly increased while mRNA levels were not changed. Stepwise deletion of the first half of the ADAM10 5`UTR revealed a striking increase in ADAM10 protein expression, suggesting that this part of the 5`UTR contains inhibitory elements for translation. Moreover, a G-quadruplex secondary structure in the first half of the ADAM10 5`UTR was identified, which inhibits ADAM10 translation (Lammich *et al.*, 2011).

These data demonstrate translational repression as a new mechanism controlling ADAM10 and BACE1 expression. RNA-binding proteins could be involved in translational control of certain genes by interacting with secondary structures or specific sequences within the 5`UTR (Derrigo *et al.*, 2000; Gray and Hentze, 1994; Gray and Wickens, 1998; Melefors and Hentze, 1993; Mignone *et al.*, 2002; Sonenberg, 1994; Wilkie *et al.*, 2003). The observed effects on the protein expression might thus be explained by proteins that bind to the 5`UTR and modulate ADAM10 and/or BACE1 translation. Such proteins binding to the 5`UTR of ADAM10 and/ or BACE1 can e.g.

inhibit the early steps of the translation process or modulate higher-ordered structures that influence translation efficiency (Khateb *et al.*, 2007; Menon *et al.*, 2008; Muckenthaler *et al.*, 1998).

Since ADAM10 plays a crucial role in the pathogenesis of AD, the goal of this PhD thesis was to identify proteins which may affect ADAM10 translation via binding to their 5`UTR. Such proteins may be important during development and may be misregulated during ageing and in AD. Thus, these proteins could provide novel therapeutic targets for AD treatment. Given that BACE1 expression plays also a crucial role in the pathogenesis of AD and that there was also a interest in the regulation of BACE1 expression in our research group, the BACE1 5`UTR was included in some of the experiments.

2 Materials and Methods

2.1 Devices and materials

2.1.1 Molecular biology

PCR machine (Mastercycler personal, Mastercyclergradient)	Eppendorf
Real-Time PCR System (7500 Fast)	Applied Biosystems
MicroAmp™ (Optical Adhesive Film)	Applied Biosystems
Photometer (Smart Spec™ 3000)	Bio-Rad
Benchtop room temperature centrifuge (Biofuge pico)	Heraeus
Benchtop 4°C centrifuge (Biofuge fresco, Fresco 17)	Heraeus, Thermo
4°C centrifuge (Megafuge 1.0R, Multifuge 3 L-R)	Heraeus
Centrifuge (Avanti™ J-20XP, J-25)	Beckman Coulter
Rotors: Type JA-10, JA-20, JA-25.50)	Beckman
Ultracentrifuge (Optima™ LE-80K)	Beckman Coulter
Rotors: 50 Ti, 70 Ti, 70.1 Ti	Beckman
Ultracentrifuge (Optima™ MAX-E Ultracentrifuge)	Beckman Coulter
Rotor: TLA 55	Beckman
37°C incubator (Function Line)	Heraeus
Freezer -20°C	Elektrolux
Fridge 4°C	Elektrolux
Autoclave (Tuttnauer 3850 EL)	Systec
Water deionizing machine (Milli-Q academic)	Millipore
Pipettier (Accu-Jet®)	Brand
Disposable pipettes (25 ml, 10 ml, 5 ml, 2 ml)	Corning, Sarstedt
Pipette tips (1 ml, 200 µl, 10 µl)	Sarstedt
Filter pipette tips (1 ml, 300 µl, 100 µl, 20 µl, 10 µl)	Sarstedt
Disposable tubes (50 ml, 15 ml, 2 ml, 1.5 ml, 0.5 ml, 0.2 ml)	Sarstedt
Waterbath (Typ 1002)	GFL
Heating blocks	Liebisch
Shaker (KM-2)	Edmund Bühler
Bacterial culture shaker (Certomat BS-1)	B. Braun Biotech
Agarose gel electrophoresis chambers	Peqlab, Owl Separation Systems
Microwave	Bosch
Rotator (Roto-Shake Genie™)	Scientific Industries

Thermo-shaker (Thermomixer compact)	Eppendorf
Magnet stirrer (RCT basic, KMO 2 basic)	IKA Labortechnik
pH-Meter (Inolab pH Level 1)	WTW
Scale (Analytical plus 200g – 0.0001 g)	Ohaus
Scale (Precision standard 2000 g – 0.01 g)	Ohaus
Disposable cuvette (Polystyrol / Polystyrene, 10 x 4 x 45 mm)	Sarstedt
Quarz spectrophotometer cuvette (10 mm)	Hellma/Bio-Rad Labs
Vortexer (Vortex Genie 2)	Scientific Industries
Gel analysis device:	MS Laborgeräte
UV lamp (White/Ultraviolet Transilluminator (UVP))	
Camera (CCD Video Camera Module)	
Software (Quickstore plus II)	
Printer (P91, Mitsubishi)	

2.1.2 Protein analysis

Plate reader (PowerWaveXS)	BioTek Instruments
Gen5™ software	BioTek Instruments
Power supplies (PowerPac 300, PowerPac™ basic)	Bio-Rad
Gel apparatus (Mini-PROTEAN® Cell)	Bio-Rad
Gel apparatus (X Cell Sure Lock™ Mini Cell)	Invitrogen
Blotting device (Mini Trans-Blot® Cell)	Bio-Rad
Film developing device (Cawomat 2000 IR)	Cawo
Slab Gel Dryer SGD2000	Savant
Gel and blot documentation system (FluorChem™ 8900)	AlphaInnotech
Luminescent Image Analyser (FujiFilm LAS4000)	FujiFilm
Scanner (V200 Photo)	Epson

2.1.3 Cell culture

Clean bench (Hera Safe HS12)	Heraeus
Bunsen burner (gasprofi 2^{SCS})	WLD-TEC
Vacuum pump	Vaccubrand
CO_2-incubator (Hera cell)	Heraeus
Centrifuge (Megafuge 1.0)	Heraeus
Waterbath (Typ 1003)	GFL

Microscope (Wilovert S)	Hund
Sterile disposable pipettes (2 ml, 5 ml, 10 ml, 25 ml)	Sarstedt, Corning
Sterile disposable tubes (15 ml, 50 ml)	Sarstedt
Glass Pasteur pipettes	VWR International
Culture dishes (92 x 17 mm, 60 x 15 mm, 6 well, 24 well)	Nunc
N_2-tank (Chronos)	Messer
Freezer -80°C (Hera freeze)	Thermo

2.2 Enzymes, Kits and Chemicals

All general chemicals were, unless otherwise stated, purchased from Merck KGaA, Darmstadt, Carl Roth GmbH & Co.KG, Karlsruhe or Sigma-Aldrich Chemie GmbH, Taufkirchen.

2.2.1 Molecular biology

Agarose	Invitrogen
Bacto-Agar	Becton, Dickson
Bacto-Trypton	Becton, Dickson
Yeast-extract	Becton, Dickson
Triton-X100	USB
Ribomax™ Large Scale RNA Production System – T7	Promega
Biotin-14-CTP	Invitrogen
GlycoBlue™ Coprecipitant	Ambion
RNase Inhibitor Cloned	Ambion
Ribonuclease Inhibitor	Fermentas
BrightStar™ Biotinylated RNA Century™ Size Markers	Ambion
BrightStar® BioDetect™ Nonisotopic Detection System	Ambion
Streptavidin agarose	Invitrogen
MAXIscript® *In vitro* Transcription Kit – T7	Ambion
MEGAscript® High-Yield Transcription Kit	Ambion
Ribo m^7G Cap Analog	Promega
Quick Spin Columns	Roche
(G-50 Sephadex Columns for Radiolabelled RNA Purification)	
µMACS™ Streptavidin Kit	Miltenyi Biotec
RNeasy® Mini Kit	Qiagen

RNase-Free DNase Set	Qiagen
SuperScript™ First-Strand Synthesis System for RT-PCR	Invitrogen
Taq DNA polymerase	Roche
GoTaq® DNA Polymerase	Promega
PCR Nucleotide Mix	Roche
2x Power SYBR Green PCR Master Mix	Applied Biosystems
2x TaqMan Buffer	Applied Biosystems
20x TaqMan Gene Expression Assay Mix	Applied Biosystems
Glutathione Sepharose 4B	GE Healthcare
Ni-NTA agarose	Qiagen
NucleoSpin Plasmid	Macherey-Nagel
NucleoBond plasmid purification (AX500)	Macherey-Nagel
NucleoBond Xtra Midi	Macherey-Nagel
NucleoSpin Extract II (PCR Clean-up, Gel Extraction)	Macherey-Nagel
DNA molecular weight marker (100 bp, 1 kb)	Invitrogen
Pwo PCR-system	Roche
T4 ligase and 10x T4 ligase buffer	Fermentas
Restriction endonucleases	NEB, Fermentas

2.2.2 Protein biochemistry

APS	Merck, Sigma
TEMED	Roth
Protease Inhibitor Cocktail	Sigma
Bio-Rad Protein Assay (Bradford)	Bio-Rad
BC Assay Reagent A + B	Interchim
BSA standard	Interchim
96 well plates for protein assay	Nunc
DTT	Biomol
PMSF	Sigma
Tropix® I-Block	Applied Biosystems
SDS	Serva
See-Blue® Plus2 Pre-Stained Standard	Invitrogen
Novex® Tricine Gels	Invitrogen
PVDF transfer membrane (Immobilion-P)	Millipore

Nitrocellulose transfer membrane (Protan®)	Schleicher & Schuell
Whatman paper	Schleicher & Schuell
ECL Western blotting Detection Reagents	GE Healthcare
ECL Plus Western blotting Detection Reagents	GE Healthcare
Tropix® CDP Star®	Applied Biosystems
Super RX, Fuji Medical X-ray Film	Fujifilm
Spectra/Por 6 Regenerated Cellulose Dialysis Membranes (MWCO 10000)	Spectrum Laboratories
SilverQuest™ Silver Staining Kit	Invitrogen
96-well MULTI-SPOT® Human (6E10) Abeta Triplex Assay	MSD

2.2.3 Cell culture

DMEM + GlutaMAX™-I, high glucose without pyruvate	Gibco Invitrogen
Foetal Bovine Serum	PAA
OPTI-MEM®I + GlutaMAX™-I (1x)	Gibco Invitrogen
Penicillin/Streptavidin (100x, 5 mg/ml)	PAA
L-Glutamine (100x, 200 mM)	PAA
Zeocin™ (100 mg/ml)	Gibco Invitrogen
Trypsin-EDTA (1x)	Gibco Invitrogen
Lipofectamine™ 2000	Invitrogen

2.2.4 Vectors

2.2.5 Eukaryotic expression vectors

pcDNA6/V5-HisA	Invitrogen
pcDNA4/Myc-HisA	Invitrogen
pcDNA3.1(+) Zeo	Invitrogen
psiCHECK-2	Promega
BSENU6	Ambion
pEGFP-N1	Clontech

2.2.6 Prokaryotic expression vectors

pGex-5X-1	GE Healthcare
pGEM-3Z	Promega
pET28a	Novagen

2.3 Oligonucleotides

All oligonucleotides were made by Thermo Electron GmbH and were all of an HPLC-purified grade (oligonucleotides are listed in Tables 2.1, 2.3 and 2.5).

2.4 Plasmids

Construct	Oligonucleotide	Vector	Restriction site	
ADAM10 5`UTR	5`cgc gct agc gcg gcg gca ggc cta g`3 5`ctc aag ctt ctg ccg ccg ccg ccg`3	pcDNA6/ V5-HisA	NheI / HindIII	§1
ADAM10 5`UTR	5`cgc aag ctt gcg gcg gca ggc cta g`3 5`ctc gaa ttc ctg ccg ccg ccg ccg`3	pGEM-3Z	HindIII / Eco RI	§3
ADAM10 5`UTR	5`cgc gaa ttc gcg gcg gca ggc cta g`3 5`ctc aag ctt ctg ccg ccg ccg ccg`3	pGEM-3Z	EcoRI / HindIII	§3
Δ251-432 ADAM10 5`UTR	5`cgc gct agc gcg gcg gca ggc cta g`3 5`aag ctt ggg acc tcc ctc ccc ctc gt`3	pcDNA6/ V5-HisA	NheI / HindIII	§3
Δ1-259 ADAM10 5`UTR	5`cgc gct agc gga gct agg agc gtt`3 5`ctc aag ctt ctg ccg ccg ccg ccg`3	pcDNA6/ V5-HisA	NheI / HindIII	§3
Δ1-215 ADAM10 5`UTR	5`cgc gct agc gga gga agg aaa cga`3 5`ctc aag ctt ctg ccg ccg ccg ccg`3	pcDNA6/ V5-HisA	NheI / HindIII	§3
Δ1-175 ADAM10 5`UTR	5`cgc gct agc gag aga ggg acc`3 5`ctc aag ctt ctg ccg ccg ccg ccg`3	pcDNA6/ V5-HisA	NheI / HindIII	§3
Δ1-155 ADAM10 5`UTR	5`cgc gct agc tga gtt tcg aag gag`3 5`ctc aag ctt ctg ccg ccg ccg ccg`3	pcDNA6/ V5-HisA	NheI / HindIII	§3
Δ164-246 ADAM10 5`UTR	5`cgc gct agc gcg gcg gca ggc cta g`3 5`aaa cag gga gaa act cag acc tcc gcc tcc`3 5`ctg agt ttc tcc ctg ttt tgg agg agc tag gag cg`3 5`ctc aag ctt ctg ccg ccg ccg ccg`3	pcDNA6/ V5-HisA	NheI / HindIII	§1
Δ164-201 ADAM10 5`UTR	5`cgc gct agc gcg gcg gca ggc cta g`3 5`ccg ctt tcc gaa act cag acc tcc gcc tcc`3 5`ctg agt ttc gga aag cgg gga aag gag aag g`3 5`ctc aag ctt ctg ccg ccg ccg ccg`3	pcDNA6/ V5-HisA	NheI / HindIII	§1
Δ204-246 ADAM10 5`UTR	5`cgc gct agc gcg gcg gca ggc cta g`3 5`cca aaa cag gga cct tcc ctt gct cgt tcc`3 5`aag gga agg tcc ctg ttt tgg agg agc tag gag cg`3 5`ctc aag ctt ctg ccg ccg ccg ccg`3	pcDNA6/ V5-HisA	NheI / HindIII	§1

Construct	Oligonucleotide	Vector	Restriction site	
Δ1-163/247-432 ADAM10 5`UTR	5`cgc aag ctt cct ccc tcc ccc tcg ttc`3 5`cgc gct agc gag gga ggg ggg gag ag`3	pcDNA6/ V5-HisA	NheI / HindIII	§1
5`UTR ADAM10	5`cgc gct agc gcg gcg gca ggc cta g`3 5`ctc aag ctt ctg ccg ccg ccg ccg`3	pcDNA6/ V5-HisA	NheI / XhoI	§1
Δ164-204 5`UTR ADAM10	5`cgc gct agc gcg gcg gca ggc cta g`3 5`ccg ctt tcc gaa act cag acc tcc gcc tcc`3 5`ctg agt ttc gga aag cgg gga aag gag gaa gg`3 5`ctc aag ctt ctg ccg ccg ccg ccg`3	pcDNA6/ V5-HisA	NheI / XhoI	§1
Δ204-246 5`UTR ADAM10	5`cgc gct agc gcg gcg gca ggc cta g`3 5`cca aaa cag gga cct tcc ctt gct cgt tcc`3 5`aag gga agg tcc ctg ttt tgg agg agc tag gag cg`3 5`ctc aag ctt ctg ccg ccg ccg ccg`3	pcDNA6/ V5-HisA	NheI / XhoI	§1
Δ164-246 5`UTR ADAM10	5`cgc gct agc gcg gcg gca ggc cta g`3 5`aaa cag gga gaa act cag acc tcc gcc tcc`3 5`ctg agt ttc tcc ctg ttt tgg agg agc tag gag cg`3 5`ctc aag ctt ctg ccg ccg ccg ccg`3	pcDNA6/ V5-HisA	NheI / XhoI	§1
Δ1-215 5`UTR ADAM10	5`cgc gct agc gga gga agg aaa cga`3 5`ctc aag ctt ctg ccg ccg ccg ccg`3	pcDNA6/ V5-HisA	NheI / XhoI	§1
Δ1-259 5`UTR ADAM10	5`cgc gct agc gga gct agg agc gtt`3 5`ctc aag ctt ctg ccg ccg ccg ccg`3	pcDNA6/ V5-HisA	NheI / XhoI	§1
UNR	5`cgc gga tcc gcc acc atg agc ttt gat cca aac ctt ctc`3 5`cgc ctc gag gtc aat gac acc agc ttg acg g`3	pcDNA4/ myc-HisA	BamHI/ XhoI	§4
UNR	5`cgc ggg atc ccc atg agc ttt gat cca aac ctt ctc c`3 5`cgc ctc gag tta gtc aat gac acc agc ttg acg`3	pGEX5X-1	BamHI/ XhoI	§4
UNR	5`cgc ctc gag atg agc ttt gat cca aac ctt ctc`3 5`cac gcg gcc gcg tca atg aca cca gct tga cgg`3	psiCHECK	XhoI / NotI	§2, 5
Unr KD	5`G aga ccg acg tga caa att aTT CAA GAG Ata at ttg tca cgt cgg tct Ctt ttt ctg ca`3 5`C tct ggc tgc act gtt taa taA GTT CTC Tatta aac agt gca gcc aga G aaaaa g`5	BSENU6	PmeI / PstI	§2
APAF-1 5`UTR	5`cgc gct agc aag aag agg tag cga gtg g`3 5`cgc aag ctt ctt ccc tca gat ctt tct c`3	pcDNA6/ V5-HisA	NheI / HindIII	§6

Construct	Oligonucleotide	Vector	Restriction site	
hnRNP A1	5`cgc gaa ttc atg tct aag tca gag tct c`3 5`cgc ctc gag tta aaa tct tct gcc act gcc`3	pET28a	EcoRI / XhoI	§6
hnRNP B1	5`cgc gaa ttc atg gag aaa act tta gaa ac`3 5`cgc ctc gag tca gta tcg gct cct ccc acc`3	pET28a	EcoRI / XhoI	§6

Table 2.1 Overview of the constructs and the vectors as well as the restriction enzyme sites, which were used to clone the constructs into the respective vector.

§1 These constructs were generated by Dr. Dominik Büll

§2 These constructs were generated by Dr. Sven Lammich

§3 Template: pcDNA6/V5-HisA ADAM10 5`UTR

§4 Template: IRATp970F0251D6 from RZPD

§5 Template: pcDNA4/myc-HisA UNR

§6 Template: cDNA library provided by Dr. Sven Lammich

2.5 Antibodies

2.5.1 Primary antibodies

Anti-ADAM10, C-terminus, polyclonal antibody	1:1000	Millipore
Anti-ADAM10, polyclonal antibody	1:7500	Calbiochem
Anti-CSDE1 (UNR)	1:2000	Sigma
b-Myb	1:200	Hybridoma Bank
Histone H3 antibody – ChIP Grade (ab1791)	1:5000	Biozol, Abcam
Rabbit serum 23 anti-Unr (Jacquemin-Sablon *et al.*, 1994)		
Anti-Actin, monoclonal antibody	1:2000	Sigma
Anti-α-tubulin, monoclonal antibody	1:1000	Sigma
β-Amyloid, 1-16 (6E10) monoclonal antibody	1:1000	Signet
mouse anti-APP A4, monoclonal antibody (22C11)	1:2000	Chemicon
APP-CT	1:1000	Sigma
192wt, polyclonal antibody	1 µg/ml	Elan Pharmaceuticals
2D8, monoclonal antibody	1 µg/ml	E. Kremmer
7C2 (UNR) , monoclonal antibody	1 µg/ml	E. Kremmer
Anti-Calnexin, polyclonal antibody	1:5000	Stressgen
Anti-V5, monoclonal antibody	1:5000	Invitrogen
Anti-GFP, monoclonal antibody	1:2000	Clontech

2.5.2 Secondary antibodies

Anti-mouse-HRP	1:10000	Promega
Anti-rabbit-HRP	1:10000	Promega
Anti-rat	1:5000	Santa Cruz

2.6 DNA techniques

2.6.1 Agarose gel electrophoresis

TAE-buffer (1x):
40 mM Tris base, 40 mM glacial acetic acid, 1 mM EDTA

TBE-buffer (1x):
89 mM Tris base, 89 mM boric acid, 2 mM EDTA

DNA loading buffer (10x):
15% Ficoll 400, 0.25% Orange G in H_2O

DNA loading buffer (5x):
50% Glycerol, 50% 10x TBE, Bromophenol, Xylene Cyanol FF

Ethidium bromide:
10 mg/ml in dH_2O

Horizontal slab gels were prepared from agarose, electrophoresis grade dissolved in 1x TAE or 1x TBE. Ethidium bromide was added to a concentration of 0.5 µg/ml. For the electrophoretic separation and analysis of linear DNA fragments, superhelical plasmid DNA and for the isolation of DNA fragments 0.8 – 2% agarose gels were used. A $1/10^{th}$ volume of gel loading buffer was added to all DNA samples before loading onto a gel. A 100-bp- or 1-kb-size marker was used to define the size of the DNA fragment. Gel electrophoresis was performed in 1x TAE or 1x TBE buffer at a constant voltage of 120 V for 30 to 60 min. Ethidium bromide-stained bands were visualized with a White/Ultraviolet Transilluminator (UVP) at 312 nm. Gel images were captured with a CCD video camera module (Kaiser) and reproduced with a Mitsubishi P91 video copy processor.

2.6.2 Quantification of DNA

DNA concentration was estimated by measuring the absorbance of aqueous DNA solutions with a Smart Spec 3000 (Bio-Rad) at 260 nm. Pure DNA at 50 ng/µl has an A_{260} of 1.0.

2.6.3 Polymerase Chain Reaction (PCR)

PCR was used to amplify the plasmid DNAs used in this thesis. PCR reactions were performed in a total volume of 50 µl containing 10 ng to 50 ng of plasmid DNA, 5 µl Pwo 10x PCR buffer (Peqlab), 100 ng forward primer, 100 ng reverse primer, 2 µl dNTPs (10 nM each) (Roche), 1 µl Pwo-polymerase (1 unit/µl) (Peqlab) and adjusted to 50 µl with distilled water. PCR was performed using a Mastercycler personal (Eppendorf) or GeneAmp PCR System 2400 (Perkin Elmer). Cycle conditions varied between the different constructs (see below).

<u>Unr program</u>

Denaturing:	94°C	3 min	
Denaturing:	94°C	30 sec	10 cycles
Annealing:	42°C	30 sec	
Elongation:	72°C	2 min	
Denaturing:	94°C	30 sec	20 cycles
Annealing:	42°C	30 sec	
Elongation:	72°C	2 min	
		+ 20 sec / cycle	
Elongation:	72°C	10 min	
hold at 4°C			

<u>5`UTR ADAM10 program</u>

Denaturing:	95°C	3 min	
Denaturing:	95°C	30 sec	35 cycles
Annealing:	50°C	30 sec	
Elongation:	72°C	2 min	
Elongation:	72°C	10 min	
hold at 4°C			

PCR products were analysed by agarose gel electrophoresis (see 2.6.1). The amplified DNA fragments were gel purified (see 2.6.4) and digested with the respective enzymes (see 2.6.5). The resulting fragments were used for further cloning (see 2.6.6).

2.6.4 DNA extraction from agarose gels

DNA was recovered and purified from agarose gels according to the NucleoSpin® Extract II kit (Macherey-Nagel) protocol. Briefly, desired DNA bands were excised from the agarose gel with a clean, sharp scalpel blade on a UV screen and weighed in a 1.5 ml tube. Two volumes of buffer NT were added to one volume of gel. Then the reaction was incubated at 50°C for 10 min to solubilize the agarose. After 10 min, the sample was transferred to a NucleoSpin® Extract II column and centrifuged for 1 minute at 13000 rpm to bind the DNA. Then 600 µl of buffer NT3 was added to the NucleoSpin® extract II column and centrifuged twice for 1 to 2 min at 13000 rpm. Finally, the NucleoSpin® Extract II column was inserted into a clean 1.5 ml microcentrifuge tube, 15-50 µl elution buffer NE was added to the NucleoSpin® Extract II column, incubated for 1 minute at room temperature and centrifuged for 1 minute at 13000 rpm to elute DNA.

2.6.5 Restriction enzyme digest

All restriction enzyme digests were performed with restriction enzymes purchased from Fermentas or NEB.

Analytical restriction enzyme digests after plasmid preparation were carried out in a total volume of 20 µl, containing 1 µg DNA, 0.5 µl of the required enzymes and 2 µl of the recommended reaction buffer. Digests were incubated for 1h at 37°C. Digested DNA products were separated by agarose gel electrophoresis (see 2.6.1).

Preparative restriction enzyme digests for cloning were carried out in a total volume of 30 µl containing 2-5 µg DNA or the respective PCR product, 1 µl of the required enzymes and 3 µl of the recommended reaction buffer. Digests were incubated for at least 1h or overnight at 37°C. Digested DNA fragments were separated by agarose gel electrophoresis and purified as described above (see 2.6.1 and 2.6.4).

Preparative restriction enzyme digests for *in vitro* transcription were carried out in a total volume of 100 µl, containing 15-30 µg plasmid DNA, 5 µl of the required enzymes and 10 µl of the recommended reaction buffer. Digests were incubated overnight at 37°C. The linearised DNA was separated by agarose gel electrophoresis and purified as described above (see 2.6.1 and 2.6.4).

2.6.6 Ligation of cDNA fragments into vector DNA

Agarose gel purified digested DNA was cloned in between the desired restriction sites of the respectively digested vector to produce the desired plasmid. Ligations were carried

out in a total volume of 20 µl, containing 2 µl digested DNA, 2 µl vector and 1 µl T4 DNA ligase in the supplied T4 ligase buffer. The mixture was incubated for 1-2 h or overnight at room temperature. In parallel, to control re-ligation of the vector, the vector was incubated without insert. 10 µl of the ligation reaction were then used for the transformation of competent bacteria of *E.coli* strain DH5α (see 2.6.8).

2.6.7 Preparation of competent DH5α and BL21 (DE3) cells

$CaCl_2$-buffer:
50 mM $CaCl_2$, 10 mM Tris, pH 8.0 in dH_20, sterile filtered

LB-Medium:
1% (w/v) Bacto-Tryptone, 0.5% (w/v) Yeast extract, 0.5% (w/v) NaCl in dH_2O, autoclaved

One colony of a freshly struck LB agar plate with DH5α or BL21 (DE3) was picked and dispersed in 3 ml LB medium to grow overnight at 37°C. The 3 ml overnight DH5α or BL21 (DE3) culture in LB medium was used to inoculate 300 ml fresh LB medium. Bacteria were cultured to a density of OD_{600} = 0.5 at 37°C by shaking at 200 rpm. Then the culture was collected into 50 ml polypropylene centrifuge tubes (e.g., Falcon tubes) and centrifuged at 3000 rpm for 5 min at 4°C. Each bacterial pellet was resuspended in 17.5 ml cold $CaCl_2$-buffer, incubated on ice for at least 30 min and centrifuged as before. The bacterial pellets were resuspended in 1 ml $CaCl_2$-buffer, supplemented with 20% glycerol, and 100-200 µl aliquots of the suspension were stored at -80°C.

2.6.8 Transformation of DNA constructs into DH5α or BL21

LB-medium:
see 2.6.7

LB agar plates:
LB-medium, 1.5% agar, autoclaved

An aliquot (100 µl) of competent DH5α or BL21 (DE3) cells was thawed on ice, 10 µl of the ligation reaction or 50 ng plasmid DNA (re-transformation) was added, mixed gently and incubated on ice for 30 min. After a heat shock at 42°C for 2 min, cells were incubated for additionally 2 min on ice. Then 300 µl of fresh LB medium was added to the mixture and bacteria were incubated for 1 h at 37°C with shaking at 750 rpm. The mixture was briefly centrifuged, the pellet resuspended in 100 µl of LB and then plated onto a LB-agar plate containing the respective antibiotic to select positive clones. LB-agar plates were incubated overnight at 37°C. Colonies were picked, inoculated into 3 ml fresh LB

medium containing the desired antibiotic and incubated overnight at 37°C. 1.5 ml of the overnight culture was used for mini prep (see 2.6.9).

2.6.9 Small-scale plasmid preparation (Mini-prep)

LB-medium:
see 2.6.7

TENS:
10 mM Tris, pH 8.0, 1 mM EDTA, pH 8.0, 100 mM NaCl, 0.5% SDS in dH_2O

Na-Acetate:
3 M Na-Acetate, pH 5.2 with acetic acid

RNase – DNase free:
10 mg/ml RNase in 10 mM Tris, pH 7.5 and 15 mM NaCl, incubation for 15 min at 95°C, slowly cooling down at room temperature, store aliquots at -20°C

Plasmid DNA was isolated in smaller amounts (Mini-preps) by the alkaline lysis method (Zhou *et al.*, 1990), described as follows: Usually, a volume of 3 ml of LB-media supplement with the appropriate antibiotic was inoculated with a single bacterial colony and cultured overnight at 37°C and 200 rpm. The next day, 1.5 ml overnight culture was collected into 1.5 ml tube and centrifuged for 1 min at 13000 rpm. The supernatant was gently discarded, leaving 50-100 µl with bacterial pellet and the bacterial pellet resuspended in the leftover supernatant by vortexing. The bacterial cells were lysed in 300 µl TENS buffer by gently inverting the suspension. Then the suspension was neutralized by adding 150 µl 3 M NaOAc, pH 5.2 by gently inverting the suspension. Afterwards the insoluble fraction (cell debris and chromosomal DNA) was removed by centrifugation at 13000 rpm for 5 min at room temperature. The supernatant was transferred into a fresh 1.5 ml tube containing 900 µl -20°C cold 100% ethanol, mixed well and incubated for at least 20 min at -80°C. Plasmid DNA and RNA were precipitated by centrifugation at 13000 rpm for 2 min at 4°C. The pellet was rinsed twice with 4°C cold 70% Ethanol and centrifuged at 13000 rpm for 2 min at 4°C. Thereafter, the pellet was dried for 5 min at 37°C, resuspended in 30 µl dH_2O/RNase solution (1 µg/µl) and incubated for 30 min at 37°C. To identify positive clones, 5 µl of the mini prep DNA was digested (see 2.6.5) with the same restriction enzymes that were used to get sticky ends before ligation and analysed by agarose gel electrophoresis (see 2.6.1).

One of typically several positive clones containing the predicted size of insert cDNA fragment was selected and used for medium- or large-scale DNA preparation.
For directly sequencing, a Mini-prep preparation the DNA was isolated using the NucleoBond Plasmid kit according to the manufacturer`s instructions.

2.6.10 Medium-scale plasmid preparation (Midi-prep)

Plasmid DNA was isolated in medium amounts (Midi-preps) using the NucleoBond Xtra Midi kit described as follows: Usually, a volume of 100 ml of LB-medium supplemented with the appropriate antibiotic was inoculated with a single bacterial colony and cultured overnight at 37°C and 200 rpm. The next day, the bacteria culture was centrifuged in centrifuge bottles at 5000 rpm for 15 min at 4°C. The supernatant was removed and the pellet resuspended in 8 ml of cold resuspension buffer RES + RNase A by pipetting the cells up and down. Afterwards, 8 ml of lysis buffer LYS was added, mixed gently by inversion and incubated for 5 min at room temperature. Next, a NucleoBond® Xtra Column together with the inserted column filter was equilibrated with 12 ml equilibration buffer EQU by applying the buffer onto the rim of the column filter. The column was allowed to empty by gravity flow. Then 8 ml of neutralisation buffer NEU was added to the suspension and the lysates was immediately mixed gently by inversion. The lysates was simultaneously cleared and loaded onto the column and the column was allowed to empty by gravity flow. The NucleoBond® Xtra column filter and column was washed with 5 ml equilibration buffer EQU. The buffer was applied to the funnel shaped rim of the filter to make sure that the lysates, which was remaining in the filter, was washed out. Afterwards, the NucleoBond® Xtra column filter was discarded and the column was washed with 8 ml wash buffer WASH. The column was transferred to a 50 ml Falcon tube and the plasmid DNA was eluted with 5 ml elution buffer ELU. To precipitate the eluted plasmid DNA, 3.5 ml isopropanol (at room temperature) was added, vortexed well and the mixture was left on the bench for 2 min. Then the plasmid DNA was recovered by centrifugation at 6000 rpm for 30 min at 4°C. Finally, the DNA pellet was washed with 2 ml 70% ethanol, dried for at least 10 min at room temperature, before being resuspended in 100 to 200 µl distilled water dependent on the pellet size and transferred to a 1.5 ml microcentrifuge tube. 5 µl DNA was diluted in 495 µl H_2O and used for DNA concentration measurement (see 2.6.2). To control the plasmid DNA, 1 µg DNA was digested with the respective enzymes (see 2.6.5) and analysed by agarose gel electrophoresis (see 2.6.1).

2.6.11 Large-scale plasmid preparation (Maxi-prep)

Plasmid DNA was isolated in larger amounts (Maxi-prep) using the NucleoBond PC500 kit described as follows: Usually, a volume of 200 ml of LB-media supplemented with the appropriate antibiotic was inoculated with a single bacterial colony and cultured

overnight at 37°C and 200 rpm. The next day, the culture was centrifuged in bottles at 5000 rpm for 15 min at 4°C. The supernatant was removed and the pellet resuspended in 10 ml of cold resuspension buffer S1 by pipetting up and down. Afterwards, 10 ml of lysis buffer S2 was added and mixed gently by inversion. Then 10 ml of neutralisation buffer S3 was added, mixed thoroughly by inversion and incubated on ice for 5 min. Before the solution was decanted through a wetted paper filter onto a column, the column was moistened with equilibration buffer N2. The column was filled with wash buffer N3, transferred to a 50 ml Falcon tube and the DNA was eluted with 15 ml elution buffer N5. Isopropanol (11 ml) was then added to the decanted supernatant, mixed thoroughly by inversion and the precipitated plasmid DNA was recovered by centrifugation at 6000 rpm for 30 min. Finally, the DNA pellet was washed with 70% ethanol, dried for at least 10 min at room temperature before being resuspended in 200 to 400 µl distilled water (dependent on the pellet size) and transferred to a 1.5 ml microcentrifuge tube. 5 µl DNA was diluted in 495 µl H_2O and used for DNA concentration measurement (see 2.6.2). To control the plasmid DNA, 1 µg DNA was digested with the respective enzymes (see 2.6.5) and analysed by agarose gel electrophoresis (see 2.6.1).

2.6.12 DNA sequencing

All cDNA constructs were confirmed by sequencing by GATC Biotech AG (Konstanz, Germany). The constructs were sequenced with the T7 or BGH primer. For UNR, two additional primers were used (see Table 2.3).

Oligonucleotide name	**Sequence**
Unr 601-620	5`aca atc aag gac aga aat gg`3
Unr 1201-1220	5`gta gaa aaa gaa gcc act tt`3

Table 2.3 Oligonucleotides used for sequencing.

Sequencing results were analysed by BLASTN (http://blast.ncbi.nlm.nih.gov) or HUSAR Prof Align, a bioinformatics service of the DKFZ (Heidelberg).

2.7 RNA techniques

2.7.1 In vitro transcription of α-^{32}Phosphate-labelled RNA

The pcDNA6-V5/HisA ADAM10 5`UTR and deletion constructs were linearised with HindIII to serve as templates for the synthesis of RNA probes. The pcDNA3.1(+) Zeo BACE1 5`UTR was linearised with EcoRI. In case of the ADAM10 5`UTR the last 12 nucleotides of the 5`UTR were removed, resulting in a 5`UTR with a length of 432 nucleotides instead of 444 nucleotides. For the BACE1 5`UTR the last 9 nucleotides of the 5`UTR were removed, resulting in a 5`UTR with a length of 437 nucleotides instead of 446 nucleotides. In addition, as the T7 promoter used for the *in vitro* transcription was not directly in front of the 5`end of the two 5`UTRs, the resulting *in vitro* transcripts for ADAM10 and BACE1 5`UTR had a length of 453 nucleotides and 474 nucleotides, respectively (Figure 2.1).

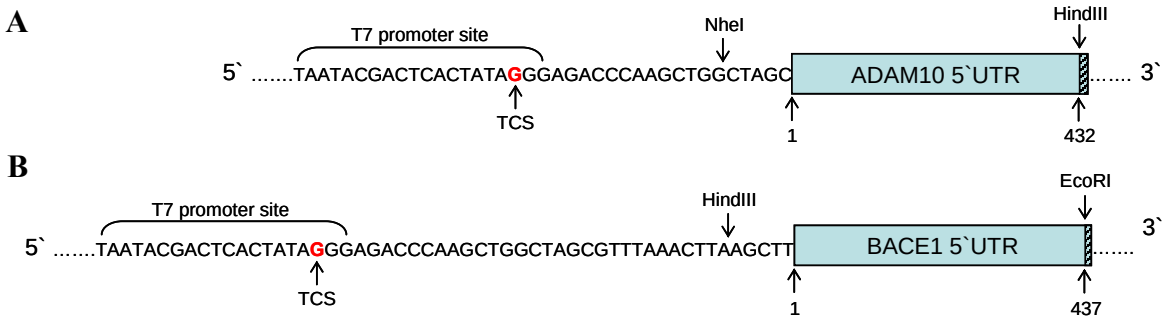

Figure 2.1 Representation of the ADAM10 and BACE1 5`UTR constructs.
The ADAM10 and BACE1 5`UTR used for *in vitro* transcription are shown. The bracket shows the T7 promoter sequence. The transcription start (TCS) is highlighted in red. (A) NheI and HindIII are the restriction sites used for cloning the ADAM10 5`UTR. HindIII was used for linearization of the ADAM10 5`UTR. The black stripped box represents the last 12 nucleotides which are missing in the *in vitro*-transcribed ADAM10 5`UTR. (B) HindIII and EcoRI were used for cloning the BACE1 5`UTR. The restriction enzyme EcoRI was used for linearization of the BACE1 5`UTR. The black stripped box represents the last 9 nucleotides which are missing in the *in vitro*-transcribed BACE1 5`UTR.

In vitro transcription was performed at room temperature. There is a trade-off between synthesis of high specific activity probe and synthesis of full-length probe. The proportion of full-length transcript increases with increasing concentration of limiting nucleotide. However, if unlabelled nucleotide is used to increase the limiting nucleotide concentration, it will lower the specific activity of the transcript. In order to find the optimal reaction setup for *in-vitro*-transcribed RNA with a high proportion of full-length transcript combined with a high specific activity, several reaction setups were prepared. Therefore, different end concentrations of α^{32}P-CTP (3.125 µM and 0.625 µM) and non-labelled CTP (0 µM, 10 µM, 50 µM, 100 µM and 500 µM) were tested for the ADAM10

5`UTR. For the BACE1 5`UTR several reaction setups with different end concentrations of non-labelled UTP (0 µM, 10 µM, 50 µM and 100 µM) and 3.125 µM α^{32}P-UTP were tested. In this work, the ADAM10 5`UTR was prepared with 3.125 µM $\alpha^{32}$P-CTP and 10 µM CTP and the BACE1 5`UTR with 3.125 µM α^{32}P-UTP and 10 µM UTP.

According to the MAXIscript® *In vitro* Transcription Kit – T7 (Ambion) a 20 µl reaction, e.g., for the ADAM10 5`UTR, included 4 µl nuclease-free water, 1 µg linearised DNA template, 2 µl 10x Transcription buffer, 1 µl 10 mM ATP, 1 µl 10 mM GTP, 1 µl 10 mM UTP, 2 µl 100 µM CTP, 50 µCi ^{32}P labelled CTP (10 µCi/µl) and 2 µl T7 Enzyme mix. The reaction was mixed by gently flicking the tube and microfuged briefly to collect the reaction mixture at the bottom of the tube. Afterwards, the reaction was incubated for 1 h at 37°C. Following the transcription reaction, the template DNA was removed by adding 1 µl TURBO DNase 1. The reaction was mixed well and incubated for an additional 15 min at 37°C. Finally, the reaction was purified according to 2.7.4 and analysed according to 2.7.7.

2.7.2 In vitro transcription of RNA

The pcDNA6-V5/HisA ADAM10 5`UTR and deletion constructs were linearised with HindIII to serve as templates for the synthesis of RNA probes. The pcDNA6-V5/HisA APAF-1 5`UTR was linearised with HindIII. The reactions were set up at room temperature according to the MEGAscript® High-Yield Transcription Kit (Ambion). A 20 µl reaction included 6 µl Nuclease-free water, 1 µg DNA, 2 µl 75 mM ATP, 2 µl 75 mM CTP, 2 µl 75 mM GTP, 2 µl 75 mM UTP, 2 µl 10x Transcription buffer, and 2 µl T7 Enzyme mix. The reaction was mixed by gently flicking the tube and microfuged briefly to collect the reaction mixture at the bottom of the tube. Afterwards the reaction was incubated for 4 h at 37°C. Following the transcription reaction, the template DNA was removed by adding 1 µl TURBO DNase 1. The reaction was mixed well and incubated for an additional 15 min at 37°C. Finally, the reaction was purified according to 2.7.5.

2.7.3 In vitro transcription of internally biotinylated RNA

The pcDNA6-V5/HisA ADAM10 5`UTR was linearised with HindIII to serve as templates for the synthesis of RNA probes. The pcDNA3.1(+) Zeo BACE1 5`UTR was linearised with EcoRI. The reaction was set up at room temperature according to the Ribomax™ Large-Scale RNA Production System – T7 (Promega). A 100 µl sample reaction included 20 µl 5x T7 Transcription buffer, 30 µl rNTPs (25 mM ATP, CTP, GTP,

UTP), 2.5 µl 10 mM Biotin-14-CTP, 37.5 µl linear DNA template (10 µg total) plus Nuclease-free water, 10 µl Enzyme mix and 1 µl RNasin. The reaction was mixed by gently pipetting and incubated at 37°C for 4 h. To remove the DNA template following the transcription reaction, RQ1 RNase-Free DNase was added to a concentration of 1 U/µg of template DNA. The reaction was incubated for 15 min at 37°C. Additionally, a control reaction without 2.5 µl 10 mM Biotin-14-CTP was set up. Afterwards the transcription reaction was purified according to 2.7.5 and analysed according to 2.7.8.

2.7.4 Purification of radiolabelled RNA

For the purification of radiolabelled RNA from 2.7.1 Quick Spin Columns G-50 Sephadex Columns for Radiolabelled RNA Purification (Roche Applied Science) were used. For the purification, a column was removed from the storage container and gently inverted several times to resuspend the column matrix. The top cap was removed from the column, then the bottom tip was removed and the buffer allowed to drain by gravity and discarded. The column was placed in a collection tube, centrifuged at 1100 x g for 2 min and the collection tube with the eluted buffer was discarded. The column was kept in an upright position, the RNA sample was carefully applied to the centre of the column bed and the column was placed in a second collection tube. Finally, the column was centrifuged for 4 min at 1100 x g, the column was discarded and the eluate from the second collection tube was saved as this contained the purified RNA sample. The purified RNA was analysed according to 2.7.7.

2.7.5 Purification of non-labelled and internally biotinylated RNA

The *in vitro*-transcribed RNAs from 2.7.2 and 2.7.3 were purified with the phenol-chloroform extraction method. Transcription reactions were brought up to 136 µl with Nuclease-free water and 15 µl ammonium acetate stop solution were added and mixed thoroughly. The transcription reaction was extracted with an equal volume (151 µl) of phenol-chloroform, mixed and centrifuged at 13000 rpm for 3 min. The upper phase was transferred to a new tube, extracted with an equal volume (115 µl) of chloroform, vortexed and centrifuged at 13000 rpm for 3 min. Then the upper aqueous phase was recovered, transferred to a new tube and the RNA was precipitated by adding 1 volume (80 µl) of isopropanol and mixed well. The mixture was chilled overnight at -20°C and centrifuged at 4°C for 15 min at 13000 rpm to pellet the RNA. The pellet was washed 2x with 70% ethanol (500 µl) at 13000 rpm for 15 min at 4°C. Finally, the pellet was dried at room

temperature, resuspended in the desired volume of nuclease-free water and the RNA concentration was determined (see 2.7.10). The RNA was stored at -80°C. The internally biotinylated RNA was analysed according to 2.7.8.

2.7.6 Denaturing polyacrylamide gel

10x TBE:
0.9 M Tris base, 0.9 M Boric acid, 20 mM EDTA solution in DEPC-H_2O

Acrylamide solution:
40% (w/v) Acrylamide-Bis 37.5:1

APS:
10% (w/v) Ammoniumpersulfate in dH_2O

Mix the following components for a 5% denaturing polyacrylamide / 8 M urea gel solution:

for 15 ml	Component
7.2 g	Urea
1.5 ml	10x TBE
1.9 ml	40% Acrylamide-Bis
to 15 ml	DEPC-H_2O

The gel solution was stirred at room temperature until the urea was completely dissolved and then the following was added:

120 µl	10% APS
16 µl	TEMED

After the last two ingredients, which catalyse polymerization, were added, the gel solution was mixed briefly, and then the gel was poured immediately.

2.7.7 Gel analysis of radiolabelled transcripts

10x TBE:
see 2.7.6

The best way to analyse the outcome of a transcription reaction is to run an aliquot on a 5% denaturing polyacrylamide / 8 M urea gel (see 2.7.6). Therefore, 1 µl of the 20 µl transcription reaction was mixed with 7 µl Gel Loading buffer II (Ambion) containing xylene cyanol and bromophenol blue and heated to 95°C for 2 min. The sample was directly loaded into the freshly rinsed well of the gel and electrophoresed at 200 volts in 1x TBE buffer until the bromophenol blue (the faster migrating dye) approached the bottom

of the gel. The loading buffer also served as size marker. On a 5% denaturing polyacrylamide / 8M urea gel xylene cyanol runs around 130 nucleotides and bromophenol blue at around 35 nucleotides (Sambrook *et al.*, 1989). Finally, the gel was removed from the glass plates, covered in plastic wrap and exposed to X-ray film.

2.7.8 Analysis of internally biotinylated transcripts

For the analysis of internally biotinylated transcripts, the BrightStar® BioDetect™ kit was used. A dilution series (1 µg, 100ng, 10 ng, 1 ng, 100 pg, 10 pg, 1 pg) of the biotinylated RNA probe (from 2.7.3 and 2.7.5) was spotted on a positively charged nylon transfer membrane Hybond-N+ and then detected using the BrightStar® BioDetect™ protocol. First, the membrane was washed 2x 5 min in approximately 1 ml 1x Wash Buffer/cm^2 membrane. Afterwards the membrane was incubated 2x 5 min in approximately 0.5 ml Blocking Buffer/cm^2 membrane followed by a 30 min incubation in approximately 1 ml Blocking Buffer/cm^2 membrane. The membrane was incubated for 30 min in diluted Strep-Alkaline Phosphatase (10 ml Blocking Buffer and 1 µl Strep-Alkaline Phosphatase) and after that incubated in 0.5 ml Blocking Buffer/cm^2 membrane for 10 min. To decrease non-specific background, the membrane was washed 3x 5 min in approximately 1 ml Wash Buffer/cm^2 membrane. Finally, the membrane was incubated 2x 2 min in 0.5 ml 1x Assay Buffer/cm^2 membrane and for 5 min in 5 ml CDP-Star. The excess CDP-Star was removed by quickly blotting the membrane on a piece of filter paper without letting the membrane dry. The membrane was wrapped in a single layer of plastic and exposed on X-ray film at room temperature.

2.7.9 RNA extraction from cells

RNA was extracted according to the RNeasy Mini Kit protocol (Qiagen) as follows. Cells were harvested with PBS, centrifuged for 5 min at 5000 rpm and the supernatant was removed. The pellet was resuspended in 30 µl H_2O and mixed with 600 µl RLT buffer (10 µl β-mercaptoethanol/ml RLT buffer were freshly added). The lysate was added to a Qia-shredder spin column and centrifuged for 2 min at 13000 rpm. The flow through was mixed with 630 µl 70% ethanol (in DEPC-H_2O). 700 µl of the lysate were transferred to an RNeasy mini column, centrifuged for 15 sec at 10000 rpm and the flow-through was discarded. The procedure was repeated with the remaining sample. Afterwards 350 µl RW1 buffer was added to the column and centrifuged for 15 sec at 10000 rpm to wash the spin column membrane. To eliminate remaining DNA contaminants, 80 µl of a DNaseI

mixture (10 µl DNaseI + 70 µl RDD buffer) was added to the RNeasy spin column membrane and incubated for 15 min at room temperature. Then 350 µl RW1 buffer were added to the column and centrifuged again for 15 sec at 10000 rpm. The RNeasy column was transferred to a new tube, then 500 µl RPE buffer were added and centrifuged for 15 sec at 10000 rpm to wash the spin column membrane. An additional 500 µl RPE buffer were added to the column, centrifuged for 2 min at 10000 rpm and again for 1 minute at 10000 rpm to remove residual ethanol. Finally, the RNeasy spin column was placed in a new 1.5 ml collection tube and the RNA was eluted in 30 µl RNase-free water by centrifugation for 1 minute at 10000 rpm. The concentration and quality of the RNA was determined with the Agilent 2100 Bioanalyser (see 2.7.10). For RNA isolated from transiently transfected cells the RNA concentration was first measured with a Jasco UV/VIS spectrophotometer V-550 (see 2.7.10). To remove residual DNA, 10 µg of the RNA were treated a second time with DNaseI (DNA-free, Ambion).

2.7.10 RNA concentration and quality determination

RNA concentration of *in vitro*-transcribed RNA and RNA isolated from transient transfected cells was estimated by measuring the absorbance of aqueous RNA solutions with a UV/VIS spectrophotometer V-550 (Jasco).

RNA concentration and quality of isolated RNA was determined with the Agilent 2100 Bioanalyser using the Agilent RNA Nano kit according to the manual.

2.7.11 cDNA synthesis

cDNA synthesis was performed according to the SuperScript™ First-Strand Synthesis System for RT-PCR as follows. The reaction was set up with 100 ng random primers, 100 ng isolated RNA, 1 µl dNTP mix (10 mM each) and filled up to 12 µl with RNase-free water. The mixture was then heated to 65°C for 5 min and quickly chilled on ice. Afterwards, the content of the tube was collected by brief centrifugation and 4 µl 5x First-Strand Buffer, 2 µl 0.1 M DTT and 1 µl RNaseOUT (40 units/µl) (optional) were added. The content of the tube was mixed gently and incubated at 25°C for 2 min. Finally, 1 µl (200 units) of SuperScript™ II RT was added and mixed by pipetting gently up and down. The tubes were incubated at 25°C for 10 min following incubation at 42°C for 50 min. The reaction was inactivated by heating at 70°C for 15 min. For the cDNA synthesis of RNA isolated of transiently transfected cells, the reaction was set up with 500 ng oligo-dT primer and 500 ng isolated RNA.

2.7.12 qRT-PCR

For quantitative RT-PCR, the Applied Biosystems 7500 Fast machine was used. For endogenous RNA the reaction was set up as follows: 10 µl TaqMan Buffer, 1 µl TaqMan Primer (20x TaqMan Gene Expression Assay Mix) (see Table 2.4), 1 µl cDNA and 8 µl RNase-free water.

Samples were measured in triplicates with the following program: holding stage with 50°C for 2 min and 95°C for 10 min following the cycling stage with 40 cycles at 95°C for 15 sec and 60°C for 1 minute.

Gene of interest	**Primer name**		
CSDE1	Hs00200261_m1	Fam/MGB	exon-exon
APP	Hs00169098_m1	Fam/MGB	exon-exon
BACE1	Hs00201573_m1	Fam/MGB	exon-exon
ADAM10	Hs00153853_m1	Fam/MGB	exon-exon
GAPDH	4326317E-0509010	VIC-MGB	exon-exon

Table 2.4 List of TaqMan primers used for qRT-PCR.

For the detection of transfected constructs, the reaction was set up as follows: 10 µl 2x Power SYBR Green PCR Master Mix (Applied Biosystems), 1 µl (1 µM) of each primer pair (see Table 2.5), 1 µl cDNA and 8 µl RNase-free water.

Samples were measured in triplicates with the same program as for endogenous RNA. The relative ADAM10 RNA expression was normalised to the $\Delta\Delta C_t$ method.

Gene of interest	**Primer name**	**Sequence**
V5-tagged ADAM10 constructs	ADAM10-2228 forward primer ADAM10-V5 reverse primer	5`cat tca gca acc cca gcg tca g`3 5`atc gag acc gag gag agg gtt ag`3
GAPDH	GAPDH forward primer GAPDH reverse primer	5`tca gtg cca ccc aga aga c`3 5`cag tga gct tcc cgt tca g`3

Table 2.5 Primers used for qRT-PCR.

2.8 Cell lines and cell culture

2.8.1 Cell lines and cell culture

PBS buffer (1x, sterile):
140 mM NaCl, 10 mM Na_2HPO_4*$2H_2O$, 1.75 mM KH_2PO_4, 2.7 mM KCl in dH_2O, set to pH 7.4 with HCl, autoclaved

Trypsin-EDTA:
0.05% Trypsin-EDTA

Culture medium:
DMEM + GlutaMAX I (with 4.5 g/l glucose, without pyruvate), 10% FCS, 2 mM L-Glutamine

Selection medium:
Culture medium supplemented with 50 units/ml penicillin, 50 µg/ml streptomycin and 200 µg/ml Zeocin

Cell lines:

293E

293E UnrKO #15

293E Unr #6

Cell culture

Human embryonic kidney 293E cells (HEK293E) were cultured in Dulbecco's modified Eagle's medium (DMEM) supplemented with 10% foetal bovine serum, 50U/ml penicillin/ 50 µg/ml streptomycin, and as appropriate, 200 µg/ml Zeocin (293E Unr, 293E Unr KO).

All cells were maintained at 37°C in an incubator (Hera Cell, Heraeus) in 5% CO_2 and 95% air humidity. The cells were grown in cell culture dishes of varying sizes depending on the application. The cells were allowed to grow until a confluency of 90% had been reached. For passage of the cells the medium was removed carefully with a sterile pasteur pipette, the cells were washed with 1x sterile PBS and then detached with Trypsin-EDTA. The trypsinised cells were resuspended in medium, transferred to a 15 ml tube and centrifuged at 1000 rpm for 5 min. The cell pellet was resuspended in fresh medium and the cells re-plated at the desired density in new cell culture dishes.

2.8.2 Counting of cells

The cell number was determined using a Neubauer counting chamber.

2.8.3 Storage of cells (cryoconservation)

PBS buffer (sterile):
see 2.8.1

Trypsin-EDTA:
see 2.8.1

Culture medium:
see 2.8.1

Freezing medium:
90% FCS, 10% DMSO

To prepare cells for storage, confluent cells were washed with 1x PBS, trypsinised and resuspended in culture medium. Cells were then centrifuged at 1000 rpm for 5 min. The medium was removed and the cells resuspended in 1 ml freezing medium and transferred into a 1.5 ml cryo tube. Cells were then transferred to a freeze box that allows a slow and defined cooling down at -80°C overnight and finally stored at -80°C or in liquid nitrogen. To repropagate cells, the microtubes were removed from -80°C or liquid nitrogen and placed at room temperature for thawing. The cells were then mixed with 9 ml fresh medium followed by centrifugation (to remove DMSO) to pellet them before being re-plated in cell culture dishes in fresh medium.

2.8.4 Coating of cell culture dishes with poly-L-lysine

Poly-L-Lysine:
1:100 dilution of 10 mg/ml poly-L-lysine in PBS

PBS:
see 2.8.1

For some experiments, the cell culture dishes had to be coated with poly-L-lysine to get a better adhesion of the cells. Therefore, cell culture dishes were incubated with poly-L-lysine for at least 30 min at 37°C in a CO_2-incubator and afterwards 2-3x washed with dH_2O. Before use, the cell culture dishes were dried under the clean bench.

2.8.5 Transient transfection by Lipofectamine™ 2000

Cells used for transfection were split and re-seeded 24 h before transfection. Usually, transient transfections were performed in either 6 cm or 10 cm cell culture dishes for cell lysates. Transient transfection was performed using Lipofectamine™ 2000 (Invitrogen). According to the manufacturer's instructions, 8 µg of plasmid DNA and 20 µl of the transfection reagent or 24 µg of plasmid DNA and 60 µl Lipofectamine per reaction were mixed separately with either 0.5 ml or 1.5 ml Optimem. As transfection control, 0.05 µg

pEGFP-N1 was added to each transfection reaction. The reaction was incubated for 5 min, and then both solutions were mixed and incubated for 20 min at room temperature. The transfection mixture was gently added onto the cells and incubated for 24 h before processing for the indicated experiment.

2.8.6 Stable Transfection by Lipofectamine™ 2000

To establish stable cell lines, cells were transfected with cDNA as described above with Lipofectamine™ 2000 (see 2.8.5). The cells were re-seeded 1:5 to 1:100 24 h post-transfection under appropriate antibiotic selection to generate clones. Single-cell clones were picked using 100 µl pipette tips, transferred to 24 well plates and cultured. The clones were screened for expression levels by Western blot and the best clones used for further experiments.

2.9 Protein biochemistry methods

2.9.1 Preparation of cell pellets

PBS:
see 2.8.1

The desired confluent cells were placed on ice and the medium was removed. Afterwards the cells were washed with 5 ml 1x PBS, 1 ml 1x PBS was added to remove the cells from the plate and transferred to a 1.5 ml tube. Cells were centrifuged for 5 min at 5000 rpm, the liquid phase was removed and pellets were stored at -20°C.

2.9.2 Collection of supernatants

Culture medium:
see 2.9.1

Culture medium without FCS:
DMEM + GlutaMAX I (with 4.5 g/l glucose, without pyruvate), 2 mM L-Glutamine

1.8 x 10^6 cells/6cm dish or 5.4 x 10^6 cells/10 cm dish of the desired cells were plated in culture medium on poly-L-lysine coated plates. The next day the medium was changed and the cells were incubated in 5 ml culture medium containing 10% FCS overnight. After 18h, the supernatants were collected, centrifuged for 5 min at 2000 rpm and Aβ levels were analysed by ELISA as described in 2.9.12. After removal of the supernatants for Aβ measurement, the plates were 3x washed with 5 ml culture medium without FCS. The cells were then incubated in 5 ml culture medium containing 10 µg/ml fatty-acid-free BSA

instead of 10% FCS. After 4h, the supernatants were collected, centrifuged for 5 min at 2000 rpm and TCA precipitated as described in 2.9.7. The TCA precipitates were used for the determination of APPst, APPsα and APPsβ. To ensure equal amounts of protein content, the cells were harvested in 1ml PBS and OD_{600} was determined and all supernatants were adjusted with medium to the same OD_{600} before TCA precipitation or Aβ measurement via ELISA.

2.9.3 Cytosolic and nuclear extracts

PBS:
see 2.8.1

Buffer A:
10 mM HEPES, pH 7.9, 1.5 mM $MgCl_2$, 10 mM KCl, add fresh 0.5 mM DTT

Buffer B:
0.3 M HEPES, pH 7.9, 1.4 M KCl, 30 mM $MgCl_2$

Buffer C:
20 mM HEPES, pH 7.9, 25% v/v glycerol, 0.42 M NaCl, 1.5 mM $MgCl_2$, 0.2 mM EDTA, add fresh 0.5 mM PMSF and 0.5 mM DTT

Buffer D:
20 mM HEPES, pH 7.9, 20% v/v glycerol, 0.1 M KCl, 0.2 mM EDTA, add fresh 0.5 mM PMSF and 0.5 mM DTT

Cytosolic and nuclear extracts were prepared according to a protocol of Dignam (Dignam *et al.*, 1983). All steps were done on ice, in the cold room and in cooled centrifuges. Pelleted cells were suspended in 5 volumes of cold PBS and collected by centrifugation for 10 min at 2000 rpm. The cells were then suspended in 5 packed cell pellet volumes of buffer A and allowed to stand for 10 min on ice. The cells were collected by centrifugation as before, suspended in 2 packed cell pellet volumes (volume prior to the initial wash with buffer A) of buffer A and lysed by 10-20 strokes with a glass douncer (Wheaton). The homogenate was centrifuged for 10 min at 2000 rpm to pellet nuclei. The supernatant was carefully decanted, mixed with 0.11 volumes of buffer B, and centrifuged for 60 min at 100000 g. The high-speed supernatant from this step, designated the cytosolic fraction, was dialyzed overnight against buffer D. The cytosolic extract was frozen in liquid nitrogen and stored at -80°C.

The nuclear extract was prepared as follows. The pellet obtained from the low-speed centrifugation of the homogenate was subjected to a second centrifugation for 20 min at 25000 g, to remove residual cytoplasmic material. This pellet was designated as crude nuclei. These crude nuclei were resuspended in 3 ml of buffer C per 10^9 cells with a glass

douncer (Wheaton). The resulting suspension was stirred gently with a magnetic stirring bar for 30 min and then centrifuged for 30 min at 25000 g. The obtained clear supernatant was dialyzed against buffer D overnight. The dialysate was centrifuged at 25000 g for 20 min and the resulting precipitate discarded. The supernatant, designated the nuclear extract, was frozen as aliquots in liquid nitrogen and stored at -80°C.

2.9.4 Cytosolic extract from mouse brains

MC buffer:
10 mM HEPES(K) pH 7.6, 10 mM K-acetate, 0.5 mM Mg-acetate, 5 mM DTT, 1x protease inhibitor

The brain tissue was washed with PBS (if the tissue was frozen, this step was skipped). The weight of the brain tissue was determined and afterwards was cut into small pieces. 2 ml of MC buffer was added per 1 g of brain tissue. The brain tissue was homogenized by 25 strokes with a tight glass douncer (Wheaton). The homogenate was centrifuged for 1 hour at 100000 g at 4°C. The supernatant was collected and aliquots were stored at -80°C.

2.9.5 STEN-Lysates

STEN-Lysis:
50 mM Tris pH 7.6, 150 mM NaCl, 2 mM EDTA, 1% Triton-X100, 1:500 PI-mix in dH_2O

Pelleted cells were suspended in 300 µl (6 cm dish) or 600 µl (10 cm dish) STEN-Lysis buffer containing 1:500 PI-mix and incubated for 20 min on ice. After the incubation on ice, the suspension was centrifuged for 20 min at 13000 rpm at 4°C. The supernatant was transferred to a fresh tube and the pellet was discarded. The concentration of the STEN-lysate was measured by the BCA assay as described in 2.9.8 and analysed by SDS-PAGE (see 2.9.9) followed by Western blotting (see 2.9.10).

2.9.6 Membrane preparations for ADAM10

Hypotonic-buffer:
10 mM Tris, pH 7.4, 1 mM EDTA, 1 mM EGTA, 1:500 PI-mix in dH_2O

STEN-Lysis:
see 2.9.5

Pelleted cells were suspended in 200 µl (6 cm dish) or 400 µl (10 cm dish) hypotonic buffer and incubated for 10 min on ice. Cells were lysed by passing the suspension approximately 15 times through a 1 ml syringe (Terumo) with 0.6 mm cannula (Braun). The suspension was centrifuged for 45 min at 13000 rpm at 4°C to pellet the nuclear

fraction and the membranes. The supernatant was removed, kept as cytosolic fraction and the pellet was resuspended in 100 µl (6 cm dish) or 200 µl (10 cm dish) STEN-Lysis buffer. The suspension was incubated for 20 min on ice and centrifuged for 20 min at 13000 rpm at 4°C. The supernatant was transferred to a new tube, designated as nuclear/ membrane fraction and the pellet was discarded. The concentration of the cytosolic fraction and the nuclear/ membrane fraction were measured by the BCA assay as described in 2.9.8 and analysed by SDS-PAGE (see 2.9.9) followed by Western blotting (see 2.9.10).

2.9.7 TCA precipitation

TCA:
6.1 M in dH_2O (= 100%)

Acetone:
100% at -20°C

SDS-sample buffer (2x):
6.4% upper Tris (4x), 4% (w/v) SDS, 0.4% (w/v) DTT, 20% Glycerol, bromophenolblue

For TCA precipitation of cell supernatants (chapter 2.9.2), several portions of cell media were precipitated with 100% TCA. For this 1 ml of cell media was treated with 113 µl freshly prepared cold 100% TCA and centrifuged for 4 min at 13000 rpm. The supernatant was removed after each centrifugation step. Finally, the pellet was washed twice with 1 ml acetone (-20°C). The pellet was dried at 95°C for 2 min and dissolved in 100 µl 1x SDS-sample buffer.

For TCA precipitation of eluted proteins (see 2.9.19), 1 volume of 100% TCA was added to 4 volumes of protein eluate (e.g., to 1 ml elution fraction add 250 µl TCA). The mixture was incubated on ice for 10 min and centrifuged for 5 min at 10000 rpm. The supernatant was removed leaving the protein pellet intact. Then the protein pellet was washed twice with 200 µl ice-cold acetone and centrifuged at 13000 rpm for 5 min. The protein pellet was dried by placing the tube in a 95°C heating block for 5 min to drive off the acetone. Finally, the protein pellet was dissolved in 30 µl 1x SDS-sample buffer.

2.9.8 Protein quantification

BSA standard:
2 mg/ml BSA (Interchim)

Protein concentration of cell lysates was determined using a BCA assay (Interchim). Briefly, the standard working solution was prepared by mixing 50 volumes of reagent A with 1 volume of reagent B. Then 200 µl standard working solution was added to 10 µl

sample, mixed and incubated for 30 min at 37°C. Protein concentration was estimated by measuring the absorbance at 562 nm with a plate reader Power WaveXS (BioTex Instruments) or Smart Spec 3000 (Bio-Rad). For the preparation of a standard curve, a concentration series of BSA from 0 µg/µl to 20µg/µl was used. All samples and the calibration standards were prepared as duplicates.

2.9.9 SDS-polyacrylamide gel electrophoresis

Lower Tris (4x):
1.5 M Tris pH 8.8, 0.4% SDS (w/v) in dH_2O

Upper Tris (4x):
0.5M Tris pH 6.8, 0.4% SDS (w/v) in dH_2O

Acrylamide solution:
see 2.8.6

APS:
see 2.8.6

SDS-sample buffer (5x):
16% upper Tris (4x), 10% (w/v) SDS, 1% (w/v) DTT, 50% Glycerol, bromophenolblue

Tris-Glycine gel running buffer without SDS (10x):
250 mM Tris, 1.92 M Glycine, in dH_2O

Tris-Glycine gel running buffer (1x):
25 mM Tris, 192 mM Glycine, 0.1% SDS

To detect different proteins, cell lysates, membrane extracts or cytosolic extracts were analysed by immunoblotting. The gel electrophoresis was done according to Laemmli (Laemmli, 1970). The separation was done in a discontinuous horizontal SDS-polyacrylamide gel electrophoresis using the gel apparatus Mini-PROTEAN® Cell (Bio-Rad) filled with Tris-Glycine gel running buffer for gels with a size of 10 x 8 cm. The gels had a thickness of 1.5 mm. The concentration of the gels ranged from 8 to 15% polyacrylamide depending on the protein size (see Table 2.6).

	8% Separating gel	10% Separating gel	12% Separating gel	15% Separating gel	Stacking gel
H_2O	4.4 ml	4.0 ml	3.6 ml	3.2 ml	3.25 ml
Acrylamide-Bis (40%)	1.6	2.0 ml	2.4 ml	2.8 ml	0.5 ml
Lower Tris	2 ml	2 ml	2 ml	2 ml	-
Upper Tris	-	-	-	-	1.25 ml
TEMED	15 µl	15 µl	15 µl	15 µl	15 µl
10% APS	15 µl	15 µl	15 µl	15 µl	15 µl

Table 2.6 Composition of one thick (1.5 mm) mini gel

10-30 µg proteins were separated by SDS-PAGE dependent on the protein to be detected. Prior to SDS-PAGE, proteins were denatured by adding SDS-sample buffer and boiling for 5 min at 95°C before applying to the gel. As size marker, 5 µl SeeBlue pre-stained Protein Standard was loaded. Electrophoresis was performed at constant voltage at 70 V until all samples migrated into the stacking gel and then at 120 V. The separated proteins were analysed by Western blotting.

2.9.10 Western blot analysis

Blotting buffer (1x):
25 mM Tris, 192 mM Glycine in dH_2O

Blocking buffer:
0.2% I-Block, 0.1% Tween20 in PBS

TBST (10x):
100 mM Tris pH 7.6, 3 M NaCl, 1% Tween20 in dH_2O

TBST (1x):
10 mM Tris pH 7.6, 300 mM NaCl, 0.1% Tween20 in dH_2O

After protein separation, the proteins were transferred from the gel onto a PVDF membrane of the size of the separating gel using the Bio-Rad system. The PVDF transfer membrane was soaked in isopropanol, washed with dH_2O, and equilibrated in blotting buffer. Gel plates were opened and gels were carefully removed from the plates. The transfer membrane was placed on the gel between blotting buffer, two filter papers soaked with blotting buffer and one sponge on both sides.

Blotting assembly:

Anode plate (transparent)
Sponge equilibrated in blotting buffer
2 pieces blotting paper equilibrated in blotting buffer
membrane equilibrated in blotting buffer
SDS gel
2 pieces blotting paper equilibrated in blotting buffer
Sponge equilibrated in blotting buffer
Cathode plate (black)

The protein transfer was performed at constant current flow of 400 mA for 65 min using as blotting device the Mini Trans-Blot® Cell (Bio-Rad) filled with Tris-Glycine buffer together with an ice cube block.

After the transfer, the apparatus was disassembled. The membrane was removed and incubated for at least 1 h in blocking buffer to saturate unspecific protein binding sites. Membranes were incubated in the desired primary antibody with appropriate dilution in I-Block containing 0.02% sodium azide at room temperature for 1 h or overnight at 4°C with shaking. Afterwards the membranes were washed 4x for 15 min in 1x TBST to remove unspecific bound antibody. After washing, the membrane was incubated with the appropriate HRP-conjugated secondary antibody at the optimal concentration in blocking buffer for 1 h at room temperature. After extensive washing of the membranes with 1x TBST as described above, the protein of interest was detected with the enhanced chemiluminescence (ECL) Western blotting detection reagent (Amersham Bioscience) according to the manufacturer's description. The chemiluminescence signals were exposed on X-ray film for an appropriate time, and the films were developed using a developer machine.

For the identification of RNA-binding proteins (see method 2.9.19) via Western blotting, the proteins were bound to PVDF membranes as described above (see 2.9.10). After the transfer, the proteins were detected via chemiluminescence as described above (see 2.9.10).

2.9.11 "Stripping" of Western blots

Strip Buffer:
2% SDS, 62.5 mM Tris-HCl, pH 6.7, 100 mM β-Mercaptoethanol

The membrane is incubated in Strip-buffer for 1 h at 50°C with shaking. After 1 h, the membrane is washed 2x for 10 min in TBST and incubated in I-Block for 1 h. Then the membrane was processed as described in 2.9.10.

2.9.12 ELISA

1x Tris wash buffer:
1:10 dilution of 10x Tris wash buffer (provided by MSD)

1% Blocker A solution:
1% Blocker A (provided by MSD) in 1x Tris wash buffer

Detection antibody solution:
1x SULFO-TAG 6E10 antibody (stock provided by MSD), 1x Blocker G (stock provided by MSD) in 1% Blocker A solution

2x MSD read buffer T:
1:2 dilution of 4 MSD read buffer T (provided by MSD)

Calibrator:
serial dilution of combined Aβ1-38, Aβ1-40 and Aβ1-42 peptide standards in cell culture medium

Aβ levels of supernatants from cells were determined by an enzyme-linked immunosorbent assay (ELISA), following the manufacturer`s recommendations. Measurements were carried out using the 96-well MULTI-SPOT® Human (6E10) Abeta Triplex Assay from MSD. The 96-well plate was blocked for 1 hour at room temperature on a shaker with 150 µl/well 1% Blocker A solution. Afterwards the plate was washed 3x with 1x Tris wash buffer. 25 µl/well of detection antibody solution were added as well as 25 µl/well of supernatant or calibrator diluted in cell culture medium. The reaction was incubated for 2 hours at room temperature with shaking. Then, the wells were washed 3x with 1x Tris wash buffer. Finally, 150 µl/well of 2x MSD read buffer T was added and the plate immediately measured using the MSD Sector Imager 2400 reader. The concentration of the Aβ peptides were calculated using the MSD Discovery Workbench software.

2.9.13 Purification of GST-fusion protein

Elution buffer: 10 mM Glutathione in 50 mM Tris-HCl, pH 9.0

In order to generate GST-fusion protein, the DNA of interest was cloned downstream of and in frame with the GST gene in the pGEX-5 expression vector (see 2.6.6). Once

sequenced (see 2.6.12) and proven to be correct, the construct was transformed into the expression *E.coli* host strain BL21 (DE3) (see 2.6.8). A single colony of bacteria was grown overnight in 5 ml LB medium supplemented with 100 µg/ml ampicillin (to select for plasmid-containing bacteria). Next morning, the culture was diluted 1:100 with fresh LB medium containing 100 µg/ml ampicillin and grown for an additional 2-3 h until OD_{600} = 0.5 was reached. Expression of the GST-fused protein was induced by the addition of IPTG to a final concentration of 1 mM and the culture was grown for another 2-3 h at 37°C. The cells were harvested by centrifugation at 5000 rpm for 10 min at 4°C. The bacterial pellet was resuspended in 20 ml PBS containing 1:200 PI mix and 200 µl lysozyme (10 mg/ml) (10 µl were removed for SDS-PAGE analysis). The suspension was stirred for 30 min on ice before it was sonified (4 min: 20 sec sonification, 20 sec pause; 3 min: 30 sec sonification, 30 sec pause) (50% Duty, left 5). After sonification 1% Triton and 1:500 PI-mix were added and stirred again for 30 min on ice (10 µl were removed for SDS-PAGE analysis). Cell debris (10 µl were removed for SDS-PAGE analysis) was removed by centrifugation at 10000 rpm for 20 min. The supernatant containing the protein (10 µl were removed for SDS-PAGE analysis) was incubated with 600 µl Glutathione-sepharose 4B by rotation for 2 h at RT or overnight at 4°C. Afterwards, the suspension was centrifuged for 10 min at 6000 rpm at 4°C and the supernatant (10 µl were removed for SDS-PAGE analysis) was discarded. In order to remove unbound material, the sepharose was washed 3 times in PBS containing 0.5% Triton by 5 min centrifugation at 6000 rpm at 4°C. The sepharose was resuspended in 5 ml PBS and loaded on a Poly-Prep® chromatography column (Bio-Rad). The column was washed with 10 ml PBS before the specific GST fusion protein was eluted by incubation of the beads for 10 min at room temperature with 10x 1 ml elution buffer. SDS-PAGE (see 2.9.9) and subsequent Coomassie staining (see 2.9.15) estimated the amount and purity of the isolated protein. Usually 20 µl of each fraction were loaded per lane. The correct fraction were pooled and dialysed against PBS.

2.9.14 Purification of His-tagged fusion-protein

Lysis buffer: 20 mM Tris-HCl pH 8.0, 1 M KCl, 0.25% NP40, 1 mM PMSF, 10 µg/ml Leupeptin

Buffer A: 24 mM Tris-HCl pH 8.0, 1.5 mM $MgCl_2$, 1M KCl, 5% glycerol

Buffer B: 1 M KCl, 20 mM Tris-HCl, 5% glycerol, 1 mM EDTA, 1 mM DTT

Elution buffer: buffer A containing 500 mM imidazole

In order to generate His-tagged fusion-protein, the DNA of interest was cloned downstream of and in frame with the His-tag in the pET28a expression vector (see 2.6.6). Once sequenced (see 2.6.12) and proven to be correct, the construct was transformed into the expression *E.coli* host strain BL21 (DE3) (see 2.6.8). A single colony of bacteria was grown overnight in 5 ml LB medium supplemented with 50 µg/ml kanamycin (to select for plasmid-containing bacteria). Next morning the culture was diluted 1:100 with fresh LB medium containing 50 µg/ml kanamycin and grown for an additional 2-3 h until OD_{600} = 0.5 was reached. Expression of the His-tagged fusion-protein was induced by the addition of IPTG to a final concentration of 1 mM and the culture was grown for another 3 h at 30°C. The cells were harvested by centrifugation at 5000 rpm for 10 min at 4°C. The bacterial pellet was resuspended in 5 ml lysis buffer (10 µl were removed for SDS-PAGE analysis) and sonified on ice (4 min: 20 sec sonification, 20 sec pause; 3 min: 30 sec sonification, 30 sec pause) (50% Duty, left 5). After sonification, 10 µl were removed for SDS-PAGE analysis and cell debris (10 µl were removed for SDS-PAGE analysis) was removed by centrifugation at 10000 rpm for 30 min at 4°C. The supernatant containing the protein (10 µl were removed for SDS-PAGE analysis) was incubated with 500 µl Ni-NTA agarose (Qiagen) by rotation for 2 h at RT or overnight at 4°C. The Ni-NTA agarose was washed twice with buffer A before the addition of the protein. In order to remove unbound material, the agarose was washed 3 times in buffer A by 5 min centrifugation at 6000 rpm at 4°C. The agarose was resuspended in 5 ml buffer A and loaded on a Poly-Prep® chromatography column (Bio-Rad). The column was washed with 10 ml buffer A before the specific His-tagged fusion-protein was eluted by incubation of the beads for 10 min at room temperature with 10x 1 ml elution buffer. The amount and purity of the isolated protein was estimated by SDS-PAGE (see 2.9.9) and subsequent Coomassie staining (see 2.9.15). Usually 20 µl of each fraction were loaded per lane. The correct fractions were pooled and dialysed against buffer B.

The group of Ostareck and Ostareck-Lederer has kindly provided recombinant His-hnRNP K and His-hnRNP E1 (Ostareck *et al.*, 1997).

2.9.15 Coomassie Blue Staining

Coomassie Brilliant Blue R staining solution:
25% Isopropanol, 1% acetic acid, 0.1% Coomassie Brilliant Blue R in dH_2O

Destaining solution:
5% Isopropanol, 7% acetic acid in dH_2O

Immediately after gel electrophoresis (see 2.9.9), gels were placed into Coomassie Brilliant Blue R staining solution and gently shaken at room temperature for 1 h followed by destaining in destaining solution until the background was clear. The gels were shortly washed with water and then dried for 3 h at 60°C on a gel dryer.

2.9.16 RNA/Protein UV-crosslinking

β-Mercaptoethanol:
3 M β-Mercaptoethanol (stock: 14.3 M)

Reaction buffer:
40 mM Tris pH 7.4, 60 mM KCl, 5 mM $MgCl_2$, 1 mM spermidine

Heparin:
125 mg/ml

RNase T1:
10 U/µl

RNase A:
0.55 U/µl

15 µg cytoplasmic or nuclear extract, prepared from HEK293E cells, were pre-treated with 200 mM β-mercaptoethanol at room temperature for 10 min and filled up with H_2O to a final volume of 15 µl. The treated extracts were then added to 6 µl reaction buffer supplemented with 0.75 mM ATP, 0.75 mM GTP, and the non-specific competitors poly d(I-C) (0.1 µg/µl) and tRNA (1 µg/µl), and preincubated at room temperature for 10 min. The radiolabelled RNA was then added, and incubation continued for 25 min at room temperature to allow the formation of specific RNA-protein complexes. Subsequently, 5 mg/ml heparin was added to remove weak and unspecific RNA-protein interactions, and the incubation continued for 10 min at room temperature. The samples were then exposed to UV irradiation (254 nm) for 25 min on ice (UVP Ultraviolet products, 8W Model UVLMS, 10 cm distance from source). The crosslinked RNA-protein complex was digested with RNase T1 (10 U/µl) and RNase A (0.055 U/µl) at room temperature for 15 min. Samples were heated to 95°C in protein sample buffer for 5 min, and resolved by SDS-PAGE. The results were obtained by autoradiography.

2.9.17 Non-denaturing 3.5% polyacrylamide gel for RNA-EMSAs

10x TBE:
see 2.7.6

Acrylamide solution:
see 2.7.6

APS:
see 2.7.6

Mix the following components for a 3.5% polyacrylamide gel solution:

for 15 ml	Component
1.5 ml	10x TBE
1.3 ml	40% Acrylamide-Bis
12.2 ml	DEPC-H_2O

The gel solution was stirred at room temperature until the urea was completely dissolved and then the following was added:

120 µl	10% APS
16 µl	TEMED

After addition of the last two ingredients, which catalyse polymerization, the gel solution was mixed briefly and poured immediately.

2.9.18 RNA-Electrophoretic mobility shift assay

Reaction buffer:
see 2.9.16

Heparin:
see 2.9.16

TBE (10x):
see 2.7.6

Non-denaturing polyacrylamide gel (3.5%):
see 2.9.17

15 µg cytoplasmic or nuclear extract, prepared from HEK293E cells, or 4 µg of recombinant protein were pre-treated with 200 mM β-mercaptoethanol at room temperature for 10 min and filled up with H_2O to a final volume of 15 µl. The treated extract and recombinant protein were then added to 6 µl reaction buffer supplemented with 0.75 mM ATP, 0.75 mM GTP, and the non-specific competitors poly d(I-C) (0.1 µg/µl) and tRNA (1 µg/µl), and preincubated at room temperature for 10 min. After addition of radiolabelled RNA, incubation continued for 25 min at room temperature to allow the

formation of specific RNA-protein complexes. Subsequently, 5 mg/ml heparin was added, and the incubation continued for 10 min at room temperature. Samples were heated to 95°C in 7 µl Gel Loading Buffer II (Ambion) containing xylene cyanol and bromophenol blue for 2 min, and resolved on a non-denaturing 3.5% polyacrylamide gel (2.9.17). The loading buffer served as size marker. On a 3.5% non-denaturing polyacrylamide gel xylene cyanol runs at around 460 nucleotides and bromophenol blue at around 100 nucleotides (Sambrook *et al.*, 1989). Electrophoresis was performed in 1x TBE at constant voltage at 100 V. The results were obtained by autoradiography.

2.9.19 Isolation of RNA-binding proteins with biotinylated RNA probes

Protein-binding buffer:
10% glycerol, 10 mM Hepes pH 7, 50 mM KCl, 1 U/ml RNase Inhibitor, 0.15 µg/ml yeast tRNA, 1 mM EDTA, 1 mM DTT, 0.5% Triton X-100

First, 2.5 ml of heparin agarose, type I were prewashed 3x with 5 ml of protein-binding buffer. Following the last wash, 4 ml protein-binding buffer and 6 mg cytosolic cell extract was added to the heparin agarose and rotated at 4°C for 1 h. The heparin agarose was removed by centrifugation at 2000 rpm for 5 min at 4°C. The precleared extract was incubated with 250 µl streptavidin agarose on a rotator at 4°C for 1 h. The streptavidin agarose was washed 3x with 500 µl of protein-binding buffer before usage. After the incubation with the cytosolic extract, the streptavidin agarose was removed by centrifugation for 5 min at 2000 rpm at 4°C. 400 pmol biotinylated RNA probe in a final volume of 100 µl containing 50 mM KCl was incubated with 100 µl of µMACS Streptavidin MicroBeads for 1 h at room temperature. The reaction mixture was incubated with the precleared cytosolic cell extract for 1 h at 4°C on a rocking platform. Following the binding reaction, a µColumn was placed in the magnetic field of the µMACS separator and prepared by washing 2x with 100 µl of equilibration buffer for protein applications. In addition, the column was rinsed with 2x 100 µl of protein-binding buffer. The entire binding reaction was added to the column held within a µMACS Separator. Once the entire incubation reaction had flowed through the column, the column was washed 4x with 200 µl of the protein-binding buffer to remove non-specifically bound molecules. Bound proteins were finally eluted with 200 µl protein-binding buffer supplemented with 1 M NaCl. Finally, eluted proteins were TCA precipitated according to 2.9.7 and loaded onto a SDS-gel according to 2.9.9. Proteins were detected by Western blotting according to 2.9.10 or by Silver staining according to 2.9.20.

2.9.20 Silver Staining

Sensitizing solution:
30 ml ethanol, 10 ml Sensitizer, up to 100 ml ultrapure water

Staining solution:
1 ml Stainer, up to 100 ml ultrapure water

Developing solution:
10 ml Developer, 1 drop Developer enhancer, up to 100 ml ultrapure water

After electrophoresis, the gel was removed from the cassette, placed in a clean staining tray of the appropriate size and silver stained following the SilverQuest^{TM} Silver Staining Kit (Invitrogen) protocol. The gel was briefly rinsed with ultrapure water and fixed in 100 ml fixative solution in a 15 cm Petri dish for at least 20 min with gentle rotation. The fixative solution was decanted and the gel was washed in 30% ethanol for 10 min, followed by 100 ml of sensitizing solution for 10 min. Afterwards, the gel was washed in 100 ml of 30% ethanol for 10 min, followed by 100 ml ultrapure water for 10 min. The gel was incubated in 100 ml of staining solution for 15 min. The staining solution was decanted and the gel was washed with 100 ml ultrapure water for 20-60 s. Then the gel was incubated in 100 ml of developing solution for 4-8 min until bands started to appear and the desired band intensity was reached. Once the appropriate staining intensity was achieved, 10 ml of stopper solution was added to the gel. The gel was gently agitated for 10 min and the colour changes from pink to colourless indicated that the development had stopped. Finally, the stopper solution was decanted, the gel was washed with 100 ml of ultrapure water for 10 min and given to mass spectrometry analysis (stored in fresh ultrapure water) (refer to 2.9.21).

2.9.21 Mass spectrometry analysis

After silver staining, mass spectrometry analysis was performed to identify RNA-binding proteins. Mass spectrometry analysis was performed by Ignasi Forne at the protein analysis unit at the Adolf-Butenandt Institute of the Ludwig-Maximilians-University in Munich.

Gel bands were manually excised and placed in a 96-well digestion plate (Proxeon Biosystems). A multiscreen vacuum manifold (Millipore) was used to digest samples with trypsin as described before (Shevchenko *et al.*, 2000; Wilm *et al.*, 1996) with minor modifications. First, gel slices were washed twice with 100 µl of ultrapure H_2O, 3 times with 100 µl of 25 mM NH_4HCO_3 and dehydrated by washing them 3 times with 100 µl of acetonitrile. Gel slices were then incubated for 1 h with 50 µl of 10 mM DTT in 25 mM

NH_4HCO_3. Afterwards slices were incubated for 30 min in a dark place with 50 µl of 55 mM iodoacetamide in 25 mM NH_4HCO_3 to carbamidomethylate the reduced cysteines. Gel fragments were washed with 100 µl of 25 mM NH_4HCO_3 and dehydrated again with 100 µl of acetonitrile. 10 µl of 25 ng/ml trypsin (Promega) dissolved in 25 mM NH_4HCO_3 were added to each gel slice, depending on the volume of the excised spot, incubated 45 min at 4ºC and then the non-absorbed trypsin was removed. Gel fragments were covered with 25 mM NH_4HCO_3 and digestion took place for 16 h at 30ºC. For the peptide extraction, gel slices were washed twice with 50 µl of acetonitrile/ultrapure H_2O 1/1 0.25% TFA and twice more with 50 µl of acetonitrile. The resulting liquid containing the digested peptides was totally evaporated. The peptides were redissolved with 10 µl of 0.1% formic acid and stored at -20 ºC until further processing.

For the mass spectrometry analysis, 8 µl were injected in an Ultimate 3000 HPLC system (LC Packings) and desalted on-line in a C18 micro column (75 µm i.d. x 15 cm, packed with C18 PepMap™, 3 µm, 100 Å by LC Packings). The desalted sample was then separated in a 15 cm analytical column C18 micro column (75 µm i.d., packed with C18 PepMap™, 3 µm, 100 Å by LC Packings) with a 40 min gradient from 5 to 60% acetonitrile in 0.1% formic acid. The effluent from the HPLC was directly electrosprayed into a LTQ-Orbitrap mass spectrometer (Thermo). The MS instrument was operated in data-dependent mode to automatically switch between full scan MS and MS/MS acquisition. Survey full scan MS spectra (from m/z 300 – 2000) were acquired in the Orbitrap with resolution R=60000 at m/z 400 (after accumulation to a 'target value' of 500000 in the linear ion trap). The six most intense peptide ions with charge states between 2 and 4 were sequentially isolated to a target value of 10000 and fragmented in the linear ion trap by collision-induced dissociation (CID). All fragment ion spectra were recorded in the LTQ part of the instrument. For all measurements with the Orbitrap detector, 3 lock-mass ions from ambient air (m/z=371.10123, 445.12002, 519.13882) were used for internal calibration as described before (Olsen *et al.*, 2005). Typical mass spectrometry conditions were: spray voltage of 1.5 kV; no sheath and auxiliary gas flow; heated capillary temperature of 200ºC; normalised collision energy of 35% for CID in LTQ. The ion selection threshold was 10000 counts for MS2. An activation q = 0.25 and activation time of 30 ms were used.

Each individual thermo binary .raw file was searched with Mascot against the Swissprot database (versions 52.2-57.10). Typical search parameters were peptide mass tolerance of 10 ppm, fragment tolerance of 0.5 Da, enzyme was set to trypsin (allowing up

to two missed cleavages), static modification, carbamidomethylated cysteine (+57.0215 Da), variable modifications and methionine oxidation (+15.9949 Da). All searches were performed considering a maximum of +3 charges for the precursor ion.

3 Results

3.1 RNA-protein-binding studies

3.1.1 Electrophoretic Mobility Shift Assay with cytosolic and nuclear extract of HEK293E cells

In initial experiments, *in vitro*-transcribed ADAM10 5`UTR and BACE1 5`UTR RNA (as defined in Figure 2.1) (referred to as ADAM10 5`UTR and BACE1 5`UTR throughout this thesis) were used to study RNA-protein interactions, which possibly contribute to the regulation of the ADAM10 and/or BACE1 expression. First, EMSAs were performed to detect putative 5´UTR-binding proteins.

To do so, cytosolic and nuclear extracts from HEK293E cells were prepared according to a well-established protocol (Dignam *et al.*, 1983). To provide conclusive evidence that the cytosolic preparation was free of nuclear proteins, the absence of b-Myb, a specific nuclear marker (Takemoto *et al.*, 1994), was demonstrated (Figure 3.1). To control the quality of the nuclear extract, the absence of tubulin, a specific cytosolic marker (Willingham *et al.*, 1980), was proven (Figure 3.1).

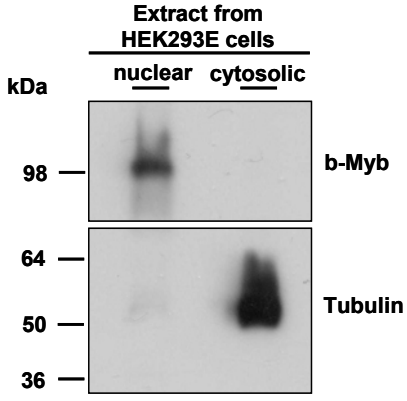

Figure 3.1 Quality control of nuclear and cytosolic extracts of HEK293E cells.
Nuclear and cytosolic extracts of HEK293E cells were separated on an 8% SDS gel and analysed by Western blot with the anti-b-Myb or anti-tubulin antibody as indicated. In the upper panel the anti-b-myb antibody detects a specific signal in the nuclear extract but not in the cytosolic extract. In the lower panel the anti-tubulin antibody detects a specific signal in the cytosolic extract but not in the nuclear extract, indicating that the cytosolic fraction is not contaminated with nuclear proteins and vice versa.

In a next step, ADAM10 5`UTR and BACE1 5`UTR RNA were prepared. Several reactions with different amounts of limiting nucleotide (mixture of labelled and unlabelled form of that nucleotide) were setup to find the optimal conditions for the generation of the ADAM10 5`UTR and BACE1 5`UTR (refer to 2.7.1). The loading buffer containing xylene cyanol and bromophenol blue served as size marker. On a 5% denaturing

polyacrylamide / 8M urea gel xylene cyanol runs around 130 nucleotides and bromophenol blue at around 35 nucleotides (Sambrook *et al.*, 1989).

The *in vitro* transcription setup in presence of 3.125 µM α^{32}P-CTP and 10 µM CTP for the ADAM10 5`UTR (Figure 3.2A) and of 3.125 µM $\alpha^{32}$P-UTP and 10 µM UTP for the BACE1 5`UTR (Figure 3.2B) were used for further experiments. These reaction setups showed an optimal combination of high specific activity and synthesis of full-length probe.

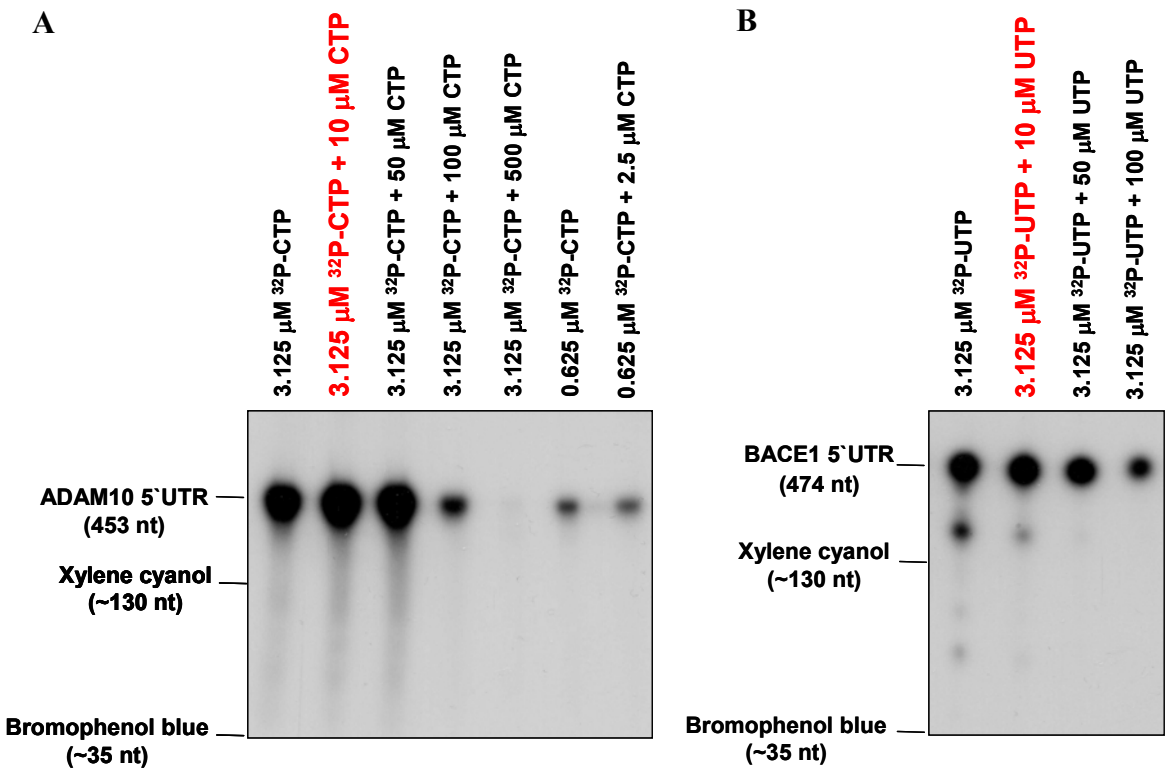

Figure 3.2 Effect of limiting nucleotide concentration on ADAM10 5`UTR and BACE1 5`UTR transcription.
An aliquot of several reactions of *in vitro*-transcribed ADAM10 (A) and BACE1 (B) 5`UTR RNA were analysed on 5% denaturing polyacrylamide / 8M urea gels and detected by autoradiography. The *in vitro*-transcribed ADAM10 and BACE1 5`UTR RNA is 453 and 474 nucleotides long, respectively (as explained in Figure 2.1). The xylene cyanol (~ 130 nt) and bromophenol blue (~ 35 nt) front on the gel served as size marker. The reaction setup used for further experiments is highlighted in red.

In order to analyze the effect of the 5`cap on protein binding, EMSAs were performed with capped and non-capped 5`UTR. Capped and non-capped α^{32}P-labelled *in vitro* transcripts of the ADAM10 5`UTR or BACE1 5`UTR (shown in Figure 3.3A) were incubated with 15 µg cytosolic extract of HEK293E cells (Figure 3.3B). Following the incubation, 5 µg/µl heparin was added to remove unspecifically bound proteins from the RNA. Heparin is a polyanion that is used to eliminate nonspecfic RNA-protein interactions (Tanguay and Gallie, 1996). Subsequently, the RNA-protein complexes were

analysed on a 3.5% non-denaturing polyacrylamide gel and visualized by autoradiography (Figure 3.3B). The loading buffer containing xylene cyanol and bromophenol blue served as size marker. On a 3.5% non-denaturing polyacrylamide gel xylene cyanol runs at around 460 nucleotides and bromophenol blue at around 100 nucleotides (Sambrook *et al.*, 1989).

The formation of a RNA-protein complex is visible in the gel through a delayed running behaviour of this complex (shift) in comparison to the free RNA (Figure 3.3B). Figure 3.3B demonstrates that the free labelled probes of ADAM10 and BACE1 5`UTR RNA have a faster-running behaviour than the 5`UTRs of ADAM10 and BACE1, which were incubated with cytosolic extract. The results presented in Figure 3.3B suggest that proteins may bind to the 5`UTR of ADAM10 and BACE1 mRNA. The binding was independent of the 5`cap. Hence, future studies were performed without 5`cap.

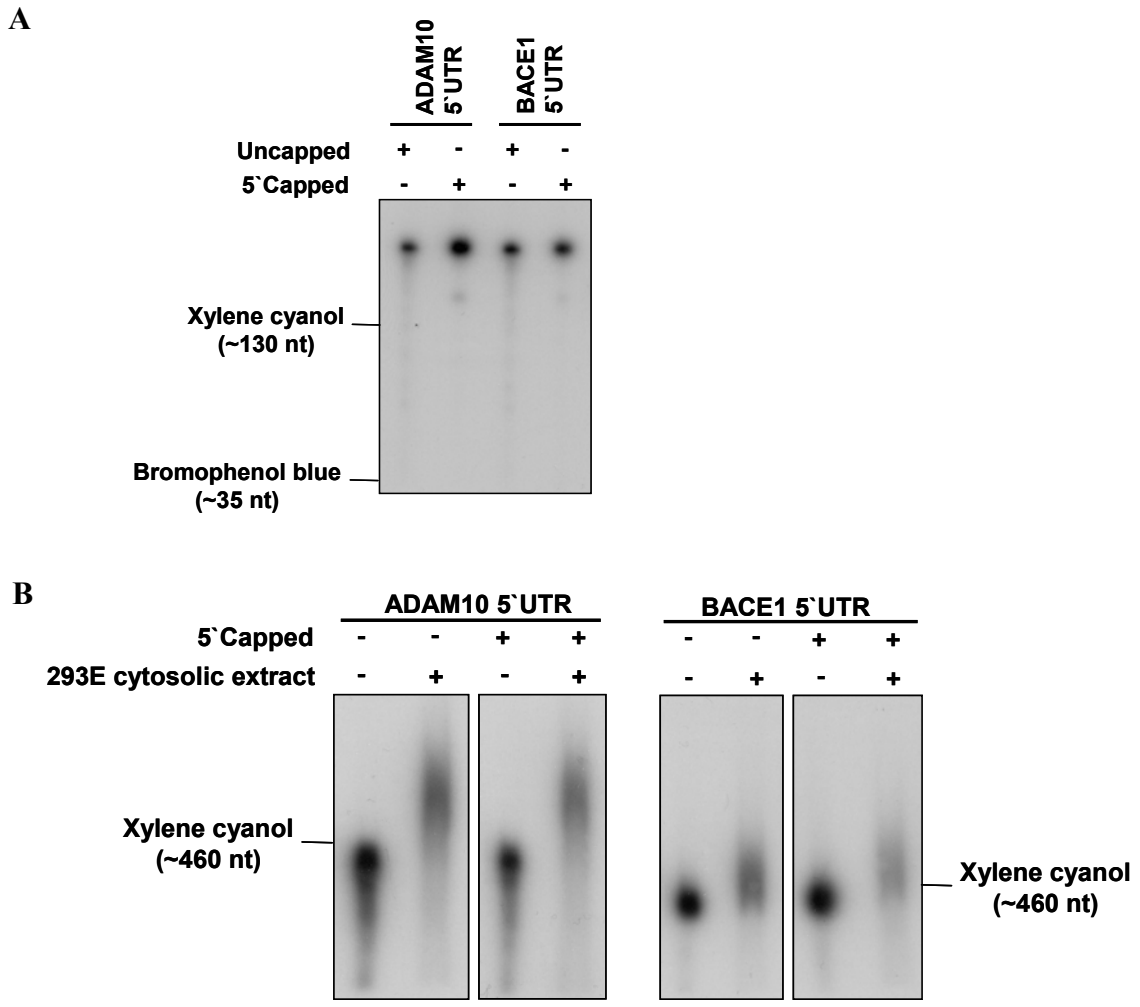

Figure 3.3 Cytosolic proteins bind to the 5`UTRs of ADAM10 and BACE1.
(A) An aliquot of the *in vitro*-transcribed α^{32}P-labelled 5`capped or uncapped ADAM10 and BACE1 5´UTR RNA was analysed on a 5% denaturing polyacrylamide / 8M urea gel to control the quality of the RNA. The xylene cyanol (~ 130 nt) and bromophenol blue (~ 35 nt) front on the gel served as size marker. (B) $10^6$ cpm $\alpha^{32}$P-labelled 5`capped or uncapped ADAM10 or BACE1 5'UTR RNA probe was incubated with 15 µg cytosolic extract from HEK293E cells in binding buffer for 30 min at room temperature. RNA-protein complexes were separated on a 3.5% non-denaturing polyacrylamide gel and visualized by autoradiography. The xylene cyanol front (~ 460 nt) on the gel served as size marker. Upon incubation of the RNA with the cytosolic extract, a shift of the RNA is visible in the gel.

In a similar experiment, the ADAM10 5`UTR RNA (shown in Figure 3.4A) was incubated with 15 µg cytosolic or nuclear extract in the presence or absence of heparin (Figure 3.4B/C). As expected, the ADAM10 5`UTR also formed an RNA-protein complex with the nuclear extract (Figure 3.4C). Omitting the heparin treatment resulted in a more delayed running behaviour because of nonspecific RNA-protein interactions (Figure 3.4B/C). Thus, these data indicate that heparin treatment is necessary to avoid unspecific binding of cytosolic and nuclear proteins to the 5`UTR of ADAM10.

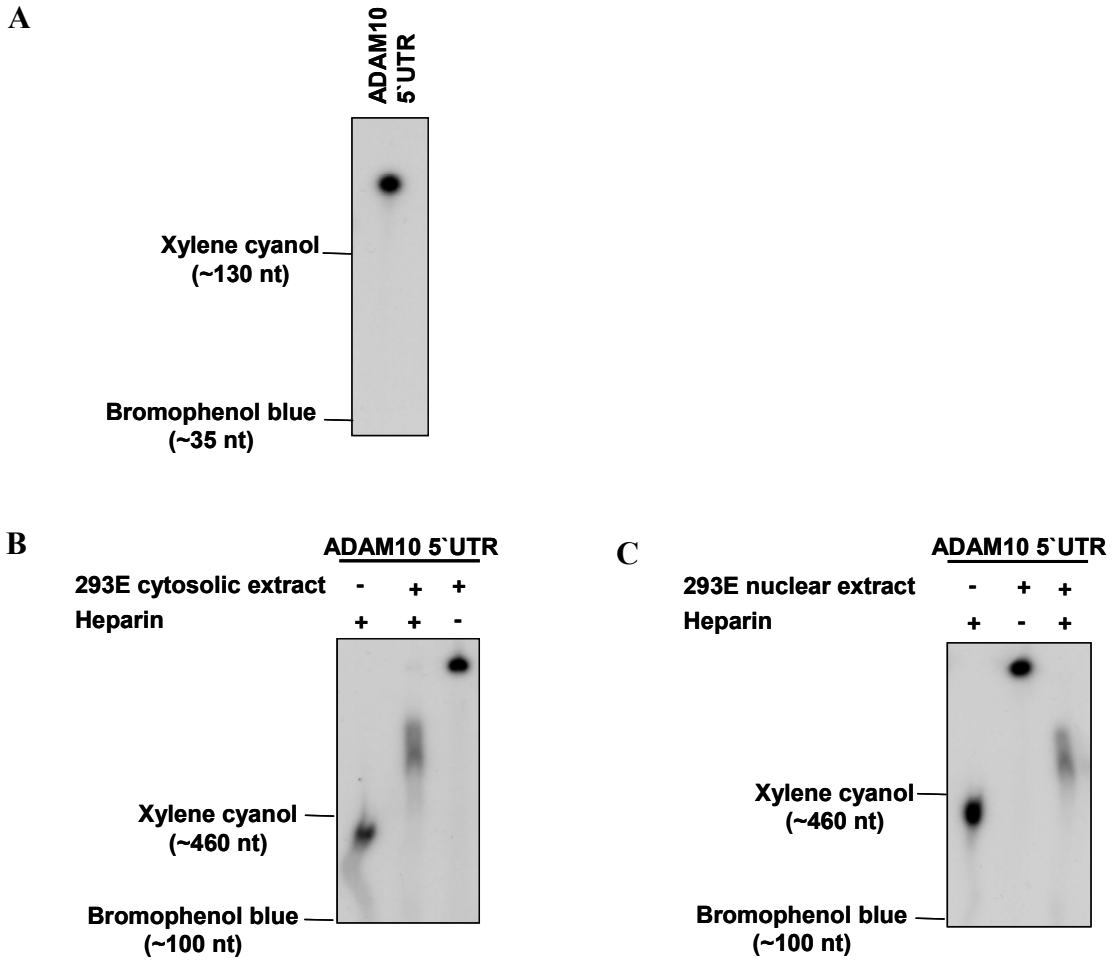

Figure 3.4 Heparin influences the binding of cytosolic proteins to the ADAM10 5`UTR. (A) An aliquot of *in vitro*-transcribed α^{32}P-labelled ADAM10 5´UTR RNA was analysed on a 5% denaturing polyacrylamide / 8M urea gel to control for RNA quality. The xylene cyanol (~ 130 nt) and bromophenol blue (~ 35 nt) front on the gel served as size marker. (B) 10^6 cpm α^{32}P-labelled ADAM10 5`UTR was incubated with 15 µg cytosolic (B) or nuclear (C) cell extract in binding buffer for 30 min at room temperature and subsequently treated with 5 µg/µl heparin as indicated. RNA-protein complexes were separated on a 3.5% non-denaturing polyacrylamide gel and visualized by autoradiography. The xylene cyanol (~ 460 nt) and bromophenol blue (~ 100 nt) front on the gel served as size marker. The incubation of RNA with cytosolic or nuclear cell extracts induced a shift due to cytosolic proteins binding to the ADAM10 5`UTR. Omitting the heparin treatment resulted in a more delayed running behaviour due to unspecifically bound proteins.

3.1.2 EMSA with cytosolic mouse brain extract

To provide *in vivo* evidence, cytosolic brain extract of postnatal-day 30 (P30) was prepared to identify possible RNA-binding proteins which bind to the 5`UTR of ADAM10 and/or BACE1. To control the quality of the cytosolic extract of P30 mice brains, extracts were analysed by Western blot with anti-histone H3, a specific nuclear antibody, and anti-tubulin antibody. This analysis revealed that the cytosolic extract was free of nuclear proteins and can be used for further experiments (Figure 3.5).

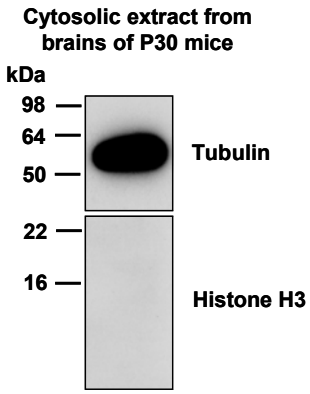

Figure 3.5 Quality control of cytosolic extract from brains of P30 mice.
Cytosolic extract of P30 mice brain was separated on a 15% gel and analysed by Western blot with anti-histone H3 or anti-tubulin antibody as indicated. In the upper panel the tubulin antibody detects a specific signal in the cytosolic extract. In the lower panel the histone H3 antibody reveals no signal which shows that the cytosolic extract is not contaminated with nuclear proteins.

In analogy to the experiments with the HEK293E cytosolic extract, the labelled *in vitro* transcript of the human ADAM10 5`UTR (Figure 3.6A) was incubated with 15 µg cytosolic extract from P30 mice brains (Figure 3.6B). Subsequently, the RNA-protein complex was analysed on a 3.5% non-denaturing polyacrylamide gel and visualized by autoradiography. The formation of an RNA-protein complex of the ADAM10 5`UTR and the cytosolic extract from the brains of P30 mice was visible in the gel through a delay in the running behaviour in comparison with the free RNA. Interestingly, the running behaviour of the RNA-protein complex from the P30 mice brain cytosolic extract (Figure 3.6B) differs from the running behaviour of the RNA-protein complex formed with the HEK293E cytosolic extract (Figure 3.3). An explanation for this might be that the protein composition binding to the ADAM10 5`UTR differs between the cytosolic extract from P30 mice brains and HEK293E cells.

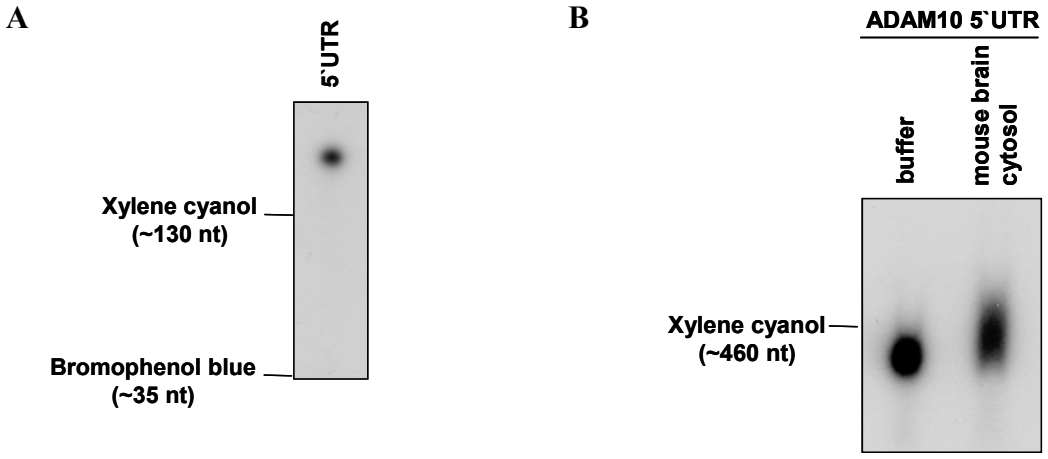

Figure 3.6 Cytosolic proteins from brains of P30 mice bind to the ADAM10 5`UTR.
(A) An aliquot of *in vitro*-transcribed α^{32}P-labelled ADAM10 5´UTR RNA was analysed on a 5% denaturing polyacrylamide / 8 M urea gel to control for RNA quality. The xylene cyanol (~ 130 nt) and bromophenol blue (~ 35 nt) front on the gel served as size marker. (B) 10^6 cpm α^{32}P-labelled human ADAM10 5'UTR RNA was incubated with 15 µg cytosolic extract from brains of P30 mice in binding buffer for 30 min at room temperature. RNA-protein complexes were separated on a 3.5% non-denaturing polyacrylamide gel and visualized by autoradiography. The xylene cyanol (~ 460 nt) front on the gel served as size marker.

3.1.3 Electrophoretic mobility shift assays with ADAM10 5`UTR deletion constructs

Recently, our laboratory could show that deletion of the first half of the ADAM10 5`UTR (Δ1-259) revealed an approximately 100-fold increase in ADAM10 protein expression in HEK293E cells while ADAM10 mRNA levels were only slightly increased (Lammich *et al.*, 2010). In contrast to these findings, deletion of the second half of the ADAM10 5`UTR (Δ251-432) resulted in decreased ADAM10 protein levels accompanied by a similar reduction of ADAM10 mRNA levels (Lammich *et al.*, 2010). These results indicate that the first half of the 5`UTR contains inhibitory elements for translation while the second half of the 5`UTR of ADAM10 might be important for mRNA stability and efficient translation of ADAM10 (Lammich *et al.*, 2010). RNA-binding proteins might bind to these regions and could be involved in this regulation.

In order to identify possible protein-binding sites within the 5`UTR of ADAM10, different parts of the 5`UTR were used in EMSA experiments. The ADAM10 5`UTR was divided into two halves namely Δ1-259 and Δ251-432 (Figure 3.7A). The formation of a RNA-protein complex was observed for the full-length and the Δ251-432 ADAM10 5`UTR (Figure 3.7C). In contrast, no RNA-protein complex was formed with the ADAM10 5`UTR lacking the first 259 nucleotides (Figure 3.7C). These data demonstrate

that cytosolic proteins bind to the first part of the 5`UTR of ADAM10 mRNA but not to the second half.

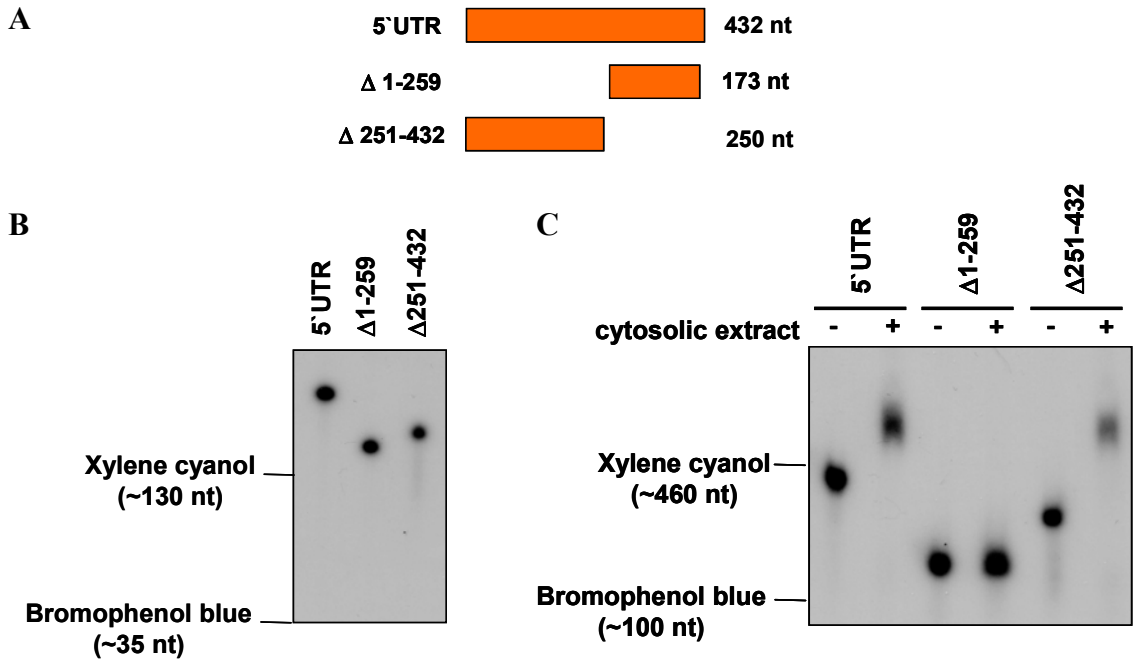

Figure 3.7 Binding of cytosolic proteins to the first half of the ADAM10 5`UTR.
(A) Representation of the ADAM10 deletion constructs. Schematic representation of the ADAM10 5`UTR, the Δ1-259 and the Δ251-432 ADAM10 5`UTR utilized in the EMSA experiments. All ADAM10 5`UTR constructs lack the last 12 nucleotides (see Figure 2.1A). (B) An aliquot of *in vitro*-transcribed α^{32}P-labelled ADAM10 5´UTR RNA was analysed on a 5% denaturing polyacrylamide / 8M urea gel to control for RNA quality. The xylene cyanol (~ 130 nt) and bromophenol blue (~ 35 nt) front on the gel served as size marker. (C) 10^6 cpm of radiolabelled RNA of full-length, Δ1-259 and Δ251-432 ADAM10 5`UTR was incubated with 15 µg cytosolic cell extract. RNA-protein complexes were separated on a 3.5% non-denaturing polyacrylamide gel and visualized by autoradiography. The xylene cyanol (~ 460 nt) and bromophenol blue (~ 100 nt) front on the gel served as size marker. The incubation of the full-length and the Δ251-432 RNA with cytosolic cell extract induced a shift due to binding of proteins. In case of the Δ1-259 ADAM10 5`UTR no protein binding was detectable.

3.1.4 UV crosslinking with cytosolic and nuclear extracts

To provide further evidence that proteins bind to the 5`UTR of ADAM10, a series of UV crosslinking studies were performed. *In vitro*-transcribed radiolabelled 5'UTR RNA of ADAM10 or BACE1 (as control for selectivity) was incubated with 15 µg cytosolic or nuclear extract from HEK293E cells. RNA and cell extract were incubated in the presence of an excess of poly d(I-C) and tRNA. After treatment with 5 µg/µl heparin to remove weak and instable unspecific RNA-protein interactions, RNA bound proteins were covalently crosslinked with UV light at 254 nm for 25 min on ice. Subsequently, the samples were treated with RNase T_1 and RNase A. RNase T_1 cleaves single-stranded RNA after G-residues near double-stranded RNA whereas RNase A cleaves single-

stranded RNA at the 3`end of pyrimidine residues (C or U). RNA nucleotides that are not involved in the RNA-protein complex and therefore not protected by the bound protein were removed by this treatment. RNase-protected RNA-protein complexes were separated on an 8% SDS gel and visualized by autoradiography. Interaction of ADAM10 5`UTR with cytosolic proteins resulted in the formation of at least four UV-crosslinked RNA-protein complexes in the region between 36 and 98 kDa (Figure 3.8A). For the ADAM10 5`UTR incubated with nuclear extract at least two protein bands were detected in the region of 36 to 64 kDa (Figure 3.8A). Importantly, all protein bands were only detected in the presence of extract and were dependent on UV crosslinking (Figure 3.8A).

In addition, the BACE1 5`UTR was analysed in an effort to prove the specificity and selectivity of the RNA-binding proteins. The data in Figure 3.8B indicate binding of several proteins to the BACE1 5`UTR. Again, the protein binding is dependent on UV irradiation.

In summary, the results show that several proteins bind to the ADAM10 and BACE1 5`UTR. However, the protein band patterns detected differ. Hence, the detected proteins seem to bind in a selective way to the 5`UTRs of ADAM10 and BACE1.

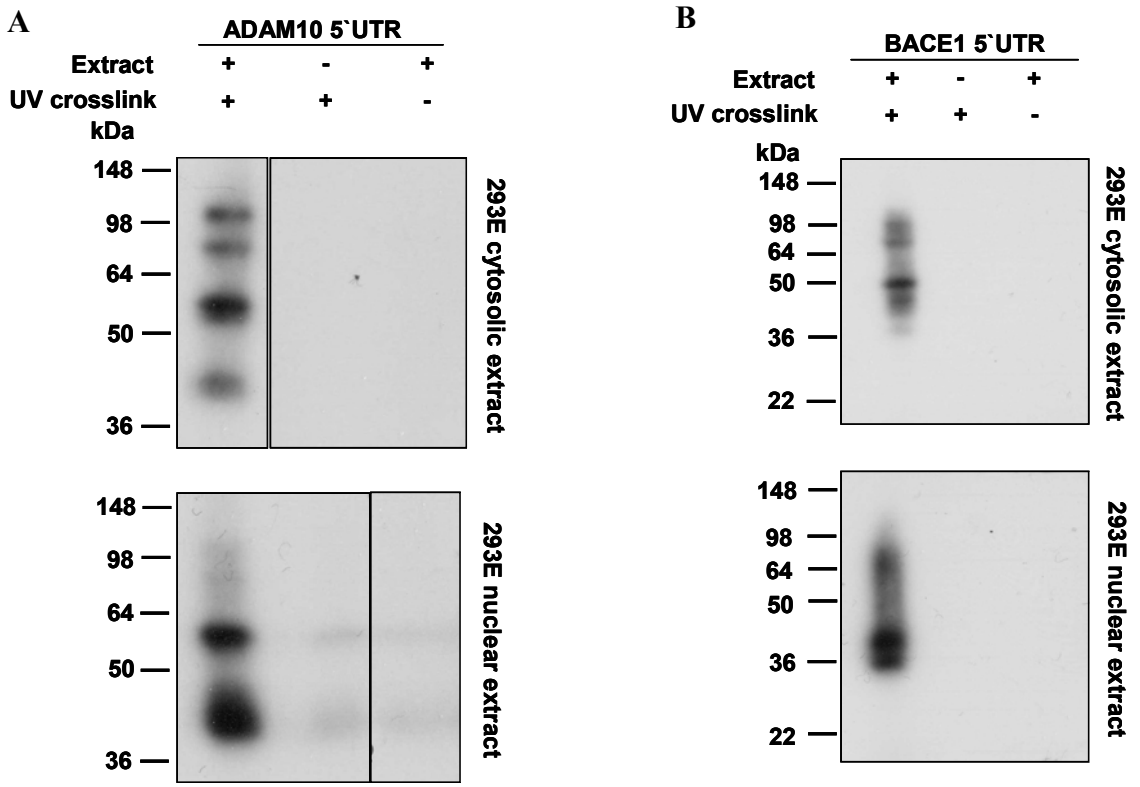

Figure 3.8 Crosslinking of cytosolic and nuclear proteins to the ADAM10 5`UTR or BACE1 5`UTR.

UV-crosslinking experiments of 10^6 cpm radiolabelled *in vitro*-transcribed 5'UTR mRNA of ADAM10 (A) or BACE1 (B) were performed in the presence or absence of HEK293E cytosolic or nuclear extract. After RNase digestion, the protected RNA-protein complexes were separated on an 8% SDS gel and visualized by autoradiography. (A) For the ADAM10 5`UTR incubated with 15 µg cytosolic extract of HEK293E cells at least 4 protein bands in the region of 36 to 98 kDa were detected. In contrast with nuclear extract, only 2 protein bands in the region of 36 to 64 kDa were detected. (B) The BACE1 5`UTR incubation with cytosolic or nuclear extract of HEK293E cells following UV light treatment results in binding of several protein bands. For (A) and (B) the reaction set ups without extract or no UV light treatment revealed no protein bands on the gel. All reactions for ADAM10 5`UTR and cytosolic extract and ADAM10 5`UTR and nuclear extract were run on one gel, respectively. The lanes were separated by other reactions that have been removed for this figure. The reactions for the BACE1 5`UTR with cytosolic extract and nuclear extract were run as well on separate gels.

To further prove the specificity of the ADAM10 5`UTR RNA-binding proteins, competition experiments were performed. The cytosolic and nuclear extracts were preincubated with a 100-fold of *in vitro*-transcribed ADAM10 5`UTR prior to the addition of 10^6 cpm radiolabelled *in vitro*-transcribed ADAM10 5`UTR. The formation of all the UV-crosslinked RNA-protein complexes could be specifically competed by unlabelled ADAM10 5`UTR RNA (Figure 3.9).

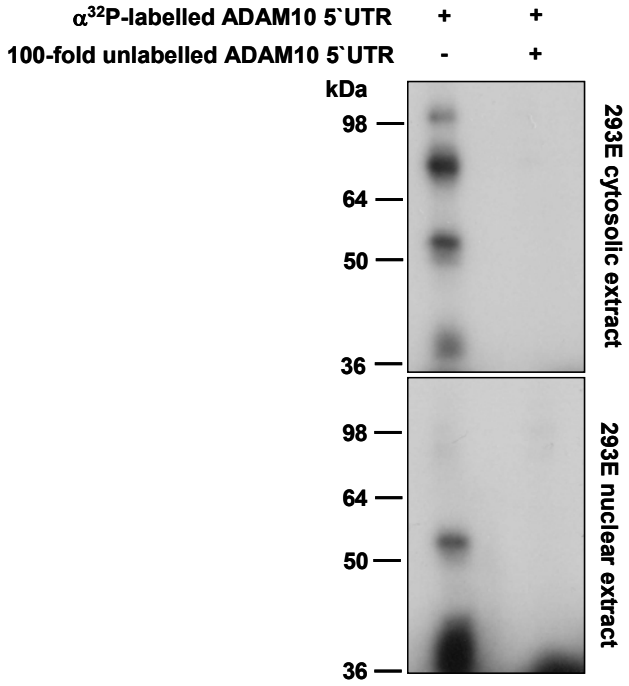

Figure 3.9 Displacement of protein binding via excess of non-radioactive-labelled ADAM10 5`UTR RNA

Cytosolic and nuclear extracts were preincubated (right) with an excess of unlabelled *in vitro*-transcribed ADAM10 5`UTR. Following the addition of radiolabelled *in vitro*-transcribed ADAM10 5`UTR, RNA and protein were UV crosslinked at 254 nm for 25 min on ice and RNA was digested. RNase-protected RNA-protein complexes were separated on an 8% SDS gel and visualized by autoradiography.

The specificity of the ADAM10 5`UTR RNA-binding proteins was proven by the use of the reverse ADAM10 5`UTR sequence (Figure 3.10A). Incubation of the reverse ADAM10 5`UTR sequence with either cytosolic or nuclear HEK293E extract following UV light treatment resulted in the detection of a slightly different protein band pattern (Figure 3.10B). The slight difference between the proteins binding to the ADAM10 5`UTR and the reverse ADAM10 5`UTR confirms the specificity of the RNA-binding proteins. Taken together, these data demonstrate that different RNA sequences are recognized by different proteins. However, proteins, which do not bind to specific nucleotides but to purine-rich or pyrimidine-rich stretches, can bind to both 5`UTRs. This might explain the similarity of the detected protein pattern.

A

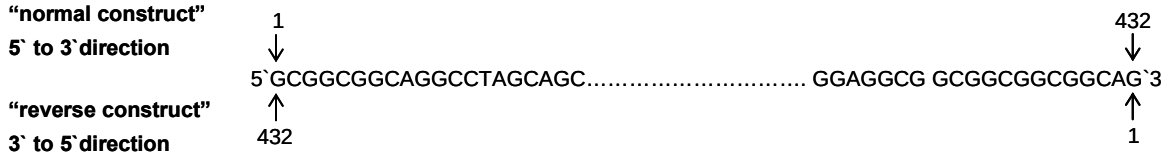

B

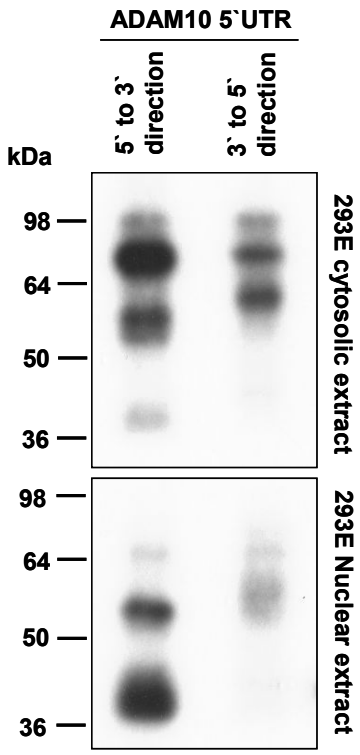

Figure 3.10 Specific binding of proteins to the ADAM10 5`UTR.
Nuclear and cytosolic extract were incubated with ADAM10 5`UTR RNA or reverse ADAM10 5`UTR and crosslinked via UV treatment at 254 nm for 25 min. The RNA-protein complex was separated on an 8% SDS gel and visualized by autoradiography. In the first lane of each gel, the same proteins were detected as in Figure 3.8. Incubation of nuclear and cytosolic extracts with reverse ADAM10 5`UTR reveals a changed protein pattern.

In summary, the UV-crosslink experiments strongly suggest that the detected RNA-binding proteins are selectively binding to the ADAM10 5`UTR.

3.1.5 Deletional analysis of ADAM10 5`UTR protein-binding sites

In the experiment described in 3.1.4, the intact ADAM10 5`UTR was used to detect RNA-protein interactions. To map the region of the RNA sequence/structure involved in protein binding, a series of 3` and 5` deletions of the 5`UTR were tested for their ability to crosslink to proteins (Figure 3.11A).

In order to test the RNA-protein interaction of the deletion constructs, UV crosslink experiments of the full-length 5`UTR and the 3` and 5` deletions were performed as

described in 3.1.4. For the 3` deletion construct Δ251-432 no reduction but an increased intensity in protein bands could be detected after incubation with 15 µg cytosolic extract in comparison to the full-length ADAM10 5`UTR (Figure 3.11B). The formation of a 70-90 kDa UV-crosslinked RNA-protein complex disappeared for the 5` deletion constructs Δ1-155 and Δ1-175 when incubated with cytosolic extract. However, an increased intensity of the remaining bands was detected for these constructs, indicating that the remaining proteins might bind more efficiently. Analysis of the 5` deletion construct Δ1-215 revealed a reduced number and intensity of detected proteins, suggesting that an important element is missing for efficient binding of the remaining proteins. Furthermore, the deletion of the first 259 nt of the 5`UTR nearly completely reduced the number of UV-crosslinked proteins (Figure 3.11B). The results are in agreement with the EMSAs performed for Δ1-259 and Δ251-432 (Figure 3.7). The two remaining bands for the Δ1-259 construct in the UV-crosslink might be some weak interactors that were stabilized by the covalent binding and can therefore not be seen by EMSAs. Taken together, these data confirm that the crosslinked proteins bind to the first half of the 5`UTR. In addition, it was demonstrated that the region between 175 and 259 contains important protein-binding sites.

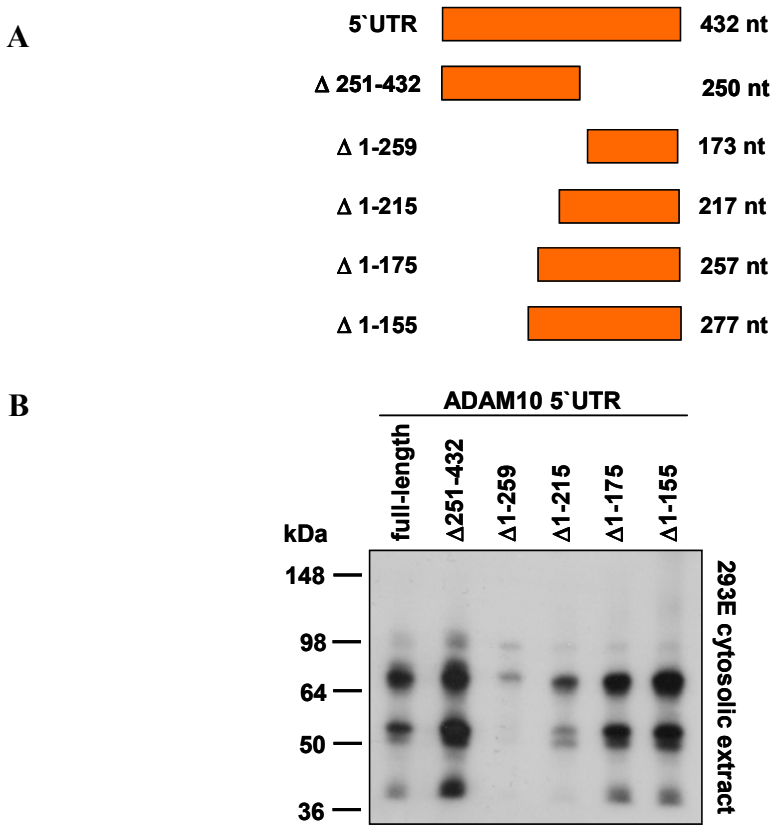

Figure 3.11 Determination of the ADAM10 5`UTR-binding domains required for protein binding.

(A) Schematic representation of the ADAM10 5`UTR deletion constructs. The complete ADAM10 5`UTR (432 nt), the 3` deleted Δ251-432 RNA as well as a series of 5` deleted RNAs (Δ1-259, Δ1-215, Δ1-175, Δ1-155) were prepared for UV-crosslinking experiments. All ADAM10 5`UTR constructs lack the last 12 nucleotides (see Figure 2.1A). (B) Crosslink experiments with full-length and deleted ADAM10 5`UTR constructs were performed in the presence of 15 µg cytosolic extract. For the Δ251-432 construct the same proteins as for the full-length 5`UTR were detected, but the intensity of the protein bands increased. The formation of the 70-90 kDa RNA-protein complex disappeared upon deletion of the first 155 and 175 nucleotides. However, the other RNA-protein complexes appear with a higher intensity. The Δ1-215 construct resulted in a reduced number of RNA-protein complexes and a decreased intensity of the complexes. Nearly no RNA-protein complexes could be detected with the first half (Δ1-259) of the ADAM10 5`UTR.

3.2 Data base search for ADAM10 and BACE1 5`UTR-binding proteins

The above described results suggest a specific binding of proteins to the 5`UTR of ADAM10 and BACE1. Therefore a database search was performed to look for potential candidate proteins. The UTR database UTRdb of the Institute for Biomedical Technologies (http://utrdb.ba.itb.cnr.it/) (Grillo *et al.*, 2010; Pesole *et al.*, 2000; Pesole *et al.*, 1998) was used for the identification of ADAM10 and BACE1 5`UTR-binding proteins. Examination of the BACE1 5`UTR revealed that there was no predicted RNA-binding protein. In contrast, for the ADAM10 5`UTR the search revealed two possible binding sites for the RNA-binding protein upstream of N-ras (Unr). These binding sites

are located within an 83-nucleotide-long stretch that is composed almost solely of purines between nucleotides 164 and 246 of the ADAM10 5`UTR (Figure 3.12).

```
  1 GCGGCGGCAG GCCUAGCAGC ACGGGAACCG UCCCCCGCGC GCAUGCGCGC GCCCCUGAAG
 61 CGCCUGGGGG ACGGGUAGGG GCGGGAGGUA GGGGCGCGGC UCCGCGUGCC AGUUGGGUGC
121 CCGCGCGUCA CGUGGUGAGG AAGGAGGCGG AGGUCUGAGU UUCGAGGGAG GGGGGGAGAG
181 AAGAGGGAAC GAGCAAGGGA AGGAAAGCGG GGAAAGGAGG AAGGAAACGA ACGAGGGGGA
241 GGGAGGUCCC UGUUUUGGAG GAGCUAGGAG CGUUGCCGGC CCCUGAAGUG GAGCGAGAGG
301 GAGGUGCUUC GCCGUUUCUC CUGCCAGGGG AGGUCCCGGC UUCCCGUGGA GGCUCCGGAC
361 CAAGCCCCUU CAGCUUCUCC CUCCGGAUCG AUGUGCUGCU GUUAACCCGU GAGGAGGCGG
421 CGGCGGCGGC AGCGGCAGCG GAAG
```

Figure 3.12 Representation of the ADAM10 5`UTR sequence and its predicted Unr binding sites.
Shown is the sequence of the ADAM10 5`UTR (Accession number: NT_010194.17, GI:224514848). The 83-nucleotide-long purine stretch is shown in bold. The two predicted optimal Unr binding sites R_8AACR_3 (R = G or A) within this purine stretch are underlined and shown in red (Triqueneaux *et al.*, 1999). The last 12 nucleotides of the ADAM10 5`UTR, which were not included in EMSA, UV-crosslink and purification experiments, are shown in green (see Figure 2.1A).

Unr is a cytoplasmic RNA-binding protein and contains five cold shock domains (CSD) (Jacquemin-Sablon *et al.*, 1994). Each CSD contains two conserved RNA recognition motifs RNP-1 (ribonucleoprotein 1) (amino acids Y/FGFI) and RNP-2 (amino acids FFH) that fold in a compact β-barrel and mediate binding to single stranded nucleic acids (Figure 3.13) (Brown and Jackson, 2004; Jacquemin-Sablon *et al.*, 1994).

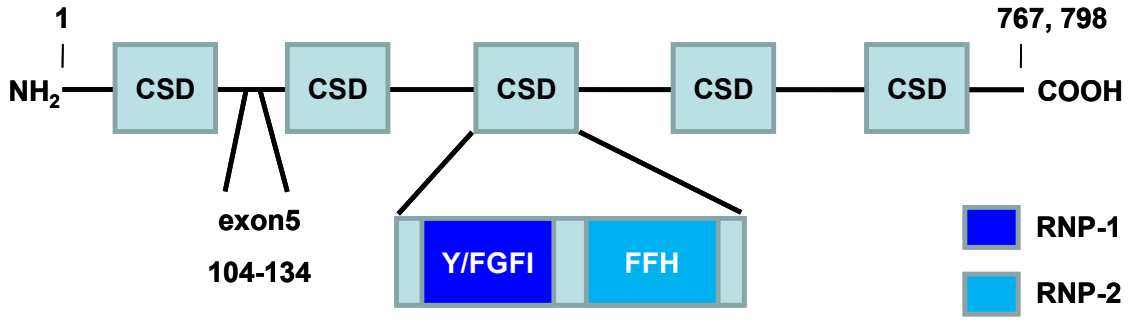

Figure 3.13 Representation of the Unr protein.
Shown is Unr with its five CSDs, each containing two conserved RNP motifs. RNP1 consists of the amino acids Y/FGFI and RNP2 consists of the amino acids FFH. Two isoforms of Unr are shown: a 767-amino-acid-long isoform lacking exon 5 and a 798 amino acid long isoform containing exon 5.

Two isoforms of Unr with an open reading frame of 767 or 798 amino acids are generated by skipping of exon 5 (Boussadia *et al.*, 1993; Ferrer *et al.*, 1999). In addition, three alternative polyadenylation sites have been described in the Unr gene (Jeffers *et al.*, 1990).

Proteins of the CSD family perform a variety of functions and are thought to behave as RNA chaperones, promoting a linear conformation of the mRNA. Unr was shown to be involved in the regulation of mRNA translation and stability by binding to purine-rich sites in UTRs (Mihailovich *et al.*, 2010). Therefore, Unr may be a potential candidate that might regulate ADAM10 protein expression by binding to its 5'UTR.

3.3 Affinity purification of RNA-binding proteins

To prove Unr as a ADAM10 5`UTR-binding protein and to identify and purify other ADAM10 5`UTR binding proteins in a large scale, a biotin-streptavidin affinity chromatography (based on Miltenyi-Biotech procedures, Figure 3.15), was established. In the original protocol from Miltenyi-Biotech, the *in vitro*-transcribed RNA was labelled with a biotinylated oligonucleotides which must be complementary to the *in vitro*-transcribed RNA and should be at least 25 – 30 bases long. However, with this labelling method no specific interaction with proteins was detectable. Therefore, the protocol was optimized with internally biotinylated *in vitro*-transcribed RNA (refer to 2.7.3). Furthermore to reduce possible background binding, two preclearing steps (streptavidin agarose and heparin agarose) for the cytosolic extract were introduced (refer to 2.9.19) instead of only one optional washing step with heparin agarose in the original protocol (www.miltenyibiotec.com/~/media/Images/Products/Import/0002500/IM0002567.ashx).

For the purification of 5`UTR-binding proteins, 400 pmol internally biotinylated *in vitro*-transcribed ADAM10 or BACE1 5`UTR mRNA (as control for selectivity) (Figure 3.14) was incubated with paramagnetic micro beads covalently conjugated with streptavidin for one hour. As a control, the same experimental setup was performed with the exception that the paramagnetic micro beads were incubated with non-biotinylated *in vitro*-transcribed mRNA (Figure 3.14).

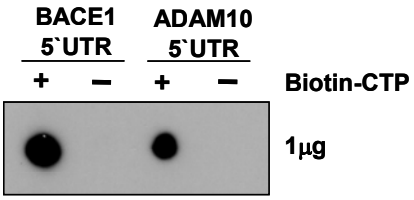

Figure 3.14 Control of biotinylated ADAM10 and BACE1 5`UTR
A dot blot for 1 µg biotinylated and non-biotinylated ADAM10 and BACE1 5`UTR decorated with a Streptavidin-Alkaline phosphatase antibody is shown.

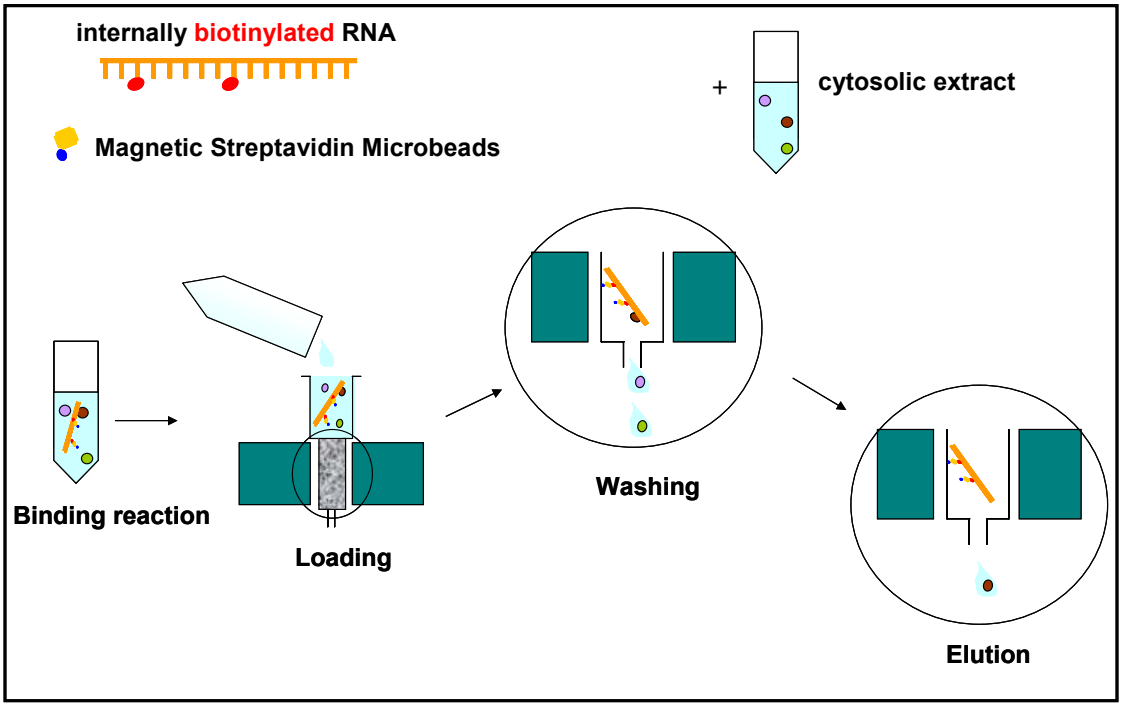

Figure 3.15 Schematic representation of the affinity purification method (adapted from Miltenyi-Biotech, www.miltenyibiotec.com)
400 pmol *in vitro*-transcribed internally biotinylated RNA was incubated with µMACS Streptavidin MicroBeads for 1 h at room temperature. Cytosolic extract was precleared with heparin and streptavidin agarose followed by the incubation with the biotinylated RNA-µMACS Streptavidin MicroBeads complex for 1 h. The entire binding reaction was added to an equilibrated µColumn in the magnetic field of a µMACS separator. Once the entire incubation reaction passed through the column, the column was washed several times with binding buffer to remove non-specifically bound molecules. Bound proteins were finally eluted with binding buffer supplemented with 1 M NaCl.

The RNA-bead complexes were incubated with 6 mg cytosolic extract from HEK293E cells (Figure 3.16A) or cytosolic brain extracts from P30 mice (Figure 3.16B) to allow the formation of RNA-protein complexes. These complexes were separated on a µColumn localized in the magnetic field of a µMACS separator. After stringent washing, the RNA-binding proteins were eluted with high-salt buffer followed by TCA precipitation. Finally, the RNA-binding proteins were separated on an 8% SDS gel for the HEK293E cytosolic extract and on a 10% SDS gel for the cytosolic extract from P30 mice brains. The gels were either stained with silver (Figure 3.16) or blotted onto a membrane (Figure 3.21). As already seen for the results of the UV crosslinking, the protein band patterns for the ADAM10 and BACE1 5`UTR differ significantly (Figure 3.16). Hence, there seems to be selective binding of proteins to either of the two 5`UTRs.

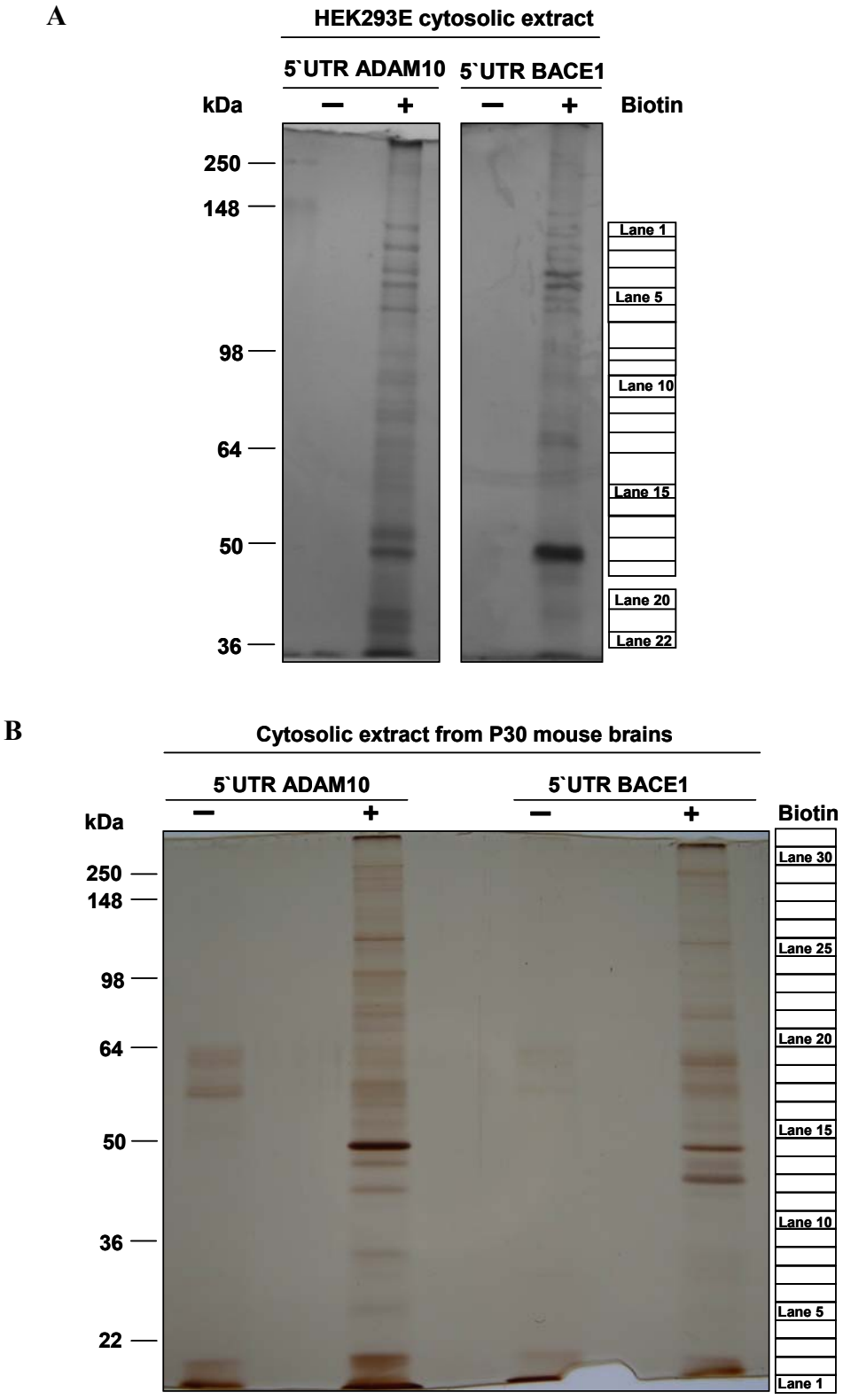

Figure 3.16 Purification of ADAM10 and BACE1 5`UTR-binding proteins.
6 mg cytosolic extract was incubated with 400 pmol non-biotinylated and biotinylated ADAM10 or BACE1 5`UTR. RNA-binding proteins were affinity purified in a magnetic field and separated on an 8% SDS gel (A) or 10% SDS gel (B), respectively. The silver-stained protein bands were cut out and subjected to LC-MS/MS. (A) Silver gel for the affinity purified TCA precipitated RNA-binding proteins from HEK293 cytosolic extract, and (B) for RNA-binding proteins from cytosolic extract from P30 mouse brains. Next to the gel pictures, the cutting paradigm is shown. Gel (A) was cut manually whereas gel (B) was cut with a moulding tool.

The silver-stained gels of the affinity purifications (Figure 3.16) comprising the complete molecular weight range from 36 kDa to 210 kDa were cut into several pieces (see cutting paradigm next to gel pictures). Each piece was subjected to in-gel trypsin digestion. Peptide mass fingerprints were generated by LC-MS/MS analysis and the results analysed by a mascot database search (LC-MS/MS analysis was performed by Dr. Ignasi Forne).

3.4 ADAM10 5`UTR RNA-binding proteins

As expected from the database search, Unr was identified in both affinity purification setups for the lane at 98 kDa (refer to Figure 3.16) with a high coverage confirming the results of the UTR scan approach. The mass spectrometry performed on the silver gel from the purification with the cytosolic extract from HEK293E cells yielded 14 different peptides covering the human Unr protein sequence from the N- to the C-terminus (20% peptide coverage) (Figure 3.17, Figure 3.18 and in detail Appendix Figure 6.1). The mascot score, describing the significance of the search result was 193. The mascot score is a measure of the reliability of the identification (Koenig *et al.*, 2008). Thus, a high score represents a reliable identification. In this work, the significance threshold was set to 100.

```
  1 MSFDPNLLHN NGHNGYPNGT SAALRETGVI EKLLTSYGFI QCSERQARLF
 51 FHCSQYNGNL QDLKVGDDVE FEVSSDRRTG KPIAVKLVKI KQEILPEERM
101 NGQVVCAVPH NLESKSPAAP GQSPTGSVCY ERNGEVFYLT YTPEDVEGNV
151 QLETGDKINF VIDNNKHTGA VSARNIMLLK KKQARCQGVV CAMKEAFGFI
201 ERGDVVKEIF FHYSEFKGDL ETLQPGDDVE FTIKDRNGKE VATDVRLLPQ
251 GTVIFEDISI EHFEGTVTKV IPKVPSKNQN DPLPGRIKVD FVIPKELPFG
301 DKDTKSKVTL LEGDHVRFNI STDRRDKLER ATNIEVLSNT FQFTNEAREM
351 GVIAAMRDGF GFIKCVDRDV RMFFHFSEIL DGNQLHIADE VEFTVVPDML
401 SAQRNHAIRI KKLPKGTVSF HSHSDHRFLG TVEKEATFSN PKTTSPNKGK
451 EKEAEDGIIA YDDCGVKLTI AFQAKDVEGS TSPQIGDKVE FSISDKQRPG
501 QQVATCVRLL GRNSNSKRLL GYVATLKDNF GFIETANHDK EIFFHYSEFS
551 GDVDSLELGD MVEYSLSKGK GNKVSAEKVN KTHSVNGITE EADPTIYSGK
601 VIRPLRSVDP TQTEYQGMIE IVEEGDMKGE VYPFGIVGMA NKGDCLQKGE
651 SVKFQLCVLG QNAQTMAYNI TPLRRATVEC VKDQFGFINY EVGDSKKLFF
701 HVKEVQDGIE LQAGDEVEFS VILNQRTGKC SACNVWRVCE GPKAVAAPRP
751 DRLVNRLKNI TLDDASAPRL MVLRQPRGPD NSMGFGAERK IRQAGVID
```

Figure 3.17 Unr peptides found by mass spectrometry.
Unr peptides found by mass spectrometry for the purification with cytosolic extract from HEK293E cells are shown. The peptides identified by mass spectrometry are marked in red. The peptides of exon5 which were not identified by mass spectrometry are marked in blue. The mascot score and the peptide coverage were 193 and 20%, respectively.

Start – End	Observed	Mr(expt)	Mr(calc)	Sequence
65 – 78	805.3696	1608.7246	1608.7380	VGDDVEFEVSSDRR
90 – 99	627.8517	1253.6889	1253.6979	IKQEILPEER
195 – 202	484.7464	967.4782	967.4763	EAFGFIER
208 – 217	673.8214	1345.6283	1345.6343	EIFFHYSEFK
218 – 234	938.9553	1875.8961	1875.9102	GDLETLQPGDDVEFTIK
247 – 269	858.4576	2572.3509	2572.3425	LLPQGTVIFEDISIEHFEGTVTK
287 – 295	529.8392	1057.6639	1057.6536	IKVDFVIPK
308 – 317	569.8107	1137.6068	1137.6142	VTLLEGDHVR
318 – 325	504.7607	1007.5068	1007.5148	FNISTDRR
331 - 348	1028.0024	2053.9903	2054.0069	ATNIEVLSNTFQFTNEAR
519 - 527	489.3065	976.5985	976.5957	LLGYVATLK
601 - 606	377.2598	752.5051	752.5021	VIRPLR
683 - 696	809.8669	1617.7192	1617.7311	DQFGFINYEVGDSK
759 - 769	586.7951	1171.5756	1171.5833	NITLDDASAPR

Figure 3.18 Detailed description of Unr peptides from HEK293E cytosolic extract found by mass spectrometry.
Start – End: amino acid number of the peptide in the protein sequence. Observed: experimental mass number / charge number (m/z) value. Mr(expt): experimental m/z transformed to a relative molecular mass. Mr(calc): relative molecular mass calculated from the matched peptide sequence.

For the silver gel from the purification with the cytosolic extract from P30 mouse brains, mass spectrometry identified 32 different peptides from the 98 kDa band, which matched peptide sequences from mouse Unr (Figure 3.19, Figure 3.20 and in detail Appendix Figure 6.2). The corresponding peptide coverage was 41% and the mascot score was 1447.

```
  1 MSFDPNLLHN NGHNGYPNGT SAALRETGVI EKLLTSYGFI QCSERQARLF
 51 FHCSQYNGNL QDLKVGDDVE FEVSSDRRTG KPIAIKLVKI KPEIHPEERM
101 NGQVVCAVPH NLESKSPAAP GQSPTGSVCY ERNGEVFYLT YTSEDVEGNV
151 QLETGDKINF VIDNNKHTGA VSARNIMLLK KKQARCQGVV CAMKEAFGFI
201 ERGDVVKEIF FHYSEFKGDL ETLQPGDDVE FTIKDRNGKE VATDVRLLPQ
251 GTVIFEDISI EHFEGTVTKV IPKVPSKNQN DPLPGRIKVD FVIPKELPFG
301 DKDTKSKVTL LEGDHVRFNI STDRRDKLER ATNIEVLSNT FQFTNEAREM
351 GVIAAMRDGF GFIKCVDRDA RMFFHFSEIL DGNQLHIADE VEFTVVPDML
401 SAQRNHAIRI KKLPKGTVSF HSHSDHRFLG TVEKEATFSN PKTTSPNKGK
451 DKEAEDGIIA YDDCGVKLTI AFQAKDVEGS TSPQIGDKVE FSISDKQRPG
501 QQIATCVRLL GRNSNSKRLL GYVATLKDNF GFIETANHDK EIFFHYSEFS
551 GDVDSLELGD MVEYSLSKGK GNKVSAEKVN KAHSVNGITE EANPTIYSGK
601 VIRPLRGVDP TQIEYQGMIE IVEEGDMKGE VYPFGIVGMA NKGDCLQKGE
651 SVKFQLCVLG QNAQTMAYNI TPLRRATVEC VKDQFGFINY EVGDSKKLFF
701 HVKEVQDGVE LQAGDEVEFS VILNQRTGKC SACNVWRVCE GPKAVAAPRP
751 DRLVNRLKNI TLDDASAPRL MVLRQPRGPD NSMGFGAERK IRQAGVID
```

Figure 3.19 Unr peptides found by mass spectrometry.
Unr peptides found by mass spectrometry for the purification with cytosolic extract from P30 mouse brains are shown. The peptides identified by mass spectrometry are marked in red. The peptides of exon5 which were not identified by mass spectrometry are marked in blue. The mascot score and the peptide coverage were 1447 and 41%, respectively.

Start – End	Observed	Mr(expt)	Mr(calc)	Sequence
33 – 45	787.3870	1572.7594	1572.7606	LLTSYGFIQCSER
65 - 78	537.2531	1608.7375	1608.7380	VGDDVEFEVSSDRR
65 - 78	805.3762	1608.7378	1608.7380	VGDDVEFEVSSDRR
79 - 86	414.2715	826.5284	826.5276	TGKPIAIK
90 - 99	416.5660	1246.6762	1246.6669	IKPEIHPEER
158 - 166	538.7904	1075.5662	1075.5662	INFVIDNNK
167 - 174	399.7144	797.4142	797.4144	HTGAVSAR
175 - 180	366.2279	730.4412	730.4411	NIMLLK
175 - 180	374.2253	746.4360	746.4360	NIMLLK Oxidation (M)
195 - 202	484.7450	967.4754	967.4763	EAFGFIER
218 - 236	716.6857	2147.0353	2147.0383	GDLETLQPGDDVEFTIKDR
237 - 246	544.7883	1087.5620	1087.5622	NGKEVATDVR
278 - 286	505.7542	1009.4938	1009.4941	NQNDPLPGR
287 - 295	353.5583	1057.6531	1057.6536	IKVDFVIPK
287 - 295	529.8340	1057.6534	1057.6536	IKVDFVIPK
296 - 305	575.2932	1148.5718	1148.5713	ELPFGDKDTK
306 - 317	451.9200	1352.7382	1352.7412	SKVTLLEGDHVR
318 - 325	504.7645	1007.5144	1007.5148	FNISTDRR
349 - 357	489.2491	976.4836	976.4834	EMGVIAAMR
349 - 357	497.2466	992.4786	992.4783	EMGVIAAMR Oxidation (M)
349 - 357	505.2438	1008.4730	1008.4732	EMGVIAAMR 2 Oxidation (M)
358 - 364	392.2054	782.3962	782.3963	DGFGFIK
416 - 427	456.2130	1365.6172	1365.6174	GTVSFHSHSDHR
428 - 442	556.6257	1666.8553	1666.8566	FLGTVEKEATFSNPK
468 - 475	446.2682	890.5218	890.5225	LTIAFQAK
476 - 496	746.6976	2237.0710	2237.0699	DVEGSTSPQIGDKVEFSISDK
497 - 508	471.9176	1412.7310	1412.7307	QRPGQQIATCVR
519 - 527	489.3049	976.5952	976.5957	LLGYVATLK
601 - 606	377.2585	752.5024	752.5021	VIRPLR
629 - 642	749.3750	1496.7354	1496.7334	GEVYPFGIVGMANK Oxidation (M)
683 - 696	809.8754	1617.7362	1617.7311	DQFGFINYEVGDSK
698 - 703	395.7344	789.4542	789.4538	LFFHVK
744 - 752	318.1821	951.5245	951.5250	AVAAPRPDR
744 - 752	476.7696	951.5246	951.5250	AVAAPRPDR
757 - 769	471.9278	1412.7616	1412.7623	LKNITLDDASAPR
757 - 769	707.3889	1412.7632	1412.7623	LKNITLDDASAPR
770 - 774	316.2017	630.3888	630.3887	LMVLR
770 - 774	324.1990	646.3834	646.3836	LMVLR Oxidation (M)
778 - 789	619.2672	1236.5198	1236.5193	GPDNSMGFGAER
778 - 789	627.2643	1252.5140	1252.5143	GPDNSMGFGAER Oxidation (M)
791 - 798	436.2534	870.4922	870.4923	IRQAGVID

Figure 3.20 Detailed description of Unr peptides from mouse brain cytosolic extract found by mass spectrometry.
Start – End: amino acid number of the peptide in the protein sequence. Observed: experimental mass number / charge number (m/z) value. Mr(expt): experimental m/z transformed to a relative molecular mass. Mr(calc): relative molecular mass calculated from the matched peptide sequence.

To prove the result of the mass spectrometry analysis regarding Unr, the TCA precipitated RNA-binding proteins from cytosolic extracts of HEK293E cells binding to the ADAM10 5`UTR were blotted onto a membrane and decorated with the Unr S23 antibody (Jacquemin-Sablon *et al.*, 1994) (Figure 3.21). Unr could be detected in the

Western blot for the purification with the biotinylated ADAM10 5`UTR RNA but not in the control lane. The lower fainter bands detected by the antibody might be degradation products of Unr whereas the upper band might be Unr including exon 5.

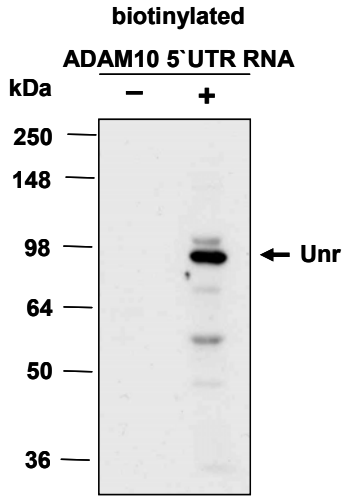

Figure 3.21 Detection of Unr after affinity purification.
Affinity purified ADAM10 5`UTR RNA-binding proteins from HEK293E cytosolic extract were precipitated with TCA after elution and separated on an 8% SDS gel. Unr was detected by immunoblotting with the Unr antibody S23 (Jacquemin-Sablon *et al.*, 1994) at 98 kDa (representative Western Blot for n=3 experiments). Note, in addition to the 98 kDa band, some fainter bands, possibly degraded Unr, could be detected.

Besides Unr several other RNA-binding proteins could be identified for the ADAM10 5`UTR, which were not predicted in the UTR database (Table 3.1 and 3.2). 22 gel bands from the purification with HEK293E cytosolic extract were analysed by mass spectrometry, which identified 90 proteins (Table 3.1). ADAM10 5`UTR associated proteins included 3 RNA transport proteins, 12 proteins involved in protein synthesis, 12 hnRNPs, 7 RNA helicases, 6 splicing factors, 15 RNA associated proteins (including Unr), 10 tRNA synthetases, 9 cytoskeletal associated proteins and 16 other known proteins.

Function / Type (number)	Protein name	Mascot score	Molecular weight (kDa)	Lane
RNA transport (3)	FXR1	400	70 kDa	**11**, 10, 12
	FXR2	172	75 kDa	**8**
	THOC6	122	38 kDa	**18**
Protein synthesis (12)	eEF1a1	254	50 kDa	**17**, 18, 14, 19
	eEF1a2	145	51 kDa	**17**
	eEF1d	181	31 kDa	**20**
	eEF1g	299	50 kDa	**17**
	eIF2a	636	36 kDa	**18**, 20, 21
	eIF2b	148	39 kDa	**17**
	eIF2g	380	52 kDa	**16**, 17
	eIF3c	116	106 kDa	**11**
	eIF3i	120	67 kDa	**13**
	IMDH2	219	56 kDa	**14**, 15
	RL6	282	33 kDa	**18**
	RLA0	171	34 kDa	**18**
hnRNP (12)	hnRNP A0	145	34 kDa	**18**
	hnRNP A1	446	39 kDa	**18**, 21, 20
	hnRNP A2/B1	1714	37 kDa	**18**, 20, 19, 21
	hnRNP A3	171	40 kDa	**18**, 20
	hnRNP C	105	34 kDa	**19**
	hnRNP F	318	46 kDa	**17**, 16, 19, 18
	hnRNP H1	491	49 kDa	**16**, 19, 17
	hnRNP H2	242	50 kDa	**16**
	hnRNP H3	171	37 kDa	**18**
	hnRNP K	110	51 kDa	**13**
	hnRNP Q	128	70 kDa	**13**
	hnRNP U	364	91 kDa	**10**, 4, 11, 9, 8, 12, 13
RNA helicases (7)	DHX9	160	142 kDa	**3**
	DHX15	141	92 kDa	**10**, 8
	DHX40	114	90 kDa	**9**
	Ku70	212	70 kDa	**11**
	UAP56	152	49 kDa	**17**
	G3BP1	462	52 kDa	**13**
	G3BP2	137	54 kDa	**14**

Function / Type (number)	Protein name	Mascot score	Molecular weight (kDa)	Lane
Splicing factors (6)	SF3A1	154	89 kDa	**4**
	SF3B1	142	146 kDa	**4**
	SF3B3	428	136 kDa	**3**
	SF3B4	105	44 kDa	**17**
	U2AF1	202	28 kDa	**18**
	U2AF2	236	54 kDa	**13**
Other RNA associated (15)	Unr	193	90 kDa	**8**, 11
	Nucleolin	567	77 kDa	**14**, 17, 15, 13, 11, 18, 9, 7, 10, 19, 8
	FBP1	221	68 kDa	**11**
	LA	123	47 kDa	**19**
	IMP4	100	34 kDa	**21**
	NONO	177	54 kDa	**22**, 18
	ILF2	320	43 kDa	**19**
	ILF3	466	96 kDa	**10**, 9
	NPM	161	33 kDa	**18**
	PRP19	107	55 kDa	**14**
	PA2G4	398	44 kDa	**17**
	CPSF6	243	59 kDa	**11**
	SND1	486	103 kDa	**5**, 6
	APEX1	102	36 kDa	**18**
	LC7L2	145	47 kDa	**18**
tRNA synthetases (10)	SYC	150	89 kDa	**9**
	SYDC	696	57 kDa	**15**, 16, 14
	SYEP	318	165 kDa	**4**, 5, 9, 8, 14, 7
	SYIC	1060	145 kDa	**2**, 3, 1
	SYK	474	68 kDa	**11**, 12
	SYLC	964	136 kDa	**3**, 4
	SYMC	516	102 kDa	**7**
	SYQ	931	89 kDa	**8**, 13
	SYRC	916	76 kDa	**12**, 11, 13
	SYSC	153	59 kDa	**14**

Function / Type (number)	Protein name	Mascot score	Molecular weight (kDa)	Lane
Cytoskeletal (9)	Drebrin	776	72 kDa	**4**, 5, 7, 10, 11, 6
	Septin-2	283	42 kDa	**19**, 18
	Septin-7	194	51 kDa	**17**, 18
	Septin-8	154	56 kDa	**15**
	Septin-9	205	66 kDa	**13**
	Septin-11	311	50 kDa	**16**
	Vimentin	109	54 kDa	**14**
	LIMA1	116	86 kDa	**10**, 13
	DC1I2	102	69 kDa	**10**
Other known proteins (16)	LONM	1167	107 kDa	**6**, 7, 8
	HSP71	236	70 kDa	**11**
	KIAA1967 homolog	338	103 kDa	**5**
	KCC2B	103	58 kDa	**17**
	IQGA1	589	190 kDa	**7**
	GTPBP1	191	72 kDa	**11**
	GLYM	232	56 kDa	**15**
	DRG1	335	41 kDa	**19**
	Moesin	137	68 kDa	**10**
	MCA1	299	35 kDa	**20**, 21
	MCA2	106	36 kDa	**21**
	MCM3	146	92 kDa	**7**
	MCM5	191	83 kDa	**8**
	P5CR2	326	34 kDa	**18**
	PP1G	146	38 kDa	**18**
	DHB4	275	72 kDa	**10**

Table 3.1 ADAM10 5`UTR interacting proteins from cytosolic extract of HEK293E cells
Cytosolic extract of HEK293E cells was incubated with ADAM10 5`UTR RNA. The RNA binding proteins were separated by gel electrophoresis, and 22 bands were analysed with mass spectrometry. The proteins were subdivided in different categories according to their function. For each identified protein the highest mascot score, the molecular weight and the lane(s), where the protein was identified, are listed. The lane number marked in bold corresponds to the mascot score. Only proteins with a mascot score higher than 100 were considered. The data listed represents n=2 experiments. Proteins colour labelled in blue were detected in the purification with cytosolic extract from HEK293E and P30 mice brains.

Fewer proteins were identified for the affinity purification with cytosolic extract from P30 mouse brains. The analysis of the 31 gel bands identified 42 proteins including 2 transcription / RNA transport proteins, 1 protein involved in proteins synthesis, 5 hnRNPs,

6 RNA associated proteins (including Unr) and 19 cytoskeletal associated proteins as well as 9 other known proteins (Table 3.2).

Function / Type (number)	Protein name	Mascot score	Molecular weight (kDa)	Lane
Transcription /	Pur-alpha	865	35 kDa	**13**, 12, 11
RNA transport (2)	Pur-beta	1224	34 kDa	**11**, 12
Protein synthesis (1)	eEF1a2	115	51 kDa	**15**
hnRNP (5)	hnRNP A1	158	34 kDa	**9**
	hnRNP F	687	46 kDa	**15**, 14, 16
	hnRNP H1	1042	49 kDa	**16**, 15, 14
	hnRNP H2	906	49 kDa	**16**
	hnRNP Q	118	70 kDa	**19**
Other RNA associated (6)	Unr	1447	90 kDa	**23**, 22
	Unrip	753	39 kDa	**11**
	Nucleolin	563	77 kDa	**23**, 20
	FBP1	344	68 kDa	**20**
	PABP	106	32 kDa	**16**
	SART-3	135	110 kDa	**25**
Cytoskeletal (19)	MAP1A	117	301 kDa	**30**
	MAP2	7553	199 kDa	**29**, 30, 28, 31, 27
	MAP6	651	97 kDa	**25**
	Coronin-2A	113	60 kDa	**18**
	Coronin-2B	174	55 kDa	**17**
	Drebrin	1100	78 kDa	**25**, 24
	Tau	153	76 kDa	**15**
	Spectrin (chain	280	285 kDa	28
	Spectrin (chain	111	275 kDa	28
	Synapsin-1	1269	74 kDa	21, 19, 20
	Synapsin-2	376	64 kDa	17
	Synapsin-3	124	64 kDa	19
	DC1I1	329	71 kDa	21
	DC1I2	125	69 kDa	**21**
	DC1L1	217	57 kDa	**17**
	DYHC1	2293	534 kDa	**29**, 30, 31
	DYN1	3227	98 kDa	**23**, 22
	DYN2	738	98 kDa	**23**
	DYN3	846	98 kDa	**23**

Function / Type (number)	Protein name	Mascot score	Molecular weight (kDa)	Lane
Other known proteins (9)	EFHD2	352	27 kDa	**8**, 7
	HS71L	195	71 kDa	**20**
	HSP72	229	70 kDa	**20**
	HSP7C	373	71 kDa	**20**
	SYNJ1	101	174 kDa	**26**
	BASP1	115	22 kDa	**16**
	NCAN	105	139 kDa	**30**
	G3P	110	36 kDa	**10**
	KIAA1967 homolog	229	104 kDa	**25**

Table 3.2 Potential ADAM10 5`UTR interacting proteins from cytosolic extract of P30 mice brains identified by mass spectrometry.
Cytosolic extract of P30 mice brains was incubated with ADAM10 5`UTR RNA. The RNA binding proteins were separated by gel electrophoresis, and 31 bands were analysed with mass spectrometry. The proteins were subdivided in different categories according to their function. For each identified protein the highest mascot score, the molecular weight and the lane(s), where the protein was identified, are listed. The lane number marked in bold corresponds to the mascot score. Only proteins with a mascot score higher than 100 were considered. The data listed represents n=1 experiment due to limited amount of cytosolic extract from P30 mice brains. Proteins colour labelled in blue were detected in the purification with cytosolic extract from HEK293E and P30 mice brains.

Interestingly, besides the total number of identified proteins also the kind of proteins identified largely differed (compare Table 3.1 and 3.2).

Comparison of the proteins identified with the cytosolic extract of HEK293E cells and the cytosolic extract of P30 mice brains implies that there are a couple of different proteins identified (compare Table 3.1 and 3.2). However, several of the proteins identified, such as Unr, Nucleolin, hnRNP A1 and hnRNP H/F, were found in both purifications (identical protein colour labelled in Table 3.1 and 3.2 and summarized in Table 3.3).

Interestingly, only for the purification with HEK293E cytosolic extract RNA helicases, splicing factors and tRNA synthetases were pulled down (compare Table 3.1 and 3.2). For the purification with mice brain cytosolic extract an increasing number of cytoskeleton-associated proteins was pulled down (compare Table 3.1 and 3.2). Furthermore, the identified RNA transport proteins differed between the two purifications (refer to Table 3.3).

Function / Type (number)	Protein name	Molecular weight (kDa)
Protein synthesis (1)	eEF1a1	50 kDa
RNA transport (4)	FXR1 [1]	70 kDa
	FXR2 [1]	75 kDa
	Pur-alpha [2]	35 kDa
	Pur-beta [2]	34 kDa
hnRNP (7)	hnRNP A1	39 kDa
	hnRNP A2/B1 [1]	37 kDa
	hnRNP F	46 kDa
	hnRNP H1	49 kDa
	hnRNP H2	50 kDa
	hnRNP Q	70 kDa
	hnRNP U [1]	91 kDa
Other RNA associated (5)	Unr	90 kDa
	Nucleolin	77 kDa
	FBP1	68 kDa
	PABP [2]	32 kDa
	Unrip [2]	39 kDa
Cytoskeletal (2)	Drebrin	72 kDa
	DC1I2	69 kDa
Other known proteins (1)	KIAA1967 homolog	103 kDa

Table 3.3 Summary of potential ADAM10 5`UTR interacting proteins from cytosolic extract of HEK293E cells and P30 mice brains identified by mass spectrometry.
Cytosolic extracts of HEK293E cells and P30 mice brains were incubated with ADAM10 5`UTR RNA. The RNA binding proteins were separated by gel electrophoresis, and the slices were analysed with mass spectrometry. The proteins were subdivided in different categories according to their function. The RNA-binding proteins, which were identified in both purifications with a mascot score higher than 100 are listed. RNA-binding proteins marked with a [1] were only identified with cytosolic extract of HEK293E cells and proteins marked with a [2] came up only in the purification with mouse cytosolic extract.

Interestingly, some of the proteins identified were described to interact with Unr. The protein hnRNP Q (Grosset *et al.*, 2000), which was identified in both purifications, belongs to the proteins interacting with Unr. hnRNP U, which has only been identified in the purification with HEK293E cytosolic extract was described to play a role in mRNA stabilisation together with hnRNP Q (Weidensdorfer *et al.*, 2009). Two other proteins, which have been described to interact with Unr in an RNA independent-manner, namely Unrip (Hunt *et al.*, 1999; Mitchell *et al.*, 2003) and PABP (Chang *et al.*, 2004; Duncan *et al.*, 2009; Grosset *et al.*, 2000; Patel *et al.*, 2005), have only been identified for the purification with P30 mice brain cytosolic extract. Moreover, FBP1 was identified in both

purifications. This protein is closely related to FBP2, which interacts with Unr (Dinur *et al.*, 2006; Nechama *et al.*, 2008; Nechama *et al.*, 2009).

3.4.1 Electrophoretic mobility shift assay with recombinant Unr

The UTR database search and the biotin-streptavidin affinity purification have revealed that Unr is an ADAM10 5`UTR RNA-binding protein. In the next step, this result was further confirmed by EMSAs with recombinant Unr. Recombinant Unr was prepared by the Glutathione S-transferase (GST) Gene Fusion System (Figure 3.22). In addition, GST and a gene associated with Parkinson`s disease and which was reported to interact with RNA, GST-DJ1 (Blackinton *et al.*, 2009; Hod *et al.*, 1999; van der Brug *et al.*, 2008), were used as negative controls (Figure 3.22).

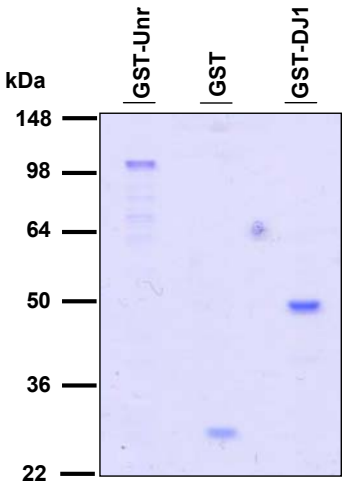

Figure 3.22 Quality control of purified recombinant GST fusion proteins.
Recombinant proteins were analysed on a 10% SDS gel. A Coomassie stained SDS gel is shown for recombinant GST-Unr (lane1), GST (lane 2) and GST-DJ1 (lane3), respectively. 1 µg of each recombinant protein was loaded.

To analyse the ability of Unr to bind specifically to the ADAM10 5`UTR RNA, $10^6$ cpm $^{32}$P-labelled ADAM10 5'UTR was incubated with recombinant GST-Unr. As positive control a cytosolic extract of HEK293E cells was incubated with ADAM10 5`UTR. GST-DJ1 and GST served as negative control. Figure 3.23 demonstrates that recombinant Unr binds to the 5'UTR of ADAM10, while GST-DJ1 or GST alone do not. Specificity of the binding of GST-Unr to radiolabelled ADAM10 5`UTR was determined by competition with non-radioactive *in vitro*-transcribed ADAM10 5`UTR. Binding of GST-Unr to the radiolabelled ADAM10 5`UTR was prevented by the addition of an excess of unlabelled ADAM10 5`UTR (100-fold). Moreover, it was described that Unr can bind to the Apaf-1 5`UTR (Mitchell *et al.*, 2001). Therefore, the Apaf-1 5`UTR was used as an additional

control to analyse the specificity of GST-Unr binding to the ADAM10 5`UTR. Addition of an excess of Apaf-1 5`UTR (100-fold) abolished the binding of the ADAM10 5´UTR to GST-Unr. In summary, the observed effects confirmed that Unr specifically binds to the ADAM10 5`UTR.

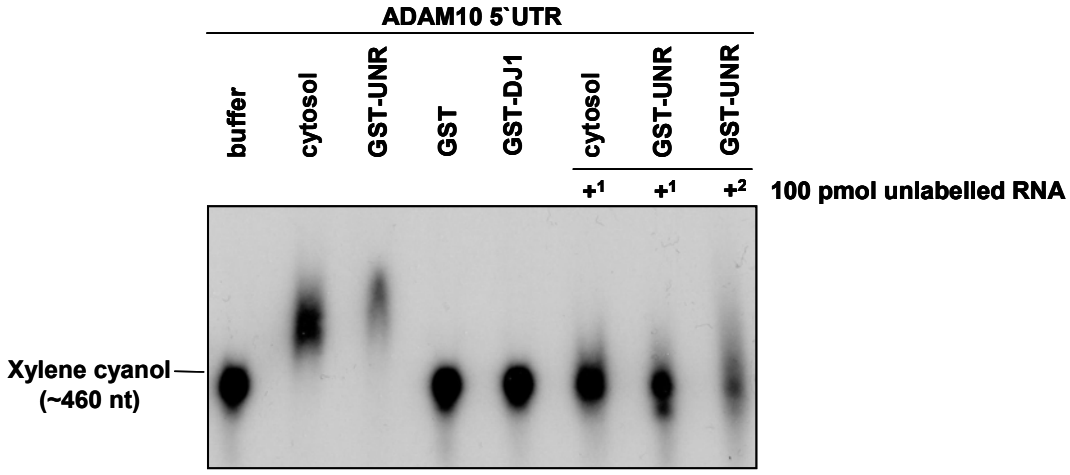

Figure 3.23 GST-Unr binds to the ADAM10 5`UTR.
10^6 cpm of ^{32}P-labelled ADAM10 5'UTR RNA was incubated either with 15 µg HEK293E cell extract or with 4 µg of the indicated recombinant proteins in binding buffer for 30 min at room temperature. RNA-protein complexes were separated on a 3.5% non-denaturing polyacrylamide gel and visualized by autoradiography. The xylene cyanol (~ 460 nt) front on the gel served as size marker. Competition studies were performed by addition of an excess of unlabelled ADAM10 5`UTR ($+^1$) or Apaf-1 5`UTR ($+^2$) as indicated. The incubation of RNA with cytosolic extract or GST-Unr induced a shift, whereas no shift was observed for GST or GST-DJ1. Addition of unlabelled ADAM10 5`UTR ($+^1$) or Apaf-1 5`UTR ($+^2$) abrogates the binding of cytosolic extract and GST-Unr.

3.4.2 Binding of Unr to the mouse 5`UTR

In chapter 3.3, the affinity purification of RNA-binding proteins was performed with cytosolic extract of mouse brains. In comparison to the human ADAM10 5`UTR, the mouse 5`UTR is shorter as it lacks the first 150 nucleotides, however, the Unr binding site appears to be evolutionary conserved (Figure 3.24).

To demonstrate the binding of proteins to the mouse ADAM10 5`UTR, radiolabelled mouse ADAM10 5`UTR (Figure 3.25A) was incubated with cytosolic extract of P30 mice brains (Figure 3.25B). The formation of a complex demonstrates that proteins bind to the mouse ADAM10 5`UTR (Figure 3.25B).

```
mouse           ------------------------------------------------------------
human           GCGGCGGCAGGCCTAGCAGCACGGGAACCGTCCCCCGCGCGCATGCGCGCGCCCCTGAAG 60

mouse           ------------------------------------------------------------
human           CGCCTGGGGGACGGGTATGGGCGGGAGGTAGGGGCGCGGCTCCGCGTGCCAGTTGGGTGC 120

mouse           ------------------------------AGGGCCGCGGCTCAGGGAAGGGGCTGAGAC 30
human           CCGCGCGTCACGTGGTGAGGAAGGAGGCGGAGGTCTGAGTTTCGAAGGAGGGGGGGAGAG 180
                                             *** * * *  **   * *****  ****

mouse           CAGGCGAA--GAGCGAGGGCAGGGAAGCGGGGAAGGGAGGAAGGAAGAGGCCGAGGGGGA 88
human           AAGAGGGAACGAGCAAGGGAAGGAAAGCGGGGAAAGGAGGAAGGAAACGAACGAGGGGGA 240
                 **  * *  **** **** *** ********** **********  *  *********

mouse           GGGAGGGCCCTGTTTTGGCGGAGCAGGGCGCGCGGCTGGGCCCCTGAAGTGGAGCGAGAG 148
human           GGGAGGTCCCTGTTTTGGAGGAGCTAGGAGCGTTGCCGG-CCCCTGAAGTGGAGCGAGAG 299
                ****** *********** *****  ** ***  ** ** ********************

mouse           GGAGGCGCTTCGCCGGGTGCCACTGCCGGGGAGGCTCG----------------TCGGGA 192
human           GGAGGTGCTTCGCCGTTTCTCCTGCCAGGGGAGGTCCCGGCTTCCCGTGGAGGCTCCGGA 359
                ***** *********  *  *    * *******  *                  ** ***

mouse           CCCAGCGCCGGTCGCGGCTCCCTCAGGATCGATGCACCGCGGTTAACCCGTGAGGAGGCG 252
human           CCAAGCCCCTTCAGCTTCTCCCTCCGGATCGATGTGCTGCTGTTAACCCGTGAGGAGGCG 419
                ** *** **    **  ******* *********  * ** ******************

mouse           GCGGCCGGGGAAG------------ 265
human           GCGGCGGCGGCAGCGGCAGCGGAAG 444
                ***** * ** **
```

Figure 3.24 Alignment of the human and mouse ADAM10 5`UTR sequence.
The ADAM10 5`UTR is conserved in human and mouse. Nucleotides shown in red are part of the purine-rich sequence. The stars below the nucleotides show the conserved residues between mouse and human ADAM10 5`UTR. The mouse 5`UTR was isolated from P5 brain mRNA via 5`RACE (data provided by Dr. Lammich). The alignment was done with Clustal.

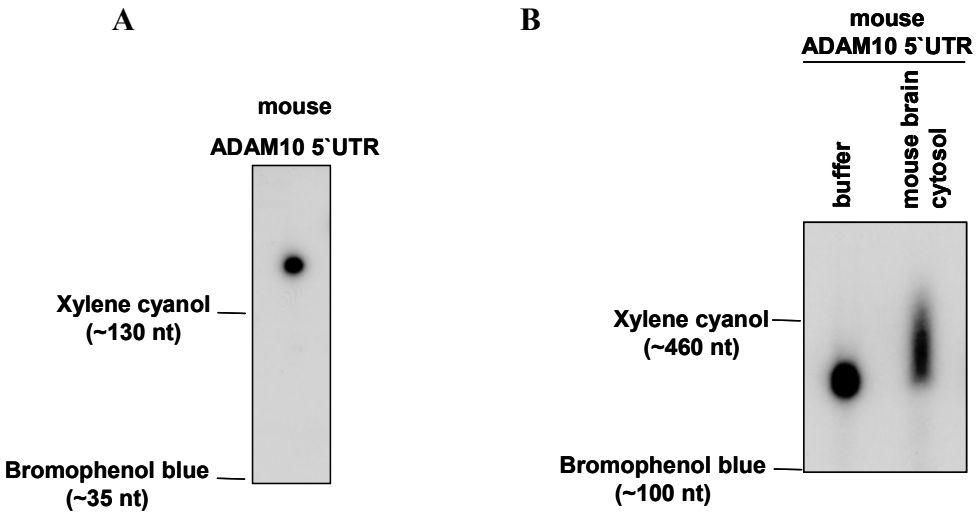

Figure 3.25 Cytosolic proteins from mice brains bind to the mouse ADAM10 5`UTR.
(A) An aliquot of *in vitro*-transcribed α^{32}P-labelled mouse ADAM10 5´UTR RNA was analysed on a 5% denaturing polyacrylamide / 8 M urea gel to control for RNA quality. The xylene cyanol (~ 130 nt) and bromophenol blue (~ 35 nt) front on the gel served as size marker. (B) 10^6 cpm α^{32}P-labelled mouse ADAM10 5'UTR was incubated with 15 µg cytosolic extract of P30 mice brains in binding buffer for 30 min at room temperature. RNA-protein complexes were separated on a 3.5% non-denaturing polyacrylamide gel and visualized by autoradiography. The xylene cyanol (~ 460 nt) and bromophenol blue (~ 100 nt) front on the gel served as size marker. Upon incubation of the RNA with the cytosolic extract, a shift of the RNA is visible in the gel.

To further confirm that Unr is a binding partner of the murine ADAM10 5`UTR, EMSAs were performed. Radiolabelled murine ADAM10 5'UTR (Figure 3.25A) was either incubated with cytosolic extract of HEK293E cells or with recombinant GST-Unr. Since mouse and human Unr have a very high sequence homology (98% identity), the human protein was used for this analysis. GST-DJ1 or GST served as negative controls (Figure 3.26). In line with the findings of the EMSAs with the human ADAM10 5`UTR, cytosolic extract and GST-Unr could bind *in vitro* to the mouse 5'UTR of ADAM10. The interaction of the radiolabelled mouse ADAM10 5`UTR with cytosolic extract or GST-Unr could be inhibited by the addition of an excess of unlabelled mouse ADAM10 5`UTR (100-fold) (Figure 3.26). In summary, these results demonstrate that Unr binds to both the human and the mouse ADAM10 5`UTR.

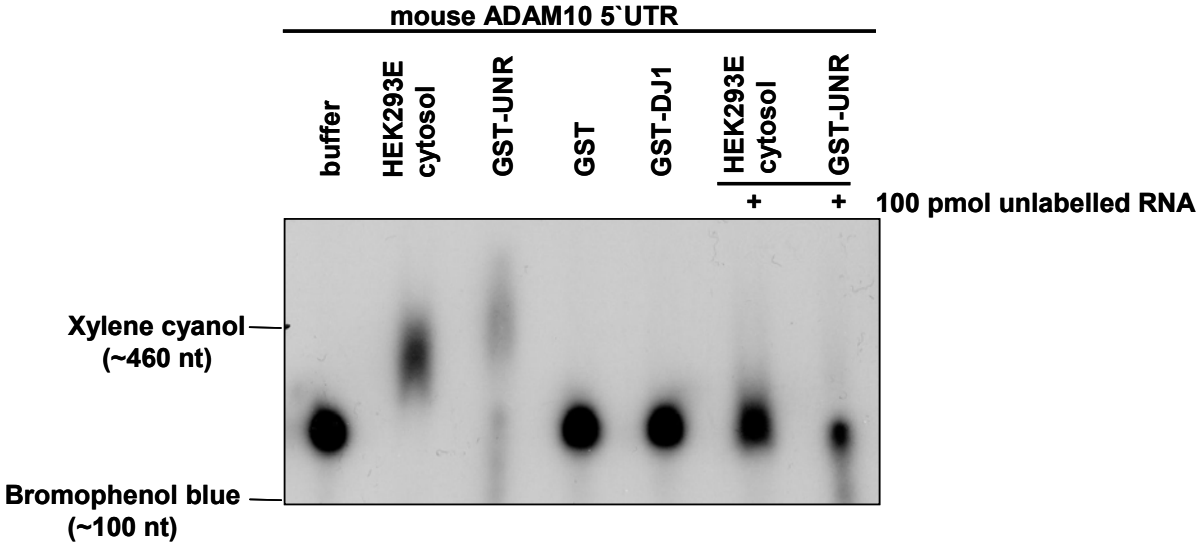

Figure 3.26 Recombinant Unr binds to the mouse ADAM10 5`UTR.
Radiolabelled mouse ADAM10 5'UTR (1x 10^6 cpm) was incubated either with 15 µg cytosolic extract of HEK293E cell or with 4 µg of the indicated recombinant proteins in binding buffer for 30 min at room temperature. RNA-protein complexes were separated on a 3.5% non-denaturing polyacrylamide gel and visualized by autoradiography. The xylene cyanol (~ 460 nt) and bromophenol blue (~ 100 nt) front on the gel served as size marker. Competition studies were performed by the addition of unlabelled mouse ADAM10 5`UTR (100-fold excess). The incubation of RNA with cytosolic or GST-Unr induced a shift due to cytosolic proteins or GST-Unr binding to the RNA. The two negative controls GST or GST-DJ1 showed no binding to the ADAM10 5`UTR. The addition of unlabelled mouse ADAM10 5`UTR to the reaction abrogates the binding of cytosolic extract and GST-Unr. Note, in the lane with GST-Unr some degradation is visible.

3.4.3 Deletion analysis of predicted Unr binding site

EMSAs showed that Unr specifically binds to the ADAM10 5`UTR. By *in vitro* selection experiments (SELEX) it was shown that Unr preferentially binds to purine-rich sequences (Triqueneaux *et al.*, 1999). Moreover, the UTR database search (3.2) predicts

that there are two optimal Unr binding sites within the purine-rich stretch of the human ADAM10 5`UTR. The first Unr binding site is located between nucleotides 180-193 and the second Unr binding site between nucleotides 218-231 (compare Figure 3.12). To confirm that these regions within the long purine stretch are part of the Unr binding site, several 5`deletions of the ADAM10 5`UTR RNA were analysed by EMSA (Figure 3.27).

As expected, the full-length ADAM10 5`UTR and the first half (Δ251-432) of the ADAM10 5`UTR bind proteins of the cytosolic extract as well as GST-Unr (Figure 3.27) in agreement with the previous results. However, for the second half (Δ1-259) of the ADAM10 5`UTR, lacking the entire purine-rich stretch, neither binding of cytosolic proteins nor binding of GST-Unr was detectable (see Figure 3.27: highlighted with a red box). To explore the importance of this purine-rich sequence, the Δ1-163/247-342, Δ164-246, Δ164-204 and Δ201-246 probes were analysed. Interestingly, cytosolic extract and recombinant GST-Unr bind to the Δ1-163/247-342 construct that extends over the entire purine-rich sequence, indicating that Unr binds to the purine-rich stretch of the ADAM10 5`UTR as predicted by the UTR database search and SELEX experiments (Triqueneaux *et al.*, 1999).

Moreover, proteins of the cytosolic extract and recombinant GST-Unr still bind to the Δ164-204 and Δ201-246 probes of the ADAM10 5`UTR, where only one half of the purine-rich sequence is present. In contrast, the binding of Unr was diminished when the complete purine-rich stretch (Δ164-246) was deleted (Figure 3.27, highlighted with an yellow box). Importantly, the Δ164-246 ADAM10 5`UTR was still capable of binding proteins of the cytosolic extract (Figure 3.27, highlighted with an orange box). This observation suggests that Unr is not the only protein that interacts with the ADAM10 5`UTR. However, Unr was able to bind to the Δ164-204 and Δ201-246 ADAM10 5`UTR, supporting the prediction that there are at least two potential Unr binding sites within the purine-rich sequence 164-246 of the ADAM10 5`UTR.

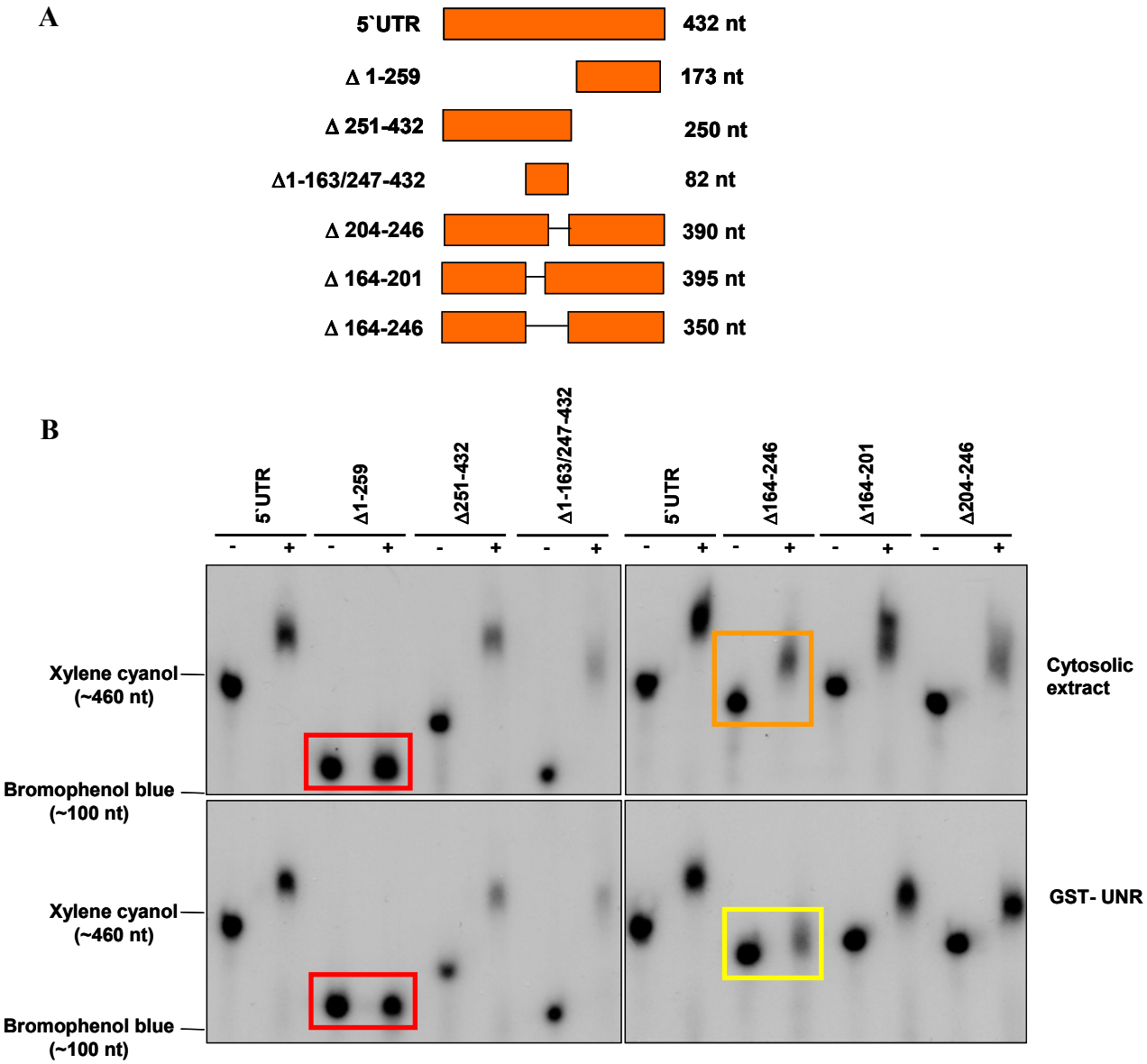

Figure 3.27 Unr binds to the purine stretch of the ADAM10 5`UTR.
(A) Schematic representation of the ADAM10 5`UTR deletion constructs lacking the predicted binding sites for Unr. Depicted are the 5`UTR and the 5`UTR deletion constructs used for EMSA. All ADAM10 5`UTR constructs lack the last 12 nucleotides; so that, e.g., the used full-length 5`UTR is only 432 nt instead of 444 nt long (compare Figure 2.1 and Figure 3.12). (B) $10^6$ cpm $^{32}$P-labelled full-length ADAM10 5`UTR and ADAM10 5'UTR deletion constructs were incubated either with 15 µg HEK293E cytosolic cell extract (upper panel) or with 4 µg of recombinant GST-Unr (lower panel) in binding buffer for 30 min at room temperature. RNA-protein complexes were separated on a 3.5% non-denaturing acrylamide gel and visualized by autoradiography. The xylene cyanol (~ 460 nt) and bromophenol blue (~ 100 nt) front on the gel served as marker. Incubation of full-length and Δ251-432 ADAM10 5`UTR with either cytosolic or GST-Unr resulted in a shift. However, no shift was observed with Δ1-259 ADAM10 5`UTR incubated with either cytosolic extract or GST-Unr (highlighted with a red box). The purine-rich sequence 164-246 as well as the deletion constructs Δ164-204 and Δ201-246 form complexes with proteins of the cytosolic extract and GST-Unr. Importantly, the deletion construct Δ164-246 ADAM10 5`UTR induced no shift with recombinant Unr but formed a complex with cytosolic extract (highlighted with an yellow or orange box).

3.4.4 Expression analysis of ADAM10 5`UTR deletion constructs

In the previous chapter, Unr has been shown to bind to the purine-rich sequence of the ADAM10 5`UTR (3.4.3). In a next step, it was addressed whether deletion of this purine-rich sequence affects ADAM10 expression at the translational level. Therefore, various 5`UTR deletion constructs in front of the ADAM10 ORF were transfected in HEK293E cells and expression levels of ADAM10 were analysed by immunoblotting (Figure 3.28A). As described previously, deletion of the first 215 and 259 nucleotides resulted in 30- and 70- to 100-fold increase of ADAM10 expression, respectively (Lammich *et al.*, 2010). Deletion of the first half of the purine-rich stretch (nucleotides 164-201) or deletion of the second half of the purine-rich stretch (nucleotides 204-246) resulted in a 2.5- and 4.5-fold increase of ADAM10 expression, respectively. However, omission of the complete purine-rich sequence (nucleotides 164-246) resulted in an 11-fold increase of ADAM10 expression (Figure 3.28B), suggesting that the purine-rich stretch is a strong translational inhibitory RNA element. Nevertheless, the constructs missing the first 215 and 259 nucleotides of the ADAM10 5`UTR resulted even in a stronger increase of ADAM10 expression, indicating that in addition to the purine-rich stretch there is another strong translational inhibitory RNA element within the first 259 nucleotides of the ADAM10 5`UTR. These results are consistent with the binding studies (3.4.3) demonstrating that there are several proteins which could bind to the ADAM10 5`UTR (Figure 3.27).

In addition, the mRNA levels of these deletion constructs were analysed to demonstrate that the observed effect on the protein expression is independent from an increase in transcription. The mRNA levels only increased 1.2-, 1.4- and 2.8-fold for the ADAM10 5`UTR deletions 164-201, 204-246 and 164-246, respectively (Figure 3.28B). For the constructs missing the first 215 and 259 nucleotides of the ADAM10 5`UTR the mRNA levels increased 3- and 4.9-fold, respectively, as described before (Lammich *et al.*, 2010), suggesting that deletion of the first 215 and 259 nucleotides could contribute to mRNA stability. However, the robust effects on protein synthesis are unlikely to emerge solely from mRNA stability. Instead, these findings suggest that there is a very strong translational inhibitory RNA element within the first 259 nucleotides of the ADAM10 5`UTR. Taken together, the Unr binding studies and ADAM10 expression data may suggest that Unr is involved in the translational repression of ADAM10.

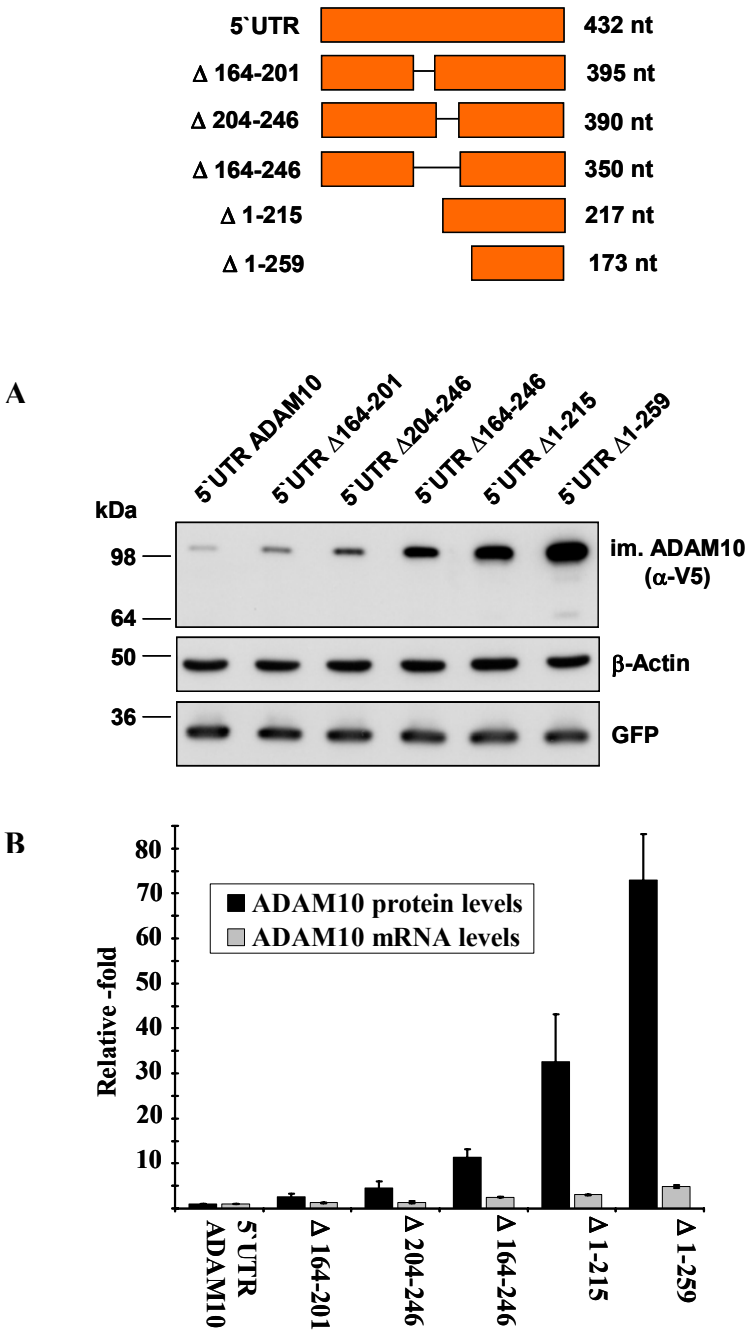

Figure 3.28 Effects of 5`UTR deletions on ADAM10 expression.
HEK293E cells were transfected with the indicated 5`UTR ADAM10 cDNA constructs. (A) Representative Western blots for V5-tagged ADAM10 and (B) Quantification of ADAM10 signals from cells transfected with ADAM10 cDNA constructs lacking parts of the 5`UTR are shown in black. The values were normalised to β-actin and GFP levels. The signal for ADAM10 with 5`UTR was set to 1. The results are expressed as the mean ± standard deviation of six independent experiments. Quantification of ADAM10 mRNA by quantitative real-time RT-PCR from cells transfected with ADAM10 cDNA constructs lacking parts of the 5`UTR are shown in grey. ADAM10 mRNA levels were normalised to GAPDH mRNA levels. The values are the mean ± standard deviation of at least two different experiments measured in triplicates and the signal of the 5`UTR ADAM10 mRNA is set to 1.

3.5 Effect of Unr on ADAM10 and APP processing

3.5.1 Unr knockdown

Based on the hypothesis that the proteins binding to the ADAM10 5`UTR could contribute to the regulation of ADAM10 expression at the translational level, the functional relationship between endogenous Unr and ADAM10 in HEK293E cells was analysed. HEK293E cells stably expressing shRNA (short hairpin RNA) against Unr were generated. To determine the level of Unr and ADAM10 protein levels in Unr knockdown (Unr KD) cells, cytosolic extract and membrane preparations were separated by SDS-PAGE and analysed by immunoblotting. Unexpectedly, Unr knockdown in HEK293E cells resulted in a significant decrease in Unr levels, accompanied by a significant decrease in the expression of ADAM10 protein (Figure 3.29), suggesting that Unr is indeed important for regulating ADAM10 synthesis although an increase of ADAM10 expression was expected. To control equal loading of protein, actin and calnexin were used as loading controls. In addition, it was shown that Unr knockdown has no general effect on protein expression, since expression of endogenous APP was not altered upon Unr knockdown.

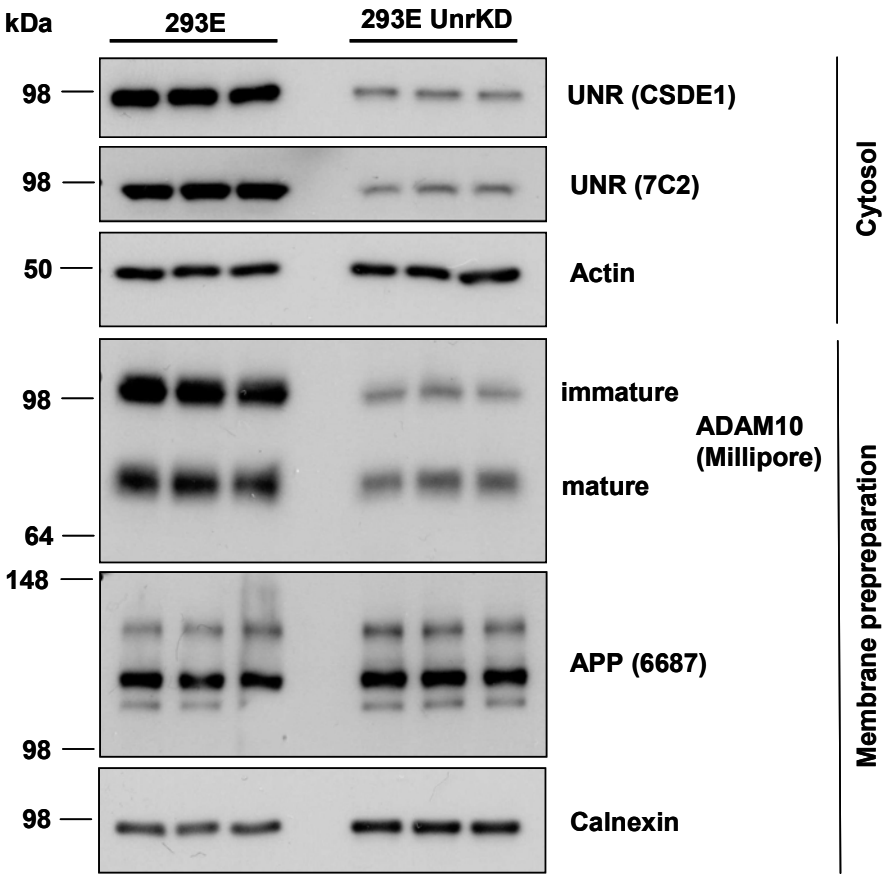

Figure 3.29 Endogenous ADAM10 levels were reduced in cells with decreased expression of Unr

Cytosolic extracts of HEK293E Unr knockdown cells were prepared to analyse the levels of Unr and β-actin as loading control by Western blot. Membranes were prepared to analyse the levels of ADAM10, APP and loading control calnexin. ADAM10 protein levels were reduced in cells that have low levels of Unr. In contrast, APP protein levels were unaffected.

To further analyse the consequences of Unr knockdown on ADAM10 expression, the processing of APP, an ADAM10 substrate, was analysed. Shedding of APP by ADAM10 results in APPsα and CTFα. Therefore, a change in ADAM10 expression levels should consequently lead to a change in the production of APPsα. Supernatants of HEK293E cells and HEK293E Unr KD cells were analysed for APPsα levels. As expected, reduced ADAM10 levels in the HEK293E Unr KD cells resulted in reduced APPsα levels compared to HEK293E cells (Figure 3.30) although APPsβ and Aβ levels did not change. The drop of total APPs levels (APPst) is due to the reduced levels of APPsα.

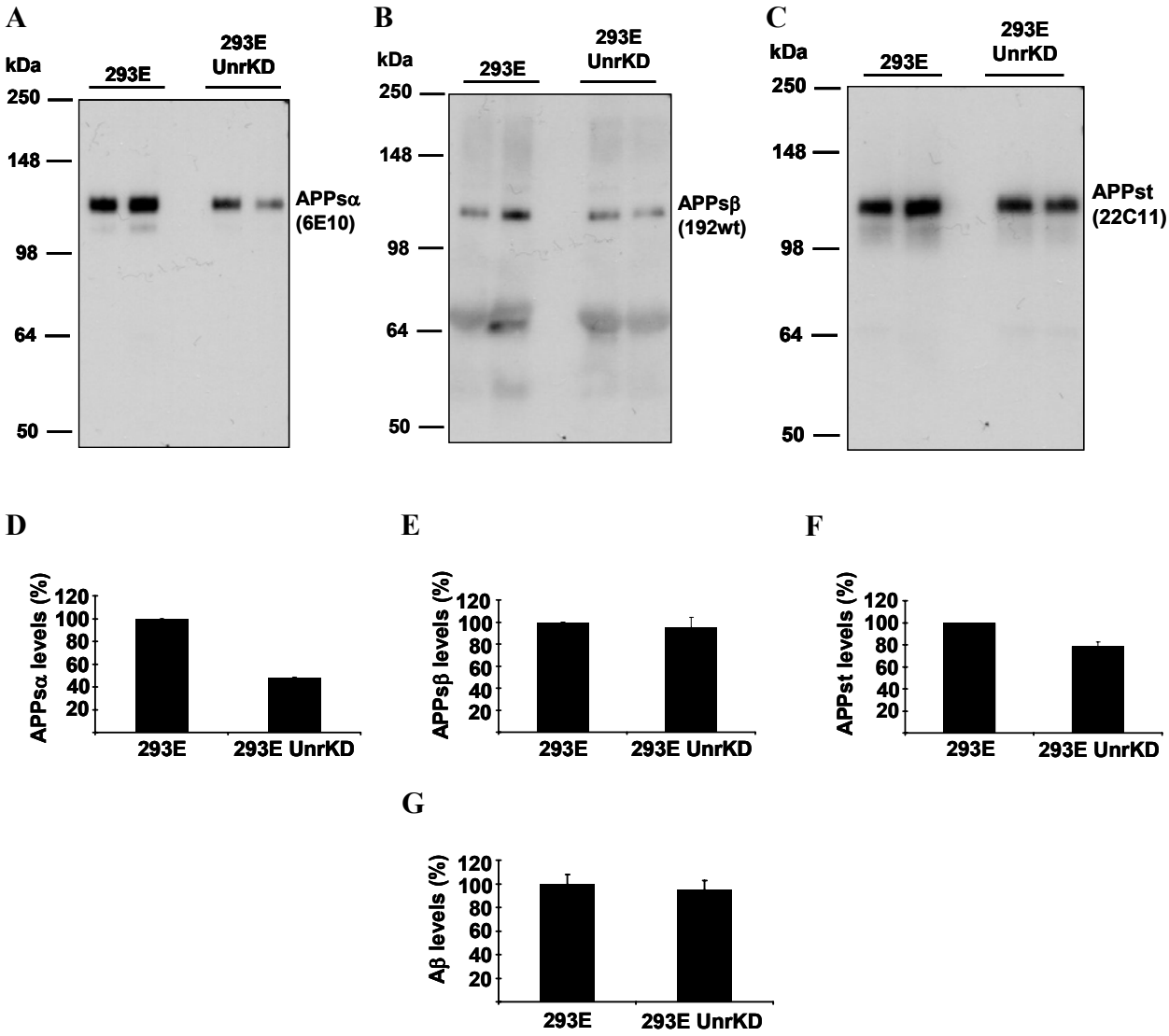

Figure 3.30 Reduced APP processing in Unr KD cells
(A-C) Representative Western blots for APPsα (A), APPsβ (B) and APPst (C) in stable HEK293E Unr knockdown (KD) cells are shown. (D-F) Quantification of APPsα (D), APPsβ (E) and APPst (F) signals from Unr KD cells. The APPsα, APPsβ, APPst and Aβ signal for HEK293E was set to 100%. Results are expressed as the mean ± standard deviation of at least six independent experiments. (G) Aβ levels were determined by ELISA (performed by Brigitte Nuscher). The Aβ signal for HEK293E was set to 100%. Results are expressed as the mean ± standard deviation of at least three independent experiments.

Overexpression of the ADAM10 5`UTR deletion constructs resulted in an increase in ADAM10 protein expression upon deletion of the Unr binding sites (purine-rich stretch) (refer to Figure 3.28). Therefore, it was expected that Unr plays a role in the translational control of ADAM10. The knockdown of Unr resulted in a decrease of ADAM10 levels, although an increase of ADAM10 expression was expected. However, since Unr is also involved in mRNA stabilisation (Chang *et al.*, 2004; Dinur *et al.*, 2006; Grosset *et al.*, 2000), reduced ADAM10 levels could conceivably be caused by decreased stability of the

ADAM10 mRNA. Therefore, RNA levels of Unr and ADAM10 were analysed by quantitative real-time PCR in these cells. The mRNA levels of Unr in the Unr knockdown cells were reduced to 15% (+/- 4.5%) (Figure 3.31). Importantly, the ADAM10 mRNA levels were reduced by 45% (+/- 10%) (Figure 3.31). This finding indicated that Unr is either essential for the stabilisation of the ADAM10 mRNA or has an effect on the ADAM10 transcription. Considering that, Unr is a cytosolic protein (Jacquemin-Sablon *et al.*, 1994), which is not found in the nucleus, a transcriptional effect could be ruled out as transcription occurs in the nucleus.

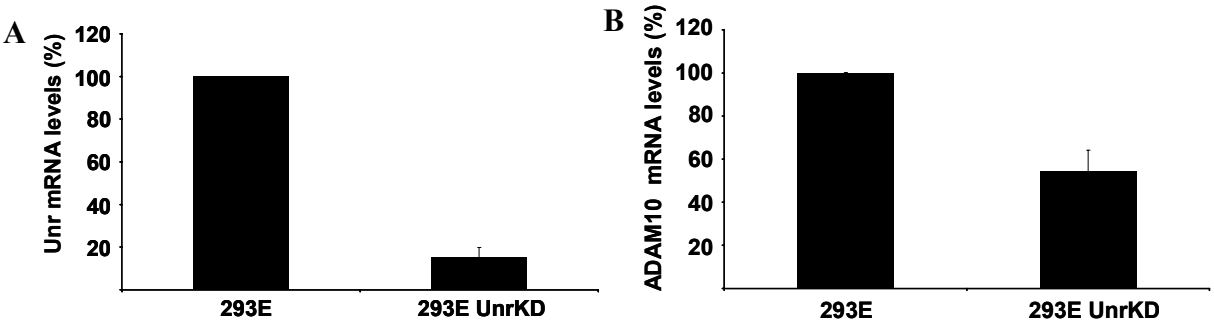

Figure 3.31 RNA levels for Unr KD cells.
Quantification of endogenous Unr (A) and ADAM10 (B) mRNA isolated from HEK293E cells and HEK293E Unr KD cells by quantitative real-time PCR with TaqMan probes. Unr and ADAM10 mRNA levels were normalised to endogenous GAPDH mRNA levels using the $2^{-\Delta\Delta CT}$ method. Values are expressed as the mean ± standard deviation of at least nine different experiments measured in triplicates. ADAM10 mRNA level and Unr mRNA level isolated from HEK293E cells were set to 100%.

3.5.2 Unr overexpression

Unr knockdown in HEK293E cells resulted in decreased ADAM10 protein expression accompanied by a decrease in ADAM10 mRNA levels. To examine the functional relationship between overexpressed Unr and endogenous ADAM10 in HEK293E cells, myc-tagged Unr was stably expressed in HEK293E cells. Cytosolic extract and membrane preparations of HEK293E cells overexpressing Unr-myc were analysed for ADAM10 expression by Western blotting. To control equal loading of protein, actin and calnexin were used as loading control. Unr-myc overexpression in HEK293E cells resulted in a replacement of the endogenous Unr levels, accompanied by a minor decrease of immature ADAM10 levels (Figure 3.32). Replacement of endogeneous Unr might be due to that Unr forms a complex with other proteins. In addition, it was shown that Unr overexpression has no general effect on protein expression by analysing the expression of APP, since the expression of APP was not altered upon Unr overexpression.

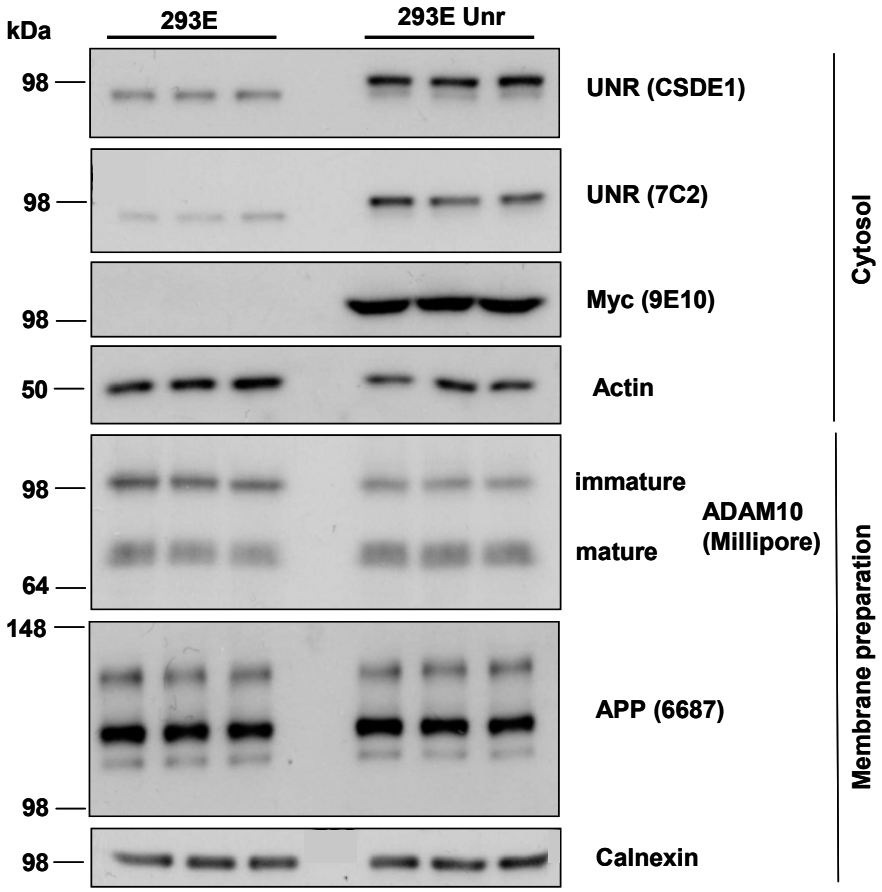

Figure 3.32 Overexpression of Unr results in a minor decrease of endogenous immature ADAM10.
Representative Western blots for Unr, ADAM10 and APP in stably Unr overexpressing HEK293E cells. β-actin as a cytosolic protein and calnexin as a membrane protein were used as loading controls. HEK293E cells with overexpressed Unr show a small decrease in immature ADAM10 protein levels. In contrast, APP protein levels were unaffected.

Overexpression of Unr resulted in a small decrease of APPsα levels compared to HEK293E cells (Figure 3.33). Surprisingly, APPsβ as well as Aβ levels increased upon overexpression of Unr, whereas APPst levels were more or less unaffected.

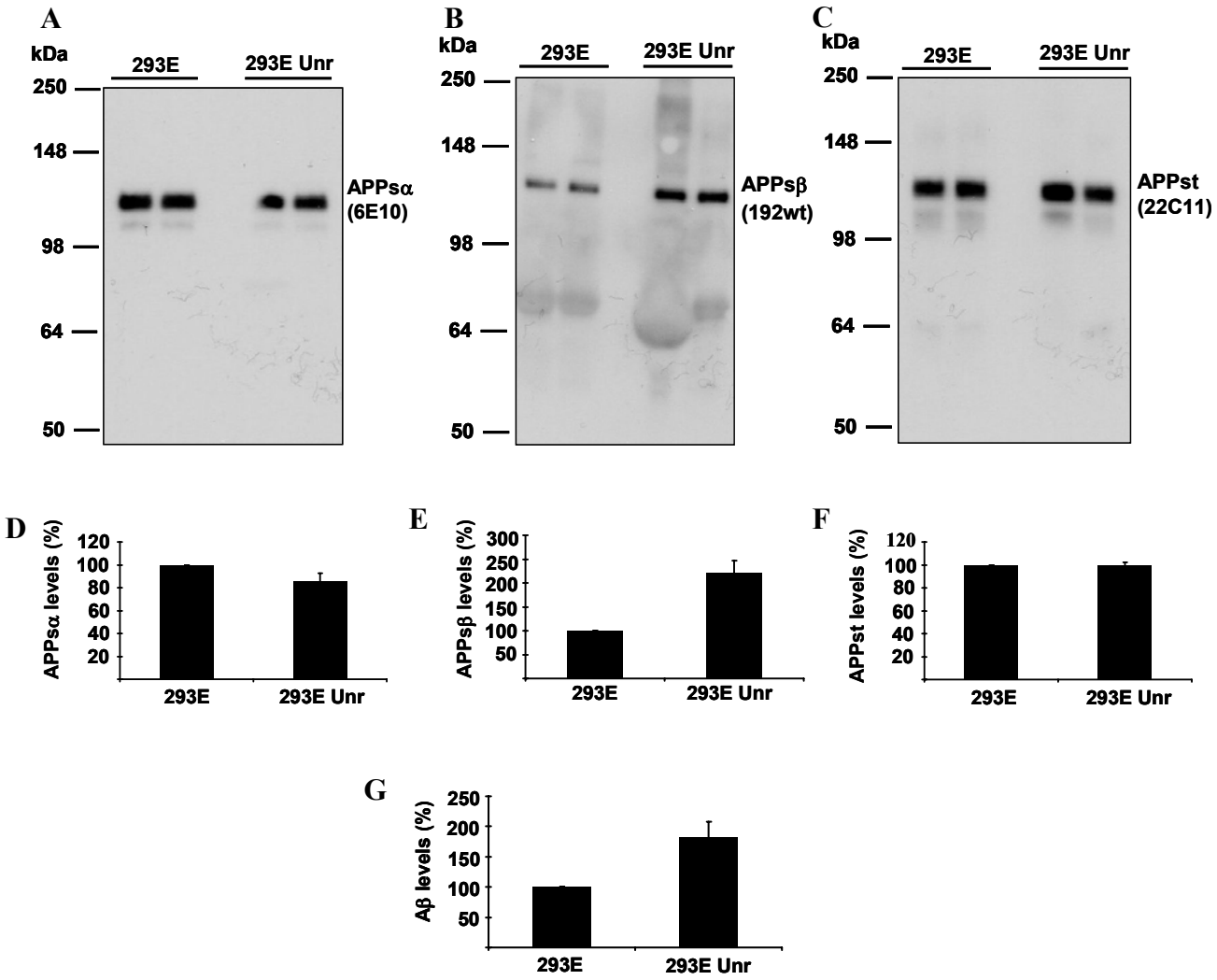

Figure 3.33 Change in APP processing in Unr overexpressing cells.
Supernatants were collected to assess the levels of APPsα (A), APPsβ (B) and APPst (C) by Western blotting. The signals of APPsα (D), APPsβ (E) and APPst (F) were quantified and represented as mean ± standard deviation of at least six independent experiments. Aβ levels (G) were determined by ELISA. The signals for APPsα, APPsβ, APPst and Aβ in HEK293E cells were set to 100%.

A decrease of ADAM10 levels upon Unr overexpression in HEK293E cells was expected from the previous results of the ADAM10 5`UTR deletion constructs in HEK293E cells shown in Figure 3.28. Since the HEK293E Unr knockdown cells showed reduced ADAM10 protein and mRNA levels (Figure 3.31), it might be possible that Unr is involved in the stabilisation of ADAM10 mRNA (3.5.1). To test the involvement of Unr in ADAM10 mRNA stabilisation, the RNA levels of Unr overexpressing cells were analysed by quantitative real-time PCR. Quantitative real-time PCR revealed that ADAM10 mRNA level did not change in response to increased Unr levels. The mRNA level of Unr in Unr overexpressing cells was increased by a factor of 4 (Figure 3.34).

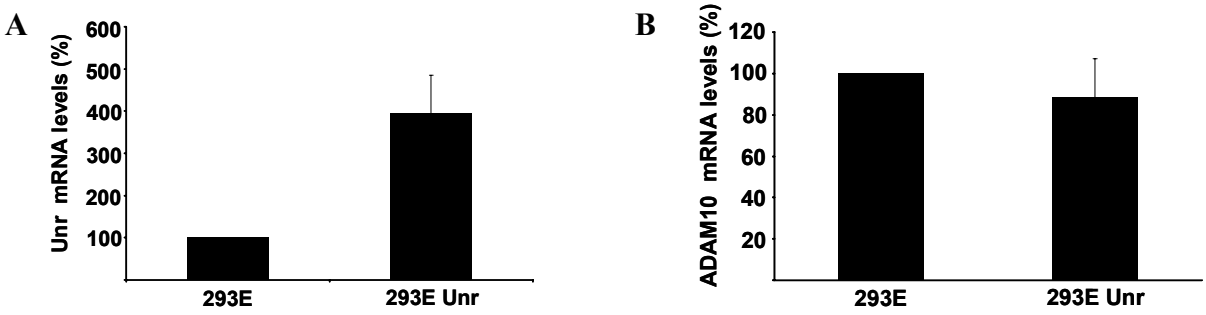

Figure 3.34 RNA levels for Unr overexpression
Quantification of Unr (A) and ADAM10 (B) mRNA isolated from HEK293E cells and HEK293E Unr overexpressing cells by quantitative real-time PCR with TaqMan probes. Unr and ADAM10 mRNA levels were normalised to endogenous GAPDH mRNA levels using the $2^{-\Delta\Delta CT}$ method. Values are expressed as the mean ± standard deviation of at least four different experiments made in triplicate. ADAM10 mRNA level and Unr mRNA level isolated from HEK293E cells were set to 100%

In summary, the analysis of the functional relationship between endogenous Unr and ADAM10 in HEK293E cells resulted in some interesting findings (summarized in Figure 3.35).

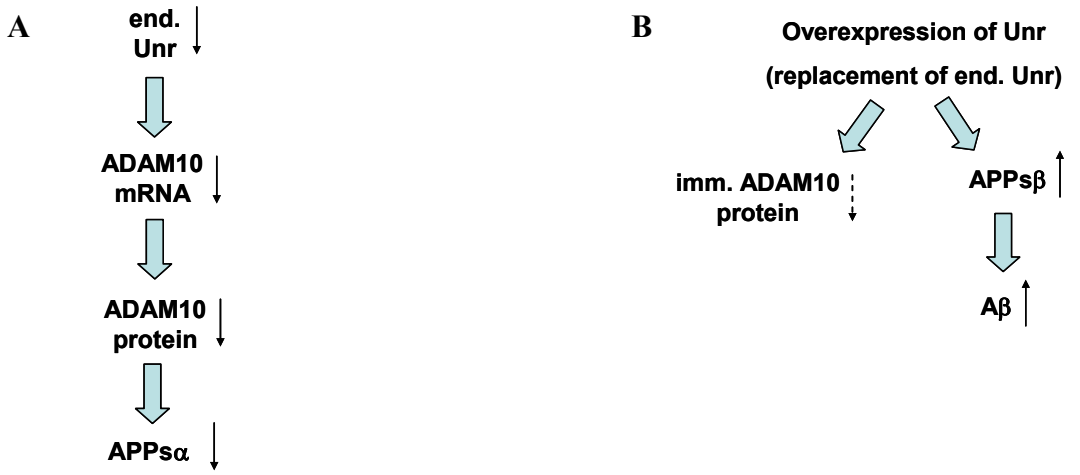

Figure 3.35 A schematic diagram depicting the major findings of the functional relationship between Unr, ADAM10 and APP processing
(A) Downregulation of Unr leads to reduced ADAM10 mRNA and protein levels as well as reduced secretion of APPsα. (B) The overexpression of Unr leads to a replacement of endogenous Unr protein complexes. Moreover a small decrease of immature (imm.) ADAM10 was observed. In addition, the levels of APPsβ and Aβ are increased.

Upon Unr downregulation, ADAM10 protein and mRNA levels were reduced. Consistent with these findings, the generation of APPsα was reduced (Figure 3.35A). The levels for APPsβ, APPst and Aβ remained unchanged. Upon overexpression of Unr in HEK293E cells, endogenous Unr was downregulated thereby the ADAM10 protein levels were hardly affected and no change was observed for ADAM10 mRNA levels, APPsα and

APPst. However, the most significant finding was that Unr overexpression results in increased levels of APPsβ consistently with increased Aβ (Figure 3.35B).

Hence, these results suggest that Unr influences the stability of the ADAM10 mRNA and surprisingly has an effect on the generation of APPsβ and Aβ.

4 Discussion

This PhD thesis deals with the translational control of ADAM10 expression. The regulation of ADAM10 expression might be critical for the development of AD. An increase in α-secretase cleavage can be considered as a therapeutic approach for AD (Endres and Fahrenholz, 2010; Fahrenholz, 2007). Consistent with this hypothesis, it was recently shown that ADAM10 expression in mice potentiates hippocampal neurogenesis (Suh *et al.*, 2013). Moreover, mutations in the ADAM10 prodomain reduced α-secretase activity, increased β-secretase activity, enhanced Aβ plaque load as well as reactive gliosis and cosegregate with late onset AD (Suh *et al.*, 2013). Therefore, it is important to understand how the expression of ADAM10 is regulated. Several studies addressed the regulation of ADAM10 expression at the level of transcription (Donmez *et al.*, 2010; Prinzen *et al.*, 2005; Tippmann *et al.*, 2009). In addition to transcription, post-transcriptional mechanisms play an important role in the control of ADAM10 expression.

The ADAM10 5`UTR has been shown to be involved in the translational regulation (Lammich *et al.*, 2010; Lammich *et al.*, 2011), but the exact mechanism mediating this effect is unknown. Therefore, the possibility that 5`UTR RNA-binding proteins regulate ADAM10 expression was explored in this work. To search for such factors forming complexes with RNA, *in vitro* binding experiments were carried out by EMSAs, UV crosslinking and affinity purification. Beyond that the functional relationship between one of these factors and ADAM10 expression was analyzed in this work.

4.1 Unr as potential regulator of ADAM10 expression

To identify potential ADAM10 5`UTR binding proteins a database search was performed. This search revealed Unr as potential binding protein of ADAM10 5´UTR. Interestingly, Unr was shown to be involved in the regulation of mRNA translation and stability by binding to sites generally located in UTRs (Mihailovich *et al.*, 2010).

4.1.1 Unr binds to a purine-rich region in the ADAM10 5`UTR

To confirm the result of the database search, binding of Unr to ADAM10 was analysed by EMSAs with recombinant Unr. EMSAs suggest that Unr indeed binds specifically to the human and mouse ADAM10 5`UTR. In a next step, the exact region of Unr binding to the ADAM10 5`UTR was investigated. By *in vitro* selection experiments (SELEX) it was shown previously that Unr preferentially binds to purine-rich sequences (Triqueneaux *et al.*, 1999). Unr binds preferentially to two related consensus sequences,

R_5AAGUAR and R_8AACR$_3$ (R = G or A) with a K_d of 10-25 nM (Triqueneaux *et al.*, 1999). Single base changes of purines to pyrimidine have limited effect on Unr-RNA recognition and the purines downstream of the pyrimidine in these motifs seem to be unimportant for efficient binding (Triqueneaux *et al.*, 1999). Interestingly, two such R_8AACR$_3$ motifs can be found in the 83-nucleotide-long purine-rich stretch of the ADAM10 5`UTR (Figure 3.12). The two Unr binding sites within this purine-rich stretch are predicted to be between nucleotides 180-193 and 218-231 (Figure 3.12). The binding of Unr is indeed dependent on the 83-nucleotide-long purine-rich sequence located between nucleotides 164-246 of the ADAM10 5'UTR since the binding of Unr is lost when this region is deleted. Moreover, deletion of this purine-rich sequence results in an 11-fold increase of ADAM10 expression after overexpression of ADAM10 cDNA (Figure 3.28). That means, upon deletion of the Unr binding site, the ADAM10 mRNA could be translated more efficiently resulting in an increase in protein expression. Hence, Unr might be a translational repressor of ADAM10 protein expression. Deletion of the first 155, 175 or 215 nucleotides, where the purine stretch is intact or partially deleted, leads to a 8-fold, 28-fold or 40-fold increase in ADAM10 expression, respectively (refer to Figure 3.28) (Lammich *et al.*, 2010). However, deletion of the purine-rich stretch together with the first 163 nucleotides results in a 70-100-fold increase of ADAM10 expression levels compared to the construct with full-length 5`UTR (refer to Figure 3.28) (Lammich *et al.*, 2010). Thus, there might be other translational inhibitory RNA elements in the first part of the 5´UTR. Interestingly, Lammich and colleagues could recently show that the ADAM10 5`UTR contains a G-quadruplex secondary structure close to the 5`end that represses ADAM10 translation (Lammich *et al.*, 2011). Upon deletion of the G-quadruplex and the purine-rich sequence, the same increase of ADAM10 expression level can be observed as for deletion of the first 259 nucleotides (Dr. S. Lammich, personal communication). G-quadruplexes are four-stranded structures formed by guanine-rich sequences (Gellert *et al.*, 1962; Sen and Gilbert, 1992).

4.1.2 Identification of Unr by affinity chromatography followed by mass spectrometry

The database search result and EMSAs could be confirmed by affinity purification followed by mass spectrometry. Since two different isoforms of Unr were described (Boussadia *et al.*, 1993; Ferrer *et al.*, 1999), the question which of these two isoforms binds to the ADAM10 5`UTR came up. The two isoforms result from an exon-skipping

mechanism. Therefore, the protein encoded by the open reading frame is either 767- or 798-amino-acid-long with a predicted molecular weight of either 85 or 88 kDa. The Unr sequences that are shown in Figure 3.17 represent the longer isoform of Unr including exon 5 (exon 5 marked in blue). The longer message containing exon 5 represents only a small fraction of Unr messages in all tissues except for the brain (Boussadia *et al.*, 1993). In the brain, both types of messages are equally abundant. However, the mass spectrometry results did not reveal which of the two Unr proteins binds to the ADAM10 5`UTR (refer to chapter 3.4) as none of the identified peptides corresponds to exon 5. The alternative splicing that leads to a difference of 31 amino acids near the N-terminus of the Unr protein does not disrupt any of the five cold shock protein motifs present in the protein. Hence, it is not clear which isoform of Unr binds to the ADAM10 5`UTR. Since the RNA recognition motifs ribonucleoprotein RNP-1 (amino acids Y/FGFI) and RNP-2 (amino acids FFH) are conserved in both Unr isoforms (Boussadia *et al.*, 1993; Ferrer *et al.*, 1999), it is likely that both isoforms are involved in ADAM10 5`UTR binding.

4.2 Other potential regulators of ADAM10 expression

As mentioned above, the affinity purification followed by mass spectrometry was conducted to confirm Unr as ADAM10 5`UTR binding protein. In addition, the affinity purification approach from cytosolic extract of HEK293E cells and from mouse brain cytosolic extract identified a large number of other proteins binding to the ADAM10 5`UTR.

4.2.1 Comparison of results from UV crosslink and affinity purification

Several of the hnRNPs identified by affinity purification in this work, such as hnRNP A1 and hnRNP A2/B1, are also involved in nuclear-cytoplasmic shuttling (Allemand *et al.*, 2005; Borer *et al.*, 1989; Nichols *et al.*, 2000). Furthermore, nucleolin, which was identified as potential ADAM10 5`UTR binding protein by affinity purification, is known to shuttle between the nucleus and cytosol (Borer *et al.*, 1989). These shuttle proteins could first bind to the ADAM10 5`UTR in the nucleus and then continue their function in the cytosol to regulate the ADAM10 mRNA expression. This would also explain the results from the UV crosslinking experiments with cytosolic and nuclear extract which show protein bands of the same molecular weight (refer to Figure 3.8). The protein bands in the cytosolic and nuclear fraction with a molecular weight above 36 kDa could be

hnRNP A1 and hnRNP A2/B1. Since these proteins are primarily localized in the nucleus, the protein band of the UV crosslink is more pronounced in the nuclear fraction. The protein band around 80 kDa, which is more pronounced in the cytosolic fraction, could be nucleolin. Preliminary results from EMSAs could confirm the binding of recombinant hnRNP A1 and hnRNP B1 to the ADAM10 5`UTR (data not shown). Therefore, they likely play a role in the translational control of the ADAM10 expression. Most interestingly, hnRNP A2/B1 has been implicated in AD and its expression is altered in the hippocampi of patients at different stages of disease (Mizukami *et al.*, 2005).

4.2.2 Specificity and selectivity of identified proteins

To prove the specificity of the RNA-binding proteins, competition experiments were conducted via UV crosslinking. Since the RNA-protein complexes could be competed with excess of non-labelled ADAM10 5`UTR, RNA-protein binding seems to be specific. The selectivity of the RNA-binding proteins was analyzed by the use of a second unrelated 5`UTR, more precisely the BACE1 5`UTR. The protein band patterns from the UV-crosslink (3.1.4) and affinity chromatography (3.3) experiments for the ADAM10 5`UTR and BACE1 5`UTR, respectively, are different, strongly suggesting that the detected RNA-binding proteins were selective for the ADAM10 5`UTR. Also the mass spectrometry results from the affinity purification of both 5`UTRs confirm the difference of proteins identified.

4.2.3 Potential role of the other identified proteins on ADAM10 expression

Many of the identified proteins are known to influence different aspects of mRNA metabolism, including translational control, splicing, transport and stability (Carpenter *et al.*, 2006; Glisovic *et al.*, 2008; Krecic and Swanson, 1999). Since the first part of the 5`UTR also seems to have a translational inhibitory function, these proteins might bind to this part. As mentioned above, Lammich and colleagues could show that the ADAM10 5`UTR contains a G-quadruplex secondary structure close to the 5`end that represses ADAM10 translation. Interestingly, several of the purified RNA-binding proteins, such as nucleolin, the hnRNP F/H family and hnRNP A family have been reported to interact with G-rich sequences (Abdelmohsen *et al.*, 2011; Dominguez *et al.*, 2010; Khateb *et al.*, 2007; Khateb *et al.*, 2004). They can either bind to G-quadruplex structures in DNA or RNA promoting its formation, and/or stabilizing the final structure or unwind this stable

secondary structure, thus facilitating transcription or translation (Brooks and Hurley, 2010; Dominguez *et al.*, 2010; Gonzalez *et al.*, 2009; Khateb *et al.*, 2007; Khateb *et al.*, 2004). For example, nucleolin is involved in the formation and stabilisation of the c-myc DNA G-quadruplex structure. Nucleolin thereby blocks the transcription of c-myc (Brooks and Hurley, 2010; Gonzalez *et al.*, 2009; Gonzalez and Hurley, 2010). hnRNP F/H can prevent G-quadruplex structure formation by binding single-stranded RNA (Dominguez *et al.*, 2010). In addition, hnRNP A2 and hnRNP A1 have been reported to destabilize G-quadruplexes in both DNA and RNA (Khateb *et al.*, 2004). hnRNP A2 relieves the translational block of FMR1 mRNA that results from G-quadruplex formation and thereby enhancing translation (Khateb *et al.*, 2007). Also preliminary results from EMSAs resulted in binding of recombinant hnRNP A1, hnRNP A2 and hnRNP B1 to the ADAM10 5`UTR (data not shown), it was not yet tested if binding occurs at the G-rich region. Therefore, these proteins might be involved in the translational repression of ADAM10 by binding to its G-quadruplex. Admittedly, the influence of these proteins on the ADAM10 5`UTR G-quadruplex has not been analysed so far.

4.3 Functional relationship of Unr and ADAM10 expression

4.3.1 Influence of Unr on ADAM10 expression levels

As mentioned above, the expression of the ADAM10 5`UTR deletion constructs lacking the Unr binding site resulted in a tremendous increase in ADAM10 expression (Figure 3.28) (Lammich *et al.*, 2010). Therefore, a decrease of ADAM10 levels upon Unr overexpression and an increase of ADAM10 levels upon Unr knockdown was expected. Normally translational repression can be reversed, and this is generally achieved by removal of the repressor from its binding site on the mRNA or by remodelling of the repressor complex (Abaza and Gebauer, 2008; Cao and Richter, 2002; Klausner *et al.*, 1993; Ostareck-Lederer *et al.*, 2002; Thomas *et al.*, 2008). However, stable knockdown of Unr resulted in a strong decrease of ADAM10 mRNA and protein levels in HEK293E cells (summarized in Figure 3.35). In line with reduced ADAM10 levels, APPsα levels were reduced in the HEK293E Unr KD cells. However, APPsβ and Aβ levels did not change. These findings are in line with the recently published data from Kuhn *et al.* and Colombo *et al.* (Colombo *et al.*, 2012; Kuhn *et al.*, 2010). They had demonstrated the same phenomenon that upon ADAM10 knockdown APPsα is decreased, however APPsβ and Aβ were not increased (Colombo *et al.*, 2012; Kuhn *et al.*, 2010). As discussed in these two publications, the results can be explained by different scenarios. One possibility is that

the cellular APP levels may not be rate limiting for α- and β-secretase cleavages in HEK293E cells and therefore the reduction of one cleavage does not increase the other cleavage. Another possibility is that the α- and β-secretase cleavages occur at different cellular compartments in HEK293 cells. This means that reduced α-secretase cleavage of APP at the plasma membrane does not increase the endosomal APP available for β-secretase cleavage.

An increase in Unr concentration in HEK293E cells does not change ADAM10 mRNA levels and hardly affects protein levels (summarized in Figure 3.35). Since endogenous levels of Unr were replaced upon Unr overexpression and Unr overexpression shows no effect on mRNA and protein levels of ADAM10, a possible explanation for this observation might be that a multiprotein complex is necessary for obtaining a change in ADAM10 expression. Furthermore, it is quite common that multiple proteins are involved in the translational regulation as mRNA-specific regulation by single proteins (e.g. IRP) is more an exception (Gebauer and Hentze, 2004). Several studies indeed have shown that Unr is part of a protein complex that regulates translation and mRNA stability. Some of the identified proteins, like hnRNP Q, PABP, FBP and Unrip are already described to form a multiprotein complex together with Unr (Abaza *et al.*, 2006; Chang *et al.*, 2004; Dinur *et al.*, 2006; Duncan *et al.*, 2006; Duncan *et al.*, 2009; Grosset *et al.*, 2000; Hunt *et al.*, 1999; Mitchell *et al.*, 2003; Nechama *et al.*, 2008; Patel *et al.*, 2005). Grosset *et al.* and Chang *et al.*, for example, could show that Unr forms a complex with PABP, PAIP1, hnRNP D and hnRNP Q to control the translationally coupled mRNA turnover of the c-fos mRNA (Chang *et al.*, 2004; Grosset *et al.*, 2000). In addition, Bannai *et al.* showed that hnRNP Q interacts in HEK293E cells with PABP1, nucleolin as well as several hnRNPs such as hnRNP A2/B1, hnRNP F/H and hnRNP U (Bannai *et al.*, 2004) which have been identified as binding partners for the ADAM10 5`UTR. Furthermore, in another study, it was shown that Unr can form a complex with PABP and IMP-1 at the 5`UTR of the PABP mRNA to repress the translation of PABP mRNA (Patel *et al.*, 2005).

Such complex components could be the limiting factor for obtaining a change in ADAM10 expression and will be discussed in the proposed model for ADAM10 regulation.

4.3.2 Proposed model for ADAM10 regulation

In this work, it was shown that Unr overexpression has no effect on ADAM10 mRNA levels (refer to Figure 3.34) and ADAM10 mRNA translation stays unchanged (refer to

Figure 3.32). However, Unr overexpression resulted in reduced levels of endogeneous Unr. A possible explanation could be that Unr forms a complex with other proteins as mentioned above. Therefore, overexpression of Unr together with other RNA-binding proteins could result in stabilization of ADAM10 mRNA. Upon Unr knockdown, the ADAM10 mRNA is reduced (refer to Figure 3.31) with the consequence of reduced ADAM10 protein expression (refer to Figure 3.29). This observation is depicted in the proposed model (Figure 4.1): upon expression of Unr and other RNA-binding proteins ADAM10 mRNA might be stabilized and protein translation might then be increased. However, it might be also possible that the mRNA is stabilized while the protein translation might be not increased since efficient ribosome recruitment is blocked. Upon Unr knockdown, Unr and other RNA-binding proteins are released from the ADAM10 5`UTR. Following the release of these proteins, another RNA-binding protein could bind to the purine-rich stretch and recruits the degradation machinery to the 5`UTR thereby mediating the mRNA turnover.

This model would also explain why deletion of the purine-rich stretch results in an increase in ADAM10 expression. Upon deletion of the purine-rich stretch, neither Unr nor the protein recruiting the degradation machinery could bind anymore. As a consequence the RNA could be translated more efficiently, along with ADAM10 mRNA stabilisation. Thus, depletion of both proteins should result in an increase in ADAM10 expression and a stabilisation of ADAM10 mRNA.

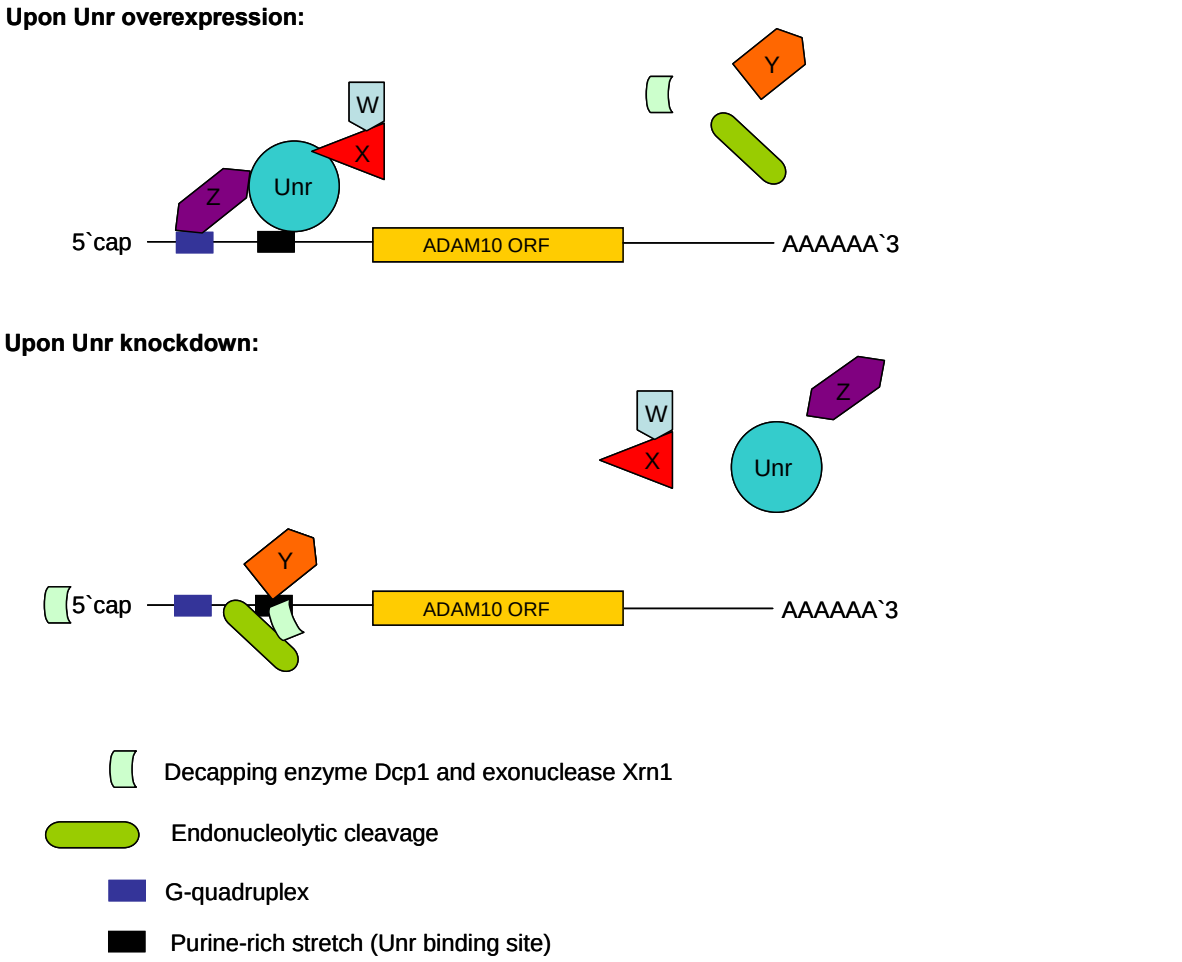

Figure 4.1 Proposed model for the regulation of ADAM10 mRNA stability.
Unr together with some other RNA-binding proteins (W, X, Z) binds to the 5`UTR of ADAM10 thereby blocking the recruitment of degrading enzymes. Upon deletion of Unr another RNA-binding protein (Y) can bind to the ADAM10 5`UTR that recruits nucleases to the mRNA.

There are several different mechanisms of eukaryotic mRNA decay described (Day and Tuite, 1998).

The first example of mRNA decay can occur via the 5´end. Binding of Unr may prevent binding of decapping enzymes and RNA degrading enzymes to the cap structure. However, when Unr is depleted mRNA decay is accelerated and mRNA stabilization is abrogated. This means, displacement of Unr makes the 5`cap accessible to degradative enzymes, such as Dcp1/Dcp2 and Xrn1. Dcp1 and Dcp2 are decapping enzymes that remove the mRNA cap and renders the 5`end of the mRNA accessible to the Xrn1 exonuclease (Amrani *et al.*, 2006). Interestingly, it was reported that Xrn1 exhibits a substrate preference for G-quadruplex RNA (Bashkirov *et al.*, 1997). Recently, Lammich and colleagues could show that the 5`UTR contains a G-quadruplex close to the 5`end (Lammich *et al.*, 2011) and might therefore be a good binding site for Xrn1.

The second example would be endonucleolytic cleavage within the gene while it is actively engaged by translating ribosomes (Dodson and Shapiro, 2002). Three mRNA endonucleases have been linked to specific decay pathways: polysomal ribonuclease 1 (PMR1) (Chernokalskaya *et al.*, 1998), G3BP (Gallouzi *et al.*, 1998) and IRE-1 (Hollien and Weissman, 2006). Endonucleolytic cleavage of some mRNAs is regulated by RNA-binding proteins that bind near the cleavage site(s) and render them inaccessible to nucleolytic attack. The c-myc mRNA is an example of an eukaryotic mRNA that is degraded by endonucleolytic cleavage before deadenylation (Barnes *et al.*, 2009; Sparanese and Lee, 2007).

The third example is based on the regulatory mechanism of the parathyroid hormone (PTH) mRNA where Unr binds to the PTH mRNA and stabilise the PTH mRNA (Dinur *et al.*, 2006). Most interestingly, PTH gene expression is regulated post-transcriptionally through the binding of the trans-acting proteins FBP2, Unr and hnRNP D to an AU-rich element (ARE) element in PTH mRNA 3`UTR (Dinur *et al.*, 2006; Nechama *et al.*, 2008; Nechama *et al.*, 2009; Sela-Brown *et al.*, 2000). While Unr together with hnRNP D stabilizes PTH mRNA, FBP2 promotes PTH mRNA decay (Dinur *et al.*, 2006; Nechama *et al.*, 2008). Calcium depletion increases the association of hnRNP D and/or Unr with the PTH mRNA ARE and decreases FBP2 binding to the ARE resulting in mRNA stabilization (Nechama *et al.*, 2008). In transfected cells, overexpression of FBP2 destabilizes the PTH mRNA and this is mediated by the PTH mRNA ARE (Nechama *et al.*, 2008). FBP2-PTH mRNA interaction is prevented by overexpression of HNRNP D and/or Unr. Overexpression of HNRNP D and/or Unr also attenuates the FBP2-mediated destabilization of PTH mRNA in transfected cells (Dinur *et al.*, 2006; Nechama *et al.*, 2008). In contrast, knockdown of Unr and/or hnRNP D led to a decrease in the expression of PTH (Dinur *et al.*, 2006). FBP2 is described to recruit labile mRNAs to the exosome and was proposed to compete with RNA-binding proteins that promote mRNA stability (Briata *et al.*, 2005; Chen *et al.*, 2001). For mRNAs recruited to the exosome by FBP2, the activity of deadenylase is also required for transcript decay, suggesting that FBP2 delivers the factors, necessary for both deadenylation and exosome-mediated degradation, onto target mRNAs (Gherzi *et al.*, 2004; Lai *et al.*, 2003). In this example, FBP2 interacts with the exosome in a phosphorylation-dependent manner and recruits the degradation machinery to the PTH mRNA thereby mediating the mRNA turnover (Gherzi *et al.*, 2004). In addition, FBP2 recruits the endonuclease PMR1 to the PTH mRNA. Upon FBP2 binding to the PTH mRNA, PMR1 cleaves the PTH mRNA and PTH mRNA decay can

proceed through exonucleolytic cleavage of both fragments (Gherzi *et al.*, 2004; Nechama *et al.*, 2009). The binding of Unr and/or HNRNP D to the PTH mRNA blocks the binding of FBP2 to the PTH mRNA (Nechama *et al.*, 2008).

A similar mechanism as the third example of mRNA decay could control the ADAM10 mRNA. However, instead of FBP2, FBP1 might play a role in here. As long as Unr could bind to the ADAM10 5`UTR, binding of FBP1 and recruitment of the degradation machinery might be blocked. Upon the deletion of Unr, FBP1 might bind to the ADAM10 5`UTR and could recruit the degradation machinery to the ADAM10 mRNA thereby mediating the ADAM10 mRNA turnover. So far, only the binding of Unr to the 5`UTR of ADAM10 and deletion of Unr leading to ADAM10 mRNA destabilization has been demonstrated. The binding of FBP1 to the ADAM10 5`UTR has to be proven.

Yet, it is important to know that several of the identified ADAM10 5`UTR act together with FBP1 or FBP2 on the translational control of different genes. For example, FBP1 together with hnRNP A2/B1, another identified ADAM10 5`UTR RNA-binding protein, was shown to interact specifically with the 3' UTR of nucleophosmin (NPM) to repress translation (Olanich *et al.*, 2011).

4.4 Influence of Unr on BACE1 expression

Although overexpression of Unr had no effect on ADAM10 and APPsα levels, surprisingly APPsβ as well as Aβ levels increased significantly upon overexpression of Unr. Since Unr was not identified by the affinity purification with the BACE1 5`UTR (refer to Appendix Table 5.1 and 5.2), Unr seems not to bind to the 5`UTR of BACE1. A possible explanation could be that Unr binds to the BACE1 3`UTR since this was predicted by the UTR database UTRdb of the Institute for Biomedical Technologies (http://utrdb.ba.itb.cnr.it/) (Grillo *et al.*, 2010; Pesole *et al.*, 2000; Pesole *et al.*, 1998). Unr binding to the 3`UTR of BACE1 could result in an increase in BACE1 protein expression thereby inducing an enhanced production of APPsβ and Aβ. If Unr overexpression influences the BACE1 expression via its 3`UTR has to be analysed in future studies. So far, there is no data available showing an influence of the BACE1 3`UTR on BACE1 expression. Another possibility is that Unr acts as a stress sensor / mediator (Dormoy-Raclet *et al.*, 2007; Tinton *et al.*, 2005) and thereby upregulates BACE1 expression. O'Connor and colleagues showed that during energy deprivation eIF2α is phosphorylated and results in increased BACE1 mRNA translation (O'Connor *et al.*, 2008). Interestingly, Tinton *et al.* demonstrated that eIF2α phosphorylation and Unr expression occur at the

same time in the cell cycle (G2/M stage) (Tinton *et al.*, 2005). Hence, there might be a direct link between Unr expression and phosphorylated eIF2α resulting in increased expression of BACE1.

4.5 Conclusion

In summary, the results demonstrate that Unr is not responsible for translational repression but rather is responsible for ADAM10 mRNA stabilisation. Unr has been characterised as a regulatory protein that binds specifically to the c-fos and PTH mRNA and influences their stability (Chang *et al.*, 2004; Grosset *et al.*, 2000; Patel *et al.*, 2005). The rate of mRNA decay is regulated by the interaction of cis-acting elements in the transcripts and sequence-specific RNA-binding proteins (Hollams *et al.*, 2002). The presented effect of Unr on ADAM10 expression might be explained by the same mechanism as described for PTH mRNA (Dinur *et al.*, 2006).

4.6 Outlook

This work describes the RNA-binding protein Unr for the ADAM10 5`UTR and shows that Unr has the potential to regulate the synthesis of the ADAM10 protein at the level of mRNA stability. The RNA-binding protein Unr provides a potential mechanism for suppression of translation of ADAM10 as well as for the stability of the ADAM10 mRNA. However, additional work is needed to obtain a detailed characterization of the physiological and pathophysiological role of Unr and possible other ADAM10 5`UTR-binding proteins in controlling ADAM10 translation. Previous results have shown that Unr is an essential gene (Boussadia *et al.*, 2003). The homozygous knockout of Unr is embryonic lethal in mice around embryonic day E10, which implies that Unr is not essential for general cell viability and cell division, but must be essential for certain stages in differentiation (Boussadia *et al.*, 1997; Dormoy-Raclet *et al.*, 2007). Interestingly, the ADAM10 homozygous knockout, showing a notch phenotype, is also embryonic lethal in mice around the same embryonic day due to major developmental defects (Hartmann *et al.*, 2002). Therefore, it might be interesting to analyse in particular the homozygous and heterozygous Unr knockout in more detail as there might be a direct link to the ADAM10 knockout. So far, the phenotype of Unr knockout mice has not been described. Further examination of the *in vivo* activities of Unr on the ADAM10 5`UTR should provide important information about the mechanism of ADAM10 translation. On the other hand, it will be important to determine whether and how the activity of Unr is regulated in the cell.

In this regard, it will be also interesting to find out which role Unr plays in the generation of APPsβ and Aβ.

In addition to Unr, a variety of other candidate RNA-binding proteins were identified for the ADAM10 5`UTR. Taken together, the finding that the ADAM10 5`UTR associates with factors that have a potentially regulatory function suggests that translation of the ADAM10 5`UTR is subject to complex regulatory mechanisms. In addition, there is the possibility that some of the detected proteins were co-purified as a complex via Unr`s interaction with the purine-rich stretch of the ADAM10 5`UTR. Therefore, it will be important to proof their binding capabilities and to analyse their effect on the translation of ADAM10. Future studies, similar to the ones performed for Unr, are required to analyse the relevance of the RNA-binding proteins in more detail.

In general, this study supports the notion that RNA-binding proteins of the 5`UTR can control translation and in particular begins to provide a molecular basis for translational regulation of ADAM10. Further investigations are necessary to positively identify the exact mechanism of the RNA-binding proteins interacting with the 5`UTR. Identification of the functions of these proteins may lead to a greater understanding of translational regulation of ADAM10 and eventually to the development of novel drug targets in the treatment of AD.

5 Literature

Abaza I., Coll O., Patalano S., Gebauer F. (2006) Drosophila UNR is required for translational repression of male-specific lethal 2 mRNA during regulation of X-chromosome dosage compensation. *Genes Dev* **20:** 380-389

Abaza I., Gebauer F. (2008) Trading translation with RNA-binding proteins. *Rna* **14:** 404-409

Abdelmohsen K., Tominaga K., Lee E.K., Srikantan S., Kang M.J., Kim M.M., Selimyan R., Martindale J.L., Yang X., Carrier F., Zhan M., Becker K.G., Gorospe M. (2011) Enhanced translation by Nucleolin via G-rich elements in coding and non-coding regions of target mRNAs. *Nucleic Acids Res* **39:** 8513-8530

Allemand E., Guil S., Myers M., Moscat J., Caceres J.F., Krainer A.R. (2005) Regulation of heterogenous nuclear ribonucleoprotein A1 transport by phosphorylation in cells stressed by osmotic shock. *Proc Natl Acad Sci U S A* **102:** 3605-3610

Allinson T.M., Parkin E.T., Turner A.J., Hooper N.M. (2003) ADAMs family members as amyloid precursor protein alpha-secretases. *J Neurosci Res* **74:** 342-352

Alzheimer A. (1907) Über eine eigenartige Erkankung der Hirnrinde [Concerning a novel disease of the cortex]. *Allgemeine Zeitschrift für Psychiatrie Psychisch-Gerichtlich Medizine* **64:** 146-148

Amadio M., Pascale A., Wang J., Ho L., Quattrone A., Gandy S., Haroutunian V., Racchi M., Pasinetti G.M. (2009) nELAV proteins alteration in Alzheimer's disease brain: a novel putative target for amyloid-beta reverberating on AbetaPP processing. *J Alzheimers Dis* **16:** 409-419

Amrani N., Sachs M.S., Jacobson A. (2006) Early nonsense: mRNA decay solves a translational problem. *Nat Rev Mol Cell Biol* **7:** 415-425

Asai M., Hattori C., Szabo B., Sasagawa N., Maruyama K., Tanuma S., Ishiura S. (2003) Putative function of ADAM9, ADAM10, and ADAM17 as APP alpha-secretase. *Biochem Biophys Res Commun* **301:** 231-235

Augustin R., Endres K., Reinhardt S., Kuhn P.H., Lichtenthaler S.F., Hansen J., Wurst W., Trumbach D. (2012) Computational identification and experimental validation of microRNAs binding to the Alzheimerrelated gene ADAM10. *BMC Med Genet* **13:** 35

Bai S., Nasser M.W., Wang B., Hsu S.H., Datta J., Kutay H., Yadav A., Nuovo G., Kumar P., Ghoshal K. (2009) MicroRNA-122 inhibits tumorigenic properties of hepatocellular carcinoma cells and sensitizes these cells to sorafenib. *J Biol Chem* **284:** 32015-32027

Baki L., Marambaud P., Efthimiopoulos S., Georgakopoulos A., Wen P., Cui W., Shioi J., Koo E., Ozawa M., Friedrich V.L., Jr., Robakis N.K. (2001) Presenilin-1 binds cytoplasmic epithelial cadherin, inhibits cadherin/p120 association, and regulates stability and function of the cadherin/catenin adhesion complex. *Proc Natl Acad Sci U S A* **98:** 2381-2386

Bannai H., Fukatsu K., Mizutani A., Natsume T., Iemura S., Ikegami T., Inoue T., Mikoshiba K. (2004) An RNA-interacting protein, SYNCRIP (heterogeneous nuclear ribonuclear protein Q1/NSAP1) is a component of mRNA granule transported with inositol 1,4,5-trisphosphate receptor type 1 mRNA in neuronal dendrites. *J Biol Chem* **279:** 53427-53434

Barnes T., Kim W.C., Mantha A.K., Kim S.E., Izumi T., Mitra S., Lee C.H. (2009) Identification of Apurinic/apyrimidinic endonuclease 1 (APE1) as the endoribonuclease that cleaves c-myc mRNA. *Nucleic Acids Res* **37:** 3946-3958

Bartel D.P. (2009) MicroRNAs: target recognition and regulatory functions. *Cell* **136:** 215-233

Bashkirov V.I., Scherthan H., Solinger J.A., Buerstedde J.M., Heyer W.D. (1997) A mouse cytoplasmic exoribonuclease (mXRN1p) with preference for G4 tetraplex substrates. *J Cell Biol* **136:** 761-773

Beaudoin M.E., Poirel V.J., Krushel L.A. (2008) Regulating amyloid precursor protein synthesis through an internal ribosomal entry site. *Nucleic Acids Res* **36:** 6835-6847

Benjannet S., Elagoz A., Wickham L., Mamarbachi M., Munzer J.S., Basak A., Lazure C., Cromlish J.A., Sisodia S., Checler F., Chretien M., Seidah N.G. (2001) Post-translational processing of beta-secretase (beta-amyloid-converting enzyme) and its ectodomain shedding. The pro- and transmembrane/cytosolic domains affect its cellular activity and amyloid-beta production. *J Biol Chem* **276:** 10879-10887

Bennett B.D., Babu-Khan S., Loeloff R., Louis J.C., Curran E., Citron M., Vassar R. (2000a) Expression analysis of BACE2 in brain and peripheral tissues. *J Biol Chem* **275:** 20647-20651

Bennett B.D., Denis P., Haniu M., Teplow D.B., Kahn S., Louis J.C., Citron M., Vassar R. (2000b) A furin-like convertase mediates propeptide cleavage of BACE, the Alzheimer's beta -secretase. *J Biol Chem* **275:** 37712-37717

Berezovska O., Frosch M., McLean P., Knowles R., Koo E., Kang D., Shen J., Lu F.M., Lux S.E., Tonegawa S., Hyman B.T. (1999) The Alzheimer-related gene presenilin 1 facilitates notch 1 in primary mammalian neurons. *Brain Res Mol Brain Res* **69:** 273-280

Bergman A., Hansson E.M., Pursglove S.E., Farmery M.R., Lannfelt L., Lendahl U., Lundkvist J., Naslund J. (2004) Pen-2 is sequestered in the endoplasmic reticulum and subjected to ubiquitylation and proteasome-mediated degradation in the absence of presenilin. *J Biol Chem* **279:** 16744-16753

Bernstein H.G., Bukowska A., Krell D., Bogerts B., Ansorge S., Lendeckel U. (2003) Comparative localization of ADAMs 10 and 15 in human cerebral cortex normal aging, Alzheimer disease and Down syndrome. *J Neurocytol* **32:** 153-160

Black R.A., Rauch C.T., Kozlosky C.J., Peschon J.J., Slack J.L., Wolfson M.F., Castner B.J., Stocking K.L., Reddy P., Srinivasan S., Nelson N., Boiani N., Schooley K.A., Gerhart M., Davis R., Fitzner J.N., Johnson R.S., Paxton R.J., March C.J., Cerretti D.P. (1997) A metalloproteinase disintegrin that releases tumour-necrosis factor-alpha from cells. *Nature* **385:** 729-733

Blackinton J., Kumaran R., van der Brug M.P., Ahmad R., Olson L., Galter D., Lees A., Bandopadhyay R., Cookson M.R. (2009) Post-transcriptional regulation of mRNA associated with DJ-1 in sporadic Parkinson disease. *Neurosci Lett* **452:** 8-11

Boissonneault V., Plante I., Rivest S., Provost P. (2009) MicroRNA-298 and microRNA-328 regulate expression of mouse beta-amyloid precursor protein-converting enzyme 1. *J Biol Chem* **284:** 1971-1981

Bonifacino J.S., Cosson P., Klausner R.D. (1990) Colocalized transmembrane determinants for ER degradation and subunit assembly explain the intracellular fate of TCR chains. *Cell* **63:** 503-513

Bonifacino J.S., Cosson P., Shah N., Klausner R.D. (1991) Role of potentially charged transmembrane residues in targeting proteins for retention and degradation within the endoplasmic reticulum. *Embo J* **10:** 2783-2793

Borer R.A., Lehner C.F., Eppenberger H.M., Nigg E.A. (1989) Major nucleolar proteins shuttle between nucleus and cytoplasm. *Cell* **56:** 379-390

Boussadia O., Amiot F., Cases S., Triqueneaux G., Jacquemin-Sablon H., Dautry F. (1997) Transcription of unr (upstream of N-ras) down-modulates N-ras expression in vivo. *FEBS Lett* **420:** 20-24

Boussadia O., Jacquemin-Sablon H., Dautry F. (1993) Exon skipping in the expression of the gene immediately upstream of N-ras (unr/NRU). *Biochim Biophys Acta* **1172:** 64-72

Boussadia O., Niepmann M., Creancier L., Prats A.C., Dautry F., Jacquemin-Sablon H. (2003) Unr is required in vivo for efficient initiation of translation from the internal ribosome entry sites of both rhinovirus and poliovirus. *J Virol* **77:** 3353-3359

Bray S.J. (2006) Notch signalling: a simple pathway becomes complex. *Nat Rev Mol Cell Biol* **7:** 678-689

Briata P., Forcales S.V., Ponassi M., Corte G., Chen C.Y., Karin M., Puri P.L., Gherzi R. (2005) p38-dependent phosphorylation of the mRNA decay-promoting factor KSRP controls the stability of select myogenic transcripts. *Mol Cell* **20:** 891-903

Brooks T.A., Hurley L.H. (2010) Targeting MYC Expression through G-Quadruplexes. *Genes Cancer* **1:** 641-649

Brown E.C., Jackson R.J. (2004) All five cold-shock domains of unr (upstream of N-ras) are required for stimulation of human rhinovirus RNA translation. *J Gen Virol* **85:** 2279-2287

Broytman O., Westmark P.R., Gurel Z., Malter J.S. (2009) Rck/p54 interacts with APP mRNA as part of a multi-protein complex and enhances APP mRNA and protein expression in neuronal cell lines. *Neurobiol Aging* **30:** 1962-1974

Buxbaum J.D., Liu K.N., Luo Y., Slack J.L., Stocking K.L., Peschon J.J., Johnson R.S., Castner B.J., Cerretti D.P., Black R.A. (1998) Evidence that tumor necrosis factor alpha converting enzyme is involved in regulated alpha-secretase cleavage of the Alzheimer amyloid protein precursor. *J Biol Chem* **273:** 27765-27767

Cai H., Wang Y., McCarthy D., Wen H., Borchelt D.R., Price D.L., Wong P.C. (2001) BACE1 is the major beta-secretase for generation of Abeta peptides by neurons. *Nat Neurosci* **4:** 233-234

Cai X.D., Golde T.E., Younkin S.G. (1993) Release of excess amyloid beta protein from a mutant amyloid beta protein precursor. *Science* **259:** 514-516

Cao Q., Richter J.D. (2002) Dissolution of the maskin-eIF4E complex by cytoplasmic polyadenylation and poly(A)-binding protein controls cyclin B1 mRNA translation and oocyte maturation. *Embo J* **21:** 3852-3862

Capell A., Beher D., Prokop S., Steiner H., Kaether C., Shearman M.S., Haass C. (2005) Gamma-secretase complex assembly within the early secretory pathway. *J Biol Chem* **280:** 6471-6478

Capell A., Grunberg J., Pesold B., Diehlmann A., Citron M., Nixon R., Beyreuther K., Selkoe D.J., Haass C. (1998) The proteolytic fragments of the Alzheimer's disease-associated presenilin-1 form heterodimers and occur as a 100-150-kDa molecular mass complex. *J Biol Chem* **273:** 3205-3211

Capell A., Steiner H., Willem M., Kaiser H., Meyer C., Walter J., Lammich S., Multhaup G., Haass C. (2000) Maturation and pro-peptide cleavage of beta-secretase. *J Biol Chem* **275:** 30849-30854

Carpenter B., MacKay C., Alnabulsi A., MacKay M., Telfer C., Melvin W.T., Murray G.I. (2006) The roles of heterogeneous nuclear ribonucleoproteins in tumour development and progression. *Biochim Biophys Acta* **1765:** 85-100

Ceman S., Brown V., Warren S.T. (1999) Isolation of an FMRP-associated messenger ribonucleoprotein particle and identification of nucleolin and the fragile X-related proteins as components of the complex. *Mol Cell Biol* **19:** 7925-7932

Chang T.C., Yamashita A., Chen C.Y., Yamashita Y., Zhu W., Durdan S., Kahvejian A., Sonenberg N., Shyu A.B. (2004) UNR, a new partner of poly(A)-binding protein,

plays a key role in translationally coupled mRNA turnover mediated by the c-fos major coding-region determinant. *Genes Dev* **18:** 2010-2023

Chantry A., Gregson N.A., Glynn P. (1989) A novel metalloproteinase associated with brain myelin membranes. Isolation and characterization. *J Biol Chem* **264:** 21603-21607

Chen C.Y., Gherzi R., Ong S.E., Chan E.L., Raijmakers R., Pruijn G.J., Stoecklin G., Moroni C., Mann M., Karin M. (2001) AU binding proteins recruit the exosome to degrade ARE-containing mRNAs. *Cell* **107:** 451-464

Chernokalskaya E., Dubell A.N., Cunningham K.S., Hanson M.N., Dompenciel R.E., Schoenberg D.R. (1998) A polysomal ribonuclease involved in the destabilization of albumin mRNA is a novel member of the peroxidase gene family. *Rna* **4:** 1537-1548

Cho H.H., Cahill C.M., Vanderburg C.R., Scherzer C.R., Wang B., Huang X., Rogers J.T. (2010) Selective translational control of the Alzheimer amyloid precursor protein transcript by iron regulatory protein-1. *J Biol Chem* **285:** 31217-31232

Citron M., Oltersdorf T., Haass C., McConlogue L., Hung A.Y., Seubert P., Vigo-Pelfrey C., Lieberburg I., Selkoe D.J. (1992) Mutation of the beta-amyloid precursor protein in familial Alzheimer's disease increases beta-protein production. *Nature* **360:** 672-674

Clemens M.J. (2001) Initiation factor eIF2 alpha phosphorylation in stress responses and apoptosis. *Prog Mol Subcell Biol* **27:** 57-89

Colciaghi F., Borroni B., Pastorino L., Marcello E., Zimmermann M., Cattabeni F., Padovani A., Di Luca M. (2002) [alpha]-Secretase ADAM10 as well as [alpha]APPs is reduced in platelets and CSF of Alzheimer disease patients. *Mol Med* **8:** 67-74

Colombo A., Wang H., Kuhn P.H., Page R., Kremmer E., Dempsey P.J., Crawford H.C., Lichtenthaler S.F. (2012) Constitutive alpha- and beta-secretase cleavages of the amyloid precursor protein are partially coupled in neurons, but not in frequently used cell lines. *Neurobiol Dis* **49C:** 137-147

Corder E.H., Saunders A.M., Strittmatter W.J., Schmechel D.E., Gaskell P.C., Small G.W., Roses A.D., Haines J.L., Pericak-Vance M.A. (1993) Gene dose of apolipoprotein E type 4 allele and the risk of Alzheimer's disease in late onset families. *Science* **261:** 921-923

Creemers J.W., Ines Dominguez D., Plets E., Serneels L., Taylor N.A., Multhaup G., Craessaerts K., Annaert W., De Strooper B. (2001) Processing of beta-secretase by furin and other members of the proprotein convertase family. *J Biol Chem* **276:** 4211-4217

Cruts M., Theuns J., Van Broeckhoven C. (1998) Locus-specific mutation databases for neurodegenerative brain diseases. *Hum Mutat*

Crystal A.S., Morais V.A., Fortna R.R., Carlin D., Pierson T.C., Wilson C.A., Lee V.M., Doms R.W. (2004) Presenilin modulates Pen-2 levels posttranslationally by protecting it from proteasomal degradation. *Biochemistry* **43:** 3555-3563

Crystal A.S., Morais V.A., Pierson T.C., Pijak D.S., Carlin D., Lee V.M., Doms R.W. (2003) Membrane topology of gamma-secretase component PEN-2. *J Biol Chem* **278:** 20117-20123

David D.C., Layfield R., Serpell L., Narain Y., Goedert M., Spillantini M.G. (2002) Proteasomal degradation of tau protein. *J Neurochem* **83:** 176-185

Davis J.A., Naruse S., Chen H., Eckman C., Younkin S., Price D.L., Borchelt D.R., Sisodia S.S., Wong P.C. (1998) An Alzheimer's disease-linked PS1 variant rescues the developmental abnormalities of PS1-deficient embryos. *Neuron* **20:** 603-609

De Pietri Tonelli D., Mihailovich M., Di Cesare A., Codazzi F., Grohovaz F., Zacchetti D. (2004) Translational regulation of BACE-1 expression in neuronal and non-neuronal cells. *Nucleic Acids Res* **32:** 1808-1817

De Strooper B. (2003) Aph-1, Pen-2, and Nicastrin with Presenilin generate an active gamma-Secretase complex. *Neuron* **38:** 9-12

De Strooper B., Annaert W., Cupers P., Saftig P., Craessaerts K., Mumm J.S., Schroeter E.H., Schrijvers V., Wolfe M.S., Ray W.J., Goate A., Kopan R. (1999) A presenilin-1-dependent gamma-secretase-like protease mediates release of Notch intracellular domain. *Nature* **398:** 518-522

De Strooper B., Saftig P., Craessaerts K., Vanderstichele H., Guhde G., Annaert W., Von Figura K., Van Leuven F. (1998) Deficiency of presenilin-1 inhibits the normal cleavage of amyloid precursor protein. *Nature* **391:** 387-390

Derrigo M., Cestelli A., Savettieri G., Di Liegro I. (2000) RNA-protein interactions in the control of stability and localization of messenger RNA (review). *Int J Mol Med* **5:** 111-123

Dignam J.D., Lebovitz R.M., Roeder R.G. (1983) Accurate transcription initiation by RNA polymerase II in a soluble extract from isolated mammalian nuclei. *Nucleic Acids Res* **11:** 1475-1489

Ding A., Nitsch R., Hoyer S. (1992) Changes in brain monoaminergic neurotransmitter concentrations in rat after intracerebroventricular injection of streptozotocin. *J Cereb Blood Flow Metab* **12:** 103-109

Dinur M., Kilav R., Sela-Brown A., Jacquemin-Sablon H., Naveh-Many T. (2006) In vitro evidence that upstream of N-ras participates in the regulation of parathyroid hormone messenger ribonucleic acid stability. *Mol Endocrinol* **20:** 1652-1660

Dodson R.E., Shapiro D.J. (2002) Regulation of pathways of mRNA destabilization and stabilization. *Prog Nucleic Acid Res Mol Biol* **72:** 129-164

Dominguez C., Fisette J.F., Chabot B., Allain F.H. (2010) Structural basis of G-tract recognition and encaging by hnRNP F quasi-RRMs. *Nat Struct Mol Biol* **17:** 853-861

Dominguez D., Tournoy J., Hartmann D., Huth T., Cryns K., Deforce S., Serneels L., Camacho I.E., Marjaux E., Craessaerts K., Roebroek A.J., Schwake M., D'Hooge R., Bach P., Kalinke U., Moechars D., Alzheimer C., Reiss K., Saftig P., De Strooper B. (2005) Phenotypic and biochemical analyses of BACE1- and BACE2-deficient mice. *J Biol Chem* **280:** 30797-30806

Donmez G., Wang D., Cohen D.E., Guarente L. (2010) SIRT1 suppresses beta-amyloid production by activating the alpha-secretase gene ADAM10. *Cell* **142:** 320-332

Donoviel D.B., Hadjantonakis A.K., Ikeda M., Zheng H., Hyslop P.S., Bernstein A. (1999) Mice lacking both presenilin genes exhibit early embryonic patterning defects. *Genes Dev* **13:** 2801-2810

Dormoy-Raclet V., Markovits J., Malato Y., Huet S., Lagarde P., Montaudon D., Jacquemin-Sablon A., Jacquemin-Sablon H. (2007) Unr, a cytoplasmic RNA-binding protein with cold-shock domains, is involved in control of apoptosis in ES and HuH7 cells. *Oncogene* **26:** 2595-2605

Dries D.R., Yu G. (2008) Assembly, maturation, and trafficking of the gamma-secretase complex in Alzheimer's disease. *Curr Alzheimer Res* **5:** 132-146

Duncan K., Grskovic M., Strein C., Beckmann K., Niggeweg R., Abaza I., Gebauer F., Wilm M., Hentze M.W. (2006) Sex-lethal imparts a sex-specific function to UNR by recruiting it to the msl-2 mRNA 3' UTR: translational repression for dosage compensation. *Genes Dev* **20:** 368-379

Duncan K.E., Strein C., Hentze M.W. (2009) The SXL-UNR corepressor complex uses a PABP-mediated mechanism to inhibit ribosome recruitment to msl-2 mRNA. *Mol Cell* **36:** 571-582

Edbauer D., Winkler E., Haass C., Steiner H. (2002) Presenilin and nicastrin regulate each other and determine amyloid beta-peptide production via complex formation. *Proc Natl Acad Sci U S A* **99:** 8666-8671

Edbauer D., Winkler E., Regula J.T., Pesold B., Steiner H., Haass C. (2003) Reconstitution of gamma-secretase activity. *Nat Cell Biol* **5:** 486-488

Eggert S., Paliga K., Soba P., Evin G., Masters C.L., Weidemann A., Beyreuther K. (2004) The proteolytic processing of the amyloid precursor protein gene family members APLP-1 and APLP-2 involves alpha-, beta-, gamma-, and epsilon-like cleavages: modulation of APLP-1 processing by n-glycosylation. *J Biol Chem* **279:** 18146-18156

Endres K., Fahrenholz F. (2010) Upregulation of the alpha-secretase ADAM10--risk or reason for hope? *Febs J* **277:** 1585-1596

Esch F.S., Keim P.S., Beattie E.C., Blacher R.W., Culwell A.R., Oltersdorf T., McClure D., Ward P.J. (1990) Cleavage of amyloid beta peptide during constitutive processing of its precursor. *Science* **248:** 1122-1124

Esler W.P., Kimberly W.T., Ostaszewski B.L., Diehl T.S., Moore C.L., Tsai J.Y., Rahmati T., Xia W., Selkoe D.J., Wolfe M.S. (2000) Transition-state analogue inhibitors of gamma-secretase bind directly to presenilin-1. *Nat Cell Biol* **2:** 428-434

Esler W.P., Wolfe M.S. (2001) A portrait of Alzheimer secretases--new features and familiar faces. *Science* **293:** 1449-1454

Evans D.A., Funkenstein H.H., Albert M.S., Scherr P.A., Cook N.R., Chown M.J., Hebert L.E., Hennekens C.H., Taylor J.O. (1989) Prevalence of Alzheimer's disease in a community population of older persons. Higher than previously reported. *Jama* **262:** 2551-2556

Faghihi M.A., Modarresi F., Khalil A.M., Wood D.E., Sahagan B.G., Morgan T.E., Finch C.E., St Laurent G., 3rd, Kenny P.J., Wahlestedt C. (2008) Expression of a noncoding RNA is elevated in Alzheimer's disease and drives rapid feed-forward regulation of beta-secretase. *Nat Med* **14:** 723-730

Fahrenholz F. (2007) Alpha-secretase as a therapeutic target. *Curr Alzheimer Res* **4:** 412-417

Fang M., Wang J., Zhang X., Geng Y., Hu Z., Rudd J.A., Ling S., Chen W., Han S. (2012) The miR-124 regulates the expression of BACE1/beta-secretase correlated with cell death in Alzheimer's disease. *Toxicol Lett* **209:** 94-105

Farzan M., Schnitzler C.E., Vasilieva N., Leung D., Choe H. (2000) BACE2, a beta -secretase homolog, cleaves at the beta site and within the amyloid-beta region of the amyloid-beta precursor protein. *Proc Natl Acad Sci U S A* **97:** 9712-9717

Fellgiebel A., Kojro E., Muller M.J., Scheurich A., Schmidt L.G., Fahrenholz F. (2009) CSF APPs alpha and phosphorylated tau protein levels in mild cognitive impairment and dementia of Alzheimer's type. *J Geriatr Psychiatry Neurol* **22:** 3-9

Ferrer N., Garcia-Espana A., Jeffers M., Pellicer A. (1999) The unr gene: evolutionary considerations and nucleic acid-binding properties of its long isoform product. *DNA Cell Biol* **18:** 209-218

Fluhrer R., Capell A., Westmeyer G., Willem M., Hartung B., Condron M.M., Teplow D.B., Haass C., Walter J. (2002) A non-amyloidogenic function of BACE-2 in the secretory pathway. *J Neurochem* **81:** 1011-1020

Fortna R.R., Crystal A.S., Morais V.A., Pijak D.S., Lee V.M., Doms R.W. (2004) Membrane topology and nicastrin-enhanced endoproteolysis of APH-1, a component of the gamma-secretase complex. *J Biol Chem* **279:** 3685-3693

Francis R., McGrath G., Zhang J., Ruddy D.A., Sym M., Apfeld J., Nicoll M., Maxwell M., Hai B., Ellis M.C., Parks A.L., Xu W., Li J., Gurney M., Myers R.L., Himes C.S., Hiebsch R., Ruble C., Nye J.S., Curtis D. (2002) aph-1 and pen-2 are required for Notch pathway signaling, gamma-secretase cleavage of betaAPP, and presenilin protein accumulation. *Dev Cell* **3:** 85-97

Fukumori A., Fluhrer R., Steiner H., Haass C. (2010) Three-amino acid spacing of presenilin endoproteolysis suggests a general stepwise cleavage of gamma-secretase-mediated intramembrane proteolysis. *J Neurosci* **30:** 7853-7862

Fukumoto H., Cheung B.S., Hyman B.T., Irizarry M.C. (2002) Beta-secretase protein and activity are increased in the neocortex in Alzheimer disease. *Arch Neurol* **59:** 1381-1389

Gallouzi I.E., Parker F., Chebli K., Maurier F., Labourier E., Barlat I., Capony J.P., Tocque B., Tazi J. (1998) A novel phosphorylation-dependent RNase activity of GAP-SH3 binding protein: a potential link between signal transduction and RNA stability. *Mol Cell Biol* **18:** 3956-3965

Garton K.J., Gough P.J., Blobel C.P., Murphy G., Greaves D.R., Dempsey P.J., Raines E.W. (2001) Tumor necrosis factor-alpha-converting enzyme (ADAM17) mediates the cleavage and shedding of fractalkine (CX3CL1). *J Biol Chem* **276:** 37993-38001

Gebauer F., Hentze M.W. (2004) Molecular mechanisms of translational control. *Nat Rev Mol Cell Biol* **5:** 827-835

Gellert M., Lipsett M.N., Davies D.R. (1962) Helix formation by guanylic acid. *Proc Natl Acad Sci U S A* **48:** 2013-2018

Georgakopoulos A., Marambaud P., Efthimiopoulos S., Shioi J., Cui W., Li H.C., Schutte M., Gordon R., Holstein G.R., Martinelli G., Mehta P., Friedrich V.L., Jr., Robakis N.K. (1999) Presenilin-1 forms complexes with the cadherin/catenin cell-cell adhesion system and is recruited to intercellular and synaptic contacts. *Mol Cell* **4:** 893-902

Gherzi R., Lee K.Y., Briata P., Wegmuller D., Moroni C., Karin M., Chen C.Y. (2004) A KH domain RNA binding protein, KSRP, promotes ARE-directed mRNA turnover by recruiting the degradation machinery. *Mol Cell* **14:** 571-583

Glenner G.G., Wong C.W. (1984) Alzheimer's disease: initial report of the purification and characterization of a novel cerebrovascular amyloid protein. *Biochem Biophys Res Commun* **120:** 885-890

Glisovic T., Bachorik J.L., Yong J., Dreyfuss G. (2008) RNA-binding proteins and post-transcriptional gene regulation. *FEBS Lett* **582:** 1977-1986

Goate A., Chartier-Harlin M.C., Mullan M., Brown J., Crawford F., Fidani L., Giuffra L., Haynes A., Irving N., James L., et al. (1991) Segregation of a missense mutation in the amyloid precursor protein gene with familial Alzheimer's disease. *Nature* **349:** 704-706

Goddard D.R., Bunning R.A., Woodroofe M.N. (2001) Astrocyte and endothelial cell expression of ADAM 17 (TACE) in adult human CNS. *Glia* **34:** 267-271

Goedert M., Spillantini M.G., Cairns N.J., Crowther R.A. (1992) Tau proteins of Alzheimer paired helical filaments: abnormal phosphorylation of all six brain isoforms. *Neuron* **8:** 159-168

Gonzalez V., Guo K., Hurley L., Sun D. (2009) Identification and characterization of nucleolin as a c-myc G-quadruplex-binding protein. *J Biol Chem* **284:** 23622-23635

Gonzalez V., Hurley L.H. (2010) The C-terminus of nucleolin promotes the formation of the c-MYC G-quadruplex and inhibits c-MYC promoter activity. *Biochemistry* **49:** 9706-9714

Goutte C., Tsunozaki M., Hale V.A., Priess J.R. (2002) APH-1 is a multipass membrane protein essential for the Notch signaling pathway in Caenorhabditis elegans embryos. *Proc Natl Acad Sci U S A* **99:** 775-779

Gray N.K., Hentze M.W. (1994) Regulation of protein synthesis by mRNA structure. *Mol Biol Rep* **19:** 195-200

Gray N.K., Wickens M. (1998) Control of translation initiation in animals. *Annu Rev Cell Dev Biol* **14:** 399-458

Grillo G., Turi A., Licciulli F., Mignone F., Liuni S., Banfi S., Gennarino V.A., Horner D.S., Pavesi G., Picardi E., Pesole G. (2010) UTRdb and UTRsite (RELEASE 2010): a collection of sequences and regulatory motifs of the untranslated regions of eukaryotic mRNAs. *Nucleic Acids Res* **38:** D75-80

Grosset C., Chen C.Y., Xu N., Sonenberg N., Jacquemin-Sablon H., Shyu A.B. (2000) A mechanism for translationally coupled mRNA turnover: interaction between the poly(A) tail and a c-fos RNA coding determinant via a protein complex. *Cell* **103:** 29-40

Grundke-Iqbal I., Iqbal K., Tung Y.C., Quinlan M., Wisniewski H.M., Binder L.I. (1986) Abnormal phosphorylation of the microtubule-associated protein tau (tau) in Alzheimer cytoskeletal pathology. *Proc Natl Acad Sci U S A* **83:** 4913-4917

Haass C. (2004) Take five--BACE and the gamma-secretase quartet conduct Alzheimer's amyloid beta-peptide generation. *Embo J* **23:** 483-488

Haass C., Hung A.Y., Selkoe D.J., Teplow D.B. (1994) Mutations associated with a locus for familial Alzheimer's disease result in alternative processing of amyloid beta-protein precursor. *J Biol Chem* **269:** 17741-17748

Haass C., Koo E.H., Mellon A., Hung A.Y., Selkoe D.J. (1992a) Targeting of cell-surface beta-amyloid precursor protein to lysosomes: alternative processing into amyloid-bearing fragments. *Nature* **357:** 500-503

Haass C., Schlossmacher M.G., Hung A.Y., Vigo-Pelfrey C., Mellon A., Ostaszewski B.L., Lieberburg I., Koo E.H., Schenk D., Teplow D.B., et al. (1992b) Amyloid beta-peptide is produced by cultured cells during normal metabolism. *Nature* **359:** 322-325

Haass C., Selkoe D.J. (1993) Cellular processing of beta-amyloid precursor protein and the genesis of amyloid beta-peptide. *Cell* **75:** 1039-1042

Haass C., Selkoe D.J. (2007) Soluble protein oligomers in neurodegeneration: lessons from the Alzheimer's amyloid beta-peptide. *Nat Rev Mol Cell Biol* **8:** 101-112

Haass C., Steiner H. (2002) Alzheimer disease gamma-secretase: a complex story of GxGD-type presenilin proteases. *Trends Cell Biol* **12:** 556-562

Hall R.J., Erickson C.A. (2003) ADAM 10: an active metalloprotease expressed during avian epithelial morphogenesis. *Dev Biol* **256:** 146-159

Haniu M., Denis P., Young Y., Mendiaz E.A., Fuller J., Hui J.O., Bennett B.D., Kahn S., Ross S., Burgess T., Katta V., Rogers G., Vassar R., Citron M. (2000) Characterization of Alzheimer's beta -secretase protein BACE. A pepsin family member with unusual properties. *J Biol Chem* **275:** 21099-21106

Hardy J., Selkoe D.J. (2002) The amyloid hypothesis of Alzheimer's disease: progress and problems on the road to therapeutics. *Science* **297:** 353-356

Harold D., Abraham R., Hollingworth P., Sims R., Gerrish A., Hamshere M.L., Pahwa J.S., Moskvina V., Dowzell K., Williams A., Jones N., Thomas C., Stretton A., Morgan A.R., Lovestone S., Powell J., Proitsi P., Lupton M.K., Brayne C., Rubinsztein D.C., Gill M., Lawlor B., Lynch A., Morgan K., Brown K.S., Passmore P.A., Craig D., McGuinness B., Todd S., Holmes C., Mann D., Smith A.D., Love S., Kehoe P.G., Hardy J., Mead S., Fox N., Rossor M., Collinge J., Maier W., Jessen F., Schurmann B., van den Bussche H., Heuser I., Kornhuber J., Wiltfang J., Dichgans

M., Frolich L., Hampel H., Hull M., Rujescu D., Goate A.M., Kauwe J.S., Cruchaga C., Nowotny P., Morris J.C., Mayo K., Sleegers K., Bettens K., Engelborghs S., De Deyn P.P., Van Broeckhoven C., Livingston G., Bass N.J., Gurling H., McQuillin A., Gwilliam R., Deloukas P., Al-Chalabi A., Shaw C.E., Tsolaki M., Singleton A.B., Guerreiro R., Muhleisen T.W., Nothen M.M., Moebus S., Jockel K.H., Klopp N., Wichmann H.E., Carrasquillo M.M., Pankratz V.S., Younkin S.G., Holmans P.A., O'Donovan M., Owen M.J., Williams J. (2009) Genome-wide association study identifies variants at CLU and PICALM associated with Alzheimer's disease. *Nat Genet* **41:** 1088-1093

Harrison S.M., Harper A.J., Hawkins J., Duddy G., Grau E., Pugh P.L., Winter P.H., Shilliam C.S., Hughes Z.A., Dawson L.A., Gonzalez M.I., Upton N., Pangalos M.N., Dingwall C. (2003) BACE1 (beta-secretase) transgenic and knockout mice: identification of neurochemical deficits and behavioral changes. *Mol Cell Neurosci* **24:** 646-655

Hartmann D., de Strooper B., Serneels L., Craessaerts K., Herreman A., Annaert W., Umans L., Lubke T., Lena Illert A., von Figura K., Saftig P. (2002) The disintegrin/metalloprotease ADAM 10 is essential for Notch signalling but not for alpha-secretase activity in fibroblasts. *Hum Mol Genet* **11:** 2615-2624

Hasegawa H., Sanjo N., Chen F., Gu Y.J., Shier C., Petit A., Kawarai T., Katayama T., Schmidt S.D., Mathews P.M., Schmitt-Ulms G., Fraser P.E., St George-Hyslop P. (2004) Both the sequence and length of the C terminus of PEN-2 are critical for intermolecular interactions and function of presenilin complexes. *J Biol Chem* **279:** 46455-46463

Hattori M., Osterfield M., Flanagan J.G. (2000) Regulated cleavage of a contact-mediated axon repellent. *Science* **289:** 1360-1365

Head E., Lott I.T. (2004) Down syndrome and beta-amyloid deposition. *Curr Opin Neurol* **17:** 95-100

Hebert S.S., Horre K., Nicolai L., Bergmans B., Papadopoulou A.S., Delacourte A., De Strooper B. (2009) MicroRNA regulation of Alzheimer's Amyloid precursor protein expression. *Neurobiol Dis* **33:** 422-428

Hebert S.S., Horre K., Nicolai L., Papadopoulou A.S., Mandemakers W., Silahtaroglu A.N., Kauppinen S., Delacourte A., De Strooper B. (2008) Loss of microRNA cluster miR-29a/b-1 in sporadic Alzheimer's disease correlates with increased BACE1/beta-secretase expression. *Proc Natl Acad Sci U S A* **105:** 6415-6420

Hebert S.S., Serneels L., Dejaegere T., Horre K., Dabrowski M., Baert V., Annaert W., Hartmann D., De Strooper B. (2004) Coordinated and widespread expression of gamma-secretase in vivo: evidence for size and molecular heterogeneity. *Neurobiol Dis* **17:** 260-272

Hennecke S., Cosson P. (1993) Role of transmembrane domains in assembly and intracellular transport of the CD8 molecule. *J Biol Chem* **268:** 26607-26612

Henricson A., Kall L., Sonnhammer E.L. (2005) A novel transmembrane topology of presenilin based on reconciling experimental and computational evidence. *Febs J* **272:** 2727-2733

Hentze M.W., Caughman S.W., Rouault T.A., Barriocanal J.G., Dancis A., Harford J.B., Klausner R.D. (1987) Identification of the iron-responsive element for the translational regulation of human ferritin mRNA. *Science* **238:** 1570-1573

Herreman A., Hartmann D., Annaert W., Saftig P., Craessaerts K., Serneels L., Umans L., Schrijvers V., Checler F., Vanderstichele H., Baekelandt V., Dressel R., Cupers P., Huylebroeck D., Zwijsen A., Van Leuven F., De Strooper B. (1999) Presenilin 2 deficiency causes a mild pulmonary phenotype and no changes in amyloid precursor

protein processing but enhances the embryonic lethal phenotype of presenilin 1 deficiency. *Proc Natl Acad Sci U S A* **96:** 11872-11877

Herreman A., Serneels L., Annaert W., Collen D., Schoonjans L., De Strooper B. (2000) Total inactivation of gamma-secretase activity in presenilin-deficient embryonic stem cells. *Nat Cell Biol* **2:** 461-462

Hinnebusch A.G. (1997) Translational regulation of yeast GCN4. A window on factors that control initiator-trna binding to the ribosome. *J Biol Chem* **272:** 21661-21664

Hod Y., Pentyala S.N., Whyard T.C., El-Maghrabi M.R. (1999) Identification and characterization of a novel protein that regulates RNA-protein interaction. *J Cell Biochem* **72:** 435-444

Holcik M., Sonenberg N. (2005) Translational control in stress and apoptosis. *Nat Rev Mol Cell Biol* **6:** 318-327

Hollams E.M., Giles K.M., Thomson A.M., Leedman P.J. (2002) MRNA stability and the control of gene expression: implications for human disease. *Neurochem Res* **27:** 957-980

Hollien J., Weissman J.S. (2006) Decay of endoplasmic reticulum-localized mRNAs during the unfolded protein response. *Science* **313:** 104-107

Holsinger R.M., McLean C.A., Beyreuther K., Masters C.L., Evin G. (2002) Increased expression of the amyloid precursor beta-secretase in Alzheimer's disease. *Ann Neurol* **51:** 783-786

Hotoda N., Koike H., Sasagawa N., Ishiura S. (2002) A secreted form of human ADAM9 has an alpha-secretase activity for APP. *Biochem Biophys Res Commun* **293:** 800-805

Howard L., Lu X., Mitchell S., Griffiths S., Glynn P. (1996) Molecular cloning of MADM: a catalytically active mammalian disintegrin-metalloprotease expressed in various cell types. *Biochem J* **317 (Pt 1):** 45-50

Hu X., He W., Diaconu C., Tang X., Kidd G.J., Macklin W.B., Trapp B.D., Yan R. (2008) Genetic deletion of BACE1 in mice affects remyelination of sciatic nerves. *Faseb J* **22:** 2970-2980

Hu X., Hicks C.W., He W., Wong P., Macklin W.B., Trapp B.D., Yan R. (2006) Bace1 modulates myelination in the central and peripheral nervous system. *Nat Neurosci* **9:** 1520-1525

Hundhausen C., Misztela D., Berkhout T.A., Broadway N., Saftig P., Reiss K., Hartmann D., Fahrenholz F., Postina R., Matthews V., Kallen K.J., Rose-John S., Ludwig A. (2003) The disintegrin-like metalloproteinase ADAM10 is involved in constitutive cleavage of CX3CL1 (fractalkine) and regulates CX3CL1-mediated cell-cell adhesion. *Blood* **102:** 1186-1195

Hunt S.L., Hsuan J.J., Totty N., Jackson R.J. (1999) unr, a cellular cytoplasmic RNA-binding protein with five cold-shock domains, is required for internal initiation of translation of human rhinovirus RNA. *Genes Dev* **13:** 437-448

Huppert J.L., Bugaut A., Kumari S., Balasubramanian S. (2008) G-quadruplexes: the beginning and end of UTRs. *Nucleic Acids Res* **36:** 6260-6268

Huse J.T., Pijak D.S., Leslie G.J., Lee V.M., Doms R.W. (2000) Maturation and endosomal targeting of beta-site amyloid precursor protein-cleaving enzyme. The Alzheimer's disease beta-secretase. *J Biol Chem* **275:** 33729-33737

Hussain I., Hawkins J., Shikotra A., Riddell D.R., Faller A., Dingwall C. (2003) Characterization of the ectodomain shedding of the beta-site amyloid precursor protein-cleaving enzyme 1 (BACE1). *J Biol Chem* **278:** 36264-36268

Hussain I., Powell D., Howlett D.R., Tew D.G., Meek T.D., Chapman C., Gloger I.S., Murphy K.E., Southan C.D., Ryan D.M., Smith T.S., Simmons D.L., Walsh F.S.,

Dingwall C., Christie G. (1999) Identification of a novel aspartic protease (Asp 2) as beta-secretase. *Mol Cell Neurosci* **14:** 419-427

Hussain I., Powell D.J., Howlett D.R., Chapman G.A., Gilmour L., Murdock P.R., Tew D.G., Meek T.D., Chapman C., Schneider K., Ratcliffe S.J., Tattersall D., Testa T.T., Southan C., Ryan D.M., Simmons D.L., Walsh F.S., Dingwall C., Christie G. (2000) ASP1 (BACE2) cleaves the amyloid precursor protein at the beta-secretase site. *Mol Cell Neurosci* **16:** 609-619

Ikeuchi T., Sisodia S.S. (2003) The Notch ligands, Delta1 and Jagged2, are substrates for presenilin-dependent "gamma-secretase" cleavage. *J Biol Chem* **278:** 7751-7754

Izumi Y., Hirata M., Hasuwa H., Iwamoto R., Umata T., Miyado K., Tamai Y., Kurisaki T., Sehara-Fujisawa A., Ohno S., Mekada E. (1998) A metalloprotease-disintegrin, MDC9/meltrin-gamma/ADAM9 and PKCdelta are involved in TPA-induced ectodomain shedding of membrane-anchored heparin-binding EGF-like growth factor. *Embo J* **17:** 7260-7272

Jacquemin-Sablon H., Triqueneaux G., Deschamps S., le Maire M., Doniger J., Dautry F. (1994) Nucleic acid binding and intracellular localization of unr, a protein with five cold shock domains. *Nucleic Acids Res* **22:** 2643-2650

Jarrett J.T., Berger E.P., Lansbury P.T., Jr. (1993a) The C-terminus of the beta protein is critical in amyloidogenesis. *Ann N Y Acad Sci* **695:** 144-148

Jarrett J.T., Berger E.P., Lansbury P.T., Jr. (1993b) The carboxy terminus of the beta amyloid protein is critical for the seeding of amyloid formation: implications for the pathogenesis of Alzheimer's disease. *Biochemistry* **32:** 4693-4697

Jeffers M., Paciucci R., Pellicer A. (1990) Characterization of unr; a gene closely linked to N-ras. *Nucleic Acids Res* **18:** 4891-4899

Joachim C.L., Morris J.H., Selkoe D.J. (1989) Diffuse senile plaques occur commonly in the cerebellum in Alzheimer's disease. *Am J Pathol* **135:** 309-319

Johnson G.V., Hartigan J.A. (1999) Tau protein in normal and Alzheimer's disease brain: an update. *J Alzheimers Dis* **1:** 329-351

Jonsson T., Atwal J.K., Steinberg S., Snaedal J., Jonsson P.V., Bjornsson S., Stefansson H., Sulem P., Gudbjartsson D., Maloney J., Hoyte K., Gustafson A., Liu Y., Lu Y., Bhangale T., Graham R.R., Huttenlocher J., Bjornsdottir G., Andreassen O.A., Jonsson E.G., Palotie A., Behrens T.W., Magnusson O.T., Kong A., Thorsteinsdottir U., Watts R.J., Stefansson K. (2012) A mutation in APP protects against Alzheimer's disease and age-related cognitive decline. *Nature* **488:** 96-99

Jorissen E., Prox J., Bernreuther C., Weber S., Schwanbeck R., Serneels L., Snellinx A., Craessaerts K., Thathiah A., Tesseur I., Bartsch U., Weskamp G., Blobel C.P., Glatzel M., De Strooper B., Saftig P. (2010) The disintegrin/metalloproteinase ADAM10 is essential for the establishment of the brain cortex. *J Neurosci* **30:** 4833-4844

Kaether C., Capell A., Edbauer D., Winkler E., Novak B., Steiner H., Haass C. (2004) The presenilin C-terminus is required for ER-retention, nicastrin-binding and gamma-secretase activity. *Embo J* **23:** 4738-4748

Kaether C., Haass C. (2004) A lipid boundary separates APP and secretases and limits amyloid beta-peptide generation. *J Cell Biol* **167:** 809-812

Kang J., Lemaire H.G., Unterbeck A., Salbaum J.M., Masters C.L., Grzeschik K.H., Multhaup G., Beyreuther K., Muller-Hill B. (1987) The precursor of Alzheimer's disease amyloid A4 protein resembles a cell-surface receptor. *Nature* **325:** 733-736

Karkkainen I., Rybnikova E., Pelto-Huikko M., Huovila A.P. (2000) Metalloprotease-disintegrin (ADAM) genes are widely and differentially expressed in the adult CNS. *Mol Cell Neurosci* **15:** 547-560

Kawas C., Gray S., Brookmeyer R., Fozard J., Zonderman A. (2000) Age-specific incidence rates of Alzheimer's disease: the Baltimore Longitudinal Study of Aging. *Neurology* **54:** 2072-2077

Khateb S., Weisman-Shomer P., Hershco-Shani I., Ludwig A.L., Fry M. (2007) The tetraplex (CGG)n destabilizing proteins hnRNP A2 and CBF-A enhance the in vivo translation of fragile X premutation mRNA. *Nucleic Acids Res* **35:** 5775-5788

Khateb S., Weisman-Shomer P., Hershco I., Loeb L.A., Fry M. (2004) Destabilization of tetraplex structures of the fragile X repeat sequence (CGG)n is mediated by homolog-conserved domains in three members of the hnRNP family. *Nucleic Acids Res* **32:** 4145-4154

Kim D.Y., Ingano L.A., Carey B.W., Pettingell W.H., Kovacs D.M. (2005) Presenilin/gamma-secretase-mediated cleavage of the voltage-gated sodium channel beta2-subunit regulates cell adhesion and migration. *J Biol Chem* **280:** 23251-23261

Kim S.H., Yin Y.I., Li Y.M., Sisodia S.S. (2004) Evidence that assembly of an active gamma-secretase complex occurs in the early compartments of the secretory pathway. *J Biol Chem* **279:** 48615-48619

Kimberly W.T., Xia W., Rahmati T., Wolfe M.S., Selkoe D.J. (2000) The transmembrane aspartates in presenilin 1 and 2 are obligatory for gamma-secretase activity and amyloid beta-protein generation. *J Biol Chem* **275:** 3173-3178

Kirschling C.M., Kolsch H., Frahnert C., Rao M.L., Maier W., Heun R. (2003) Polymorphism in the BACE gene influences the risk for Alzheimer's disease. *Neuroreport* **14:** 1243-1246

Kitazume S., Tachida Y., Oka R., Shirotani K., Saido T.C., Hashimoto Y. (2001) Alzheimer's beta-secretase, beta-site amyloid precursor protein-cleaving enzyme, is responsible for cleavage secretion of a Golgi-resident sialyltransferase. *Proc Natl Acad Sci U S A* **98:** 13554-13559

Klausner R.D., Rouault T.A., Harford J.B. (1993) Regulating the fate of mRNA: the control of cellular iron metabolism. *Cell* **72:** 19-28

Koenig T., Menze B.H., Kirchner M., Monigatti F., Parker K.C., Patterson T., Steen J.J., Hamprecht F.A., Steen H. (2008) Robust prediction of the MASCOT score for an improved quality assessment in mass spectrometric proteomics. *J Proteome Res* **7:** 3708-3717

Koike H., Tomioka S., Sorimachi H., Saido T.C., Maruyama K., Okuyama A., Fujisawa-Sehara A., Ohno S., Suzuki K., Ishiura S. (1999) Membrane-anchored metalloprotease MDC9 has an alpha-secretase activity responsible for processing the amyloid precursor protein. *Biochem J* **343 Pt 2:** 371-375

Koo E.H., Lansbury P.T., Jr., Kelly J.W. (1999) Amyloid diseases: abnormal protein aggregation in neurodegeneration. *Proc Natl Acad Sci U S A* **96:** 9989-9990

Koo E.H., Squazzo S.L. (1994) Evidence that production and release of amyloid beta-protein involves the endocytic pathway. *J Biol Chem* **269:** 17386-17389

Krebs L.T., Xue Y., Norton C.R., Shutter J.R., Maguire M., Sundberg J.P., Gallahan D., Closson V., Kitajewski J., Callahan R., Smith G.H., Stark K.L., Gridley T. (2000) Notch signaling is essential for vascular morphogenesis in mice. *Genes Dev* **14:** 1343-1352

Krecic A.M., Swanson M.S. (1999) hnRNP complexes: composition, structure, and function. *Curr Opin Cell Biol* **11:** 363-371

Kuhn P.H., Koroniak K., Hogl S., Colombo A., Zeitschel U., Willem M., Volbracht C., Schepers U., Imhof A., Hoffmeister A., Haass C., Rossner S., Brase S., Lichtenthaler S.F. (2012) Secretome protein enrichment identifies physiological BACE1 protease substrates in neurons. *Embo J* **31:** 3157-3168

Kuhn P.H., Wang H., Dislich B., Colombo A., Zeitschel U., Ellwart J.W., Kremmer E., Rossner S., Lichtenthaler S.F. (2010) ADAM10 is the physiologically relevant, constitutive alpha-secretase of the amyloid precursor protein in primary neurons. *Embo J*

Kusenda B., Mraz M., Mayer J., Pospisilova S. (2006) MicroRNA biogenesis, functionality and cancer relevance. *Biomed Pap Med Fac Univ Palacky Olomouc Czech Repub* **150:** 205-215

Laemmli U.K. (1970) Cleavage of structural proteins during the assembly of the head of bacteriophage T4. *Nature* **227:** 680-685

LaFerla F.M., Oddo S. (2005) Alzheimer's disease: Abeta, tau and synaptic dysfunction. *Trends Mol Med* **11:** 170-176

Lai W.S., Kennington E.A., Blackshear P.J. (2003) Tristetraprolin and its family members can promote the cell-free deadenylation of AU-rich element-containing mRNAs by poly(A) ribonuclease. *Mol Cell Biol* **23:** 3798-3812

Laird F.M., Cai H., Savonenko A.V., Farah M.H., He K., Melnikova T., Wen H., Chiang H.C., Xu G., Koliatsos V.E., Borchelt D.R., Price D.L., Lee H.K., Wong P.C. (2005) BACE1, a major determinant of selective vulnerability of the brain to amyloid-beta amyloidogenesis, is essential for cognitive, emotional, and synaptic functions. *J Neurosci* **25:** 11693-11709

Lambert J.C., Heath S., Even G., Campion D., Sleegers K., Hiltunen M., Combarros O., Zelenika D., Bullido M.J., Tavernier B., Letenneur L., Bettens K., Berr C., Pasquier F., Fievet N., Barberger-Gateau P., Engelborghs S., De Deyn P., Mateo I., Franck A., Helisalmi S., Porcellini E., Hanon O., de Pancorbo M.M., Lendon C., Dufouil C., Jaillard C., Leveillard T., Alvarez V., Bosco P., Mancuso M., Panza F., Nacmias B., Bossu P., Piccardi P., Annoni G., Seripa D., Galimberti D., Hannequin D., Licastro F., Soininen H., Ritchie K., Blanche H., Dartigues J.F., Tzourio C., Gut I., Van Broeckhoven C., Alperovitch A., Lathrop M., Amouyel P. (2009) Genome-wide association study identifies variants at CLU and CR1 associated with Alzheimer's disease. *Nat Genet* **41:** 1094-1099

Lammich S., Buell D., Zilow S., Ludwig A.K., Nuscher B., Lichtenthaler S.F., Prinzen C., Fahrenholz F., Haass C. (2010) Expression of the anti-amyloidogenic secretase ADAM10 is suppressed by its 5'-untranslated region. *J Biol Chem* **285:** 15753-15760

Lammich S., Kamp F., Wagner J., Nuscher B., Zilow S., Ludwig A.K., Willem M., Haass C. (2011) Translational repression of the Disintegrin and Metalloprotease ADAM10 by a stable G-quadruplex secondary structure in its 5'-untranslated region. *J Biol Chem*

Lammich S., Kojro E., Postina R., Gilbert S., Pfeiffer R., Jasionowski M., Haass C., Fahrenholz F. (1999) Constitutive and regulated alpha-secretase cleavage of Alzheimer's amyloid precursor protein by a disintegrin metalloprotease. *Proc Natl Acad Sci U S A* **96:** 3922-3927

Lammich S., Okochi M., Takeda M., Kaether C., Capell A., Zimmer A.K., Edbauer D., Walter J., Steiner H., Haass C. (2002) Presenilin-dependent intramembrane proteolysis of CD44 leads to the liberation of its intracellular domain and the secretion of an Abeta-like peptide. *J Biol Chem* **277:** 44754-44759

Lammich S., Schobel S., Zimmer A.K., Lichtenthaler S.F., Haass C. (2004) Expression of the Alzheimer protease BACE1 is suppressed via its 5'-untranslated region. *EMBO Rep* **5:** 620-625

Laudon H., Hansson E.M., Melen K., Bergman A., Farmery M.R., Winblad B., Lendahl U., von Heijne G., Naslund J. (2005) A nine-transmembrane domain topology for presenilin 1. *J Biol Chem* **280:** 35352-35360

LaVoie M.J., Selkoe D.J. (2003) The Notch ligands, Jagged and Delta, are sequentially processed by alpha-secretase and presenilin/gamma-secretase and release signaling fragments. *J Biol Chem* **278:** 34427-34437

Lee E.K., Kim H.H., Kuwano Y., Abdelmohsen K., Srikantan S., Subaran S.S., Gleichmann M., Mughal M.R., Martindale J.L., Yang X., Worley P.F., Mattson M.P., Gorospe M. (2010) hnRNP C promotes APP translation by competing with FMRP for APP mRNA recruitment to P bodies. *Nat Struct Mol Biol* **17:** 732-739

Lee J.H., Cheng R., Schupf N., Manly J., Lantigua R., Stern Y., Rogaeva E., Wakutani Y., Farrer L., St George-Hyslop P., Mayeux R. (2007) The association between genetic variants in SORL1 and Alzheimer disease in an urban, multiethnic, community-based cohort. *Arch Neurol* **64:** 501-506

Lee S.F., Shah S., Li H., Yu C., Han W., Yu G. (2002) Mammalian APH-1 interacts with presenilin and nicastrin and is required for intramembrane proteolysis of amyloid-beta precursor protein and Notch. *J Biol Chem* **277:** 45013-45019

Lee V.M., Goedert M., Trojanowski J.Q. (2001) Neurodegenerative tauopathies. *Annu Rev Neurosci* **24:** 1121-1159

Leem J.Y., Vijayan S., Han P., Cai D., Machura M., Lopes K.O., Veselits M.L., Xu H., Thinakaran G. (2002) Presenilin 1 is required for maturation and cell surface accumulation of nicastrin. *J Biol Chem* **277:** 19236-19240

Levitan D., Greenwald I. (1998) Effects of SEL-12 presenilin on LIN-12 localization and function in Caenorhabditis elegans. *Development* **125:** 3599-3606

Levy-Lahad E., Lahad A., Wijsman E.M., Bird T.D., Schellenberg G.D. (1995a) Apolipoprotein E genotypes and age of onset in early-onset familial Alzheimer's disease. *Ann Neurol* **38:** 678-680

Levy-Lahad E., Wasco W., Poorkaj P., Romano D.M., Oshima J., Pettingell W.H., Yu C.E., Jondro P.D., Schmidt S.D., Wang K., et al. (1995b) Candidate gene for the chromosome 1 familial Alzheimer's disease locus. *Science* **269:** 973-977

Levy-Lahad E., Wijsman E.M., Nemens E., Anderson L., Goddard K.A., Weber J.L., Bird T.D., Schellenberg G.D. (1995c) A familial Alzheimer's disease locus on chromosome 1. *Science* **269:** 970-973

Li Q., Sudhof T.C. (2004) Cleavage of amyloid-beta precursor protein and amyloid-beta precursor-like protein by BACE 1. *J Biol Chem* **279:** 10542-10550

Li X., Greenwald I. (1998) Additional evidence for an eight-transmembrane-domain topology for Caenorhabditis elegans and human presenilins. *Proc Natl Acad Sci U S A* **95:** 7109-7114

Li Y.M., Xu M., Lai M.T., Huang Q., Castro J.L., DiMuzio-Mower J., Harrison T., Lellis C., Nadin A., Neduvelil J.G., Register R.B., Sardana M.K., Shearman M.S., Smith A.L., Shi X.P., Yin K.C., Shafer J.A., Gardell S.J. (2000) Photoactivated gamma-secretase inhibitors directed to the active site covalently label presenilin 1. *Nature* **405:** 689-694

Lichtenthaler S.F., Dominguez D.I., Westmeyer G.G., Reiss K., Haass C., Saftig P., De Strooper B., Seed B. (2003) The cell adhesion protein P-selectin glycoprotein ligand-1 is a substrate for the aspartyl protease BACE1. *J Biol Chem* **278:** 48713-48719

Lin X., Koelsch G., Wu S., Downs D., Dashti A., Tang J. (2000) Human aspartic protease memapsin 2 cleaves the beta-secretase site of beta-amyloid precursor protein. *Proc Natl Acad Sci U S A* **97:** 1456-1460

Lleo A., Saura C.A. (2011) gamma-secretase substrates and their implications for drug development in Alzheimer's disease. *Curr Top Med Chem* **11:** 1513-1527

Lu P.D., Harding H.P., Ron D. (2004) Translation reinitiation at alternative open reading frames regulates gene expression in an integrated stress response. *J Cell Biol* **167:** 27-33

Luo Y., Bolon B., Damore M.A., Fitzpatrick D., Liu H., Zhang J., Yan Q., Vassar R., Citron M. (2003) BACE1 (beta-secretase) knockout mice do not acquire compensatory gene expression changes or develop neural lesions over time. *Neurobiol Dis* **14:** 81-88

Luo Y., Bolon B., Kahn S., Bennett B.D., Babu-Khan S., Denis P., Fan W., Kha H., Zhang J., Gong Y., Martin L., Louis J.C., Yan Q., Richards W.G., Citron M., Vassar R. (2001) Mice deficient in BACE1, the Alzheimer's beta-secretase, have normal phenotype and abolished beta-amyloid generation. *Nat Neurosci* **4:** 231-232

Ma G., Li T., Price D.L., Wong P.C. (2005) APH-1a is the principal mammalian APH-1 isoform present in gamma-secretase complexes during embryonic development. *J Neurosci* **25:** 192-198

Mann G.B., Fowler K.J., Gabriel A., Nice E.C., Williams R.L., Dunn A.R. (1993) Mice with a null mutation of the TGF alpha gene have abnormal skin architecture, wavy hair, and curly whiskers and often develop corneal inflammation. *Cell* **73:** 249-261

Marambaud P., Shioi J., Serban G., Georgakopoulos A., Sarner S., Nagy V., Baki L., Wen P., Efthimiopoulos S., Shao Z., Wisniewski T., Robakis N.K. (2002) A presenilin-1/gamma-secretase cleavage releases the E-cadherin intracellular domain and regulates disassembly of adherens junctions. *Embo J* **21:** 1948-1956

Marcinkiewicz M., Seidah N.G. (2000) Coordinated expression of beta-amyloid precursor protein and the putative beta-secretase BACE and alpha-secretase ADAM10 in mouse and human brain. *J Neurochem* **75:** 2133-2143

Marshall A.J., Rattray M., Vaughan P.F. (2006) Chronic hypoxia in the human neuroblastoma SH-SY5Y causes reduced expression of the putative alpha-secretases, ADAM10 and TACE, without altering their mRNA levels. *Brain Res* **1099:** 18-24

Matthews V., Schuster B., Schutze S., Bussmeyer I., Ludwig A., Hundhausen C., Sadowski T., Saftig P., Hartmann D., Kallen K.J., Rose-John S. (2003) Cellular cholesterol depletion triggers shedding of the human interleukin-6 receptor by ADAM10 and ADAM17 (TACE). *J Biol Chem* **278:** 38829-38839

Maurer K., Maurer U. (1998) Alzheimer. Das Leben eines Arztes und die Karriere einer Krankheit. *Piper, München*

Mechtersheimer S., Gutwein P., Agmon-Levin N., Stoeck A., Oleszewski M., Riedle S., Postina R., Fahrenholz F., Fogel M., Lemmon V., Altevogt P. (2001) Ectodomain shedding of L1 adhesion molecule promotes cell migration by autocrine binding to integrins. *J Cell Biol* **155:** 661-673

Melefors O., Hentze M.W. (1993) Translational regulation by mRNA/protein interactions in eukaryotic cells: ferritin and beyond. *Bioessays* **15:** 85-90

Menon L., Mader S.A., Mihailescu M.R. (2008) Fragile X mental retardation protein interactions with the microtubule associated protein 1B RNA. *Rna* **14:** 1644-1655

Miettinen P.J., Berger J.E., Meneses J., Phung Y., Pedersen R.A., Werb Z., Derynck R. (1995) Epithelial immaturity and multiorgan failure in mice lacking epidermal growth factor receptor. *Nature* **376:** 337-341

Mignone F., Gissi C., Liuni S., Pesole G. (2002) Untranslated regions of mRNAs. *Genome Biol* **3:** REVIEWS0004

Mihailovich M., Militti C., Gabaldon T., Gebauer F. (2010) Eukaryotic cold shock domain proteins: highly versatile regulators of gene expression. *Bioessays* **32:** 109-118

Mihailovich M., Thermann R., Grohovaz F., Hentze M.W., Zacchetti D. (2007) Complex translational regulation of BACE1 involves upstream AUGs and stimulatory elements within the 5' untranslated region. *Nucleic Acids Res* **35:** 2975-2985

Millichip M.I., Dallas D.J., Wu E., Dale S., McKie N. (1998) The metallo-disintegrin ADAM10 (MADM) from bovine kidney has type IV collagenase activity in vitro. *Biochem Biophys Res Commun* **245:** 594-598

Mitchell S.A., Brown E.C., Coldwell M.J., Jackson R.J., Willis A.E. (2001) Protein factor requirements of the Apaf-1 internal ribosome entry segment: roles of polypyrimidine tract binding protein and upstream of N-ras. *Mol Cell Biol* **21:** 3364-3374

Mitchell S.A., Spriggs K.A., Coldwell M.J., Jackson R.J., Willis A.E. (2003) The Apaf-1 internal ribosome entry segment attains the correct structural conformation for function via interactions with PTB and unr. *Mol Cell* **11:** 757-771

Mizukami K., Ishikawa M., Iwakiri M., Ikonomovic M.D., Dekosky S.T., Kamma H., Asada T. (2005) Immunohistochemical study of the hnRNP A2 and B1 in the hippocampal formations of brains with Alzheimer's disease. *Neurosci Lett* **386:** 111-115

Morris H.R., Khan M.N., Janssen J.C., Brown J.M., Perez-Tur J., Baker M., Ozansoy M., Hardy J., Hutton M., Wood N.W., Lees A.J., Revesz T., Lantos P., Rossor M.N. (2001) The genetic and pathological classification of familial frontotemporal dementia. *Arch Neurol* **58:** 1813-1816

Moss M.L., Jin S.L., Milla M.E., Bickett D.M., Burkhart W., Carter H.L., Chen W.J., Clay W.C., Didsbury J.R., Hassler D., Hoffman C.R., Kost T.A., Lambert M.H., Leesnitzer M.A., McCauley P., McGeehan G., Mitchell J., Moyer M., Pahel G., Rocque W., Overton L.K., Schoenen F., Seaton T., Su J.L., Becherer J.D., et al. (1997) Cloning of a disintegrin metalloproteinase that processes precursor tumour-necrosis factor-alpha. *Nature* **385:** 733-736

Mowrer K.R., Wolfe M.S. (2008) Promotion of BACE1 mRNA alternative splicing reduces amyloid beta-peptide production. *J Biol Chem* **283:** 18694-18701

Muckenthaler M., Gray N.K., Hentze M.W. (1998) IRP-1 binding to ferritin mRNA prevents the recruitment of the small ribosomal subunit by the cap-binding complex eIF4F. *Mol Cell* **2:** 383-388

Murai T., Miyazaki Y., Nishinakamura H., Sugahara K.N., Miyauchi T., Sako Y., Yanagida T., Miyasaka M. (2004) Engagement of CD44 promotes Rac activation and CD44 cleavage during tumor cell migration. *J Biol Chem* **279:** 4541-4550

Murakami D., Okamoto I., Nagano O., Kawano Y., Tomita T., Iwatsubo T., De Strooper B., Yumoto E., Saya H. (2003) Presenilin-dependent gamma-secretase activity mediates the intramembranous cleavage of CD44. *Oncogene* **22:** 1511-1516

Nakajima M., Shimizu T., Shirasawa T. (2000) Notch-1 activation by familial Alzheimer's disease (FAD)-linked mutant forms of presenilin-1. *J Neurosci Res* **62:** 311-317

Navarro V., Vincent J.P., Mazella J. (2002) Shedding of the luminal domain of the neurotensin receptor-3/sortilin in the HT29 cell line. *Biochem Biophys Res Commun* **298:** 760-764

Nechama M., Ben-Dov I.Z., Briata P., Gherzi R., Naveh-Many T. (2008) The mRNA decay promoting factor K-homology splicing regulator protein post-transcriptionally determines parathyroid hormone mRNA levels. *Faseb J* **22:** 3458-3468

Nechama M., Peng Y., Bell O., Briata P., Gherzi R., Schoenberg D.R., Naveh-Many T. (2009) KSRP-PMR1-exosome association determines parathyroid hormone mRNA levels and stability in transfected cells. *BMC Cell Biol* **10:** 70

Ni C.Y., Murphy M.P., Golde T.E., Carpenter G. (2001) gamma -Secretase cleavage and nuclear localization of ErbB-4 receptor tyrosine kinase. *Science* **294:** 2179-2181

Nichols R.C., Wang X.W., Tang J., Hamilton B.J., High F.A., Herschman H.R., Rigby W.F. (2000) The RGG domain in hnRNP A2 affects subcellular localization. *Exp Cell Res* **256:** 522-532

Norris C.M., Kadish I., Blalock E.M., Chen K.C., Thibault V., Porter N.M., Landfield P.W., Kraner S.D. (2005) Calcineurin triggers reactive/inflammatory processes in astrocytes and is upregulated in aging and Alzheimer's models. *J Neurosci* **25:** 4649-4658

O'Connor T., Sadleir K.R., Maus E., Velliquette R.A., Zhao J., Cole S.L., Eimer W.A., Hitt B., Bembinster L.A., Lammich S., Lichtenthaler S.F., Hebert S.S., De Strooper B., Haass C., Bennett D.A., Vassar R. (2008) Phosphorylation of the translation initiation factor eIF2alpha increases BACE1 levels and promotes amyloidogenesis. *Neuron* **60:** 988-1009

Oh Y.S., Turner R.J. (2005a) Evidence that the COOH terminus of human presenilin 1 is located in extracytoplasmic space. *Am J Physiol Cell Physiol* **289:** C576-581

Oh Y.S., Turner R.J. (2005b) Topology of the C-terminal fragment of human presenilin 1. *Biochemistry* **44:** 11821-11828

Ohno M., Sametsky E.A., Younkin L.H., Oakley H., Younkin S.G., Citron M., Vassar R., Disterhoft J.F. (2004) BACE1 deficiency rescues memory deficits and cholinergic dysfunction in a mouse model of Alzheimer's disease. *Neuron* **41:** 27-33

Olanich M.E., Moss B.L., Piwnica-Worms D., Townsend R.R., Weber J.D. (2011) Identification of FUSE-binding protein 1 as a regulatory mRNA-binding protein that represses nucleophosmin translation. *Oncogene* **30:** 77-86

Olsen J.V., de Godoy L.M., Li G., Macek B., Mortensen P., Pesch R., Makarov A., Lange O., Horning S., Mann M. (2005) Parts per million mass accuracy on an Orbitrap mass spectrometer via lock mass injection into a C-trap. *Mol Cell Proteomics* **4:** 2010-2021

Ostareck-Lederer A., Ostareck D.H., Cans C., Neubauer G., Bomsztyk K., Superti-Furga G., Hentze M.W. (2002) c-Src-mediated phosphorylation of hnRNP K drives translational activation of specifically silenced mRNAs. *Mol Cell Biol* **22:** 4535-4543

Ostareck D.H., Ostareck-Lederer A., Wilm M., Thiele B.J., Mann M., Hentze M.W. (1997) mRNA silencing in erythroid differentiation: hnRNP K and hnRNP E1 regulate 15-lipoxygenase translation from the 3' end. *Cell* **89:** 597-606

Pan D., Rubin G.M. (1997) Kuzbanian controls proteolytic processing of Notch and mediates lateral inhibition during Drosophila and vertebrate neurogenesis. *Cell* **90:** 271-280

Parihar M.S., Hemnani T. (2004) Alzheimer's disease pathogenesis and therapeutic interventions. *J Clin Neurosci* **11:** 456-467

Pastorino L., Ikin A.F., Lamprianou S., Vacaresse N., Revelli J.P., Platt K., Paganetti P., Mathews P.M., Harroch S., Buxbaum J.D. (2004) BACE (beta-secretase) modulates the processing of APLP2 in vivo. *Mol Cell Neurosci* **25:** 642-649

Pastorino L., Ikin A.F., Nairn A.C., Pursnani A., Buxbaum J.D. (2002) The carboxyl-terminus of BACE contains a sorting signal that regulates BACE trafficking but not the formation of total A(beta). *Mol Cell Neurosci* **19:** 175-185

Patel G.P., Ma S., Bag J. (2005) The autoregulatory translational control element of poly(A)-binding protein mRNA forms a heteromeric ribonucleoprotein complex. *Nucleic Acids Res* **33:** 7074-7089

Patel N., Hoang D., Miller N., Ansaloni S., Huang Q., Rogers J.T., Lee J.C., Saunders A.J. (2008) MicroRNAs can regulate human APP levels. *Mol Neurodegener* **3:** 10

Periz G., Fortini M.E. (2004) Functional reconstitution of gamma-secretase through coordinated expression of presenilin, nicastrin, Aph-1, and Pen-2. *J Neurosci Res* **77:** 309-322

Peschon J.J., Slack J.L., Reddy P., Stocking K.L., Sunnarborg S.W., Lee D.C., Russell W.E., Castner B.J., Johnson R.S., Fitzner J.N., Boyce R.W., Nelson N., Kozlosky C.J., Wolfson M.F., Rauch C.T., Cerretti D.P., Paxton R.J., March C.J., Black R.A. (1998) An essential role for ectodomain shedding in mammalian development. *Science* **282:** 1281-1284

Pesole G., Liuni S., Grillo G., Licciulli F., Larizza A., Makalowski W., Saccone C. (2000) UTRdb and UTRsite: specialized databases of sequences and functional elements of 5' and 3' untranslated regions of eukaryotic mRNAs. *Nucleic Acids Res* **28:** 193-196

Pesole G., Liuni S., Grillo G., Saccone C. (1998) UTRdb: a specialized database of 5'- and 3'-untranslated regions of eukaryotic mRNAs. *Nucleic Acids Res* **26:** 192-195

Postina R., Schroeder A., Dewachter I., Bohl J., Schmitt U., Kojro E., Prinzen C., Endres K., Hiemke C., Blessing M., Flamez P., Dequenne A., Godaux E., van Leuven F., Fahrenholz F. (2004) A disintegrin-metalloproteinase prevents amyloid plaque formation and hippocampal defects in an Alzheimer disease mouse model. *J Clin Invest* **113:** 1456-1464

Preece P., Virley D.J., Costandi M., Coombes R., Moss S.J., Mudge A.W., Jazin E., Cairns N.J. (2003) Beta-secretase (BACE) and GSK-3 mRNA levels in Alzheimer's disease. *Brain Res Mol Brain Res* **116:** 155-158

Prinzen C., Muller U., Endres K., Fahrenholz F., Postina R. (2005) Genomic structure and functional characterization of the human ADAM10 promoter. *Faseb J* **19:** 1522-1524

Prokop S., Haass C., Steiner H. (2005) Length and overall sequence of the PEN-2 C-terminal domain determines its function in the stabilization of presenilin fragments. *J Neurochem* **94:** 57-62

Prokop S., Shirotani K., Edbauer D., Haass C., Steiner H. (2004) Requirement of PEN-2 for stabilization of the presenilin N-/C-terminal fragment heterodimer within the gamma-secretase complex. *J Biol Chem* **279:** 23255-23261

Pruessmeyer J., Ludwig A. (2009) The good, the bad and the ugly substrates for ADAM10 and ADAM17 in brain pathology, inflammation and cancer. *Semin Cell Dev Biol* **20:** 164-174

Qian S., Jiang P., Guan X.M., Singh G., Trumbauer M.E., Yu H., Chen H.Y., Van de Ploeg L.H., Zheng H. (1998) Mutant human presenilin 1 protects presenilin 1 null mouse against embryonic lethality and elevates Abeta1-42/43 expression. *Neuron* **20:** 611-617

Rajagopalan L.E., Westmark C.J., Jarzembowski J.A., Malter J.S. (1998) hnRNP C increases amyloid precursor protein (APP) production by stabilizing APP mRNA. *Nucleic Acids Res* **26:** 3418-3423

Ratovitski T., Slunt H.H., Thinakaran G., Price D.L., Sisodia S.S., Borchelt D.R. (1997) Endoproteolytic processing and stabilization of wild-type and mutant presenilin. *J Biol Chem* **272:** 24536-24541

Rio C., Buxbaum J.D., Peschon J.J., Corfas G. (2000) Tumor necrosis factor-alpha-converting enzyme is required for cleavage of erbB4/HER4. *J Biol Chem* **275:** 10379-10387

Roberds S.L., Anderson J., Basi G., Bienkowski M.J., Branstetter D.G., Chen K.S., Freedman S.B., Frigon N.L., Games D., Hu K., Johnson-Wood K., Kappenman K.E., Kawabe T.T., Kola I., Kuehn R., Lee M., Liu W., Motter R., Nichols N.F., Power M., Robertson D.W., Schenk D., Schoor M., Shopp G.M., Shuck M.E., Sinha S., Svensson K.A., Tatsuno G., Tintrup H., Wijsman J., Wright S., McConlogue L. (2001) BACE knockout mice are healthy despite lacking the primary beta-secretase activity in brain: implications for Alzheimer's disease therapeutics. *Hum Mol Genet* **10:** 1317-1324

Rogaev E.I., Sherrington R., Rogaeva E.A., Levesque G., Ikeda M., Liang Y., Chi H., Lin C., Holman K., Tsuda T., et al. (1995) Familial Alzheimer's disease in kindreds with missense mutations in a gene on chromosome 1 related to the Alzheimer's disease type 3 gene. *Nature* **376:** 775-778

Rogers G.W., Jr., Edelman G.M., Mauro V.P. (2004) Differential utilization of upstream AUGs in the beta-secretase mRNA suggests that a shunting mechanism regulates translation. *Proc Natl Acad Sci U S A* **101:** 2794-2799

Rogers J.T., Leiter L.M., McPhee J., Cahill C.M., Zhan S.S., Potter H., Nilsson L.N. (1999) Translation of the alzheimer amyloid precursor protein mRNA is up-regulated by interleukin-1 through 5'-untranslated region sequences. *J Biol Chem* **274:** 6421-6431

Rogers J.T., Randall J.D., Cahill C.M., Eder P.S., Huang X., Gunshin H., Leiter L., McPhee J., Sarang S.S., Utsuki T., Greig N.H., Lahiri D.K., Tanzi R.E., Bush A.I., Giordano T., Gullans S.R. (2002) An iron-responsive element type II in the 5'-untranslated region of the Alzheimer's amyloid precursor protein transcript. *J Biol Chem* **277:** 45518-45528

Rohan de Silva H.A., Jen A., Wickenden C., Jen L.S., Wilkinson S.L., Patel A.J. (1997) Cell-specific expression of beta-amyloid precursor protein isoform mRNAs and proteins in neurons and astrocytes. *Brain Res Mol Brain Res* **47:** 147-156

Ruberti F., Barbato C., Cogoni C. (2010) Post-transcriptional regulation of amyloid precursor protein by microRNAs and RNA binding proteins. *Commun Integr Biol* **3:** 499-503

Sahin U., Weskamp G., Kelly K., Zhou H.M., Higashiyama S., Peschon J., Hartmann D., Saftig P., Blobel C.P. (2004) Distinct roles for ADAM10 and ADAM17 in ectodomain shedding of six EGFR ligands. *J Cell Biol* **164:** 769-779

Sambrook J., Fritsch E.F., Maniatis T. (1989) Molecular Cloning: A Laboratory Manual. *Cold Spring Harbor Laboratory*

Sastre M., Steiner H., Fuchs K., Capell A., Multhaup G., Condron M.M., Teplow D.B., Haass C. (2001) Presenilin-dependent gamma-secretase processing of beta-amyloid precursor protein at a site corresponding to the S3 cleavage of Notch. *EMBO Rep* **2:** 835-841

Sato M., Sato K., Nakano A. (2004) Endoplasmic reticulum quality control of unassembled iron transporter depends on Rer1p-mediated retrieval from the golgi. *Mol Biol Cell* **15:** 1417-1424

Saura C.A., Tomita T., Davenport F., Harris C.L., Iwatsubo T., Thinakaran G. (1999) Evidence that intramolecular associations between presenilin domains are obligatory for endoproteolytic processing. *J Biol Chem* **274:** 13818-13823

Scheinfeld M.H., Ghersi E., Laky K., Fowlkes B.J., D'Adamio L. (2002) Processing of beta-amyloid precursor-like protein-1 and -2 by gamma-secretase regulates transcription. *J Biol Chem* **277:** 44195-44201

Schmechel A., Strauss M., Schlicksupp A., Pipkorn R., Haass C., Bayer T.A., Multhaup G. (2004) Human BACE forms dimers and colocalizes with APP. *J Biol Chem* **279:** 39710-39717

Sela-Brown A., Silver J., Brewer G., Naveh-Many T. (2000) Identification of AUF1 as a parathyroid hormone mRNA 3'-untranslated region-binding protein that determines parathyroid hormone mRNA stability. *J Biol Chem* **275:** 7424-7429

Selkoe D.J. (1997) Alzheimer's disease: genotypes, phenotypes, and treatments. *Science* **275:** 630-631

Selkoe D.J. (2001a) Alzheimer's disease: genes, proteins, and therapy. *Physiol Rev* **81:** 741-766

Selkoe D.J. (2001b) Clearing the brain's amyloid cobwebs. *Neuron* **32:** 177-180

Selkoe D.J. (2004) Cell biology of protein misfolding: the examples of Alzheimer's and Parkinson's diseases. *Nat Cell Biol* **6:** 1054-1061

Sen D., Gilbert W. (1992) Guanine quartet structures. *Methods Enzymol* **211:** 191-199

Sennvik K., Bogdanovic N., Volkmann I., Fastbom J., Benedikz E. (2004) Beta-secretase-cleaved amyloid precursor protein in Alzheimer brain: a morphologic study. *J Cell Mol Med* **8:** 127-134

Sennvik K., Fastbom J., Blomberg M., Wahlund L.O., Winblad B., Benedikz E. (2000) Levels of alpha- and beta-secretase cleaved amyloid precursor protein in the cerebrospinal fluid of Alzheimer's disease patients. *Neurosci Lett* **278:** 169-172

Serneels L., Dejaegere T., Craessaerts K., Horre K., Jorissen E., Tousseyn T., Hebert S., Coolen M., Martens G., Zwijsen A., Annaert W., Hartmann D., De Strooper B. (2005) Differential contribution of the three Aph1 genes to gamma-secretase activity in vivo. *Proc Natl Acad Sci U S A* **102:** 1719-1724

Shah S., Lee S.F., Tabuchi K., Hao Y.H., Yu C., LaPlant Q., Ball H., Dann C.E., 3rd, Sudhof T., Yu G. (2005) Nicastrin functions as a gamma-secretase-substrate receptor. *Cell* **122:** 435-447

Sherrington R., Rogaev E.I., Liang Y., Rogaeva E.A., Levesque G., Ikeda M., Chi H., Lin C., Li G., Holman K., et al. (1995) Cloning of a gene bearing missense mutations in early-onset familial Alzheimer's disease. *Nature* **375:** 754-760

Shevchenko A., Chernushevich I., Wilm M., Mann M. (2000) De Novo peptide sequencing by nanoelectrospray tandem mass spectrometry using triple quadrupole and quadrupole/time-of-flight instruments. *Methods Mol Biol* **146:** 1-16

Shirotani K., Edbauer D., Prokop S., Haass C., Steiner H. (2004) Identification of distinct gamma-secretase complexes with different APH-1 variants. *J Biol Chem* **279:** 41340-41345

Sinha S., Anderson J.P., Barbour R., Basi G.S., Caccavello R., Davis D., Doan M., Dovey H.F., Frigon N., Hong J., Jacobson-Croak K., Jewett N., Keim P., Knops J., Lieberburg I., Power M., Tan H., Tatsuno G., Tung J., Schenk D., Seubert P., Suomensaari S.M., Wang S., Walker D., Zhao J., McConlogue L., John V. (1999) Purification and cloning of amyloid precursor protein beta-secretase from human brain. *Nature* **402:** 537-540

Sonenberg N. (1994) mRNA translation: influence of the 5' and 3' untranslated regions. *Curr Opin Genet Dev* **4:** 310-315

Sonenberg N., Hinnebusch A.G. (2009) Regulation of translation initiation in eukaryotes: mechanisms and biological targets. *Cell* **136:** 731-745

Sparanese D., Lee C.H. (2007) CRD-BP shields c-myc and MDR-1 RNA from endonucleolytic attack by a mammalian endoribonuclease. *Nucleic Acids Res* **35:** 1209-1221

St George-Hyslop P., Haines J., Rogaev E., Mortilla M., Vaula G., Pericak-Vance M., Foncin J.F., Montesi M., Bruni A., Sorbi S., et al. (1992) Genetic evidence for a novel familial Alzheimer's disease locus on chromosome 14. *Nat Genet* **2:** 330-334

Steiner H. (2004) Uncovering gamma-secretase. *Curr Alzheimer Res* **1:** 175-181

Steiner H., Capell A., Pesold B., Citron M., Kloetzel P.M., Selkoe D.J., Romig H., Mendla K., Haass C. (1998) Expression of Alzheimer's disease-associated presenilin-1 is controlled by proteolytic degradation and complex formation. *J Biol Chem* **273:** 32322-32331

Steiner H., Winkler E., Edbauer D., Prokop S., Basset G., Yamasaki A., Kostka M., Haass C. (2002) PEN-2 is an integral component of the gamma-secretase complex required for coordinated expression of presenilin and nicastrin. *J Biol Chem* **277:** 39062-39065

Struhl G., Greenwald I. (2001) Presenilin-mediated transmembrane cleavage is required for Notch signal transduction in Drosophila. *Proc Natl Acad Sci U S A* **98:** 229-234

Suh J., Choi S.H., Romano D.M., Gannon M.A., Lesinski A.N., Kim D.Y., Tanzi R.E. (2013) ADAM10 missense mutations potentiate beta-amyloid accumulation by impairing prodomain chaperone function. *Neuron* **80:** 385-401

Sunnarborg S.W., Hinkle C.L., Stevenson M., Russell W.E., Raska C.S., Peschon J.J., Castner B.J., Gerhart M.J., Paxton R.J., Black R.A., Lee D.C. (2002) Tumor necrosis factor-alpha converting enzyme (TACE) regulates epidermal growth factor receptor ligand availability. *J Biol Chem* **277:** 12838-12845

Suzuki N., Cheung T.T., Cai X.D., Odaka A., Otvos L., Jr., Eckman C., Golde T.E., Younkin S.G. (1994) An increased percentage of long amyloid beta protein secreted by familial amyloid beta protein precursor (beta APP717) mutants. *Science* **264:** 1336-1340

Takasugi N., Tomita T., Hayashi I., Tsuruoka M., Niimura M., Takahashi Y., Thinakaran G., Iwatsubo T. (2003) The role of presenilin cofactors in the gamma-secretase complex. *Nature* **422:** 438-441

Takemoto Y., Tashiro S., Handa H., Ishii S. (1994) Multiple nuclear localization signals of the B-myb gene product. *FEBS Lett* **350:** 55-60

Tanguay R.L., Gallie D.R. (1996) Isolation and characterization of the 102-kilodalton RNA-binding protein that binds to the 5' and 3' translational enhancers of tobacco mosaic virus RNA. *J Biol Chem* **271:** 14316-14322

Thinakaran G., Borchelt D.R., Lee M.K., Slunt H.H., Spitzer L., Kim G., Ratovitsky T., Davenport F., Nordstedt C., Seeger M., Hardy J., Levey A.I., Gandy S.E., Jenkins N.A., Copeland N.G., Price D.L., Sisodia S.S. (1996) Endoproteolysis of presenilin 1 and accumulation of processed derivatives in vivo. *Neuron* **17:** 181-190

Thomas J.D., Dias L.M., Johannes G.J. (2008) Translational repression during chronic hypoxia is dependent on glucose levels. *Rna* **14:** 771-781

Tinton S.A., Schepens B., Bruynooghe Y., Beyaert R., Cornelis S. (2005) Regulation of the cell-cycle-dependent internal ribosome entry site of the PITSLRE protein kinase: roles of Unr (upstream of N-ras) protein and phosphorylated translation initiation factor eIF-2alpha. *Biochem J* **385:** 155-163

Tippmann F., Hundt J., Schneider A., Endres K., Fahrenholz F. (2009) Up-regulation of the alpha-secretase ADAM10 by retinoic acid receptors and acitretin. *Faseb J* **23:** 1643-1654

Tomita T., Katayama R., Takikawa R., Iwatsubo T. (2002) Complex N-glycosylated form of nicastrin is stabilized and selectively bound to presenilin fragments. *FEBS Lett* **520:** 117-121

Triqueneaux G., Velten M., Franzon P., Dautry F., Jacquemin-Sablon H. (1999) RNA binding specificity of Unr, a protein with five cold shock domains. *Nucleic Acids Res* **27:** 1926-1934

van der Brug M.P., Blackinton J., Chandran J., Hao L.Y., Lal A., Mazan-Mamczarz K., Martindale J., Xie C., Ahmad R., Thomas K.J., Beilina A., Gibbs J.R., Ding J., Myers A.J., Zhan M., Cai H., Bonini N.M., Gorospe M., Cookson M.R. (2008) RNA binding activity of the recessive parkinsonism protein DJ-1 supports involvement in multiple cellular pathways. *Proc Natl Acad Sci U S A* **105:** 10244-10249

Vassar R., Bennett B.D., Babu-Khan S., Kahn S., Mendiaz E.A., Denis P., Teplow D.B., Ross S., Amarante P., Loeloff R., Luo Y., Fisher S., Fuller J., Edenson S., Lile J., Jarosinski M.A., Biere A.L., Curran E., Burgess T., Louis J.C., Collins F., Treanor J., Rogers G., Citron M. (1999) Beta-secretase cleavage of Alzheimer's amyloid

precursor protein by the transmembrane aspartic protease BACE. *Science* **286:** 735-741

Vassar R., Kovacs D.M., Yan R., Wong P.C. (2009) The beta-secretase enzyme BACE in health and Alzheimer's disease: regulation, cell biology, function, and therapeutic potential. *J Neurosci* **29:** 12787-12794

Vattem K.M., Wek R.C. (2004) Reinitiation involving upstream ORFs regulates ATF4 mRNA translation in mammalian cells. *Proc Natl Acad Sci U S A* **101:** 11269-11274

Vincent B., Paitel E., Saftig P., Frobert Y., Hartmann D., De Strooper B., Grassi J., Lopez-Perez E., Checler F. (2001) The disintegrins ADAM10 and TACE contribute to the constitutive and phorbol ester-regulated normal cleavage of the cellular prion protein. *J Biol Chem* **276:** 37743-37746

von Arnim C.A., Kinoshita A., Peltan I.D., Tangredi M.M., Herl L., Lee B.M., Spoelgen R., Hshieh T.T., Ranganathan S., Battey F.D., Liu C.X., Bacskai B.J., Sever S., Irizarry M.C., Strickland D.K., Hyman B.T. (2005) The low density lipoprotein receptor-related protein (LRP) is a novel beta-secretase (BACE1) substrate. *J Biol Chem* **280:** 17777-17785

Walter J., Kaether C., Steiner H., Haass C. (2001) The cell biology of Alzheimer's disease: uncovering the secrets of secretases. *Curr Opin Neurobiol* **11:** 585-590

Walter J., Schindzielorz A., Hartung B., Haass C. (2000) Phosphorylation of the beta-amyloid precursor protein at the cell surface by ectocasein kinases 1 and 2. *J Biol Chem* **275:** 23523-23529

Wang W.X., Rajeev B.W., Stromberg A.J., Ren N., Tang G., Huang Q., Rigoutsos I., Nelson P.T. (2008) The expression of microRNA miR-107 decreases early in Alzheimer's disease and may accelerate disease progression through regulation of beta-site amyloid precursor protein-cleaving enzyme 1. *J Neurosci* **28:** 1213-1223

Webster N.J., Green K.N., Settle V.J., Peers C., Vaughan P.F. (2004) Altered processing of the amyloid precursor protein and decreased expression of ADAM 10 by chronic hypoxia in SH-SY5Y: no role for the stress-activated JNK and p38 signalling pathways. *Brain Res Mol Brain Res* **130:** 161-169

Weidensdorfer D., Stohr N., Baude A., Lederer M., Kohn M., Schierhorn A., Buchmeier S., Wahle E., Huttelmaier S. (2009) Control of c-myc mRNA stability by IGF2BP1-associated cytoplasmic RNPs. *Rna* **15:** 104-115

Weskamp G., Cai H., Brodie T.A., Higashyama S., Manova K., Ludwig T., Blobel C.P. (2002) Mice lacking the metalloprotease-disintegrin MDC9 (ADAM9) have no evident major abnormalities during development or adult life. *Mol Cell Biol* **22:** 1537-1544

Weskamp G., Kratzschmar J., Reid M.S., Blobel C.P. (1996) MDC9, a widely expressed cellular disintegrin containing cytoplasmic SH3 ligand domains. *J Cell Biol* **132:** 717-726

Westmark C.J., Malter J.S. (2001a) Extracellular-regulated kinase controls beta-amyloid precursor protein mRNA decay. *Brain Res Mol Brain Res* **90:** 193-201

Westmark C.J., Malter J.S. (2001b) Up-regulation of nucleolin mRNA and protein in peripheral blood mononuclear cells by extracellular-regulated kinase. *J Biol Chem* **276:** 1119-1126

Westmark C.J., Malter J.S. (2007) FMRP mediates mGluR5-dependent translation of amyloid precursor protein. *PLoS Biol* **5:** e52

Westmeyer G.G., Willem M., Lichtenthaler S.F., Lurman G., Multhaup G., Assfalg-Machleidt I., Reiss K., Saftig P., Haass C. (2004) Dimerization of beta-site beta-amyloid precursor protein-cleaving enzyme. *J Biol Chem* **279:** 53205-53212

Wilkie G.S., Dickson K.S., Gray N.K. (2003) Regulation of mRNA translation by 5'- and 3'-UTR-binding factors. *Trends Biochem Sci* **28:** 182-188

Willem M., Garratt A.N., Novak B., Citron M., Kaufmann S., Rittger A., DeStrooper B., Saftig P., Birchmeier C., Haass C. (2006) Control of peripheral nerve myelination by the beta-secretase BACE1. *Science* **314:** 664-666

Willem M., Lammich S., Haass C. (2009) Function, regulation and therapeutic properties of beta-secretase (BACE1). *Semin Cell Dev Biol* **20:** 175-182

Willingham M.C., Yamada S.S., Pastan I. (1980) Ultrastructural localization of tubulin in cultured fibroblasts. *J Histochem Cytochem* **28:** 453-461

Wilm M., Shevchenko A., Houthaeve T., Breit S., Schweigerer L., Fotsis T., Mann M. (1996) Femtomole sequencing of proteins from polyacrylamide gels by nano-electrospray mass spectrometry. *Nature* **379:** 466-469

Wolfe M.S., Xia W., Ostaszewski B.L., Diehl T.S., Kimberly W.T., Selkoe D.J. (1999) Two transmembrane aspartates in presenilin-1 required for presenilin endoproteolysis and gamma-secretase activity. *Nature* **398:** 513-517

Wolfsberg T.G., Primakoff P., Myles D.G., White J.M. (1995) ADAM, a novel family of membrane proteins containing A Disintegrin And Metalloprotease domain: multipotential functions in cell-cell and cell-matrix interactions. *J Cell Biol* **131:** 275-278

Wong H.K., Sakurai T., Oyama F., Kaneko K., Wada K., Miyazaki H., Kurosawa M., De Strooper B., Saftig P., Nukina N. (2005) beta Subunits of voltage-gated sodium channels are novel substrates of beta-site amyloid precursor protein-cleaving enzyme (BACE1) and gamma-secretase. *J Biol Chem* **280:** 23009-23017

Wong P.C., Zheng H., Chen H., Becher M.W., Sirinathsinghji D.J., Trumbauer M.E., Chen H.Y., Price D.L., Van der Ploeg L.H., Sisodia S.S. (1997) Presenilin 1 is required for Notch1 and DII1 expression in the paraxial mesoderm. *Nature* **387:** 288-292

Xie H., Litersky J.M., Hartigan J.A., Jope R.S., Johnson G.V. (1998) The interrelationship between selective tau phosphorylation and microtubule association. *Brain Res* **798:** 173-183

Yan R., Bienkowski M.J., Shuck M.E., Miao H., Tory M.C., Pauley A.M., Brashier J.R., Stratman N.C., Mathews W.R., Buhl A.E., Carter D.B., Tomasselli A.G., Parodi L.A., Heinrikson R.L., Gurney M.E. (1999) Membrane-anchored aspartyl protease with Alzheimer's disease beta-secretase activity. *Nature* **402:** 533-537

Yan R., Munzner J.B., Shuck M.E., Bienkowski M.J. (2001) BACE2 functions as an alternative alpha-secretase in cells. *J Biol Chem* **276:** 34019-34027

Yang D.S., Tandon A., Chen F., Yu G., Yu H., Arawaka S., Hasegawa H., Duthie M., Schmidt S.D., Ramabhadran T.V., Nixon R.A., Mathews P.M., Gandy S.E., Mount H.T., St George-Hyslop P., Fraser P.E. (2002) Mature glycosylation and trafficking of nicastrin modulate its binding to presenilins. *J Biol Chem* **277:** 28135-28142

Yang L.B., Lindholm K., Yan R., Citron M., Xia W., Yang X.L., Beach T., Sue L., Wong P., Price D., Li R., Shen Y. (2003) Elevated beta-secretase expression and enzymatic activity detected in sporadic Alzheimer disease. *Nat Med* **9:** 3-4

Yasojima K., Akiyama H., McGeer E.G., McGeer P.L. (2001a) Reduced neprilysin in high plaque areas of Alzheimer brain: a possible relationship to deficient degradation of beta-amyloid peptide. *Neurosci Lett* **297:** 97-100

Yasojima K., McGeer E.G., McGeer P.L. (2001b) Relationship between beta amyloid peptide generating molecules and neprilysin in Alzheimer disease and normal brain. *Brain Res* **919:** 115-121

Yu G., Chen F., Levesque G., Nishimura M., Zhang D.M., Levesque L., Rogaeva E., Xu D., Liang Y., Duthie M., St George-Hyslop P.H., Fraser P.E. (1998) The presenilin 1

protein is a component of a high molecular weight intracellular complex that contains beta-catenin. *J Biol Chem* **273:** 16470-16475

Yu G., Chen F., Nishimura M., Steiner H., Tandon A., Kawarai T., Arawaka S., Supala A., Song Y.Q., Rogaeva E., Holmes E., Zhang D.M., Milman P., Fraser P.E., Haass C., George-Hyslop P.S. (2000a) Mutation of conserved aspartates affects maturation of both aspartate mutant and endogenous presenilin 1 and presenilin 2 complexes. *J Biol Chem* **275:** 27348-27353

Yu G., Nishimura M., Arawaka S., Levitan D., Zhang L., Tandon A., Song Y.Q., Rogaeva E., Chen F., Kawarai T., Supala A., Levesque L., Yu H., Yang D.S., Holmes E., Milman P., Liang Y., Zhang D.M., Xu D.H., Sato C., Rogaev E., Smith M., Janus C., Zhang Y., Aebersold R., Farrer L.S., Sorbi S., Bruni A., Fraser P., St George-Hyslop P. (2000b) Nicastrin modulates presenilin-mediated notch/glp-1 signal transduction and betaAPP processing. *Nature* **407:** 48-54

Zaidi S.H., Denman R., Malter J.S. (1994) Multiple proteins interact at a unique cis-element in the 3'-untranslated region of amyloid precursor protein mRNA. *J Biol Chem* **269:** 24000-24006

Zaidi S.H., Malter J.S. (1994) Amyloid precursor protein mRNA stability is controlled by a 29-base element in the 3'-untranslated region. *J Biol Chem* **269:** 24007-24013

Zaidi S.H., Malter J.S. (1995) Nucleolin and heterogeneous nuclear ribonucleoprotein C proteins specifically interact with the 3'-untranslated region of amyloid protein precursor mRNA. *J Biol Chem* **270:** 17292-17298

Zerangue N., Schwappach B., Jan Y.N., Jan L.Y. (1999) A new ER trafficking signal regulates the subunit stoichiometry of plasma membrane K(ATP) channels. *Neuron* **22:** 537-548

Zhang Z., Nadeau P., Song W., Donoviel D., Yuan M., Bernstein A., Yankner B.A. (2000) Presenilins are required for gamma-secretase cleavage of beta-APP and transmembrane cleavage of Notch-1. *Nat Cell Biol* **2:** 463-465

Zhou C., Yang Y., Jong A.Y. (1990) Mini-prep in ten minutes. *Biotechniques* **8:** 172-173

Zhou L., Barao S., Laga M., Bockstael K., Borgers M., Gijsen H., Annaert W., Moechars D., Mercken M., Gevaert K., De Strooper B. (2012) The Neural Cell Adhesion Molecules L1 and CHL1 are cleaved by BACE1 in vivo. *J Biol Chem*

Zhou W., Song W. (2006) Leaky scanning and reinitiation regulate BACE1 gene expression. *Mol Cell Biol* **26:** 3353-3364

Zhu H.C., Wang L.M., Wang M., Song B., Tan S., Teng J.F., Duan D.X. (2012) MicroRNA-195 downregulates Alzheimer's disease amyloid-beta production by targeting BACE1. *Brain Res Bull* **88:** 596-601

Zong Y., Wang H., Dong W., Quan X., Zhu H., Xu Y., Huang L., Ma C., Qin C. (2011) miR-29c regulates BACE1 protein expression. *Brain Res* **1395:** 108-115

6 Appendix

Function /Type (number)	Protein name	Mascot score	Molecular weight (kDa)	Lane
Protein synthesis (4)	eEF1a1	185	50 kDa	**17**, 18
	eEF1a2	107	51 kDa	**17**
	eIF2a	139	36 kDa	**20**
	eIF2b	220	39 kDa	**17**
hnRNP(4)	hnRNP K	110	51 kDa	**18**, 19, 1
	hnRNP E1	304	38 kDa	**19**, 20
	hnRNP E2	288	39 kDa	**19**
	hnRNP U	202	91 kDa	**9**, 3/4, 1
Other RNA associated (5)	ILF2	115	43 kDa	**19**
	ILF3	201	96 kDa	**9**
	PA2G4	347	44 kDa	**17**
	SFPQ	203	76 kDa	**18**
	YBOX1	176	36 kDa	**17**
tRNA synthetases (6)	SYEP	569	165 kDa	**1**, 3/4
	SYIC	794	146 kDa	**1**
	SYLC	616	136 kDa	**1**, 3/4
	SYMC	309	102 kDa	**7**, 6
	SYQ	653	89 kDa	**8**
	SYRC	179	76 kDa	**1**
Cytoskeletal (6)	Drebrin	1051	78 kDa	**3/4**, 5, 1, 7, 6, 8, 19, 9
	LIMA1	125	86 kDa	**9**
	Spectrin α chain	106	285 kDa	**1**
	Septin-2	118	74 kDa	**1**, 19
	Septin-7	169	64 kDa	**17**
	TMOD3	191	40 kDa	**19**
Other known proteins (2)	LONM	641	107 kDa	**6**, 5
	MCA1	331	35 kDa	**20**

Appendix Table 6.1 Potential BACE1 5`UTR interacting proteins from cytosolic extract of HEK293E cells identified by mass spectrometry.
Cytosolic extract of HEK293E cells was incubated with BACE1 5`UTR RNA. The RNA binding proteins were separated by gel electrophoresis, and 13 slices were analysed with mass spectrometry. The proteins were subdivided in different categories according to their function. For each identified protein the highest mascot score, the molecular weight and the lane(s), where the protein was identified, are listed. The lane number marked in bold corresponds to the mascot score. Only proteins with a mascot score higher than 100 were considered.

Function / Type (number)	Protein name	Mascot score	Molecular weight (kDa)	Lane
Protein synthesis (2)	eEF1a1	157	50 kDa	**14**
	eEF1a2	157	51 kDa	**14**, 15
hnRNP (4)	hnRNP K	705	51 kDa	**18**
	hnRNP E1	2294	38 kDa	**11**, 12, 13, 10, 6
	hnRNP E2	1451	39 kDa	**12**, 11, 13, 10, 6, 9, 15, 16, 7
	hnRNP E3	948	36 kDa	**12**, 11, 13
Cytoskeletal (10)	MAP2	5905	199 kDa	**29**, 30, 28, 31, 27
	Drebrin	521	78 kDa	**25**
	Tau	169	77 kDa	**15**, 14
	Spectrin α chain	270	285 kDa	**28**
	Synapsin-1	654	74 kDa	**21**, 20
	Synapsin-2	183	64 kDa	**17**
	DYHC1	981	534 kDa	**29**, 30
	DYN1	616	98 kDa	**23**
	DYN2	144	98 kDa	**23**
	DYN3	148	98 kDa	**23**
Other known proteins (3)	EFHD2	244	27 kDa	**7**
	FIBB	173	55 kDa	**8**
	FIBG	174	50 kDa	**8**

Appendix Table 6.2 Potential BACE1 5`UTR interacting proteins from cytosolic extract of P30 mice brains identified by mass spectrometry.
Cytosolic extract of P30 mice brains was incubated with BACE1 5`UTR RNA. The RNA binding proteins were separated by gel electrophoresis, and 31 bands were analysed with mass spectrometry. Only proteins with a mascot score higher than 100 were considered. The proteins were subdivided in different categories according to their function. For each identified protein the highest mascot score, the molecular weight and the lane(s), where the protein was identified, are listed. The lane number marked in bold corresponds to the mascot score

Start – End	Observed	Mr(expt)	Mr(calc)	ppm	Miss	Sequence	Ion score
65 – 78	805.3696	1608.7246	1608.7380	-8	1	K.VGDDVEFEVSSDRR.T	12
90 – 99	627.8517	1253.6889	1253.6979	-7	1	K.IKQEILPEER.M	40
195 – 202	484.7464	967.4782	967.4763	2	0	K.EAFGFIER.G	30
208 – 217	673.8214	1345.6283	1345.6343	-4	0	K.EIFFHYSEFK.G	16
218 – 234	938.9553	1875.8961	1875.9102	-8	0	K.GDLETLQPGDDVEFTIK.D	11
247 – 269	858.4576	2572.3509	2572.3425	3	0	R.LLPQGTVIFEDISIEHFEGTVTK.V	12
287 – 295	529.8392	1057.6639	1057.6536	10	1	R.IKVDFVIPK.E	46
308 – 317	569.8107	1137.6068	1137.6142	-7	0	K.VTLLEGDHVR.F	44
318 – 325	504.7607	1007.5068	1007.5148	-8	1	R.FNISTDRR.D	19
331 - 348	1028.0024	2053.9903	2054.0069	-8	0	R.ATNIEVLSNTFQFTNEAR.E	52
519 - 527	489.3065	976.5985	976.5957	3	0	R.LLGYVATLK.D	15
601 - 606	377.2598	752.5051	752.5021	4	0	K.VIRPLR.S	9
683 - 696	809.8669	1617.7192	1617.7311	-7	0	K.DQFGFINYEVGDSK.K	28
759 - 769	586.7951	1171.5756	1171.5833	-7	0	K.NITLDDASAPR.L	68

Appendix Figure 6.1 Unr peptides from HEK293E cytosolic extract found by mass spectrometry.

Start – End: amino acid number of the peptide in the protein sequence. Observed: experimental mass number / charge number (m/z) value. Mr(expt): experimental m/z transformed to a relative molecular mass. Mr(calc): relative molecular mass calculated from the matched peptide sequence. ppm: difference (error) between the experimental and calculated masses. Miss: Number of missed cleavage sites. Sequence: identified peptide sequence. The point shows the cleavage site. Ion score: the ions score for an MS/MS match is based on the calculated probability, P, that the observed match between the experimental data and the database sequence is a random event. The reported score is -10Log(P).

Start – End	Observed	Mr(expt)	Mr(calc)	ppm	Miss	Sequence	Ion Score
33 – 45	787.3870	1572.7594	1572.7606	-1	0	K.LLTSYGFIQCSER.Q	70
65 – 77	727.3258	1452.6370	1452.6369	0	0	K.VGDDVEFEVSSDR.R	56
65 – 77	727.3262	1452.6378	1452.6369	1	0	K.VGDDVEFEVSSDR.R	36
65 - 77	727.3264	1452.6382	1452.6369	1	0	K.VGDDVEFEVSSDR.R	63
65 - 78	537.2531	1608.7375	1608.7380	-0	1	K.VGDDVEFEVSSDRR.T	16
65 - 78	537.2532	1608.7378	1608.7380	-0	1	K.VGDDVEFEVSSDRR.T	37
65 - 78	805.3762	1608.7378	1608.7380	-0	1	K.VGDDVEFEVSSDRR.T	17
65 - 78	805.3764	1608.7382	1608.7380	0	1	K.VGDDVEFEVSSDRR.T	11
65 - 78	537.2534	1608.7384	1608.7380	0	1	K.VGDDVEFEVSSDRR.T	42
65 - 78	805.3777	1608.7408	1608.7380	2	1	K.VGDDVEFEVSSDRR.T	17
79 - 86	414.2715	826.5284	826.5276	1	0	R.TGKPIAIK.L	24
90 - 99	416.5660	1246.6762	1246.6669	7	0	K.IKPEIHPEER.M	17
158 - 166	538.7904	1075.5662	1075.5662	0	0	K.INFVIDNNK.H	40
167 - 174	399.7144	797.4142	797.4144	-0	0	K.HTGAVSAR.N	10
167 - 174	399.7146	797.4146	797.4144	0	0	K.HTGAVSAR.N	17
175 - 180	366.2274	730.4402	730.4411	-1	0	R.NIMLLK.K	6
175 - 180	366.2279	730.4412	730.4411	0	0	R.NIMLLK.K	17
175 - 180	366.2280	730.4414	730.4411	0	0	R.NIMLLK.K	8
175 - 180	374.2253	746.4360	746.4360	0	0	R.NIMLLK.K Oxidation (M)	23
175 - 180	374.2255	746.4364	746.4360	1	0	R.NIMLLK.K Oxidation (M)	22
175 - 180	374.2256	746.4366	746.4360	1	0	R.NIMLLK.K Oxidation (M)	26
175 - 180	374.2258	746.4370	746.4360	1	0	R.NIMLLK.K Oxidation (M)	17
195 - 202	484.7450	967.4754	967.4763	-1	0	K.EAFGFIER.G	26
195 - 202	484.7451	967.4756	967.4763	-1	0	K.EAFGFIER.G	24
195 - 202	484.7458	967.4770	967.4763	1	0	K.EAFGFIER.G	27
195 - 202	484.7460	967.4774	967.4763	1	0	K.EAFGFIER.G	33
218 - 236	716.6857	2147.0353	2147.0383	-1	1	K.GDLETLQPGDDVEFTIKDR.N	12
237 - 246	544.7883	1087.5620	1087.5622	-0	1	R.NGKEVATDVR.L	23
278 - 286	505.7532	1009.4918	1009.4941	-2	0	K.NQNDPLPGR.I	26
278 - 286	505.7541	1009.4936	1009.4941	-0	0	K.NQNDPLPGR.I	15
278 - 286	505.7542	1009.4938	1009.4941	-0	0	K.NQNDPLPGR.I	38
278 - 286	505.7546	1009.4946	1009.4941	1	0	K.NQNDPLPGR.I	25

continued on next page

Start – End	Observed	Mr(expt)	Mr(calc)	ppm	Miss	Sequence	Ion Score
287 - 295	353.5583	1057.6531	1057.6536	-0	1	R.IKVDFVIPK.E	37
287 - 295	529.8340	1057.6534	1057.6536	-0	1	R.IKVDFVIPK.E	25
287 - 295	529.8340	1057.6534	1057.6536	-0	1	R.IKVDFVIPK.E	59
287 - 295	353.5585	1057.6537	1057.6536	0	1	R.IKVDFVIPK.E	31
287 - 295	353.5589	1057.6549	1057.6536	1	1	R.IKVDFVIPK.E	28
287 - 295	529.8348	1057.6550	1057.6536	1	1	R.IKVDFVIPK.E	28
296 - 305	575.2932	1148.5718	1148.5713	0	1	K.ELPFGDKDTK.S	6
296 - 305	575.2944	1148.5742	1148.5713	3	1	K.ELPFGDKDTK.S	17
306 - 317	451.9200	1352.7382	1352.7412	-2	1	K.SKVTLLEGDHVR.F	38
306 - 317	451.9207	1352.7403	1352.7412	-1	1	K.SKVTLLEGDHVR.F	41
308 - 317	380.2118	1137.6136	1137.6142	-1	0	K.VTLLEGDHVR.F	28
308 - 317	569.8143	1137.6140	1137.6142	-0	0	K.VTLLEGDHVR.F	36
308 - 317	569.8144	1137.6142	1137.6142	0	0	K.VTLLEGDHVR.F	20
308 - 317	569.8144	1137.6142	1137.6142	0	0	K.VTLLEGDHVR.F	26
308 - 317	380.2121	1137.6145	1137.6142	0	0	K.VTLLEGDHVR.F	24
308 - 317	380.2123	1137.6151	1137.6142	1	0	K.VTLLEGDHVR.F	20
308 - 317	380.2124	1137.6154	1137.6142	1	0	K.VTLLEGDHVR.F	22
318 - 324	426.7135	851.4124	851.4137	-2	0	R.FNISTDR.R	32
318 - 324	426.7140	851.4134	851.4137	-0	0	R.FNISTDR.R	17
318 - 325	04.7645	1007.5144	1007.5148	-0	1	R.FNISTDRR.D	4
318 - 325	504.7647	1007.5148	1007.5148	0	1	R.FNISTDRR.D	16
318 - 325	336.8456	1007.5150	1007.5148	0	1	R.FNISTDRR.D	15
318 - 325	504.7652	1007.5158	1007.5148	1	1	R.FNISTDRR.D	10
349 - 357	489.2487	976.4828	976.4834	-1	0	R.EMGVIAAMR.D	10
349 - 357	489.2491	976.4836	976.4834	0	0	R.EMGVIAAMR.D	20
349 - 357	489.2491	976.4836	976.4834	0	0	R.EMGVIAAMR.D	18
349 - 357	497.2466	992.4786	992.4783	0	0	R.EMGVIAAMR.D Oxidation (M)	36
349 - 357	497.2466	992.4786	992.4783	0	0	R.EMGVIAAMR.D Oxidation (M)	30
349 - 357	497.2466	992.4786	992.4783	0	0	R.EMGVIAAMR.D Oxidation (M)	23
349 - 357	505.2438	1008.4730	1008.4732	-0	0	R.EMGVIAAMR.D 2 Oxidation (M)	17
358 - 364	392.2054	782.3962	782.3963	-0	0	R.DGFGFIK.C	36
358 - 364	392.2055	782.3964	782.3963	0	0	R.DGFGFIK.C	29
358 - 364	392.2057	782.3968	782.3963	1	0	R.DGFGFIK.C	16
358 - 364	392.2059	782.3972	782.3963	1	0	R.DGFGFIK.C	21
358 - 364	392.2062	782.3978	782.3963	2	0	R.DGFGFIK.C	41

continued on next page

Start – End	Observed	Mr(expt)	Mr(calc)	ppm	Miss	Sequence	Ion Score
416 - 427	456.2130	1365.6172	1365.6174	-0	0	K.GTVSFHSHSDHR.F	2
416 - 427	456.2131	1365.6175	1365.6174	0	0	K.GTVSFHSHSDHR.F	8
428 - 434	397.2259	792.4372	792.4382	-1	0	R.FLGTVEK.E	11
428 - 434	397.2263	792.4380	792.4382	-0	0	R.FLGTVEK.E	20
428 - 434	397.2264	792.4382	792.4382	0	0	R.FLGTVEK.E	12
428 - 434	397.2265	792.4384	792.4382	0	0	R.FLGTVEK.E	34
428 - 434	397.2266	792.4386	792.4382	1	0	R.FLGTVEK.E	12
428 - 434	397.2272	792.4398	792.4382	2	0	R.FLGTVEK.E	19
428 - 434	397.2277	792.4408	792.4382	3	0	R.FLGTVEK.E	9
428 - 442	556.6257	1666.8553	1666.8566	-1	1	R.FLGTVEKEATFSNPK.T	7
435 - 442	447.2216	892.4286	892.4290	-0	0	K.EATFSNPK.T	10
435 - 442	447.2218	892.4290	892.4290	0	0	K.EATFSNPK.T	24
435 - 442	447.2218	892.4290	892.4290	0	0	K.EATFSNPK.T	8
435 - 442	447.2220	892.4294	892.4290	0	0	K.EATFSNPK.T	14
468 - 475	446.2682	890.5218	890.5225	-1	0	K.LTIAFQAK.D	17
468 - 475	446.2684	890.5222	890.5225	-0	0	K.LTIAFQAK.D	26
468 - 475	446.2687	890.5228	890.5225	0	0	K.LTIAFQAK.D	17
476 - 488	666.8168	1331.6190	1331.6205	-1	0	K.DVEGSTSPQIGDK.V	90
476 - 488	666.8174	1331.6202	1331.6205	-0	0	K.DVEGSTSPQIGDK.V	53
476 - 488	666.8176	1331.6206	1331.6205	0	0	K.DVEGSTSPQIGDK.V	60
476 - 488	666.8180	1331.6214	1331.6205	1	0	K.DVEGSTSPQIGDK.V	56
476 - 496	746.6976	2237.0710	2237.0699	0	1	K.DVEGSTSPQIGDKVEFSISDK.Q	13
476 - 496	746.6979	2237.0719	2237.0699	1	1	K.DVEGSTSPQIGDKVEFSISDK.Q	23
497 - 508	471.9176	1412.7310	1412.7307	0	0	K.QRPGQQIATCVR.L	18
497 - 508	471.9176	1412.7310	1412.7307	0	0	K.QRPGQQIATCVR.L	16
497 - 508	707.3730	1412.7314	1412.7307	1	0	K.QRPGQQIATCVR.L	10
519 - 527	489.3045	976.5944	976.5957	-1	0	R.LLGYVATLK.D	11
519 - 527	489.3049	976.5952	976.5957	-0	0	R.LLGYVATLK.D	22
519 - 527	489.3051	976.5956	976.5957	-0	0	R.LLGYVATLK.D	44
519 - 527	489.3056	976.5966	976.5957	1	0	R.LLGYVATLK.D	47
601 - 606	377.2585	752.5024	752.5021	0	0	K.VIRPLR.G	9
601 - 606	377.2585	752.5024	752.5021	0	0	K.VIRPLR.G	8
629 - 642	749.3750	1496.7354	1496.7334	1	0	K.GEVYPFGIVGMANK.G (M)	22
683 - 696	809.8754	1617.7362	1617.7311	3	0	K.DQFGFINYEVGDSK.K	54
683 - 696	809.8787	1617.7428	1617.7311	7	0	K.DQFGFINYEVGDSK.K	62

continued on next page

Start – End	Observed	Mr(expt)	Mr(calc)	ppm	Miss	Sequence	Ion Score
698 - 703	395.7344	789.4542	789.4538	1	0	K.LFFHVK.E	6
698 - 703	395.7346	789.4546	789.4538	1	0	K.LFFHVK.E	9
744 - 752	318.1821	951.5245	951.5250	-1	0	K.AVAAPRPDR.L	12
744 - 752	476.7696	951.5246	951.5250	-0	0	K.AVAAPRPDR.L	36
744 - 752	476.7697	951.5248	951.5250	-0	0	K.AVAAPRPDR.L	11
744 - 752	476.7698	951.5250	951.5250	0	0	K.AVAAPRPDR.L	19
744 - 752	476.7699	951.5252	951.5250	0	0	K.AVAAPRPDR.L	16
744 - 752	318.1824	951.5254	951.5250	0	0	K.AVAAPRPDR.L	17
744 - 752	318.1824	951.5254	951.5250	0	0	K.AVAAPRPDR.L	19
744 - 752	318.1824	951.5254	951.5250	0	0	K.AVAAPRPDR.L	12
757 - 769	471.9278	1412.7616	1412.7623	-1	1	R.LKNITLDDASAPR.L	38
757 - 769	471.9281	1412.7625	1412.7623	0	1	R.LKNITLDDASAPR.L	42
757 - 769	471.9282	1412.7628	1412.7623	0	1	R.LKNITLDDASAPR.L	39
757 - 769	707.3889	1412.7632	1412.7623	1	1	R.LKNITLDDASAPR.L	31
757 - 769	707.3891	1412.7636	1412.7623	1	1	R.LKNITLDDASAPR.L	38
759 - 769	586.7985	1171.5824	1171.5833	-1	0	K.NITLDDASAPR.L	25
759 - 769	586.7991	1171.5836	1171.5833	0	0	K.NITLDDASAPR.L	51
759 - 769	586.7999	1171.5852	1171.5833	2	0	K.NITLDDASAPR.L	57
759 - 769	586.7999	1171.5852	1171.5833	2	0	K.NITLDDASAPR.L	39
759 - 769	586.8008	1171.5870	1171.5833	3	0	K.NITLDDASAPR.L	56
770 - 774	316.2017	630.3888	630.3887	0	0	R.LMVLR.Q	19
770 - 774	316.2021	630.3896	630.3887	2	0	R.LMVLR.Q	12
770 - 774	324.1990	646.3834	646.3836	-0	0	R.LMVLR.Q Oxidation (M)	20
770 - 774	324.1992	646.3838	646.3836	0	0	R.LMVLR.Q Oxidation (M)	26
778 - 789	619.2672	1236.5198	1236.5193	0	0	R.GPDNSMGFGAER.K	44
778 - 789	619.2679	1236.5212	1236.5193	2	0	R.GPDNSMGFGAER.K	31
778 - 789	627.2643	1252.5140	1252.5143	-0	0	R.GPDNSMGFGAER.K (M)	64
778 - 789	627.2646	1252.5146	1252.5143	0	0	R.GPDNSMGFGAER.K (M)	56
778 - 789	627.2650	1252.5154	1252.5143	1	0	R.GPDNSMGFGAER.K (M)	46
778 - 789	627.2661	1252.5176	1252.5143	3	0	R.GPDNSMGFGAER.K (M)	49
791 - 798	436.2534	870.4922	870.4923	-0	1	K.IRQAGVID.-	0

Appendix Figure 6.2 Unr peptides from mouse brain cytosolic extract found by mass spectrometry.
Start – End: amino acid number of the peptide in the protein sequence. Observed: experimental mass number / charge number (m/z) value. Mr(expt): experimental m/z transformed to a relative molecular mass. Mr(calc): relative molecular mass calculated from the matched peptide sequence. ppm: difference (error) between the experimental and calculated masses. Miss: Number of missed cleavage sites. Sequence: identified peptide sequence. The point shows the cleavage site. Ion score: the ions score for an MS/MS match is based on the calculated probability, P, that the observed match between the experimental data and the database sequence is a random event. The reported score is -10Log(P)

7 Publications

Mori K, Lammich S, Mackenzie IR, Forné I, **Zilow S**, Kretzschmar H, Edbauer D, Janssens J, Kleinberger G, Cruts M, Herms J, Neumann M, Van Broeckhoven C, Arzberger T, Haass C.
hnRNP A3 binds to GGGGCC repeats and is a constituent of p62-positive/TDP43-negative inclusions in the hippocampus of patients with C9orf72 mutations. Acta Neuropathol. 2013 Mar;125(3):413-23

Lammich S, Kamp F, Wagner J, Nuscher B, **Zilow S**, Ludwig AK, Willem M, Haass C.
Translational repression of the Disintegrin and Metalloprotease ADAM10 by a stable G-quadruplex secondary structure in its 5'-untranslated region. J Biol Chem. 2011 Dec30;286(52):45063-72

Lammich S, Buell D, **Zilow S**, Ludwig AK, Nuscher B, Lichtenthaler SF, Prinzen C, Fahrenholz F, Haass C.
Expression of the anti-amyloidogenic secretase ADAM10 is suppressed by its 5'-untranslated region. J Biol Chem. 2010 May 21;285(21):15753-60.

Kaether C, Scheuermann J, Fassler M, **Zilow S**, Shirotani K, Valkova C, Novak B, Kacmar S, Steiner H, Haass C.
Endoplasmic reticulum retention of the gamma-secretase complex component Pen2 by Rer1. EMBO Rep. 2007 Aug;8(8):743-8.